The Role of Apoptosis and Ineffective Haematopoiesis in the Myelodysplastic Syndromes (MDS)

Andrew Adel Guirguis

Submitted in total fulfilment of the requirements of the degree of Doctor of Philosophy

June 2015

Faculty of Medicine, Nursing & Health Sciences
Department of Haematology
Monash University

ABSTRACT

The myelodysplastic syndromes (MDS) are defined as clonal haematopoietic stem cell disorders whose key features are those of ineffective haematopoiesis, bone marrow dysplasia and an increased likelihood of transformation to acute leukaemia. From a clinical perspective, although these disorders are notable for their heterogeneity, the presence of recurrent cytopenias and leukaemic progression remains a common theme.

With an ever-ageing Australian population, the incidence of MDS is predicted to rise exponentially in years to come. In spite of this, research in MDS has been hampered over the years by a lack of adequately representative cell lines or useful xenograft models that accurately recapitulate features of the disease. Additionally, the mechanism of action of the limited armamentarium of therapies such as azacitidine and lenalidomide has not been fully elucidated at the present moment. Although this is likely to change as our understanding of the heterogeneous molecular basis of human MDS is further refined, there are still some significant deficiencies in our current knowledge and approach.

Early-stage MDS has long been characterized by an increase in apoptosis or 'programmed cell death'. This is thought to contribute to the disparity between marrow hypercellularity and peripheral blood cytopenias – a phenomenon referred to as 'ineffective haematopoiesis'. However, the mechanism of apoptosis has been a contentious one with some groups supporting a cell extrinsic model and others postulating a cell intrinsic one. Additionally, the majority of this data remains observational.

In this body of work, we have used the *Nup98-HoxD13 (NHD13)* murine model as a tool for studying apoptosis in MDS. We have specifically sought to determine how apoptosis contributes to the MDS phenotype, which proteins might be involved and the functional benefit and significance of abrogating apoptosis on the associated cytopenias and on leukaemic progression.

Our work identifies that apoptosis is dependent on p53 and its transcriptional target *Puma*. Using a breeding approach to target p53, PUMA and other BH-3 only proteins, we show evidence that targeting p53 or PUMA rescues apoptosis, but has a differential effect on disease progression to acute myeloid leukaemia.

Our work challenges the paradigm that resistance to apoptosis associates with disease progression in myeloid disease and will raise the possibility that current therapeutics, which often work by inducing apoptosis, might actually be detrimental in the long-term, accelerating disease progression. In this context, we show evidence for an 'anti-inflammatory' effect through prevention of apoptosis and postulate that preventing apoptosis or ameliorating the associated inflammatory milieu may present an alternative means for disease control.

DECLARATION

This is to certify that:

i. This thesis is comprised of my original work alone towards my PhD except where indicated in the Preface; and that this work has not been accepted for the award of any other degree or diploma,

ii. Acknowledgement has been made in the text to all other material used as appropriate,

iii. The thesis is less than 100,000 words in length – exclusive of tables, figures and bibliography.

Andrew Adel Guirguis

June 2015

PREFACE

I have assessed my contribution to the results described in each Chapter as original to be as follows:

Chapter 3: 75%
Chapter 4: 95%
Chapter 5: 85%

I acknowledge the important contribution of others to results presented in this work:

Chapter 3: Christopher Slape, Jesslyn Saw and David Powell
Chapter 4: Christopher Slape and Jesslyn Saw
Chapter 5: Ashwin Unnikrishnan

My overall contribution to the results presented in this thesis is therefore ~ 85%

PUBLICATIONS

Publications and papers arising from the findings presented in this thesis include:

Guirguis AA, Slape C, Saw J, Failla L, Powell D, Strasser A, Rossello F and Curtis DJ. Puma promotes apoptosis of haematopoietic progenitors driving leukaemic progression in a mouse mode of myelodysplasia. *Cell Death and Differentiation – Under Review*

Guirguis AA, Slape C, Saw J, Wei A, Failla L, Bouillet P, Strasser A and Curtis DJ. Puma is the critical BH3-only protein mediating apoptosis in the *Nup98-HoxD13 (NHD13)* mouse model of human MDS. *Blood (ASH Annual Meeting Abstracts). 2013, 122(21): 1563*

ACKNOWLEDGEMENTS

The past four years during my PhD studies have been challenging in a significant number of ways. Although frustrating at times, they have nonetheless been rewarding and enjoyable all the same. Through this work, I have been exposed to the rigors of scientific research and have developed significant admiration for the tireless efforts of many of my fellow colleagues and friends. Many people have played a significant part in my journey and for this I am deeply grateful. First and foremost, I would like to thank my primary supervisor, Associate Professor David Curtis for his encouragement, support, criticisms, patience and honesty over the past four years. David has encouraged me to reach for and achieve my potential throughout my PhD and beyond this, for my career in general. He has been a great mentor during this journey. I would also like to thank Dr Andrew Wei and Dr Christopher Slape for their mentorship over the last few years and their guidance. The journey has certainly not been an easy one, but through it, I have learnt a lot about myself.

I have been privileged to be part of an amazing laboratory comprised of competent, intelligent, passionate and supportive colleagues with whom I have developed a significant number of friendships. To all those people I have shared a corridor-conversation with, through to those I have sought specific technical support, I would like to say a big thankyou! It has been an honour to work with each of you and I have appreciated the help that has been freely given whenever I have needed guidance or assistance. I would like to thank specific members of the Stem Cell Research Group including Ms Jesslyn Saw and Ms Loretta Cerruti. Thank you for all your advice and guidance over the past four years. I have thoroughly enjoyed my time in the laboratory. A big thanks must also be extended to Dr Cédric Tremblay for his mentorship and advice and his friendship. This has been invaluable for learning new techniques and for general experimental advice. I would also like to thank Dr Stefan Sonderegger and Dr Emma Toulmin for their input over the years. The post-doctorate fellows in the lab have led by example and have shown me what it means to mentor,

educate and encourage fellow doctors and scientists in their work. During my time in the lab, I have developed many new friendships – a significant number of which will continue to play a part in my life, as I move forwards onto the next exciting chapter of my career.

I would also like to thank Dr Tiffany Khong for her career advice, support and friendship over the years. This has meant a great deal to me and is indeed very much appreciated. Specific thanks must also go to members of the AMREP Flow Cytometry Group – Geza, Phil and Jeanne. Thank you for all your tireless efforts in maintaining a fantastic Flow Cytometry facility. Additional thanks also goes to members of the animal house for caring after all my mouse lines and for your support and patience. In particular, I would like to thank Ms Kylie Spark, Ms Elyse Eble and Ms Naomi Borg for all their hard work that goes on behind the scenes.

Finally, there is no doubt I would not have survived the past four years without the support of my family, my partner and my close friends. The past twelve months in particular have been monumental somewhat and I have been blessed with genuine people who have cared for and nurtured me. That these past four years are finally coming to an end, is a tribute to your care and support for me. Thank you to my dear mother, who although not alive, has always instilled in me the value of hard work, dedication, integrity and passion. To my dearest father, Adel thank you for raising me to be the person I am today. To Dad, Randa, Aunty Nabila, Aunty Mervat, Jason, Amber, Nevine and Sam, I know that you are all as happy to see this day arrive as I am. I cannot thank any of you enough for everything you have done for me.

TABLE OF CONTENTS

LIST OF FIGURES

LIST OF TABLES

ABBREVIATIONS

2-βME	2-betamercaptoethanol
7-AAD	7-aminoactinomycin D
α	alpha
AML	acute myeloid leukaemia
ALL	acute lymphoblastic leukaemia
APAF-1	apoptotic protease activating factor 1
APC(-Cy7)	allophycocyanin(-Cy7)
APS	ammonium presulfate
ATP	adenosine triphosphate
β	beta
BAD	BCL-2 associated death
BAK	BCL-2-antagonist killer
BAX	BCL-2-associated X-protein
BCL-2	B-cell CLL / lymphoma 2
BD	Becton Dickinson
BFU-E	burst-forming unit, erythroid
BH1-4	BCL-2 homology domains 1-4
BIM	BCL-2-interacting mediator
Bio	biotin / biotinylated
bp	base pairs
BSA	bovine serum albumin
BSGC	buffered saline glucose citrate
cDNA	complementary DNA
CFU-E	colony-forming unit, erythroid
c-KIT	CD117/stem cell factor tyrosine-protein kinase receptor Kit
cm	centimetre(s)
CMP	common myeloid progenitor
CO_2	carbon dioxide

DAB	3,3'-diamino-benzidine
DAPI	4',6-diamidino-2-phenylinodole
DEPC	diethyl pyrocarbonate
dH_2O	distilled water
DMEM	Dulbecco's Modified Eagle Medium
DMSO	dimethyl sulphoxide
DNA	deoxyribonucleic acid
dsDNA	double-stranded DNA
ECL	enhanced chemiluminescence
EDTA	ethylenediaminetetra-acetic acid
EPO	erythropoietin
EtBr	ethidium bromide
EtOH	ethanol
FAB	French-American-British
FACS	fluorescence-activated cell sorting
FCS	foetal calf serum
FITC	fluorescein isothiocyanate
γ	gamma
g	gram(s)
GMP	granulocyte-macrophage/monocyte progenitor
H_2O	water
Hb	haemoglobin
HCl	hydrochloric acid
HPC	haematopoietic progenitor cell
hr	hour(s)
HRP	horseradish peroxidase
HSC	haematopoietic stem cell
IPA	Ingenuity Pathway Analysis
IPSS	International Prognostic Scoring System
KCl	potassium chloride
KO	knock-out
L	litre(s)
LK	$lineage^{negative}$, $c\text{-}Kit^{positive}$ ($Sca\text{-}1^{negative}$)

LSK	lineage^{negative}, Sca-1^{positive}, c-Kit^{positive}
LT-HSC	long-term haematopoietic stem cells (LSK, CD150^{+}, CD48^{-})
M	molar
MCL-1	myeloid cell leukaemia-1
MDS	myelodysplastic syndrome
MeC	methylcellulose
Meg-E	megakaryocyte erythroid progenitor
MeOH	methanol
mg	milligram(s)
µg	microgram(s)
min	minute(s)
mIL-3/IL-6	murine interleukin 3/6
mL	millilitre(s)
mM	millimolar
µL	microlitre(s)
$MgCl_2$	magnesium chloride
MOMP	mitochondrial outer membrane permeability
MPP	multi-potent progenitor
MQ H_2O	milli-Q water
mRNA	messenger ribonucleic acid
$Na_2HPO_4.2H_2O$	sodium hydrogen phosphate, dihydrate
NaCl	sodium chloride
$NaH_2PO_4.1H_2O$	sodium phosphate, monobasic anhydrous
NaN_3	sodium azide
NaOH	sodium hydroxide
NHD13	Nup98-HoxD13 fusion protein
NH_4Cl	ammonium chloride
NOD/SCID	non-obese diabetic / severe combined immunodeficiency
PB	pacific blue
PBS	phosphate buffered saline
PCR	polymerase chain reaction
PE-(Cy5/7)	phycoerythrin- (Cy5/7)
PerCP-Cy5.5	perdinin chlorophyll protein complex- Cy5.5

PFA	paraformaldehyde
PI	propidium iodide
Puma	p53 upregulated modulator of apoptosis
PVDF	polyvinylidene fluoride
qPCR	quantitative polymerase chain reaction
RA	refractory anaemia
RAEB	refractory anaemia with excess blasts
RBC	red blood cells
RCUD / RCMD	refractory cytopenias with unilineage / multi-lineage dysplasia
RNA	ribonucleic acid
RPMI	Roswell Park Memorial Institute medium
RPS14	ribosomal protein S14
rSCF	rat stem cell factor
RT	room temperature
s	seconds
SA	streptavidin
SCA-1	stem cell antigen 1
SCF	stem cell factor
SDS	sodium dodecyl sulphate
SLAM	Signaling lymphocyte activation molecule
ST-HSC	short-term haematopoietic stem cells (LSK, $CD150^-$, $CD48^-$)
TAE	Tris-Acetate-EDTA
TBS(T)	Tris buffered saline (Tween)
TE	Tris-EDTA
TEMED	tetramethylethylenediamine
V	volt(s)
v /v	volume per volume
w/v	weight per volume
WHO	World Health Organization

CHAPTER ONE

Introduction

Abstract

Myelodysplastic syndrome (MDS) refers to a heterogeneous group of disorders characterized by ineffective haematopoiesis, peripheral blood cytopenias and an increased propensity for transformation to acute leukaemia. Its onset occurs most frequently in those > 60 years of age and represents aberrant and defective haematopoiesis. Programmed cell death or apoptosis is believed to be a key process that accounts for the associated cytopenias and is most prominent in early-stage disease. Although many have implicated the extrinsic apoptotic pathway, other groups have demonstrated a cell intrinsic mechanism may be of equally important significance; although much of this data remains observational. As with other malignancies, it is generally thought that overcoming apoptosis associates with a more aggressive disease phenotype and leukaemic transformation. However, as will be discussed, there are exceptions to this concept. In this Chapter, our current understanding of the clinical and biological features of MDS is summarised, whilst deficiencies in our current knowledge are highlighted. The apoptotic pathway is examined in some detail and how this currently relates to the pathogenesis of early-stage MDS is assessed. A discussion about triggers of apoptosis, the bone marrow microenvironment and the limited array of MDS models and their limitations is also presented. Using the Nup98-HoxD13 (*NHD13*) mouse model of MDS, we propose to examine in more detail the mechanism by which various apoptotic proteins contribute to the phenotype of MDS and to study the effect modulating apoptosis has on myeloid disease progression.

Background

1.1. Haematopoiesis

'Haematopoiesis' refers to a tightly regulated process conserved throughout vertebrate evolution - in which a rare population of pluripotent haematopoietic stem cells (HSCs) gives rise to a series of lineage-committed haematopoietic progenitor cells (HPCs) which eventually mature into terminally differentiated blood cells. In line with this somewhat sequential process, is the gradual loss of self-renewal capacity. Adult pluripotent HSCs from the bone marrow are usually maintained in a quiescent state and are defined by their ability to self-renew and to ultimately differentiate into the various cellular components of a person's blood system (Orkin and Zon 2008) – a process often maintained through asymmetrical cell division. This same quiescent and slowly cycling population is capable of dramatic expansion and contraction in an attempt to maintain homeostasis as required particularly during times of increased haematopoietic stress (Passegué et al. 2005). Differentiation of this immature stem cell population is tightly regulated and relies upon the execution of specific gene expression programs.

In humans, the stem cell population is generally derived from lineage negative cells (i.e cells that do not express any of the lineage markers associated with more mature cells). These cells are generally CD34 positive. Within this population, cells that are additionally $CD38^-$ have been shown to possess multi-lineage repopulation capabilities best demonstrated in NOD/SCID recipient mice (Bhatia et al. 1997).

In mice, the stem cell population is similarly derived from lineage-negative cells. A proportion of these immature cells express the stem cell factor tyrosine kinase receptor, c-KIT and a proportion of these also express stem-cell antigen 1 (SCA-1). In combination, the more primitive subset of these cells is defined as being lineage negative (Lin^{neg}), SCA-1 positive (Sca^+) and c-KIT positive (Kit^+) (i.e LSK cells) (Okada et al. 1991; Okada et al. 1992). These immature cells comprise about 0.1% of total nucleated bone marrow cells and consist of a

population of cells with long-term reconstitution capacity. In contrast, less primitive cells are typically SCA-1 negative (LK cells), comprise 2.5% of total nucleated bone marrow cells and do not possess long-term reconstitution capabilities. Unlike human stem cells which are typically $CD34^{+}$, murine stem cells with delayed but long-term multi-lineage reconstitution capacity are generally negative for CD34 (Osawa et al. 1996).

Despite their purported ability for multi-lineage reconstitution, < 20% of LSK cells are actually capable of this in lethally irradiated mice. By analysing gene expression profiles, Kiel et al identified a series of markers from the SLAM family that additionally differentiate between long-term haematopoietic stem cells (LT-HSCs) and the more mature multi-potent progenitors (MPPs). These markers will be alluded to extensively throughout this study. LT-HSCs are typically $CD150^{+}$, $CD244^{-}$ and $CD48^{-}$. Of significance, CD150 is at least 4x more highly upregulated in HSCs cf MPPs (Pronk et al. 2007) and $CD150^{+}CD48^{-}$ cells are capable of inducing long-term haematopoietic reconstitution in lethally irradiated mice compared to their $CD150^{-}$ counterparts (Kiel et al. 2005). In some cases, the combination of CD34 and flk2 has been used to define similar functional subsets (Adolfsson et al. 2001; Christensen and Weissman 2001).

Within the more mature, $lineage^{neg}$, Kit^{+}, $Sca\text{-}1^{-}$ (LK) cell population, additional cell surface markers such as Endoglin (CD105) and the megakaryocytic marker, CD41, together with CD150 have been used to define more mature, terminally differentiated and lineage-restricted subsets (Pronk et al. 2007). These include granulocyte-macrophage/monocyte progenitors (GMPs), which generate monocytes and granulocytes and pre-megakaryocyte erythroid progenitors (Meg-E) that give rise to megakaryocytes and erythroid precursors (including burst-forming units erythroid (BFU-E) and colony-forming units erythroid (CFU-E)). The gating strategy used to define these populations has been outlined in detail by Pronk et al and is relevant to components of this current study (Pronk et al. 2008; Pronk and Bryder 2011).

A summary of the haematopoietic hierarchy together with details of cell-surface markers that have been defined for individual populations is presented in ***Figure 1.1.***

1.2. Myelodysplastic syndrome

1.2.1. Definition and features

Myelodysplastic syndrome (MDS) is a clonal haematopoietic stem cell disorder characterized by abnormal haematopoiesis (Nimer 2008; Pang et al. 2013). With an incidence that rises significantly with increasing age (Ma 2012; McQuilten et al. 2014), it is typified by clinical heterogeneity – a reflection of its underlying genetic variability (Starczynowski et al. 2010; Bejar et al. 2011a; Yoshida et al. 2011; Papaemmanuil et al. 2013; Haferlach et al. 2014). In spite of this, a number of key features are seen across the spectrum of the disease.

These include:

1. The presence of peripheral blood cytopenias of variable severity including anaemia, neutropenia and/or thrombocytopenia. These features occur in spite of an often normocellular or hypercellular bone marrow giving rise to a phenomenon known as *'ineffective haematopoiesis';*
2. Abnormal morphology or *dysplasia* – involving bone marrow precursors and carried through to terminally differentiated peripheral blood cells;
3. An increased propensity for transformation to acute myeloid leukaemia – often associated with clonal evolution (Greenberg et al. 2012)

Historically, Leube coined the term 'leukanaemia' as early as 1900 - describing what was thought to be the co-existence of leukaemia with an associated pernicious anaemia. The disorders noted were variably grouped with other 'atypical leukaemias' or 'idiopathic anaemia' in the following years (Blair et al. 1966). The term 'pre-leukaemia' was subsequently favoured for a period of time up until the 1970's - when it became increasingly evident that some patients died of their disease before they ever developed leukaemia. In 1976, the French-American-British (FAB) co-operative group begun the first steps of

differentiating and reclassifying these disorders under the heading 'dysmyelopoietic syndromes', excluding them from other 'acute leukaemias' (Streuli et al. 1980; Albain et al. 1983; Coiffier et al. 1983). This reclassification was further revised in 1982. From this time onwards this group of disorders was entitled the 'myelodysplastic syndromes' (Bennett et al. 1982).

1.2.2. Apoptosis and its contribution to ineffective haematopoiesis

Increased apoptosis is a predominant characteristic of low-grade MDS (Raza et al. 1995; Parker and Mufti 2000; Wu et al. 2012). It is believed to be the main, but not the only contributing factor to 'ineffective haematopoiesis' where a disparity is noted between a hypercellular marrow and peripheral blood cytopenias (Pang et al. 2013). What remains somewhat unclear is whether the concurrent hyperproliferation drives apoptosis as a physiological mechanism of controlling cell numbers; or whether proliferation of cells is compensatory in nature (Raza et al. 1997). Apoptosis in MDS will be discussed in greater detail in later sections of this Chapter.

1.2.3. Dysplasia – a hallmark of the disease

In MDS, the presence of dysplastic changes is thought to reflect aberrant and ineffective blood cell differentiation – although the genetic basis of these changes has not been fully elucidated as yet. The abnormalities themselves may manifest in one or more cell lineages, this being the basis of the previous FAB classification (Bennett et al. 1982) and the current classification by the World Health Organization (2008). Erythroid cells may exhibit nuclear or cytoplasmic asynchrony, megaloblastoid changes, multinucleate figures and nuclear budding or blebbing. Neutrophils are often hypogranular and are notable for abnormal nuclear morphology. Platelets may be large and their megakaryocyte precursors may be hypolobular or may exhibit nuclear separation (Bennett et al. 1982)

1.2.4. The haematopoietic stem cell origin of MDS

That MDS originates from a haematopoietic stem cell has been assumed for some time and corroborated more recently. Earlier studies within the '5q-' syndrome confirmed this hypothesis, demonstrating that a significant number of pro-B cells

contain the same '5q-' marker seen in other $CD34^{+}CD38^{-}$ HSCs, thus supporting the theory that 5q deletions occur in HSCs with combined lympho-myeloid potential (Nilsson et al. 2000; Nilsson et al. 2002).

Transplantation of human MDS bone marrow into NOD-SCID β2 microglobulin deficient mice revealed that clonal engraftment was possible albeit at extremely low levels (Thanopoulou et al. 2004). Of note, in one case, both human lymphoid and myeloid cells were found with the original cytogenetic abnormality (trisomy 8). Again, this indicates the origin of the MDS clone was most likely a self-renewing stem cell, capable of both myeloid and lymphoid differentiation.

In similar fashion, more recently, Pang et al. demonstrated an ability to transplant and engraft clonal MDS disease into immunodeficient mice using purified human HSCs ($Lin^{-}CD34^{+}CD38^{-}CD90^{+}CD45RA^{-}$) (Pang et al. 2013). The mice were again shown to harbour the same cytogenetic abnormality as the human MDS clone in a proportion of cases and confirm that HSCs are the disease-initiating cells in MDS.

Additional examination of normal- and MDS-associated HSCs has shown that both groups of HSCs align at a phenotypic, molecular and functional level with a reasonably high correlation rate (Woll et al. 2014). Significantly, the ability to generate other myeloid progenitors in vitro was shown to be restricted to these same stem cells. In vivo, mice were only reconstituted when stem cells were transplanted, but not when purified CMPs, GMPs, MEPs or CD34- cells were used.

1.2.5. The clonal nature of MDS

That MDS is a clonal disease is suggested perhaps by the presence and at times, excess number of immature progenitors (blasts) with abnormal cell surface marker characteristics and abnormal cytogenetic profiles. However, abnormal cytogenetics are only present in around 50% of cases (Haase et al. 2007; Schanz et al. 2012) and morphology is a crude measure for demonstrating clonality. Recent whole genome sequencing has in fact shown that up to 85-90% of bone marrow cells are clonal in MDS patients even before AML transformation and

even with blast counts < 5% (Walter et al. 2012). Analysis of secondary AML samples derived from prior MDS has suggested a hierarchy of mutations or form of 'clonal architecture' ultimately leading to disease evolution. However, despite this work, heterogeneity still significantly underlies this disease and it remains unclear whether a single gene is exclusively mutated in the founding clone (Walter et al. 2013). Work by Walter et al. also highlights the genetic variability that differentiates de novo MDS from de novo AML – highlighting these diseases as two distinct entities. These has been demonstrated by other groups as well (Albitar et al. 2002).

1.3. Epidemiology of MDS in Australia

In this section, I discuss the increasing incidence of MDS and possible contributing factors to its under-diagnosis. This section highlights the need for a better understanding of the underlying pathogenesis of MDS with the hope that this will ultimately translate into improved therapeutics.

MDS is predominantly considered a disease of the elderly with a slight male preponderence (Haase et al. 2007). In a recent Australian-based epidemiological study, the mean age at diagnosis was approximately 79 years of age (McQuilten et al. 2013). The median survival of 0.5-6 years is a reflection of the clinical heterogeneity of the disease.

In 2012, data from the Australian Institute of Health and Welfare revealed MDS to be the second most common haematological cause for cancer-based hospitalizations in Australia (AIHW 2012). Recent data from a local hospital retrospective analysis reveals that of patients with a haematological diagnosis, MDS was the most common indication (53% of cases) for receipt of a cumulative quantity of $\geq$ 10 units of RBC over a 5 year period (Poster 149) (HSANZ 2014).

MDS as a disease entity, has only been reportable to the Victorian Cancer Registry in Australia since 2001. In spite of this, the true age-standardized incidence (ASI) from cancer registry data appears to be underestimated. More recent linkage analysis that compared Victorian Cancer Registry data with that

from the Victorian Admitted Episodes Dataset (VAED) revealed a significant number of patient encounters that were not captured by registry data alone (McQuilten et al. 2013). In line with this, the ASI rose from 44 / 100,000 people to 68 / 100,000 people. Using a multivariate model, data was further extrapolated to determine a more accurate incidence figure based on cases that were missed by both data sources. From this analysis, the incidence has been reported to sit closer to 96 / 100,000 (McQuilten et al. 2014).

The above discrepancy between the captured data ASI and the extrapolated ASI is most likely explained by under-reporting and under-diagnosis of MDS. Two main factors are likely contributors to this:

1. The lack of a 'formal' diagnosis of MDS – As a significant number of patients are elderly, they may be 'presumed' to have MDS based on peripheral blood macrocytosis and cytopenias without ever undergoing an 'invasive' bone marrow biopsy. One study reveals that almost 18% of patients > 65 years old with unexplained anaemia have features most in keeping with a diagnosis of underlying MDS (Guralnik et al. 2004) .
2. Patients presenting with acute myeloid leukaemia – in which a pre-existing myelodysplastic syndrome is never diagnosed or recorded in registry data.

In considering aetiology, the majority of adult MDS cases tend to be idiopathic in nature. However, a proportion of patients present with therapy-related MDS having been previously treated with chemotherapy or radiotherapy (Morrison et al. 2002). Cases have also been associated with exposure to benzene and other agricultural compounds (Rigolin et al. 1998; Nisse et al. 2001). Of the various chemotherapeutic agents used, alkylating drugs and topoisomerase inhibitors in particular, have been associated with an increasing incidence of disease. In children, MDS is exceedingly rare; although there is a higher incidence seen in those with hereditary diseases in which DNA repair genes are mutated. These include diseases such as ataxia telangiectasia, Fanconi anaemia (Kutler et al. 2003) and Li-Fraumeni syndrome (Talwalkar et al. 2010).

As our population continues to age and with patients surviving other malignancies due to better treatments, the incidence of MDS is predicted to follow an ongoing upward trajectory (Ng and Travis 2008). Coupled with the need for significant resource allocation through hospitalizations, blood product use and treatment-associated complications, this disease will likely present an ever-increasing burden to our Australian society (and universally) in years to come.

In this context, a better understanding of the underlying pathophysiology of MDS and better disease models replicating the disease are required if we hope to ultimately alter the natural course of the disease and prevent leukaemic transformation.

1.4. Pathophysiology of MDS

The heterogeneity of MDS at presentation (variable cytopenias, blast count, likelihood of progression to AML) is a reflection of its underlying genetic landscape (Papaemmanuil et al. 2013; Haferlach et al. 2014) and complex pathogenesis. This is extensively reviewed by Raza et al (Raza and Galili 2012). A myriad of factors are thought to contribute to the biology of the disorder although whether these define discrete entities or how they actually fit together remains unclear. Contributing pathologies include but are not limited to:

- dysfunctional ribosomal protein biogenesis with associated p53 activation - particularly prominent in the 5q- syndrome (Ebert et al. 2008; Dutt et al. 2011),
- epigenetic modifications including histone deacetylation, histone methylation and DNA promoter hypermethylation (del Rey et al. 2013),
- abnormal RNA splicing (Yoshida et al. 2011; Graubert et al. 2012),
- changes in microRNAs (Starczynowski et al. 2010),
- abnormalities of the bone marrow microenvironment (Geyh et al. 2013),
- and abnormal DNA repair mechanisms (Zhou et al. 2013)

In line with these pathological processes, a number of associated genetic mutations have been described (Bejar et al. 2011b; Wang et al. 2014a; Haferlach et al. 2014). These mutations affect genes which regulate RNA splicing (eg SF3B1, SRSF2, U2AF1, ZRSR2) (Yoshida et al. 2011; Papaemmanuil et al. 2011), DNA methylation (eg TET2, DNMT3A, IDH1/2) , chromatin modification (ASXL1, EZH2, ATRX) (Boultwood et al. 2010), transcription regulation (RUNX1, TP53, ETV6, NPM1, CEBPA, GATA2) (Adamson et al. 1995; Harada et al. 2004; Wen et al. 2015), DNA repair (ATM, BRCC3, FANCL), signal transduction (CBL, NRAS, KRAS) (Reindl et al. 2009) and the cohesin complex (STAG2, RAD21, SMC3) (Thota et al. 2014). Different mutations have been found to associate with specific MDS subgroups. Some have positive correlations with each other, whilst others appear to be mutually exclusive (Haferlach et al. 2014).

These genetic mutations build on a previously well defined group of cytogenetic mutations (Haase et al. 2007) which have been associated with distinct gene expression profiles (Pellagatti et al. 2010).

Ongoing work is now underway to understand: 1) how these processes come together and contribute to the pathogenesis of MDS; 2) to what degree they are mutually exclusive; 3) how they might portend prognosis and 4) which of these processes can be therapeutically targeted.

1.5. Diagnosis, classification and prognosis of MDS

Diagnosis and classification

Diagnosing MDS is fraught with some difficulty for a number of reasons. Unlike chronic myeloid leukaemia in which the diagnostic 'BCR-ABL' mutation can be detected in the peripheral blood, there is no single diagnostic "marker" for MDS. Furthermore, in elderly patients, where a bone marrow biopsy is not always appropriate due to its invasive nature, the diagnosis is often 'assumed' based on a peripheral blood macrocytosis and the presence of cytopenias. As other diagnoses such as vitamin B12 deficiency, folate deficiency, drug therapies including methotrexate or erythropoietin and thyroid and liver dysfunction can 'masquerade' as MDS, these need to be excluded before a definitive diagnosis can

be made (Kaferle and Strzoda 2009; Steensma 2012; Veda 2013; Shah et al. 2014). The morphological presence of 'dysplasia' which forms a vital part of the diagnostic algorithm, may also be subject to significant inter-observer variability with studies reporting discordance rates ranging from 12% - 27% (Naqvi et al. 2011b; Font et al. 2013). These findings highlight the need somewhat for a more standardized and objective means of MDS diagnosis.

When MDS is suspected, a bone marrow aspirate and trephine are usually required to make a 'definitive diagnosis'. This allows the presence and degree of dysplasia in all three cell lineages (erythroid, myeloid and megakaryocytic) to be assessed together with enumeration of immature precursors or blasts (Garcia-Manero 2014).

A bone marrow biopsy also provides an opportunity to undertake cytogenetic analysis – which may be of additional diagnostic benefit. In MDS, up to 50% of de novo cases may exhibit cytogenetic abnormalities (up to 80% with secondary MDS) – the majority being deletions or chromosomal duplications. Common abnormalities include del(5q), monosomy 5 or 7, trisomy 8, del(20q), 17p abnormalities and loss of Y (Haase et al. 2007; Schanz et al. 2012). Unlike AML and other leukaemias, the presence of a balanced cytogenetic abnormality such as a reciprocal translocation, inversion or insertion is less common. Importantly, although cytogenetic abnormalities may assist in making a diagnosis; in isolation, not all cytogenetic abnormalities have been deemed 'diagnostic' (WHO Classification of Tumours of Haematopoietic and Lymphoid Tissue 2008) – again highlighting a potential deficiency in the current diagnostic algorithm.

In an attempt to standardize nomenclature, the WHO has used parameters such as number of cytopenias, number of cell lines affected by dysplasia and percentage of bone marrow blasts together with cytogenetic analysis to devise a diagnostic classification system (WHO Classification of Tumours of Haematopoietic and Lymphoid Tissue 2008). Last updated in 2008, the current criteria do not take into consideration recently described molecular abnormalities. As the implications of recently discovered genetic mutations

becomes apparent, it is likely that these findings will significantly reconstruct our diagnostic approach in years to come (Bejar et al. 2011b) .

At present, broadly speaking, the system classifies MDS into low-risk / early-stage MDS (including refractory anaemia (RA) and refractory cytopenia with unlineage or multi-lineage dysplasia (RCUD or RCMD respectively)) and high-risk / late-stage MDS (including refractory anaemia with excess blasts (RAEB)) in which there is an increased risk of leukaemic progression and worse overall survival (Schanz et al. 2012). As more recently described molecular abnormalities refine our stratification particularly of early-stage disease (Bejar et al. 2012), the basis of this distinction remains an important one particularly when predicting a patient's prognosis and deciding on appropriate treatment.

The use of flow cytometry in the diagnosis of MDS has been well documented in recent years (van de Loosdrecht et al. 2009; van de Loosdrecht and Westers 2011), but unlike AML its uptake into mainstream diagnostics remains incomplete at present due to the heterogeneity of the disease and variability between patients. As such, a better knowledge of what comprises normal variation is required to detect aberrant phenotypes. Guidelines for the integration of flow cytometry results into the WHO classification of MDS have been provided by Porwit et al (Porwit et al. 2014). It is likely that flow cytometry will provide more sensitive diagnostic capabilities over and above that of morphological analysis in years to come.

Prognosis

Prognostic scoring systems are used in MDS with the goal of predicting the likelihood of leukaemic transformation and guiding therapeutic intervention. The 'International Prognostic Scoring System' (IPSS) devised by Greenberg et al in 1997 is the most well known scoring system. Dividing patients into four subgroups portending prognosis, it draws on a number of criteria determined prior to treatment. These include percentage of bone marrow blasts, presence of cytopenias and cytogenetic abnormalities (Greenberg et al. 1997). This system has drawn a number of criticisms, as it does not take into consideration the

severity of the cytopenias or transfusion dependence. Additionally, it attributes little weight to cytogenetics and appears to be a poor predictor of prognosis in those with lower-risk disease whose outcomes seem to vary significantly even within the same prognostic category (Bejar et al. 2012).

As a result, further refinements have been made in recent years, to build upon the strength of the IPSS and to increase its prognostic value and significance. These have included:

a) The WHO Classification-Based Prognostic Scoring System (WPSS) – which considers transfusion dependency in its algorithm (Malcovati et al. 2007). This system has been validated for use at any time during disease progression, not just at diagnosis (Malcovati et al. 2011).
b) The Revised-IPSS (R-IPSS) - which now uses a more refined blast count and comprehensive cytogenetic scoring system to divide patients into 5 sub-categories – improving prognostication for those in the lower-risk IPSS category (Schanz et al. 2012; Greenberg et al. 2012).
c) Adult Comorbidity Evaluation 27 (ACE27) – which takes concomitant comorbidities into account (Naqvi et al. 2011a)
d) The MD Anderson Cancer Centre Classification (MDACC) - (Kantarjian et al. 2008)

For those patients who present with normal cytogenetic analysis, two developments over recent years have provided a further means of prognostication. The first is that of array analysis used to detect small copy number alterations (Gondek et al. 2007b; Mohamedali et al. 2007). This abnormality has been associated with a poorer prognosis particularly in those with otherwise normal cytogenetics (Gondek et al. 2007a).

The genomic era has additionally heralded an explosive discovery of new genetic mutations that underlie MDS. Bejar et al. initially demonstrated that of 111 cancer-related genes, 5 particular genes predict poor survival (Bejar et al. 2011b). Furthermore, mutation status may have prognostic and treatment implications. For instance, it may serve to upgrade a patient's IPSS-R score (Bejar

et al. 2012) or may additionally predict sensitivity or resistance to various treatments (Bejar et al. 2014). Recent work has shown that apart from SF3B1, DNMT3A, JAK2 and MPL mutations, the majority of common mutations occur more frequently in high-risk MDS and that the total number of mutations in one patient tends to increase with high-risk disease (Haferlach et al. 2014). Importantly, mutations have now been discovered in up to 68% of patients with MDS who have previously had normal cytogenetics. Using targeted deep sequencing and array-based genomic hybridization, a significant 89.5% of MDS patients harbour at least one genetic mutation when analyzed (Haferlach et al. 2014). These findings suggest that we are likely to see a shift in years to come from a diagnosis made based on morphological and cytogenetic abnormalities alone to that based on more robust and reproducible molecular analyses.

1.6. Disease progression in MDS

In up to 1/3 of patients, MDS eventually progresses to overt acute myeloid leukaemia (Greenberg et al. 1997). This may be due to the acquisition of additional driver mutations involved in epigenetic regulation or mutations which alter the balance between proliferation and apoptosis (Walter et al. 2012). As with other malignancies, progression in MDS is thought to reflect reduction or resistance to apoptosis and enhanced proliferation (Parker et al. 2000; Hanahan and Weinberg 2011). In keeping with this, immature progenitors in higher grade MDS have been shown to express higher levels of the anti-apoptotic proteins, BCL-2 (Kurotaki et al. 2000) and BCL-xL (Boudard et al. 2002) as well as CD47 – an anti-phagocytic signal (Pang et al. 2013). Conversely, a pro-apoptotic phenotype appears to correlate with early-stage disease. In this context, reduced BCL-2 levels have been associated with low-risk disease (Rajapaksa et al. 1996), as have higher levels of the pro-apoptotic proteins, BAD and BAK – all of which may sensitize or drive cells towards apoptosis (Boudard et al. 2002). Higher BCL-2, Bcl-xL and MCL-1 levels have also been associated with a higher risk of leukaemic transformation (Boudard et al. 2002). These findings suggest a pivotal role for apoptosis in leukaemic progression. A number of additional genes have more recently been shown to associate with apoptosis resistance and disease

progression and may serve as surrogate markers for this (Xu et al. 2012a; Wu et al. 2012).

In spite of these findings, much of what we know about apoptosis and its link to transformation in MDS is largely observational and has been extrapolated from lymphoid models of disease. The functional role of apoptosis in MDS has not been properly evaluated, thus forming the basis of this current work. Specifically, how does apoptosis account for the MDS phenotype, what role does it play in disease progression and how does modulating apoptosis ultimately impact on leukaemic transformation?

1.7. Treatment strategies for MDS

The distinct prognoses associated with early-stage and late-stage disease has driven strikingly different management strategies in patients with MDS. As early-stage disease is characterized by cytopenias and a lower risk of leukaemic progression, the goal of treatment has been the management of specific cytopenias and their associated complications. In many cases, this is provided through supportive care – in the form of transfusional support for anaemia and thrombocytopenia, antibiotics and antifungals for infection and management of bleeding complications. Although supportive care measures have generally improved over the years, these continue to impose a significant financial burden on the health care system and on patient independence (Frytak et al. 2009). In an attempt to overcome the apoptosis associated with MDS, haematopoietic growth factors have been used in various ways. These commonly include G-CSF (Tehranchi et al. 2003; Tehranchi et al. 2005), erythropoiesis-stimulating agents (ESAs) such as erythropoietin and darbopoietin and thrombopoietin (TPO) mimetics which stimulate platelet production. These have been met with variable success and in some cases, concern regarding potential complications – eg fibrosis associated with romiplostim and the risk of accelerating disease progression (Gonzalez and Freeman 2012; Kirito and Komatsu 2013). Although these agents may ameliorate cytopenias somewhat, it is unclear to what degree they alter the natural progression of the disease, if at all. Additionally, not all of these agents are licenced for use in MDS in Australia.

Lenalidomide, a thalidomide analog, has also proven to be of benefit particularly in the '5q-' subgroup of patients with MDS who are transfusion-dependent and non-responsive to ESAs (List et al. 2005; List et al. 2006); or additionally those who do not have the '5q-' abnormality, albeit not as effectively (Raza et al. 2008). Although it has pleiotropic properties that range from cytokine modulation including suppression of TNF-α, angiogenesis inhibition, effects on inflammation, cellular adhesion and T-cell co-stimulation, lenalidomide's exact mechanism of action in MDS remains somewhat obscure. Apart from the presence of the '5q-' abnormality, it is also difficult to predict which patients are more likely to respond to therapy.

For high-grade disease, in which the threat of transformation is often imminent, therapy has attempted to prevent disease progression. Treatment developments in this area have previously remained barren for a long time, apart from the use of conventional chemotherapy, which is not appropriate in all patients due to age constraints. In the last 5 years, the use of hypomethylating agents such as azacitidine and decitabine has been warmly welcomed with evidence that these drugs may control disease progression and improve overall survival for a period of time (Silverman et al. 2002; Kantarjian et al. 2007; Fenaux et al. 2009; Seymour et al. 2010; Lübbert et al. 2011). However, as for lenalidomide, the exact mechanism of action of azacitidine is poorly understood. Furthermore, we do not have a current means of predicting which subset of patients will exhibit sensitivity to azacitidine and which will demonstrate resistance.

A number of additional treatment combinations have been trialled in this area including the HDAC inhibitors, thalidomide and the multi-kinase inhibitor, rigosertib (Silverman et al. 2014) with variable success. However, a clear rationale for their use, based on the underlying genetic pathogenesis of MDS, has not always been apparent.

As the complex pathogenesis of MDS is unravelled, this will no doubt drive the development of more targeted therapies and approaches; however we are still a

way off 'individualizing' therapy and predicting responses to current drugs. In those who are eligible, stem cell transplantation remains the only curative option. The use of reduced-intensity conditioning regimens may enable this modality of treatment to be offered to a greater number of patients who may have otherwise been ineligible. However, this approach is not without its own risks – particularly in the older patient with associated comorbidities.

1.8. Apoptosis

1.8.1. Defining apoptosis and its role in cellular homeostasis

'Programmed cell death' or 'apoptosis' is an active and 'inherently controlled' means by which an organism eliminates redundant or damaged cells. Morphological features of this form of cell death were first described by Kerr et al in 1972 and include nuclear condensation, cell shrinkage and plasma membrane blebbing (Kerr et al. 1972). Concurrent work in *C. elegans* at this time was initiated to map the fate of a specific set of 131 cells that invariantly underwent involution on each occasion. From this work, genes homologous to the currently recognized apoptotic machinery in mammals were identified indicating significant evolutionary conservation over the years (Hengartner and Horvitz 1994).

Unlike the "disordered" process of necrosis, the destruction of a cell during apoptosis is reported to occur in an orderly and controlled fashion exhibiting multiple layers of regulation. This is highlighted by abnormalities that occur when this process becomes deregulated through insufficient or excessive and accelerated apoptosis and is manifested by developmental anomalies (Lindsten et al. 2000), autoimmune dysregulation (Bouillet et al. 1999), neurodegeneration (Jeffers et al. 2003), immunodeficiency or malignancy (Michalak et al. 2009).

Depending on the cell of origin and stage of development, apoptosis can play a number of different roles – ranging from cellular homeostasis in embryogenesis and neuronal development to the elimination of cells that acquire and accumulate oncogenic mutations with age (Strasser et al. 2011). Once the dead

cell undergoes nuclear fragmentation, it is removed by the reticulo-endothelial system through phagocytic cell engulfment and lysosomal digestion.

Two main apoptotic pathways are named according to the origin of the signals that drive the apoptotic process itself. These are summarized in ***Figure 1.2***. The 'extrinsic pathway' relies upon the activation of cell surface receptors such as Fas and the tumour necrosis factor (TNF) receptor by Fas ligand (FasL) and TNF-α respectively. In contrast, the 'intrinsic pathway' relies upon a cascade of proteins 'intrinsic' to the cell to drive the apoptotic pathway - ultimately converging on the mitochondrial apparatus. These pathways will be discussed in more detail in subsequent sections.

The aforementioned pathways invariably converge and rely upon the activity of a number of downstream effector enzymes to execute the apoptotic process itself. These intracellular endonucleases or cysteine-dependent aspartate-specific proteases (i.e caspases) act to cleave substrates at specific amino acid sites (Thornberry and Lazebnik 1998; Shi 2002) and typically exist as inactive zymogens. Based on their order of activation in the cell death cascade, caspases are divided into upstream initiators, capable of autocatalytic activation or downstream effectors (Adams and Cory 2007). Substrate specificity is usually dictated by a four amino-acid motif within each caspase protein. As such, caspase 8 is often associated with activation of the extrinsic pathway and caspase 9 with the intrinsic. Downstream, these pathways converge on activation of caspases 3 and 7 and this usually signals an irreversible commitment to apoptosis.

1.8.2. Pathways of apoptosis

1.8.2.1. Intrinsic Pathway

Cellular stressors resulting in DNA damage may act to trigger the intrinsic or mitochondrial apoptotic pathway. Triggers that are relevant to MDS will be discussed in more detail in subsequent sections. The ensuing death signal, mediated by a number of proteins 'intrinsic' to the cell (the BCL-2 family of proteins) ultimately targets the permeability of the outer mitochondrial membrane.

Based on their function and structural homology, the BCL-2 family of proteins is subdivided into three distinct groups ***(Figure 1.2)***:

1. **The pro-apoptotic BH3 (Bcl-2 homology 3)-only proteins** – these include PUMA (p53 upregulated modulator of apoptosis), NOXA, BIM (BCL-2 interacting mediator of cell death), BID (BCL-2 interacting domain death agonist), BIK (BCL-2 interacting killer) and BMF (BCL-2 modifying factor);
2. **The anti-apoptotic BCL-2-like proteins** – including BCL-2 itself, BCL-w, BCL-xL, MCL-1 and A1; and
3. **The pro-apoptotic effectors**: BCL-2 antagonist killer 1 (BAK) and BCL-2 Associated X protein (BAX).

These lists are by no means exhaustive and additional members of all three groups have been described.

Homology is shared through a number of conserved regions termed BCL-2 homology domains (BH). These are typically labelled as BH1-4. As their name suggests, the BH3-only proteins only share homology for the BH3 domain. In contrast, the anti-apoptotic BCL-2-like proteins are made up of all four BH domains; whilst BAX and BAK share BH1-3 only (Suzuki et al. 2000; Moldoveanu et al. 2006). The typical interaction between proteins is thought to involve the insertion of the hydrophobic face of the amphipathic alpha helix (formed by ~ 16 residues from the BH3 domain) into a hydrophobic groove formed by the BH1, BH2 and BH3 domains of the prosurvival proteins or the effectors BAK/BAX (Sattler et al. 1997; Liu et al. 2003; Denisov et al. 2006). The importance of the BH3-domain in inducing apoptosis is highlighted by cases in which the domain is mutated (Nakano and Vousden 2001). Variation in the depth of the associated binding pockets and certain structural variations account for the complexity of interactions between pro- and anti-apoptotic members and ensure that not all proteins remain in an 'open' configuration at all times (Chen et al. 2005; Moldoveanu et al. 2006).

From a functional perspective, the means by which members of the intrinsic pathway interact to drive apoptosis is one that has been debated significantly over the years. The previously upheld 'rheostat' model argues that apoptosis is a result of the balance between anti-apoptotic and pro-apoptotic proteins (Rajapaksa et al. 1996). However, this explanation is considered to be oversimplified somewhat. Two other models have been proposed and are discussed below. These are relevant to some of the work presented in this study in subsequent Chapters.

1. **Anti-apoptotic protein neutralization model (indirect activation) –**

In this model, BAX and BAK are believed to be inherently active and are inhibited by the anti-apoptotic proteins (including BCL-2, BCL-xL, BCL-w, MCL-1 and A1). Mitochondrial permeability is only altered when all anti-apoptotic proteins are functionally neutralized. By binding various anti-apoptotic Bcl-2 like proteins, the BH3-only proteins indirectly activate BAX and BAK (Oda et al. 2000; Nakano and Vousden 2001; Willis et al. 2007). To further complicate this model, not all BH3-only proteins have equal affinity or binding capacity to the various Bcl-2 like proteins (Chen et al. 2005).

2. **Direct activation of BAX and BAK model**

Although the existence of this model has been questioned by some (Willis et al. 2007), proponents of this mode of activation postulate that a subset of BH3-only proteins can directly induce conformational changes in BAX and BAK – without inhibiting the intermediate group of BCL-2-related proteins as discussed above. This subset of proteins is referred to as direct 'activators' and includes BIM, tBID (Wei et al. 2000; Letai et al. 2002; Walensky et al. 2006) and possibly PUMA (Cartron et al. 2004; Gallenne et al. 2009; Garrison et al. 2012). However, not all BH3-only proteins are capable of binding BAX and BAK directly. The remaining BH3-only proteins typically act as 'sensitizers' – displacing BIM, tBID and PUMA from their usual binding to BCL-2 related proteins allowing them to directly bind BAK or BAX. Some argue that as the direct binding affinity in these cases is fairly weak (Moldoveanu et al. 2006) and is only demonstrable in the setting of non-

ionic detergents (Willis et al. 2007), this means of activation is unlikely to be as important as the indirect means discussed above.

In spite of these distinctions, it is important to note that these 'activation models' may not necessarily be mutually exclusive. Regardless of the mode of activation, both models agree that there is convergence on BAX and BAK as the main effector proteins driving 'intrinsic' apoptosis and mediating mitochondrial outer membrane permeability (MOMP).

1.8.2.1.1. BH3-only proteins

These proteins will be discussed in more detail in Chapter 4.

1.8.2.1.2. Anti-apoptotic BCL-2-related proteins

The anti-apoptotic BCL-2 protein and its related partners (BCL-w, BCL-xL, MCL-1, A1) all function downstream of the BH3-only proteins (discussed in Chapter 4) and exhibit different binding specificities to upstream BH3-only proteins (Chen et al. 2005).

Mouse models exploring deficiencies of various BCL-2 related proteins exhibit a common theme of increased apoptosis; although the specific cell type in which this occurs is variable. As an example, BCL-2 deficient mice develop profound lymphopenia and renal defects resulting in polycystic kidney disease (Lindsten et al. 2000); lack of Bcl-xL is associated with massive apoptosis in the nervous system and early embryonic death; lack of A1 is associated with accelerated neutrophil apoptosis and lack of MCL-1 is embryonically lethal due to its requirement for survival and implantation of the zygote. In the haematopoietic system, Mcl-1 is also required for survival of haematopoietic progenitors (Adams and Cory 2007).

1.8.2.1.3. Intrinsic apoptosis effectors: BAX and BAK

The two effector proteins of the intrinsic pathway, BAK and BAX, drive apoptosis through their effect on the permeability of the outer mitochondrial membrane. As with the pro-survival proteins, much of the action of BAK and BAX appears to

be mediated through their BH3-specific hydrophobic groove (Suzuki et al. 2000); although some groups have proposed alternate binding sites particularly for BAX (Gavathiotis et al. 2008).

In either case, BAX and BAK subsequently undergo a conformational change, dimerize and form homo-oligomers. Although the exact mechanism by which the outer membrane is porated remains a contentious one (Danial and Korsmeyer 2004; Basañez et al. 2012; Kushnareva et al. 2012), the ultimate result is the release of cytochrome c and other death-promoting mediators into the surrounding cytoplasm. A multimeric complex, the 'apoptosome' is formed (Acehan et al. 2002) bringing together Apaf-1 (apoptotic protease-activating factor 1) and cytochrome c. In the presence of ATP/dATP, the apoptosome acts to recruit and activate caspase-9 with subsequent activation of caspases 3 and 7 as previously discussed.

One significant difference between these two proteins is their cellular localization and their respective binding partners. Unlike BAK which forms an integral part of the mitochondrial membrane, BAX is largely cytosolic – often translocating to the mitochondrial membrane in response to cytotoxic signals (Wolter et al. 1997). BAK appears to be sequestered by MCL-1 and BCL-xL alone, but not by BCL-2, BCL-w or A1 (Sattler et al. 1997; Willis et al. 2005). This means that for apoptosis to proceed through BAK, both MCL-1 and BCL-xL must be neutralized.

Unlike the pro-survival proteins, deficiency of either BAX or BAK results in either no significant phenotype or only a very mild one at worst. Mice lacking BAK alone are developmentally and reproductively normal; whilst those lacking BAX exhibit mild lymphoid hyperplasia and male sterility with no developmental defects (Knudson et al. 1995; Lindsten et al. 2000). Of significance, mice lacking both genes do not undergo apoptosis in many cells types. Significant developmental defects may also occur during embryogenesis with many tissues failing to undergo attrition in both the central nervous and haematopoietic systems. Interestingly, a single wild-type copy of either gene eliminates many of

the noted abnormalities and indicates some degree of redundancy. Of note however, the function of these effector proteins is not redundant in all tissues and exceptions have been reported (Hikita et al. 2012). Despite the increase in resistance to apoptosis, mice lacking BAX and BAK do not show evidence of increased spontaneous tumour formation.

1.8.2.2. Extrinsic Pathway

As its name suggests, the extrinsic pathway is triggered by stimuli extrinsic to the cell through ligation of the so-called 'death receptors'. Common triggers of this pathway include Fas ligand (FasL), TNF and TRAIL which bind through their respective receptors (Laster et al. 1988; Suda et al. 1993; Wiley et al. 1995; Zamai et al. 2000). In each case, these receptors contain respective intracellular domains that are thought to contribute to the formation of a death-inducing signaling complex (DISC) (Scott et al. 2009). This complex is comprised of a number of proteins including Fas itself, FasL, Fas-associated protein with death domain (FADD), TNFR-associated protein with death domain (TRADD) and pro-caspase 8 (Raza and Galili 2012). Once formed, this complex proceeds to activate caspase 8 and additional caspases further downstream. By and large, this pathway functions independent of the mitochondrial pathway, except in cases where BID is cleaved and activated (Wei et al. 2000). Particularly prominent in hepatocytes, this cleavage generates a pro-death C-terminal fragment, truncated Bid (t-Bid), which allows for crossover between the two pathways.

1.8.3. Measurement of apoptosis

In the early phases of apoptosis, DNA is first cleaved into nucleosomal fragments. Subsequently and over time, nuclear fragmentation or karyorrhexis occurs and this ultimately culminates in removal of the apoptotic cell by the reticuloendothelial system (Kerr et al. 1972). Although karyorrhexis can be morphologically identified, morphology in its own right remains a fairly insensitive and late means of identifying the 'apoptotic cell' (Raza et al. 1995; Bogdanović et al. 1996). As a result, more sensitive techniques have been developed over time to enable more accurate detection and quantification of the apoptotic process, particularly in its earlier phases.

Previously used techniques for measuring apoptosis in MDS have included DNA laddering or fragmentation assays by gel electrophoresis (Tsoplou et al. 1999), in- situ end-labeling (Wijsman et al. 1993; Kurotaki et al. 2000) and the detection of a subG1 DNA population (Rajapaksa et al. 1996; Nakano and Vousden 2001). In-situ end- labeling (ISEL) is reported to be a more reliable method of detecting early-stage apoptosis, particularly when compared and correlated with the detection of DNA laddering using gel electrophoresis (Raza et al. 1995). In other cases, the terminal deoxynucleotidetransferase-mediated dUTP nick-end labeling (TUNEL) assay has been used as an alternative measure of apoptosis (Bouscary et al. 1997; Ramos et al. 2002; Yu et al. 2010).

In an attempt to improve sensitivity, flow cytometric techniques have been developed which enable apoptosis to be detected at a much earlier time point. These techniques also allow multiple parameters to be measure concurrently and provide a fairly rapid means of analysis. The use of annexin-V as a marker of apoptosis was first described in 1995. It relies upon the binding of phophatidylserine – an anionic phospholipid on the internal surface of the cellular plasma membrane - which is externalized in cells undergoing programmed cell death (Vermes et al. 1995). As this marker alone does not distinguish between apoptosis and necrosis, it must be combined with a dye exclusion test (eg propidium iodide (PI) or 7-AAD) to establish whether the integrity of the cell membrane is preserved – thus helping to differentiate the two processes.

More recently, a number of 'Fluorescent Labeled Inhibitor of Caspase Assays' (FLICA) have come into favour. These are comprised of an affinity peptide inhibitor sequence, a fluoromethyl ketone (FMK) moiety, which allows for irreversible binding with the caspase enzyme and a fluorescent tag. The probes are usually membrane-permeant, are not retained in non-apoptotic cells and can be used to distinguish between activation of the extrinsic and/or intrinsic pathways of apoptosis (Smolewski et al. 2002; Wlodkowic et al. 2009). Throughout this study, we have used caspase-3/7 as a general marker of apoptosis.

1.9. MDS + apoptosis

That early-stage MDS is characterized by increased apoptosis has been well-demonstrated using a number of different techniques and by many different groups (Rajapaksa et al. 1996; Mundle et al. 1999a; Bouscary et al. 2000; Parker et al. 2000; Pang et al. 2013). However, the exact mechanism by which this occurs and the upstream triggers involved are openly disputed. Additionally, there has been some controversy over time as to which specific cells within the bone marrow undergo apoptosis (Amin et al. 2003; Li et al. 2004; Pang et al. 2013). The variation in cell populations analyzed and the techniques used to do so may account for some of this variability in results.

Earliest studies which suggested increased apoptosis as a feature of MDS – used in-situ end labelling of fragmented DNA and showed increased staining in more differentiated bone marrow cells from all three cell lineages as well as associated stromal cells (Raza et al. 1995). Ramos et al. reported an increase in apoptotic index based on TUNEL staining in MDS patients in general cf controls in both parenchymal and stromal cells. The specific identity of TUNEL-positive parenchymal cells was not reported in this case. Additionally, the high apoptotic indices noted in control subjects raises some suspicion about the specificity of the technique itself (Ramos et al. 2002). In other cases, apoptosis has been reported to occur in both $CD34^+$ and $CD34^-$ subsets, particularly in early stage MDS (Tsoplou et al. 1999), while other groups have reported this process to be a particular feature of $CD34^+$ cells alone (Rajapaksa et al. 1996; Pang et al. 2013). These reports highlight some of the confusion regarding the specific identity of the apoptotic cell population in MDS.

Increased apoptosis in early MDS as measured by TUNEL staining, in-situ end-labeling or annexin-V is also matched by gene expression data that reveals the 'apoptosis signalling pathway' to be the most significantly upregulated pathway in refractory anaemia but not in RAEB (Pellagatti et al. 2010).

With respect to prognosis, increased apoptosis itself has generally been correlated with better overall survival (Tsoplou et al. 1999), low blast counts (Bouscary et al. 2000; Parker et al. 2000) and reduced leukaemic transformation (Boudard et al. 2002); although not all studies have demonstrated a prognostic value (Ramos et al. 2002). These findings suggest that apoptosis may be a useful surrogate marker of early-stage disease and also support the concept that resistance to apoptosis typically associates and is a feature of disease progression (Hanahan and Weinberg 2011).

Although many studies have implicated factors extrinsic to the cell as being the main drivers of apoptosis in MDS, a number of other studies have identified cell intrinsic factors particularly in the 5q- syndrome in association with ribosomal dysfunction and through the activation of p53. Some of these studies will be discussed in more detail below.

1.9.1. Extrinsic pathway of apoptosis and MDS

For a long time, cell extrinsic signals such as TNF-α, Fas ligand (Fas-L) (and TRAIL) have been considered the main drivers of apoptosis in MDS progenitors (Bouscary et al. 1997; Gersuk et al. 1998; Claessens et al. 2002; Sawanobori et al. 2003; Campioni et al. 2005). As per differing opinions on which cell population actually undergoes apoptosis, the source of TNF- α or Fas has similarly been debated. Different cell populations have been shown to overexpress TNF-α or Fas ranging from BM macrophages, erythroid precursors (Stifter et al. 2005), CD34+ cells (Gersuk et al. 1996; Gersuk et al. 1998) or peripheral blood mononuclear cells. A dual mechanism for TNF-α's action has been proposed in which it induces apoptosis in more mature progenitors accounting for the associated cytopenias and concomitantly, induces proliferation of primitive progenitors accounting for the associated bone marrow hypercellularity (Raza et al. 1996). Those who support a role for the microenvironment, suggest that the source of TNF-α (and IFN-γ) may originate from bystanding T-cells and BM stromal cells (Shetty et al. 1996).

In similar fashion to TNF-α, Bouscary et al report upregulation of Fas on CD34+ cells, CD33+ populations and glycophorin (a marker of red cells) positive cells in those with MDS. Of note, variation is also highlighted in the techniques used to measure Fas or Fas-L and TNF (Bouscary et al. 1997).

In their study, Stifter et al demonstrate an inverse correlation between 'in situ' TNF-α expression on erythroid precursors and Hb levels supporting the idea that TNF-α may be responsible for the apoptosis of these cells. The positive correlation with marrow hypercellularity suggests this might be a compensatory response to apoptosis or a direct effect of TNF-α itself. Although TNF-α staining was increased in all MDS subtypes, it reportedly only reached statistical significance in the 'refractory anaemia' subgroup (early MDS). Of note and somewhat unexplained, the overexpression of TNF appeared to be associated with an overall worse prognosis (Stifter et al. 2005).

Another study examined 'in situ' TNF-α and found a positive correlation with caspase 3 levels and in-situ end labelling as a measure of apoptosis in the same specimens. The cell of origin expressing TNF-α was unclear in this study, although staining was reportedly more prominent in the interstitium and occasionally in the cytoplasm of immature cells. In this case, no difference was found between low-risk and high-risk MDS although numbers were low and IHC staining remains a fairly insensitive technique (Mundle et al. 1999b).

These studies in combination highlight the variability in identifying the actual source of TNF-α, although there is evidence that a correlation with erythroid cell apoptosis exists.

1.9.2. Intrinsic pathway of apoptosis and MDS

Although many of the above studies have implicated the extrinsic pathway in driving apoptosis of MDS progenitors, other studies have demonstrated that members of the intrinsic pathway may play an equally important role. This has been particularly evident and most well characterised for the del(5q) subtype of MDS in which ribosomal dysfunction underlies the activation of p53. The

resultant phenotype is one of excessive erythroid apoptosis as has been recently reported (Ebert et al. 2008; Dutt et al. 2011). This will be discussed in more detail in Chapter 3.

In other cases, observational studies have examined expression levels of the BCL-2 family of proteins. However, the functional role of these proteins has not been properly elucidated in these cases. In early-stage MDS, Rajapaksa et al identified lower BCL-2 levels in CD34+ cells from patients with low-risk disease in comparison with high-grade disease and correlated this with DNA fragmentation and an increased subG1 DNA population – in keeping with increased apoptosis (Rajapaksa et al. 1996). Parker et al calculated the ratio of pro-apoptotic proteins: anti-apoptotic proteins in CD34+ cells and noted a higher ratio in early stage disease (Parker et al. 1998; Parker et al. 2000). In similar fashion, based on examination of BMMNCs, Boudard et al report higher expression of anti-apoptotic proteins, BCL-2 and BCL-xL in high-grade MDS and higher expression of pro-apoptotic proteins, BAD and BAK in early-stage MDS (Boudard et al. 2002). Therefore, although many of these studies have variably examined mRNA or protein expression levels of BCL-2 and other intrinsic pathway relatives and implicated their role in the apoptosis of MDS, none of these studies have directly examined the effect of abrogating apoptosis per se on the MDS phenotype.

As somewhat of a contrast, others have postulated apoptosis to occur through combined interaction between the intrinsic and extrinsic pathways, which may also be plausible. Tehranchi et al proposed a model in which heightened sensitivity to death receptor ligation (extrinsic pathway) occurs due to constitutive activation of the mitochondrial axis (intrinsic pathway) (Tehranchi et al. 2003). Meanwhile, Gyan et al demonstrated activation of caspase 8 most likely results in cleavage of B-cell Receptor Associated Protein 31 (BAP31) and subsequently triggers mitochondrial cell death. In these cases, inhibition of caspase 8 resulted in inhibition of BAP31 cleavage and rescue of MDS cell apoptosis. Of significance, BCL-2 overexpression was also associated with reduced cleavage of BAP31, inhibition of mitochondrial membrane

depolarization, cytochrome c release and caspase 3 activation in MDS precursors (Gyan et al. 2008). These findings in combination implicate both the intrinsic and extrinsic pathways of apoptosis.

1.10. Triggers of apoptosis in MDS

The underlying triggers driving apoptosis in MDS are poorly understood although a number of possible mechanisms have been implicated including the generation of reactive oxygen species, ribosomal dysfunction as observed in the 5q- syndrome (discussed in Chapter 3) and defects in the supporting bone marrow microenvironment which will be discussed in later sections.

Reactive oxygen species (ROS) contribute to increased DNA damage by inducing endogenous double-strand breaks (DSBs). In some cases, MDS cells from human samples have been characterized by higher levels of ROS with a concomitant reduction in antioxidant defences (Voukelatou et al. 2009). Importantly, error-prone or defective repair of the induced breaks through non-homologous end-joining (NHEJ) may drive the generation of additional mutations. Sources of oxidative stress and ROS generation include mitochondrial dysfunction through the action of non-transferrin bound iron (NTBI) (Cortelezzi et al. 2000), generalized inflammation as will be discussed in Chapter 5 and bone marrow stromal defects. Mouse models of myeloid disease have certainly supported the hypothesis that ROS may contribute to the phenotype of increased apoptosis and disease progression (Rassool et al. 2007; Chung et al. 2014). Additionally, a reduction in antioxidant defence mechanisms with age together with increased sensitivity to oxidative stress may explain the basis that MDS is primarily a disease of the elderly.

Iron overload resulting from a high frequency of blood transfusions or as a by-product of ineffective haematopoiesis warrants specific mention as a source of oxidative stress. This has been correlated with higher expression of APAF-1 (Gu et al. 2014), a key component of the apoptosome and with higher rates of erythroid apoptosis. In keeping with this, treatment of MDS cell lines with iron-

chelating therapy such as deferoxamine, reduced the iron load and appeared to ameliorate erythroid apoptosis (Gu et al. 2014).

From a clinical perspective, there is some evidence that transfusion dependence and high ferritin levels generally portend a worse prognosis in MDS patients (Malcovati 2007). In the pre-transplant setting, elevated ferritin levels in patients with acute leukaemia and MDS have also been associated with inferior outcomes (Armand et al. 2007). In this context, there are now many reports of iron-chelation therapy being used in MDS. In some cases, this has been associated with achievement of transfusion independence (Messa et al. 2008; Rose et al. 2010; Sanford and Hsai 2015) and/or improved overall survival (Neukirchen et al. 2012). Although the majority of this data is retrospective in nature, it remains an area of ongoing clinical and research interest, but is beyond the current scope of this work.

1.11. Models of MDS

One of the greatest difficulties in MDS research has been the ability to generate an MDS model that accurately recapitulates features of human disease. Clinically, MDS presents with significant heterogeneity – a feature in keeping with the varied underlying genomic landscape that is now beginning to unravel (Papaemmanuil et al. 2013; Haferlach et al. 2014). Unfortunately, cells extracted from human samples particularly in cases of early-stage MDS, undergo significant apoptosis making it difficult to study these in vitro. Additionally, in human MDS, there is no easy way of distinguishing immature $CD34^+$ cells that belong to the aberrant MDS clone from normal $CD34^+$ cells, adding a further layer of complexity to the equation.

In this section, I will discuss the limitations of cell lines for this disorder and the significant issues to date with generation of xenograft models. A discussion will ensue regarding genetically engineered murine models of MDS – with specific attention to the *NHD13* (Nup98-HoxD13) fusion gene model that has been used to study MDS for this body of work. Finally, some thoughts will be given regarding future models for this disorder in years to come. This is particularly

relevant in the genomic era where the complex molecular pathophysiology of MDS is becoming somewhat clearer (Starczynowski et al. 2010; Bejar and Ebert 2010; Bejar et al. 2011a; Bejar et al. 2011b; Yoshida et al. 2011).

1.11.1. MDS cell lines

Although a large number of MDS cell lines have been reported in the literature, there have been a significant number of concerns regarding the validity of these lines for a number of reasons as elegantly reviewed by Drexler et al (Drexler et al. 2009). Firstly, a number of MDS lines have been deemed false due to cross-contamination by older established leukaemia cell lines. This has been ascertained through the use of DNA profiling. Secondly, a significant number of MDS cell lines have been established during the later stages of MDS and are therefore more representative of the leukaemic phase rather than early-stage disease. References for the 21 cell lines that fall into this category are provided by Drexler et al. Having excluded lines that fall into these two categories, of a total 31 'reported' MDS cell lines analyzed, only 3 apparently seem valid. However, these lines have invariably been incompletely described or are difficult to maintain in culture. These findings suggest a significant lack of robust cell line models that emulate features of early-stage MDS.

1.11.2. Xenograft models

Given concerns raised regarding the purported purity of reported MDS cell lines and difficulty maintaining them in culture, a number of attempts have been made to generate xenograft models of MDS, in which human MDS cells are transplanted into immunodeficient mice. Unfortunately, many of these attempts have been met with limited success. In general, poor reconstitution appears to be the rule (Nilsson et al. 2000; Nilsson et al. 2002). Additionally, when transplanting human samples, it is difficult to differentiate between normal bone marrow progenitors and those belonging to the MDS clone. Benito et al reported engraftment following transplant of human bone marrow into NOD/SCID mice but were unable to show any evidence of clonal precursors using FISH or X-linked clonal analysis possibly indicating the BM cells that had engrafted were of a non-MDS clone. Additionally, the mice did not develop any clinical features of

MDS and engraftment was only transient (Benito et al. 2003). Contributing factors for poor engraftment may relate to an inherent problem within the actual cells transplanted or increased susceptibility to external factors (poor microenvironmental support or immune-mediated attack).

To try and improve success rates of xenograft transplantation, NOD-SCID mice lacking β2 microglobulin and expressing endogenously generated cytokines including IL-3, GM-CSF and c-KIT have been used. Although clonal engraftment was demonstrated in these mice, repopulation was again transient and occurred at extremely low levels. Additionally, these mice did not develop clinical MDS (Thanopoulou et al. 2004). A similar study at the time, confirmed human MDS cells were transplantable if NOD/SCID-β2m^{null} mice were used and if BMMCs were injected into the intramedullary space with supportive stromal cells. Although clonal abnormalities were again detectable, no comments were made regarding the phenotype of the mice (Kerbauy et al. 2004). These studies have also been hampered somewhat by the reduced lifespan of the immunodeficient mice used.

In constellation, these results reveal significant deficiencies in the generation of xenograft models that recapitulate true features of MDS – both genetically and phenotypically.

1.11.3. Genetically engineered murine models of MDS

As genetic engineering technology has flourished and with the poor outcomes generally associated with the generation of xenograft models, a number of genetically engineered 'MDS' mice have been generated. Approaches have often involved retroviral infection (for instance, to overexpress ectopic virus integration site 1 (EVI-1)) (Buonamici et al. 2004) or knock-out / knock-in technologies (eg knockout of NPM (Grisendi et al. 2005; Sportoletti et al. 2008)).

In many cases, the resultant models have not accurately recapitulated all the phenotypic features of MDS. An in-depth analysis of some of these models is provided by Beachy et al (Beachy and Aplan 2010). This discussion is

summarized in ***Table 1.1*** where the phenotype of each model is described; together with the associated limitations or shortcomings in each case. The most common limitations across the board include the lack of reproducible cytopenias in certain cases and the lack of progression to acute leukaemia in a number of models.

1.11.3.1. *NUP98-HOXD13* mouse model of MDS

Of the transgenic models described, one of the models that recapitulates all the features of MDS most accurately is the NUP98-HOXD13 (*NHD13*) model. Although this fusion gene results from a rare balanced translocation (t(2:11)(q31;p15)) in human therapy-related MDS and AML (Raza-Egilmez et al. 1998) – the resultant phenotype closely mimics that of human MDS.

As this model forms the basis of this study, its generation has been described in much greater detail below.

Typically, the NUP98-HOXD13 translocation approximates the N terminus of the NUclear Pore complex protein (NUP98) with the homeobox containing HoxD13 protein ***(Figure 1.3A)***. On its own, NUP98 acts to mediate RNA and protein transport across the nuclear membrane (Radu et al. 1995). It is a promiscuous protein that is reported to fuse to at least 25 different partners (Slape and Aplan 2004) in various haematological conditions including the highly conserved group of homeobox (HOX) genes - which play an important role in embryogenic development. Of NUP98's partner HOX cluster genes, *HOXD13* and *HOXD11* have been associated with myeloid malignancies.

By injecting the *NUP98-HOXD13* (*NHD13*) fusion gene into mouse blastocysts under the control of 'vav1' regulatory elements, Dr Peter Aplan's group generated a mouse model of MDS in which the protein is expressed throughout all haematopoietic tissues (Lin et al. 2005). The resultant mice exhibit features that closely recapitulate features of human MDS. *NHD13* mice develop multiple cytopenias from 4 months of age onwards in spite of a reasonably cellular bone marrow – in keeping with 'ineffective haematopoiesis'. Typically, a peripheral

blood thrombocytopenia is subsequently followed by a macrocytic anaemia. Bone marrow cells are notable for their dysplastic features and from 10 months of age onwards, ~ 40-50% of these mice develop acute leukaemia (both AML and T-ALL) with a variable latency period ***(Figure 1.3B)***. Progression to leukaemia is associated with the acquisition of additional mutations such as *N-RAS, K-RAS* and *CBL* (Slape et al. 2008b) which some have postulated may be the result of increased reactive oxygen species (Chung et al. 2014).

In keeping with early-stage MDS, we have shown that apoptosis is significantly increased in *NHD13* HSCs (Slape et al. 2012) and that this can be correlated with a significant reduction in the LSK compartment (Xu et al. 2012b). By transplanting bone marrow nucleated cells (BMNC) from these mice into lethally irradiated recipient wild-type mice, Chung et al have been able to demonstrate that MDS is transplantable from a long-term repopulating cell – although the identity of this cell has not been fully elucidated to date (Chung et al. 2008).

To provide an unbiased view however, a number of caveats do exist. As the *NHD13* translocation is rare in human MDS/AML, some critics argue that this model is not an accurate representation of human MDS. That these mice develop ALL is also somewhat atypical. However, in spite of this, phenotypically these mice do closely mimic a significant number of features of human MDS and can therefore be used as a tool to study apoptosis and leukaemic transformation.

1.11.3.2. Future MDS models

As our understanding of the molecular basis of MDS improves, it is likely that better models of this disease will be developed. This area remains thwarted with some difficulties at present, as we try to determine the 'clonal architecture' of MDS development and which mutations are the key founding lesions. As one example, models that have targeted *ASXL1* for instance have shown some promise in replicating the MDS phenotype (Abdel-Wahab et al. 2013; Wang et al. 2014a). Although this remains an area of ongoing work, it lies beyond the scope of this current study.

1.12. The bone marrow microenvironment and MDS

The difficulty in maintaining viability of human MDS cells in culture (Mundle et al. 1999a) and in generating xenograft models with long-term reconstitution (Benito et al. 2003; Thanopoulou et al. 2004) has implicated a potential role for the microenvironment in permitting ongoing survival of the abnormal cell population.

As one example, the deletion of the *Dicer1* gene (an RNase III endonuclease which plays an important role in microRNA biogenesis and RNA processing) from osteoprogenitor cells, induces bone progenitor dysfunction and generates a phenotype in haematopoietic progenitors that accurately recapitulates features of MDS. Of importance is the dependence of these changes on the microenvironment. Transplantation of haematopoietic cells from mice exhibiting MDS into wild-type mice reversed the phenotype; whilst the opposite was also true. These findings suggest a role for the microenvironment in inducing and potentially propagating the MDS phenotype (Raaijmakers et al. 2010).

In other cases, functionally abnormal macrophages and fibroblasts from within the bone marrow microenvironment of MDS patients have been implicated in the secretion of pro-inflammatory cytokines such as TNF-α and IL-6 at levels higher than those produced in normal non-MDS patients (Shetty et al. 1996; Flores-Figueroa et al. 2002). Additionally, Kondo et al report that the production of TNF-α and IFN-γ by cells within the bone marrow niche itself may play a role in permitting disease progression by upregulating the costimulatory B7-H1 molecule on MDS blasts via NF-κB activation, inducing T-cell apoptosis and enhancing blast proliferation (Kondo et al. 2010; Ishibashi et al. 2011). This scenario may set the scene for acquisition of additional genetic mutations. That cells undergo ongoing apoptosis after being removed from this environment suggests a persistent intrinsic propensity to undergo apoptosis or loss of a pro-survival signal from the surrounding milieu.

1.13. Abrogation of apoptosis in MDS

That abrogating apoptosis in MDS may yield a certain therapeutic benefit with respect to cytopenias has certainly been considered; albeit in a fairly non-specific manner. Use of growth factors such as G-CSF and erythropoietin has become part of the armamentarium of supportive care for some patients (Tehranchi et al. 2005) with some evidence that G-CSF may directly inhibit release of cytochrome c. In keeping with this, other studies have suggested that such therapy may reduce sub G1 DNA levels seen in early-stage MDS correlating with reduced apoptosis (Rajapaksa et al. 1996).

In one study, Bouscary et al attempted to use caspase inhibitors to prevent apoptosis. However, less than 50% of patient samples showed any evidence of reduced apoptosis in vitro, and treatment with the inhibitor did not enhance colony formation in any case. In this study, the authors suggested that inhibiting caspase might be insufficient to rescue cells that were already committed to undergoing programmed cell death (Bouscary et al. 2000). Despite these findings, other groups have demonstrated a rescue of apoptosis in association with caspase inhibition (Ali et al. 1999). Possible causes for these discrepancies have been discussed (Mundle et al. 2000). Importantly, despite these varied observations, no 'in vivo' data is presented regarding the clinical effect on the MDS phenotype.

A number of equally comparable observations have been demonstrated for the extrinsic pathway. Claessens et al reported transduction of a dominant negative mutation of FADD which inhibited caspase-8 activation and rescued erythroid colony growth (Claessens et al. 2005). Similarly, Gersuk et al reported increased haematopoietic colony formation with TNF-α blockade (Gersuk et al. 1998). The findings for TNF-α subsequently led to a series of clinical trials from 2001 using etanercept (a TNF-α inhibitor) initially as a single agent (Maciejewski et al. 2002) and subsequently in combination with other agents known to be effective in MDS (Scott et al. 2010). Although well-tolerated, the efficacy in most cases as a single agent was generally low. In their study, Deeg et al evaluated 12 patients with MDS treated with etanercept. ¼ had rises in their haemoglobin but only one

had a fall in transfusion requirements. Platelet and neutrophil responses were more modest in nature and in some cases, blood counts declined with treatment (Deeg et al. 2002). Importantly, baseline levels of TNF-α and treatment responses could not be correlated. In contrast, a number of reports have shown more favourable results for combination therapies with etanercept, over and above that of individual therapies alone (Scott et al. 2010). The uptake of these treatments however has not been overwhelming to date.

1.13.1. *NHD13* model of MDS and role of BCL-2

In an attempt to understand the functional significance of apoptosis on the MDS phenotype, our group has previously examined the effect of BCL-2 overexpression on the features of the *NHD13* mouse (Slape et al. 2012). A summary of these findings is presented here as this forms the basis of work presented in this study.

Initial gene expression data reveals that of the five anti-apoptotic BCL-2 related genes (*Bcl-2, Bcl-w, Bcl-xL, Mcl-1* and *A1)*, *Bcl-2* alone is significantly reduced (FDR $5.43e^{-4}$ and log 2-fold reduction of -1.77) at the mRNA in *NHD13* HSCs. This corresponds to a reduction, at the protein level as well. In this context, overexpression of BCL-2 was found to prevent apoptosis of *NHD13* HSCs and rescue their numbers implicating the intrinsic pathway as the main driver of apoptosis in our model.

We reported two subsequent effects on the phenotype. Firstly, prevention of apoptosis rescued the macrocytic anaemia associated with the *NHD13* phenotype; but not the concomitant thrombocytopenia. Secondly, and somewhat counterintuitively, prevention of apoptosis of *NHD13* HSCs through BCL-2 overexpression prevented leukaemic progression to acute myeloid leukaemia (Slape et al. 2012). In association with reduced progression to AML, the increased cycling state (i.e reduced quiescence) associated with *NHD13* HSCs was normalized to wild-type levels through BCL2 overexpression and DNA damage, (which is also increased in *NHD13* HSCs) was also normalized.

These findings raise a number of important issues that will be discussed in the subsequent two sections.

1.13.2. Apoptosis and tumorigenesis

One of the key hallmarks of cancer development and progression as extensively reviewed by Hanahan et al is that of overcoming apoptosis (Hanahan and Weinberg 2000; Hanahan and Weinberg 2011). Resistance to apoptosis in the presence of an oncogene allows for the accrual of additional mutations ultimately driving tumour development and progression (Vaux et al. 1988; Pelengaris et al. 2002).

However, our findings with BCL-2 overexpression suggest that in some cases the opposite may also be true. Under certain circumstances and although counterintuitive, prevention of apoptosis may actually prevent tumour formation rather than drive its progression.

A number of disease models of other malignancies indicate this may be the case under particular circumstances. A few examples are discussed below:

- γ-irradiation of mice is typically associated with the development of radiation-induced thymic lymphoma. A number of groups have reported that thymocytes from mice lacking *Puma* at the time of irradiation fail to undergo apoptosis and subsequently do not develop cancer (Labi et al. 2010; Michalak et al. 2010). This is in contrast to loss of p53 which also abrogates apoptosis but is associated with an increase in the incidence of tumour development - likely reflecting the importance of p53's tumour suppressive function beyond apoptosis alone. Of significance, when lymphocyte apoptosis was again induced through treatment of the *Puma*-deficient mice with dexamethasone, thymic lymphoma was noted in up to 30% of treated mice. The authors argue that prevention of apoptosis reduces a compensatory proliferative stimulus that would ordinarily drive tumour formation by encouraging quiescent cells that have acquired mutations to begin cycling (Labi et al. 2010).

- In an alternative disease model, mice lacking hepatocyte-specific Mcl-1 or Bcl-xL exhibit increased apoptosis with an associated increase in the incidence of liver tumours in the context of increased oxidative stress and DNA damage (Hikita et al. 2012). Knocking out BAK (but not BAX) is sufficient to reduce the associated apoptosis and ultimately results in reduced incidence of liver tumour formation.

These cases suggest that under particular circumstances, the induction of apoptosis may be detrimental to a cell. By inducing a compensatory hyperproliferative response, apoptosis in such cases may drive the acquisition of additional mutations and ultimately support disease progression and malignant transformation. This concept will be further examined throughout this work with a particular focus on how it relates to the less well-characterized progression of myeloid disease.

1.13.3. Caveats of BCL-2 overexpression findings

Whilst the findings associated with BCL-2 overexpression in our model are extremely interesting, there are a number of limitations that warrant further discussion and investigation. The overexpression of transgenic BCL-2 in this model is likely significantly higher than that which would be found in human MDS. Additionally, there is some evidence that BCL-2 may act to negatively regulate entry into the cell cycle (as seen in this case) (Linette et al. 1996; Deng et al. 2003). As such, it is difficult to dissect whether the effect on leukaemic progression stems from prevention of apoptosis or BCL-2's effect on cell cycle. From a therapeutic perspective, it is also more difficult to overexpress BCL-2 than to inhibit a protein that is overexpressed. In this context, although BCL-2 agonists have been described; to date, they have been associated with limited therapeutic application from a clinical perspective.

Aims

1.14. Aims of this study

Although many reports have confirmed that apoptosis contributes to the ineffective haematopoiesis associated with early-stage MDS and despite divided opinions as to whether the intrinsic or extrinsic pathways contribute more significantly to this phenotype - it remains unclear what role apoptosis actually plays. Specifically, how does it contribute to disease progression in myeloid disease? And what effect might we see by modulating apoptosis on the disease phenotype and subsequent disease progression?

Our findings with BCL-2 overexpression implicate the intrinsic pathway as a driver of apoptosis in *NHD13* HSCs and suggest that this is responsible (at least in part) for the associated cytopenias. Although leukaemic progression was prevented, it is difficult to tease out whether this is the result of BCL-2's anti-apoptotic or cell cycle inhibitory effect. In this study, we have therefore sought to:

1. **Characterize apoptosis upstream of BCL-2 within the model focusing on the role of p53 in this context;**

2. **Understand the role apoptosis alone plays by targeting a number of pro-apoptotic BH3-only proteins (also upstream of BCL-2) and observing the resultant phenotype;**

3. **Understand at a molecular level how apoptosis may contribute to disease progression.**

Tables

Table 1.1 ***Genetically engineered mouse models of MDS***

Table adapted from Beachy et al (Beachy and Aplan 2010). The table lists a number of genetically engineered mouse models of myelodysplastic syndrome, the means of genetic alteration and their clinical phenotype. The limitations of each model are briefly listed in each case.

Genes involved	**Alteration**	**Phenotype**	**Limitations of the model**	**References**
Pten/Ship	Haploinsufficiency of *Pten* / Ship knockout	Leukocytosis, neutrophilia, anaemia, TCP, HSM, extramedullary haematopoiesis.	No leukaemia; short survival of 5 weeks	(Moody et al. 2004)
Evi1	Retroviral transduction	Anaemia, TCP, leukopenia (variable), hypercellular BM, BM dysplasia, uniformly fatal (14mo)	No leukaemia; risk of insertional mutagenesis	(Louz et al. 2000; Buonamici et al. 2004)
Npm1	Haploinsufficiency	Variable thrombocytosis or TCP, BM hypercellularity and dysplasia. Lung and liver tumours, AML and lymphoma at advanced age	No anaemia and additional tumours	(Grisendi et al. 2005; Sportoletti et al. 2008)
Dido	Knockout	Variable anaemia, leucocytosis, splenomegaly. BM dysplasia. Survival 55% at 26 months, BUT no leukaemia	No leukaemia	(Fütterer et al. 2005)
NUP98-HOXD13	Transgenic (Vav promoter)	Macrocytic anaemia, leukopenia, variable TCP, hypercellular BM, dysplasia, leukaemic transformation in 60% of cases (AML and ALL)	Rare translocation in human MDS; Develop AML and ALL	(Lin et al. 2005; Slape et al. 2008a; Chung et al. 2008)
SALL4B	Transgenic (CMV promoter)	Mild anaemia and neutropenia, variable thrombocytosis, BM dysplasia + hypercellularity. 50% leukaemic transformation at 24 months (AML)	Majority develop polycystic kidney disease	(Ma et al. 2006)

Genes involved	**Alteration**	**Phenotype**	**Limitations of the model**	**References**
BCL2/ NRASD13	Transgenic	No anaemia, mild leucocytosis, mild TCP, hypercellular BM, HSM.	No leukaemia or anaemia	(Omidvar et al. 2007)
RUNX1	Retroviral transduction	Macrocytic anaemia, leukopenia, TCP, hypercellular marrow. At 14mo – 60% leukaemic transformation	Very short latency in some cases (3-5 months)	(Watanabe-Okochi et al. 2008)
Arid4a	Knockout	Mild anaemia, leukopenia, TCP, hypercellular marrow with fibrosis. 12% AML at 12-22mo	Low AML transformation rate	(Wu et al. 2008)
Polg	Knockin of mutant	Anaemia, lymphopenia, BM dysplasia, mitochondrial dysfunction.	Death from megaloblastic anaemia – no leukaemia	(Chen et al. 2009)

Figures

Figure 1.1. ***The Haematopoietic Hierarchy***

Schematic of haematopoietic hierarchy: Self-renewing haematopoietic stem cells (HSCs) are capable of undergoing asymmetric cell division thus replenishing their own reservoir and differentiating to form mature terminally differentiated cells. In each case, flow cytometric characteristics used to identify each population are noted (Kiel et al. 2005; Pronk et al. 2008; Pronk and Bryder 2011). Markers in **bold blue** represent those that are different from the preceding population. As cells progress down this pathway, they are characterised by a reduced capacity for self-renewal and greater commitment and restriction to a particular lineage. It is important to note that this schematic is somewhat an oversimplification of the haematopoietic process and is unlikely to be quite as linear as depicted (Orkin and Zon 2008); LT = long-term; ST = short-term; MPP = multipotent progenitors; CMP = common myeloid progenitors; CLP = common lymphoid progenitors; GMP = granulocyte macrophage progenitors; Meg-E = megakaryocyte erythroid; BFU-E = burst-forming units erythroid; CFU-E = colony-forming units erythroid.

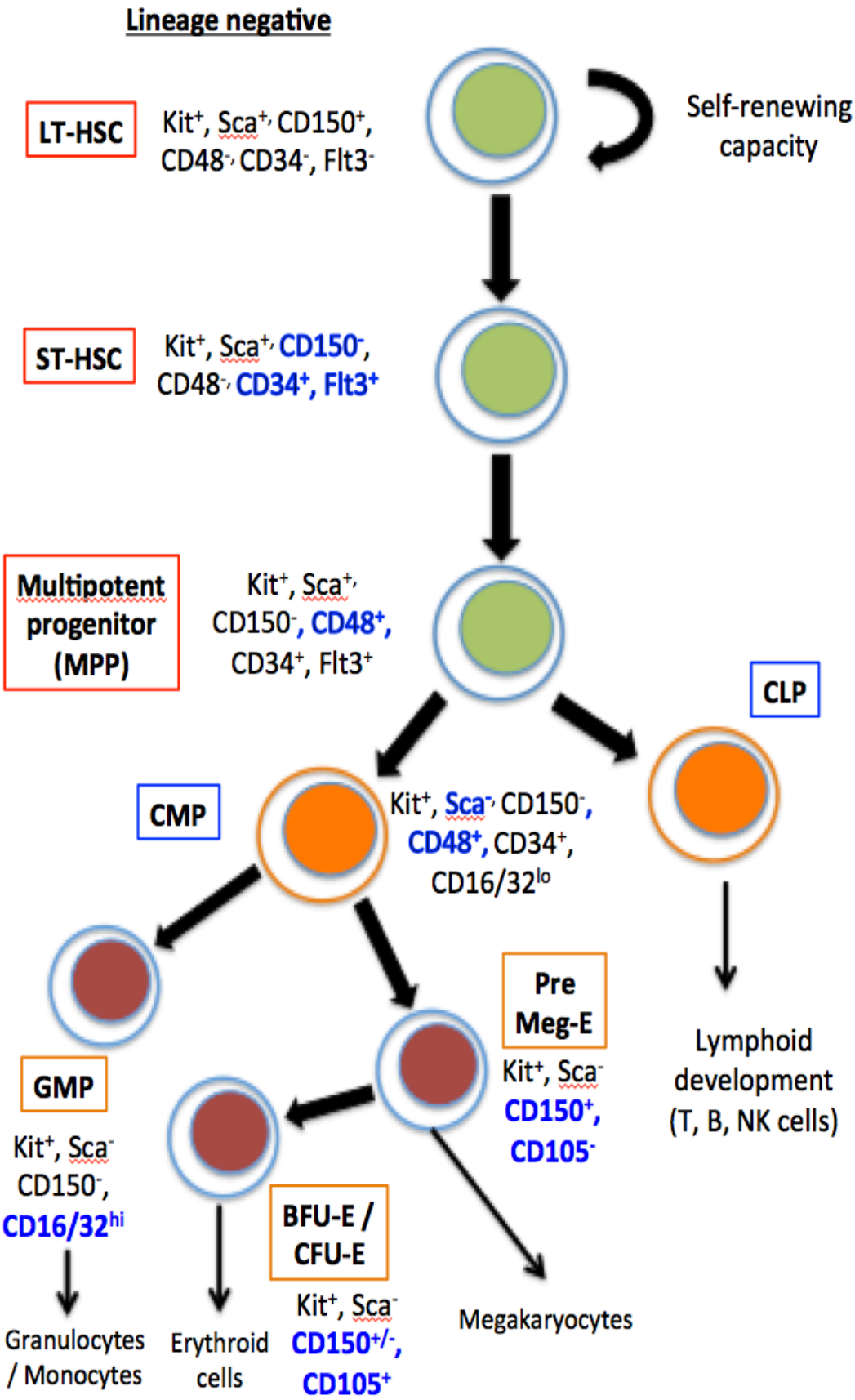
Lineage negative
LT-HSC
Kit+, Sca+, CD150+, CD48-, CD34-, Flt3-
Self-renewing capacity
ST-HSC
Kit+, Sca+, CD150-, CD48-, CD34+, Flt3+
Multipotent progenitor (MPP)
Kit+, Sca+, CD150-, CD48+, CD34+, Flt3+
CLP
CMP
Kit+, Sca-, CD150-, CD48+, CD34+, CD16/32lo
Pre Meg-E
Kit+, Sca-, CD150+, CD105-
Lymphoid development (T, B, NK cells)
GMP
Kit+, Sca-, CD150-, CD16/32hi
BFU-E / CFU-E
Kit+, Sca-, CD150+/-, CD105+
Granulocytes / Monocytes
Erythroid cells
Megakaryocytes

<u>Figure 1.2.</u> ***The Apoptotic Pathway***

Schematic of the apoptotic pathway comprised of the intrinsic and extrinsic pathway. Activation of the intrinsic pathway is primarily mediated by p53 and is regulated at a number of different stages ultimately culminating in altered mitochondrial permeability, release of cytochrome c and activation of downstream effector caspases. Within the intrinsic pathway, the BH3-only proteins and BAX and BAK are pro-apoptotic in nature and BCL-2 and its related proteins are anti-apoptotic. *Noxa* and *Puma* are transcriptionally regulated by p53. BAX and BAK can be activated indirectly through the binding of BH3-only proteins to BCL-2 and its related proteins – thus alleviating the usual inhibition of BAX and BAK. Alternatively, they can be directly engaged and activated by the BH3-only proteins or p53. The extrinsic pathway is mediated by engagement of the 'death receptors' by TNF or Fas ligand. Receptor binding results in activation of caspase 8 and further downstream caspases. Caspase 3 and 7 are common to both pathways. Crosstalk between the two pathways is at times possible depending on the cell involved; activated caspase-8 may activate BID, generating a functional truncated form that is then capable of signaling through the mitochondria.

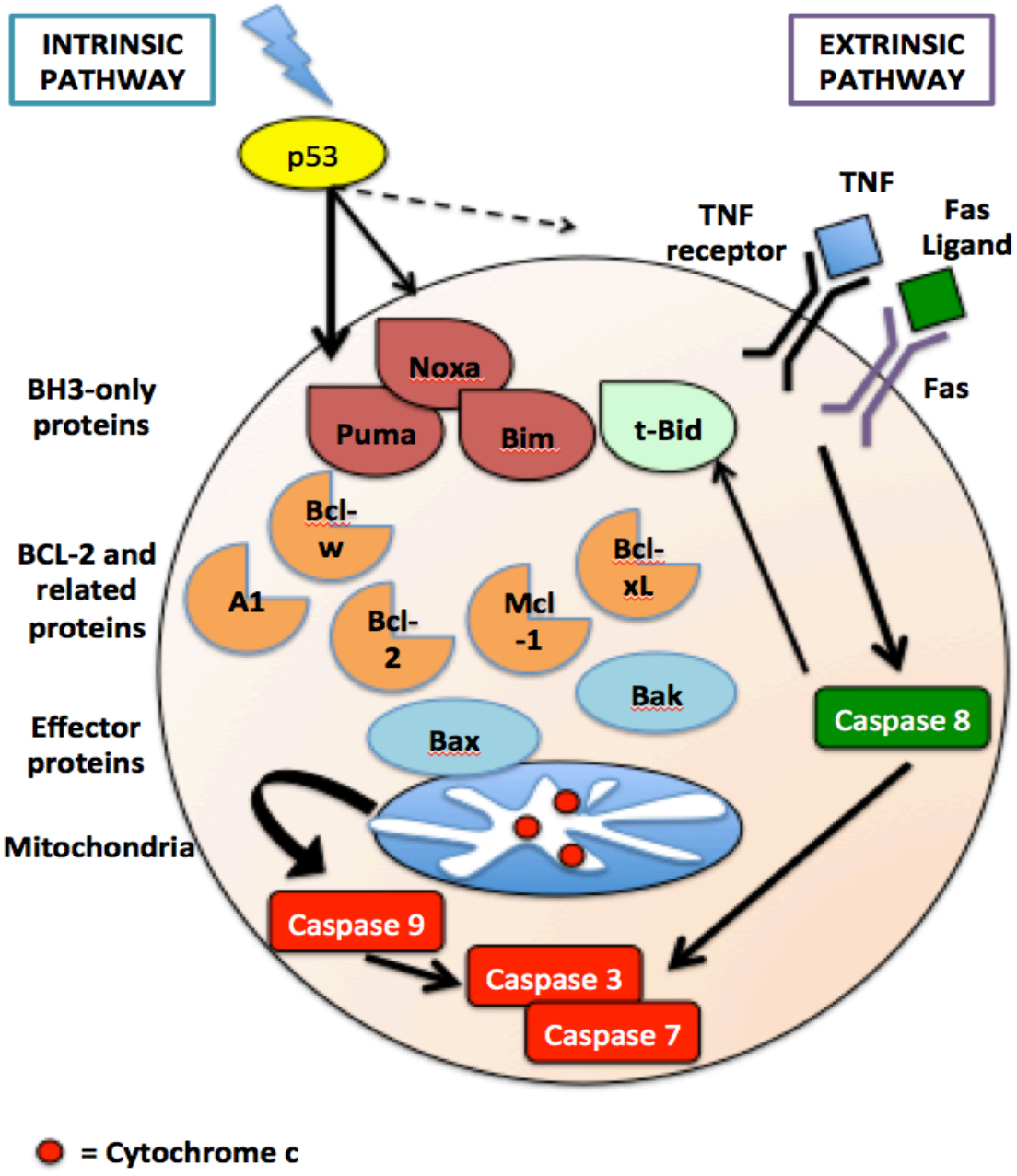
INTRINSIC PATHWAY
EXTRINSIC PATHWAY
p53
TNF
TNF receptor
Fas Ligand
Fas
BH3-only proteins
Noxa
Puma
Bim
t-Bid
BCL-2 and related proteins
Bcl-w
A1
Bcl-2
Mcl-1
Bcl-xL
Effector proteins
Bak
Bax
Caspase 8
Mitochondria
Caspase 9
Caspase 3
Caspase 7
= Cytochrome c

<u>Figure 1.3.</u> ***Generation of the NHD13 mouse model of MDS***

(A) The generation of the *Nup98-HoxD13 (NHD13)* fusion gene consisting of the N-terminus of the *Nup98* gene with the characteristic GLFG repeats and the C-terminus of the *HoxD13* gene; (B) *NHD13* mice were generated by expressing the *NHD13* gene in haematopoietic cells using the vav promoter and injecting this gene into blastocysts. Features of the mouse including development of dysplasia, pancytopenia and increased leukaemic transformation are all in keeping with human MDS.

A

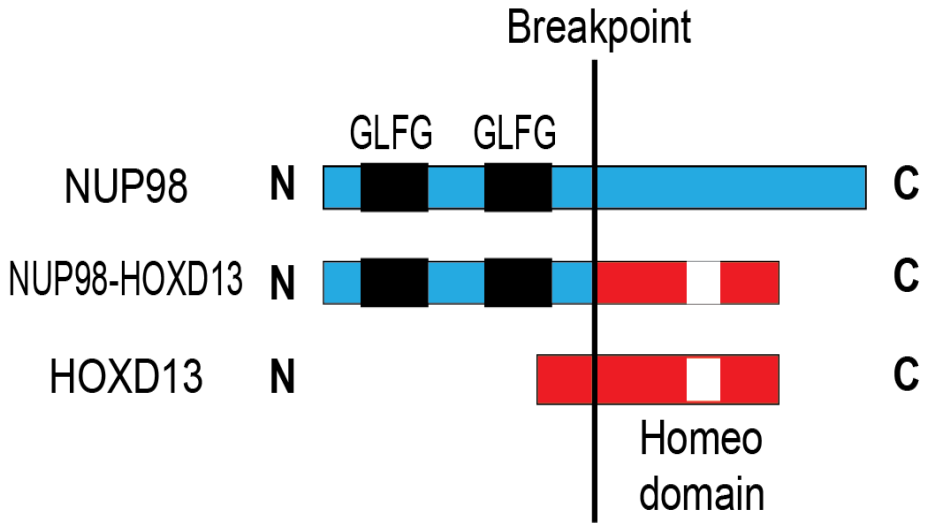
Breakpoint
GLFG
GLFG
NUP98
N
C
NUP98-HOXD13
N
C
HOXD13
N
C
Homeo
domain

B

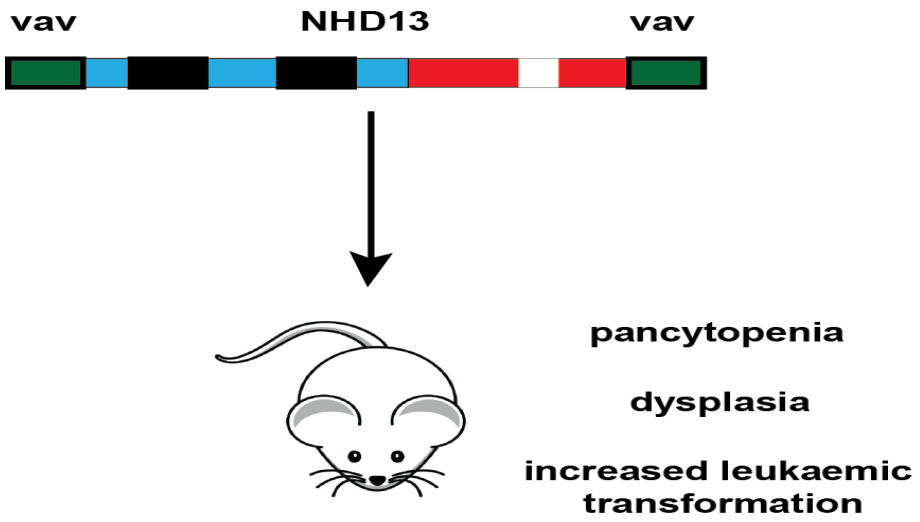
vav
NHD13
vav
pancytopenia
dysplasia
increased leukaemic
transformation

CHAPTER TWO

Materials and Methods

Abstract

This chapter outlines the various materials and methods that have been used for the purpose of experiments used in this thesis. In order to maintain clarity, details of well-established experiments have been kept to a minimum.

Materials

2.1. General buffers and solutions

All chemicals used in this study were of laboratory or analytical grade and were purchased from standard distributors as listed below. All solutions were stored at room temperature unless stated otherwise.

General Buffers and Solutions:

DEPC H_2O:

DEPC	1mL
dH_2O	999mL

After adding DEPC to the dH_2O, the solution was left overnight at room temperature before autoclaving.

Ethylene-diamine-tetra-acetic acid (EDTA) - 0.5M:

EDTA-disodium salt	186.12g
dH_2O	up to 1L

EDTA was dissolved with gentle heating and stirring; pH was adjusted to 8.0

Potassium chloride:

For 1M solution:

KCl	74.55g
dH_2O	up to 1L

Potassium chloride was dissolved by gentle heat and stirring.

Mouse Phosphate-buffered saline (PBS):

For 10 x solution (2L):

$Na_2HPO_4.2H_2O$	57g
$NaH_2PO_4.1H_2O$	11.03g
NaCl	174g

Reagents were combined and dissolved in 500ml of $MQ.H_2O$ before being made up to 2L.

SDS solution:

For 20% (w/v) solution:

SDS powder	100g
dH_2O	up to 500mL

SDS powder was dissolved with gentle heat and stirring.

Sodium chloride:

For 5M solution:

NaCl	292.2g
dH_2O	up to 1L

Sodium chloride was dissolved by gentle heat and stirring

Tris:

For 1M solution:

Tris	121.1g
dH_2O	up to 1L

Adjusted to appropriate pH using NaOH or HCl.

TE buffer:

For 1L solution:

Tris 10mM (pH 8.0)	10mL (of 1M)
EDTA 1mM	2mL (of 0.5M)
dH_2O	up to 1L

Table 2.1. Commonly used chemicals / reagents and their suppliers

Chemical / Reagent	Supplier	Location of supplier	Catalogue Number
2-betamercaptoethanol (2-βME)	Sigma-Aldrich	St Louis, USA	M7522
Ammonium chloride (NH_4Cl)	BDH	Gibbstown, USA	10017
Chloroform	Merck/BDH	Kilsyth, Australia	10077.68

Chemical / Reagent	Supplier	Location of supplier	Catalogue Number
Coomassie Plus	Thermo Scientific Pierce	Rockford, USA	23238
D-glucose	Sigma-Aldrich	St Louis, USA	G-5767
DePeX mounting medium	Merck/BDH	Kilsyth, Australia	361254D
Devondale instant skim milk powder	Devondale	-	-
Diethyl pyrocarbonate (DEPC)	Sigma-Aldrich	St Louis, USA	D-5758
Dimethyl sulphoxide (DMSO)	Sigma-Aldrich	St Louis, USA	D-5879
Ethylene-diamine-tetra-acetic acid disodium salt (EDTA)	Sigma-Aldrich	St Louis, USA	EDS
Hydrochloric acid	Merck /BDH	Kilsyth, Australia	1.09057.2500
Hydrogen peroxide	Merck/BDH	Kilsyth, Australia	10366.0500
Methanol	Fisher Scientific	Leics, UK	M/4000/PB17
Paraformaldehyde	Sigma-Aldrich	St Louis, USA	76240
Potassium chloride (KCl)	Sigma-Aldrich	St Louis, USA	P-3911
Potassium phosphate	Sigma-Aldrich	St Louis, USA	P-5379
Sodium chloride (NaCl)	Sigma-Aldrich	St Louis, USA	S-5886
Sodium citrate	Sigma-Aldrich	St Louis, USA	S-4641
Sodium dodecyl sulphate (SDS)	ICN Biomedicals	Irvine, USA	811030
Sodium hydrogen phosphate (Na_2HPO_4) - dihydrate	Merck/BDH	Kilsyth, Australia	10245.4R
Sodium hydroxide (NaOH)	Merck/BDH	Kilsyth, Australia	106498

Chemical / Reagent	Supplier	Location of supplier	Catalogue Number
Sodium phosphate (monobasic anhydrous) – NaH_2PO_4	Sigma-Aldrich	St Louis, USA	S-3139
Tris	Sigma-Aldrich	St Louis, USA	T-6066

2.2. Molecular biology solutions and reagents

All molecular biology reagents used in this study were of laboratory or analytical grade and were purchased from standard distributors as listed below. All solutions were stored at room temperature unless stated otherwise.

Molecular biology solutions

DNA ladder:

λ/DNA HindIII marker	100µL
ΦX 174 marker/HaeIII	50µL
Blue/Orange 6x DNA loading dye	100µL
dH_2O	350µL

For each agarose gel, 6µL of the ladder was used per required lane.

6 x DNA loading dye:

Bromophenol blue	25mg
Xylene cyanol FF	25mg
Orange G	25mg
Glycerol	3mL
dH_2O	up to 10mL

Reagents were combined and made up to 10mL with dH_2O giving a final solution containing 0.25% (w/v) bromophenol blue, 0.25% (w/v) xylene cyanol, 0.25% (w/v) orange G and 30% glycerol.

Glycine (1M):

Glycine	3.75g
dH_2O	50mL

After dissolving, pH was adjusted to 2.25.

Heat inactivating tail lysis buffer (for genotyping):

For 1L:

Gelatin 0.1% (w/v)	100mg
dH_2O	100mL
KCl 500mM	500mL of 1M
Tris 100mM (pH 8.3)	50mL of 2M
Nonidet P-40 (NP-40) – 1%	10mL
Tween 20 – 1%	10mL

Gelatin was first dissolved in 100mL of dH_2O. Solution was made up to 1L after additional reagents were added to achieve the listed concentrations.

Ponceau S staining solution:

Ponceau S	250mg
Acetic acid (glacial)	12.5mL
dH_2O	up to 250mL

Final concentration achieved = 0.1% (w/v) Ponceau S in 5% (v/v) acetic acid.

TAE:

For 50 x stock solution:

Tris (pH 8.2)	242g
Acetic acid (glacial)	57.1mL
EDTA	100mL of 0.5M

For 1L of stock solution – Tris was dissolved in ~ 600mL of dH_2O, then the EDTA and acetic acid were added. The solution was then made up to a final volume of 1L with dH_2O and stored at room temperature. For 1 x working concentration – solution was further diluted with dH_2O.

Tail lysis buffer:

For 1L:

Tris (pH 8.0) 100mM	100mL (of 1M)
NaCl 200mM	40mL (of 5M)
EDTA 5mM	10mL (of 0.5M)
SDS 0.2%	2mL
Proteinase K (20mg/mL)	15µL

Reagents were combined as above. Proteinase K was added prior to use.

TBST wash buffer:

TBS (10 x)	100mL
dH_2O	900mL

Supplemented with 0.1% (v/v) Tween 20 (1mL).

Tris buffered saline (TBS) – 10x –

Tris	24.2g
NaCl	80g
dH_2O	up to 1L

After dissolving, pH was adjusted to 7.6. Stock was diluted with dH_2O 1:10 prior to use.

Western Blot antibody dilution buffers:

a) ***Primary antibody dilution buffer:*** As per manufacturer recommendations and dissolved in 5% BSA + TBST
b) ***Secondary antibody dilution buffer:*** As per manufacturer recommendations and dissolved in 5% BSA / skim milk + TBST

Western Blot blocking buffers:

a) ***5% BSA + TBST:*** BSA (2.5g) was dissolved in TBST (50mL) and filter sterilized through a 0.22µm membrane giving a final concentration of 5% (w/v) BSA. Solution was kept at-30°C until use.
b) ***5% skim milk + TBST:*** Skim milk powder (5g) in 100mL TBST. Solution was kept at -30°C until use.

Western Blot running buffer – 10 x:

Tris	30g
Glycine	144g
SDS	10g
dH_2O	up to 1L

Solution was gently warmed to ensure adequate dissolving of reagents. Stock was diluted with dH_2O 1:10 prior to use.

Western Blot separating / stacking gels:

Separating gel (4 x buffer)

Tris	18.17g
20% SDS	2mL
dH_2O	up to 100mL

pH adjusted to 8.8 with HCl

Stacking gel (4 x buffer)

Tris	6.06g
20% SDS	2mL
dH_2O	up to 100mL

pH adjusted to 6.8 with HCl

SDS-Polyacrylamide Separating gels:

For a 10% gel:

Separating gel buffer	3.8mL
Acrylamide 40%	3.8mL
10% APS	224µL
TEMED	10µL

SDS-Polyacrylamide Separating gels:

Tris	18.17g
20% SDS	2mL
dH_2O	up to 100mL

pH adjusted to 8.8 with HCl

Western Blot transfer buffer – 10 x:

Tris	30g
Glycine	144g
dH_2O	up to 1L

Solution was gently warmed to ensure adequate dissolving of reagents and then stored at 4°C. For use, 100mL was combined with 200mL of methanol (MeOH) and 700mL of dH_2O.

Table 2.2. ***Commonly used molecular biology reagents***

Reagent	Supplier	Location of supplier	Catalogue Number
λ DNA/HindIII marker	Promega	Madison, USA	G1711
ΦX 174 DNA/HaeIII marker	Promega	Madison, USA	G1761
Acetic acid (glacial)	Merck/BDH	Kilsyth, Australia	1.0063
Bovine serum albumin (BSA)	Sigma-Aldrich	St Louis, USA	A-4503
Bromophenol blue	Sigma-Aldrich	St Louis, USA	B-8026
Ethidium bromide (EtBr)	Sigma-Aldrich	St Louis, USA	E-8751
Gelatin	Sigma-Aldrich	St Louis, USA	G-1890
Glycerol	Sigma-Aldrich	St Louis, USA	G-6376
Glycogen (molecular biology)	Roche	Mannheim, Germany	10901393001
GoTaq® Green Master Mix	Promega	Madison, USA	M7123
GoTaq® qPCR Master Mix	Promega	Madison, USA	A600A
Nonidet P-40 (NP-40)	Sigma-Aldrich	St Louis, USA	N-6507
Orange G	Sigma-Aldrich	St Louis, USA	O-3756
Ponceau S	Sigma-Aldrich	St Louis, USA	P-3504
Proteinase K, recombinant PCR grade	Roche	Mannheim, Germany	03115852001
Stripping buffer (Re-Blot Plus Strong 10 x)	Merck/ Millipore	California, USA	2504

Reagent	Supplier	Location of supplier	Catalogue Number
TRIzol reagent	Invitrogen	Mount Waverley, Australia	15596-018
Tween 20	Amresco	Solon, USA	0777-1L
SYBR® Safe DNA gel stain	Life Technologies	Scoresby, Australia	
Xylene cyanol FF	Sigma-Aldrich	St Louis, USA	X-4126

2.3. Cellular biology solutions and reagents

Cellular biology and animal experimentation solutions

4% paraformaldehyde (PFA):

Paraformaldehyde	20g
10M NaOH	250µ***L***
PBS	500mL

PBS was heated to 65°C. Reagents were added in a fume hood and pH was adjusted to 7.5 to allow adequate dissolution. After allowing the solution to cool down to RT, it was filter-sterilized and stored at -20°C in aliquots of 50mL. A working solution of 2% PFA was prepared by a 1:2 dilution with PBS.

Buffered saline glucose citrate (BSGC) buffer (for mouse bleeds):

NaCl	7g
Potassium phosphate	218mg
Sodium phosphate	1.2g
D-glucose	2g
Sodium citrate	4g
dH_2O	up to 1L

pH was adjusted to 7.3. Prior to use, solution was filter sterilized.

FACS block stock solution:

IgG (from rat serum)	10mg
PBS	10mL

Rat serum was diluted in PBS to give a final concentration of 1mg/ml (50 x). For working solutions, the stock was diluted 1:50 with PBS and stored at 4°C.

FACS fixative solution (FACS fix): Used in cases when immediate flow analysis was not possible.

Formaldehyde	1mL
D-glucose	2g
NaN_3 20% (w/v)	100µL
PBS	up to 100mL

Final solution: 1% (v/v) formaldehyde, 2% (w/v) glucose and 0.02% (v/v) NaN_3.

FACS wash buffer:

FCS	40mL
NaN_3	2mL
PBS	up to 2L

Reagents were added to give final concentrations of 2% (v/v) FCS and 0.02% (v/v) NaN_3. Solution was kept at 4°C to avoid contamination.

Neomycin trisulfate acidified water:

For prevention of infection in mice after irradiation and transplantation.

To prepare acidified water - a 2L bottle was filled with MQH_2O. pH was then adjusted to 2.5 using HCl. Water was then autoclaved and left at room temperature until required.

For neomycin sulfate stock (100 x)

Neomycin sulfate powder	17.55g
MQH_2O	to 100mL

After adding antibiotic to the water, the bottle was covered with foil and gently stirred until completely dissolved (yielding a yellow solution). This was stored at 4°C and protected from light.

To prepare neomycin sulfate acidified water:

Neomycin sulfate (100x)	10mL
Acidified water	up to 1L

After making up the working solution, the bottle was covered with foil to prevent deterioration of the antibiotic. The water was dispensed into dark drinking bottles when given to the mice and was replaced 1-2 x / week.

Red cell lysis buffer:

NH_4Cl (final conc. 156mM)	16.68g
dH_2O	up to 2L

After dissolving, pH was adjusted to 7.4. Lysis buffer was stored at 4°C and was allowed to reach room temperature prior to use.

Table 2.3. ***Commonly used cellular biology solutions / reagents and their suppliers***

Chemical / Reagent	Supplier	Location of supplier	Catalogue Number
Bacto™ agar	Difco	Lawrence, USA	0140-01
BD Calibite™ Beads	BD Biosciences	San Diego, USA	340486
BD Cytofix/Cytoperm	BD Biosciences	San Diego, USA	554722
BD PermWash	BD Biosciences	San Diego, USA	554723
BioMag Goat Anti-Rat IgG beads	QIAGEN	Hilden, Germany	310107
3,3' Diaminobenzidine tetrahydrochloride tablets (DAB)	MP Biomedicals	Ohio, USA	980681
Foetal calf serum	Sigma-Aldrich	St Louis, USA	F2442
Glutaraldehyde	Merck/BDH	Kilsyth, Australia	360802F
IgG (from rat serum)	Sigma-Aldrich	St Louis, USA	I4131-10mg
Isopropanol (propan-2-ol)	Merck	Damstadt, Germany	1.07022.2511

Chemical / Reagent	Supplier	Location of supplier	Catalogue Number
Methocult™	StemCell Technologies	Tullamarine	M3134
Muse™ Count & Viability Kit	Merck	Darmstadt, Germany	MCH600103
Neomycin sulphate	Sigma-Aldrich	St Louis, USA	N-1876
Penicillin/Streptomycin	Gibco / Life Technologies	NY, USA	15140-122
Sodium azide (NaN_3)	Sigma-Aldrich	St Louis, USA	S-2002
TEMED	Sigma-Aldrich	St Louis, USA	T-7024
Trypan blue solution (0.4%)	Sigma-Aldrich	St Louis, USA	T8154
0.5% Trypsin-EDTA	Gibco / Life Technologies	NY, USA	15400-054

2.4. Antibodies

2.4.1. Flow based

All antibodies used for flow cytometry in this study were purchased from Becton Dickinson Pharmingen (BD, San Diego, USA) unless otherwise stated in the following table and were stored at 4°C shielded from the light.

Table 2.4. ***Antibodies used in this study for flow cytometry***

Antibody (Supplier)	Conjugate	Clone	Specificity	Catalogue Number
7-AAD	-	-		559925
Annexin V	FITC PE	51-6874	Apoptotic cells	FITC: 556420 PE: 556422

Antibody (Supplier)	Conjugate	Clone	Specificity	Catalogue Number
B220	Bio PECy5 APC B220	RA3-6B2	B-cells	Bio: 51-01082J PECy5: 553091 APC: 553092 B220:553089
Caspase -3/7 (Molecular Probes)	FITC	35118	Apoptotic cells	V35118
CD3	Bio PE	145-2C11	T-cells	Bio: 51-01082J PE: 553063
CD4	APC	RM4-5	T-cells	APC: 553051
CD8a	PB FITC	53-6.7	T-cells	PB: 558106 FITC: 553030
CD11b (Mac-1)	Bio APC	M1/70	Macrophages, neutrophils, NK cells	Bio: 51-01712J APC: 553312
CD16/32 (FcγR)	PerCP5.5	2.4G2	Progenitor subsets - GMP	560540
CD19	APC-Cy7	1D3	B-cells	557655
CD25	PECy7	PC61	T-cell subsets	552880
CD41 (eBioscience)	Bio	eBioMWReg30	Platelets/ Megakaryoctes	13-0411-81
CD44	APC-Cy7	IM7	T-cell subsets	560568
CD45.1	PE	A20	Ly5.1 cells	553776
CD45.2	FITC	104	Ly5.2 cells	553772
CD48	APC-Cy7	HM48-1	SLAM marker	561242
CD71	FITC	C2F2	Erythroid progenitors	553266
c-Kit (CD117)	APC PE-Cy7 PCP5.5	2B8	HSCs + progenitor (LK / LSK cells)	APC: 553356 PECy7:558163 PCP5.5: 560557

Antibody (Supplier)	Conjugate	Clone	Specificity	Catalogue Number
CD105	PB	MJ7/18	Progenitor subsets-BFU-E, CFU-E, Meg-E	120411
CD150 (BioLegend)	PE	TC15-12F12.2	SLAM marker	115903
γH2AX (Cell signaling)	Alexa-647	20E3	DNA damage	#9720
DAPI (Life Technologies)	-	-	Cellular DNA content	D1306
Ki67	FITC	B56	Proliferating cells	556026
Ly6G (Gr-1)	Bio PE PECy7	PECy7: RB6-8C5 PE: 1A8	Granulocytes, neutrophils	Bio: 51-01212J PECy7: 552985 PE: 551461
Propidium Iodide (PI) (Life tech.)	-	-	Viability stain	V35118
SCA-1	PECy7 Bio	PECy7: Dy Bio: E13-161.7	HSCs (LK/LSK cells)	PECy7: 558162 Bio: 553334
Streptavidin (SA)-APC	Secondary antibody	-	2° antibody for Bio conjugates	554067
SA-APC-Cy7	Secondary antibody	-	2° antibody for Bio conjugates	554063
SA-BV605™ (BioLegend)	Secondary antibody	-	2° antibody for Bio conjugates	405229
TCRβ	PE	H57-597	T cells	553172
Ter119	Bio FITC	TER-119	Erythroid cells	Bio: 51-09082J FITC: 557915
Thy1.2	FITC	53-2.1	T-cells	553003

2.4.2. Western Blot

Table 2.5. ***Antibodies used in this study for Western Blotting***

All Western Blot antibodies were stored at 4°C.

Antibody	Species (Origin)	Size	Supplier	Catalogue Number
β-actin	Rabbit	45kDa	Cell Signaling Technologies	# 5125
Caspase-8	Rabbit	45 and 47kDa	Cell Signaling Technologies	# 4927
GAPDH	Rabbit	37kDa	Cell Signaling Technologies	# 8884
p53 (Total)	Mouse	53 kDa	Cell Signaling Technologies	# 2524
Phospho-p53 (Ser15) = Murine Ser18	Rabbit	53kDa	Cell Signaling Technologies	# 9824

2.5 Growth factors and cytokines

Recombinant murine interleukin-3 (IL-3) was supplied as a 10µg pellet from Peprotech (Rocky Hill, USA). This was reconstituted in 1ml PBS/2% FCS, divided into 200µL aliquots and stored at -20°C. For a 50 x working solution (250ng/mL final), a 200µL aliquot was diluted in 7.8mL of PBS/2% FCS, filter sterilized using a 0.22µm membrane and stored at 4°C.

Recombinant murine interleukin-6 (IL-6) was supplied as a 10µg pellet from Peprotech (Rocky Hill, USA). This was dissolved in 100µL of sterile H_2O to which a further 100µL of PBS/2% FCS was added. Aliquots of 10µL were stored at -20°C. For a 50 x working solution (50ng/mL final), a 10µL aliquot was diluted in 10mL PBS/2% FCS and filter sterilized before being stored at 4°C.

Recombinant rat Stem Cell Factor (rSCF) was purchased from Amgen (Thousand Oaks, USA) and also supplied as a 10µg pellet. This was reconstituted in 400µL PBS/2% FCS, divided into 200µL aliquots and stored at -20°C. For a 50 x working

solution (2.5µg/mL final), a 200µL aliquot was diluted in 1.8mL of PBS/2% FCS, filter sterilized using a 0.22µm membrane and stored at 4°C.

Purified recombinant human Erythropoietin (EPO) was also purchased from Amgen and supplied at 10,000U/mL. For a 100 x working solution (800U/mL final), 800µL of stock was diluted in 9.2mL of PBS/2% FCS, filter sterilized using a 0.22µm membrane and stored at 4°C.

2.6 Cell lines

The murine Eµ−Myc lymphoma cell line, murine myelomonocytic M1 cell line, murine factor-dependent cell progenitor (FDCP) cell line and the murine mouse embryonic fibroblast 3T3 cell line were used throughout the study to prepare controls for qPCR analysis or for Western Blot work.

2.7 Cell culture solutions (media)

Commercially acquired media including Roswell Park Memorial Institute medium (RPMI) and Dulbecco's Modified Eagle Medium (DMEM) was purchased from Gibco (Life technologies, USA). Media was usually supplemented with FCS and Penicillin/Streptomycin (Gibco) to give a final concentration of 10%(v/v) and 1%(v/v) respectively (i.e 50mL and 5ml). Additional media obtained from the Walter and Eliza Hall Institute of medical research (WEHI) and used for the purpose of progenitor cell assays included Dulbecco's Modified Eagle's Medium (mod-DME) and Iscove's Modification of Dulbecco's Medium (IMDM x 2). All media was stored at 4°C unless otherwise specified.

2.8 Supplements

2.8.1. Foetal calf serum (FCS)

Foetal calf serum was purchased from Gibco (Life Technologies). Heat inactivation was undertaken by immersion in a 56°C water-bath for one hour prior to storage at 4°C. This was filter sterilized through a 0.22µm membrane prior to use to remove any precipitates.

2.8.2. Penicillin / Streptomycin

For cell culture purposes, Penicillin and Streptomycin were added to culture medium. For a 500mL bottle of cell culture medium (DMEM or RPMI), a 1/100 dilution of the antibiotic preparation was used (i.e 5mL) equating to 50,000 units of penicillin and 50,000µg of streptomycin.

2.9 Oligonucleotides

All oligonucleotide primers used for genotyping and quantitative PCR were obtained as desalted pellets from GeneWorks (Hindmarsh, Australia). Master stocks at 100µM concentrations and working stocks at 10µM concentrations were prepared in MQH_2O and stored at -20°C.

2.9.1. Genotyping

All oligonucleotide primers used for genotyping are summarised in the following table.

<u>Table 2.6.</u> ***Oligonucleotides used for genotyping***

PCR conditions listed consist of an initial denaturation step, followed by amplification cycles (denaturation, annealing and elongation) and finally an extension period prior to cooling to 4°C until further analysis.

Primers	**5' → 3' sequence**	**Concentration**	**Size of amplicon**	**PCR conditions**
BCL-2	CPAL2: 5'-AAA ACC TCC CAC ACC TCC CCC TGA A-3' Bcl2GTF:5'-GGG ATG CCT TTG TGG AAC TGT ACG-3'	1µM 10µM	Transgene: 400 bp	96°C – 2 min 30 x (96°C – 30 s, 55°C – 30 s, 72°C – 60 s); 72°C – 7 min.
BIM	Bim KO1: 5'-AAG AAT CTA GGT TGA CTC TAG-3' Bim KO2: 5'-CAT TGC ACT GAG ATA GTG GTT GA-3' Bim KO3: 5'-CCC GTT GCA CCA CAG ATG AA-3'	10 µM 10 µM 10 µM	WT: 500 bp KO: 620 bp	94°C – 5 min 35 x (94°C – 15 s, 55°C – 20 s, 72°C – 30 s); 72°C – 7 min.
NHD13	Nup98-001: 5'-TGG AGG GCC TCT TGG TAC AGG-3' HoxD13L1: 5'-GGC TTC TAA GCT GTC TGT GGG C-3'	1µM 10µM	Transgene: 400 bp	96°C – 2 min 30 x (96°C – 30 s, 55°C – 30 s, 72°C – 60 s); 72°C – 7 min.
NOXA	Noxa 3'-2:5'-GAT GCT TCT TGG GTG CAC CCA CAC-3' Noxa 3'-del: 5'-AAA GCA ATC CCA AAC GAC-3' Noxa 5'-1: 5'-GGA GGG CAT AAA TGG GCA ATG ACA C-3'	10 µM 10 µM 10 µM	WT: 188 bp KO: 212 bp	96°C – 2 min 30 x (96°C – 30 s, 55°C – 30 s, 72°C – 60 s); 72°C – 7 min.

Primers	5’ → 3’ sequence	Concentration	Size of amplicon	PCR conditions
P21	P21 (1962): 5’-AAG CCT TGA TTC TGA TGT GGG C-3’ P21 (1963): 5’-TGA CGA AGT CAA AGT TCC ACC-3’ P21 (1964): 5’-GCT ATC AGG ACA TAG CGT TGG C-3’	10 µM 10 µM 10 µM	WT: 800 bp KO: 700 bp	94°C – 5 min 35 x (94°C – 30 s, 58°C – 60 s, 72°C – 60 s); 72°C – 10 min.
p53	p53x6s: 5’-TTA TGA GCC ACC CGA GGT-3’ p53x7as: 5’-TAT ACT CAG AGC CGG CCT-3’ p53neo: 5’-TCC TCG TGC TTT ACG GTA TC-3’	10 µM 10 µM 10 µM	WT: 450 bp KO: 600 bp	96°C – 2 min 30 x (96°C – 30 s, 55°C – 30 s, 72°C – 60 s); 72°C – 7 min.
PUMA	mPuma 3’-Del: 5’-ACC GCG GGC TCC GAG TAG C-3’ mPuma 3’-2: 5’-GGA CTG TCG CGG GCT AGA CCC TCT G-3’ mPuma 5’-1: 5’-AGG CTG TCC CTG GGG TCA TCC C-3’	10 µM 10 µM 10 µM	WT: 203 bp KO: 376 bp	94°C – 4 min 30 x (94°C – 40 s, 60°C – 30 s, 72°C – 60 s); 72°C – 5 min.

2.9.2. Primer sequences – RT-PCR

All oligonucleotide stock solutions were diluted to 10µM concentration in MQH_2O prior to use for the SYBR Green based qPCR.

Table 2.7. ***Oligonucleotides used for qPCR analysis***

Primers	Primer pair	5' → 3' sequence
Noxa	Sense Anti-Sense	5'- ACTGTGGTTCTGGCGCAGAT-3' 5'- TTGAGCACACTCGTCCTTCAA-3
Puma	Sense Anti-Sense	5'- ATGCCTGCCTCACCTTCATCT-3' 5'- AGCACAGGATTCACAGTCTGGA-3
P21	Sense Anti-Sense	5'- GGTGGGCCCGGAACATCT-3' 5'- GGCCCTACCGTCCTACTAAT-3'
GADD45	Sense Anti-Sense	5'- GCTGCCAAGCTGCTCAAC-3' 5'- TCGTCGTCTTCGTCAGCA-3'
HPRT	Sense Anti-Sense	5'- GCTGGTGAAAAGGACCTCT -3' 5'- CACAGGACTAGAACACCTGC -3
β-Actin	Sense Anti-Sense	5'- GTACCTGAACCGGCATCTG -3' 5'- GGGGCCATATAGTTCCACAA -3

2.10 Experimental mouse strains used in the study

Table 2.8. ***Mouse strains used in current study***

Mouse strain	Abbrev	Use in this work	Source / Reference
Nup98-HoxD13	*NHD13*	MDS mouse model	Dr Peter Aplan - (Lin et al. 2005)
TNF knockout	$TNF^{-/-}$	Crossed with *NHD13* to generate *NHD13* TNF-null mice (extrinsic pathway)	Dr B Saunders (Uni of Sydney) - (Körner et al. 1997)
Fas mutated mice	$Fas^{gld/gld}$	Crossed with *NHD13* to generate *NHD13* Fas-mutated mice (extrinsic pathway)	WEHI - (Roths et al. 1984; Takahashi et al. 1994)
P53 knockout	P53 KO / $p53^{-/-}$	Crossed with *NHD13* to generate *NHD13* p53-null mice	WEHI - (Donehower et al. 1992; Jacks et al. 1994)
Noxa knockout	Noxa KO/ $Noxa^{-/-}$	Crossed with *NHD13* to generate *NHD13* NOXA-null mice (intrinsic pathway)	WEHI - (Shibue et al. 2003)
Puma knockout	Puma KO / $Puma^{-/-}$	Crossed with *NHD13* to generate *NHD13* PUMA-null mice (intrinsic pathway)	WEHI - (Jeffers et al. 2003; Villunger et al. 2003)
Bcl-2 transgenic	BCL-2	For overexpression of *Bcl-2;* crossed with *NHD13* to generate double transgenic mice	WEHI - (Vaux et al. 1988; Strasser et al. 1990)
Bim knockout	Bim KO / $Bim^{-/-}$	Crossed with *NHD13* to generate *NHD13* Bim null mice (intrinsic pathway)	WEHI - (Bouillet et al. 1999)
Ly5.1	Ly 5.1	Wild-type mice – used as transplant recipients	WEHI
C57BL/6	BL/6	Wild-type mice – used as controls for various experiments	Monash University

Methods

Molecular biology techniques

2.11 DNA preparation + techniques

2.11.1. Genomic DNA extraction from tails

Tail biopsies were performed on mice upon weaning and collected into microfuge tubes. Ear clips were used in older mice. Genomic DNA was extracted using heat inactivation techniques. For each tail, 100µL of heat inactivating tail lysis buffer and 2µL of Proteinase K (at 10mg/mL) was added (usually made up as 1mL of buffer with 20µL of Proteinase K). Samples were incubated at 55°C overnight to allow for lysis. On the following day, samples were vortexed to ensure adequate digestion had occurred and then centrifuged for 5 min at maximum speed to pellet the debris. Samples were then heat-inactivated at 95°C-100°C for 5 min, centrifuged for 1 min at maximum speed and stored at 4°C until required.

2.11.2. Polymerase chain reaction (PCR)

For genotyping, extracted DNA was first amplified with the appropriate primers as listed in ***Table 2.6.*** Generally, for PCR for each sample, 1µL of template genomic DNA was added to 12.5µL of the appropriate DNA polymerase (JumpStart™, Sigma-Aldrich or GoTaq, Promega) and the appropriate concentration of primers for the gene of interest (generally 2µL of each 10µM primer mix solution or alternate concentration as indicated). The mix was supplemented with RNase free water to make up a final volume of 25µL. PCR conditions for each gene of interest are outlined in ***Table 2.5***. In each case, a positive and negative control was run to ensure the reaction was successful with no contamination.

2.11.3. Agarose gel electrophoresis of DNA

Gel electrophoresis was used to separate DNA based on fragment length to enable genotyping analysis. Generally, 1% agarose gels were prepared in 1 x TAE buffer to which 0.05µg/mL of EtBr was added. Samples were mixed with Orange G dye. To estimate the size of various DNA fragments – samples were loaded

adjacent to DNA markers. Two ladders were commonly used depending on the size of the DNA fragment of interest: a mix of ΦX 174 DNA/HaeIII and λ DNA/HindIII marker for larger fragments (Promega) or the 100bp ladder (New England Biolabs) for smaller fragments. Electrophoresis was performed in 1 x TAE buffer at 90V for 60-90 min. For visualization, bands were examined under UV light.

2.12. RNA preparation + techniques

2.12.1. RNA isolation with TRIzol®

Total RNA was isolated from lineage-depleted and sorted bone marrow cells for the purpose of sample preparation for qPCR and RNA-seq analysis. TRIzol® reagent (Invitrogen) was used as per the manufacturer's guidelines. This method relies on chloroform-phenol methodology as previously described (Chomczynski and Sacchi 1987). In general, cells were pelleted and resuspended in 500µL – 1mL of TRIzol® reagent as per guidelines. Samples were subsequently stored at -80°C until use. On thawing, samples were incubated at RT for 5 min to allow dissociation of nucleoprotein complexes. To eliminate debris, samples were initially centrifuged (12000 g for 10 min) after which 0.2mL of chloroform per 1mL of TRIzol® reagent was added to each sample. The resulting mixture was shaken vigorously for 15-20 seconds and then incubated at RT for 2-3 min. Samples were then centrifuged (12,000g for 15 min) to allow for separation into a colourless upper aqueous phase (where RNA resides), and a white interphase together with a lower red organic phase from which DNA and protein can be extracted. The aqueous phase was transferred into a fresh microfuge tube to which 0.5mL of isopropanolol and 10µg glycogen were added. Samples were then incubated at RT for 10 min to allow for RNA precipitation. RNA was then pelleted by centrifugation (12,000g for 10 min). 1mL of 75% EtOH was used per 1mL of initial TRIzol® reagent to wash the RNA pellets. The sample was then vortexed and centrifuged once more (7,500g for 5 min). Supernatants were discarded and the RNA pellets were allowed to air dry briefly (5-10 min) before being completely dissolved in nuclease-free water (Promega). For quantification of RNA concentration, a NanoDrop (ND-1000 - BioLab) Spectrophotometer was used. Samples were stored at -80°C until required. All centrifugation was carried

out at 4°C and samples were kept on ice between spins. Appropriate precautions were undertaken including use of gloves, barrier tips and specific RNA-only equipment in order to maintain the integrity of RNA.

2.12.2. RNA isolation with hybrid TRIzol®/RNeasy extraction protocol

To ensure RNA was produced with minimal impurities, at times (particularly for RNA-seq analysis), a hybrid extraction protocol was used – combining use of the TRIzol® reagent and the RNeasy MiniKit (Qiagen). The TRIzol® technique outlined above was executed through until the aqueous phase removal step. Subsequently, an equal volume of 100% RNA-free EtOH was added and slowly mixed in. The resultant sample was loaded into an RNeasy column (up to 700µL at a time) seated in a collection tube and centrifuged (8000g for 30 seconds). The flow-through was discarded. For samples > 700µL in volume, these steps were repeated. 700µL of the RW1 buffer was then added onto the column and centrifuged again (8,000g for 30 seconds). The flow through was discarded. The column was transferred into a new collection tube, to which 500µL of RPE buffer (with added ethanol) was added and centrifuged (8,000g for 30 seconds). After discarding the flow through again, an additional 500µL of RPE buffer was added and centrifuged (8,000g for 2 min). Flow through was discarded and the column was spun for an additional 1 minute. After transferring to a new 1.5mL microfuge tube, 35µL of nuclease-free water was added directly to the column and was allowed to sit at room temperature for 1-2 min. A final centrifuge step was undertaken (8,000g for 1 minute) to elute the RNA. Samples were stored at -80°C until use. Once again, all centrifugation was carried out at 4°C and samples were kept on ice between spins. For quantification of RNA concentration, a NanoDrop (ND-1000 - BioLab) Spectrophotometer was used. Appropriate precautions were again undertaken including use of gloves, barrier tips and specific RNA-only equipment in order to maintain the integrity of RNA.

2.12.3. RNA-seq analysis

RNA-seq was undertaken at the Australian Genome Research Facility (AGRF). For each sample provided to AGRF, a minimum of 3 mice were pooled from

which LK cells were sorted. RNA was extracted as outlined above. 3 samples were provided for each of the wild-type, *NHD13, BCL-2* and *NHD13-BCL-2* mouse lines. Samples were subjected to quality testing before being run on the Illumina True Seq platform with a 50bp read length used. Subsequent data analysis was provided through the Bioinformatics Platform from Monash University. Sequence reads were aligned against the mouse genome (mm10) using Bowtie 2 (Langmead and Salzberg 2012) and read counts were quantified using HTSeq (HTSeq-a Python framework to work with high-throughput sequencing data., 2015). Differential expression analysis was performed using Voom/Limma (Law et al. 2014) and visualization was performed using Degust software (http://victorian-bioinformatics-consortium.github.io/degust/). Genes were sorted by log-fold change and GSEA was used to test for rank-based enrichment of particular gene sets (Subramanian et al. 2005).

2.13. cDNA preparation and manipulation

2.13.1. cDNA synthesis using Reverse Transcription

Complementary DNA (cDNA) was synthesized by reverse transcription of total RNA using the Roche Transcriptor First Strand cDNA Synthesis Kit (Mannheim, Germany). This was subsequently used for the purpose of quantitative PCR (qPCR) reactions. As qPCR analysis was often performed on rare stem cell populations, 10µL of template RNA (or 1µg for higher concentrations of RNA) was used for each reaction. This was combined with 2µL of Random Hexamer Primer (at 600pmol/µL) and made up to 13µL in RNase free water. The primer/template mix was next incubated at 65°C for 10 min to ensure denaturation of RNA secondary structures. After incubation, 4µL of 5x reaction buffer (with 8mM $MgCl_2$), 0.5µL of Protector RNase Inhibitor (at 40U/µL), 2µL of dNTP mix (10mM = 10 x) and 0.5µL of Transcriptor Reverse Transcriptase (at 20U/µL) were added, giving a final volume of 20µL. The sample was mixed gently to enable collection at the bottom of the tube. For reverse transcription, the sample was then incubated for 10 min at 25°C followed by 60 min at 50°C. After incubation, reverse transcription was inactivated by heating the sample to 85°C for 5 min and then placing it on ice. For longer-term storage, samples were frozen and stored at -20°C.

2.13.2. Quantitative polymerase chain reaction (qPCR)

Quantitative polymerase chain reaction (qPCR) analyses were undertaken to measure the expression of various target genes in cDNA samples relative to housekeeper genes. Reactions were generated in a Roche LightCycler® 480 Real-Time PCR system using SYBR® Green-based reaction mixtures (Molecular Probes / Roche). Oligonucleotide primer sequences used for qPCR in this study are listed in ***Table 2.5.***

For each qPCR SYBR® Green-based reaction, 2μL of template cDNA, 0.25μL of each of the appropriate forward and reverse primers (at a concentration of 10μM), 2.5μL of RNase-free water and 5μL of GoTaq (2x) were combined to make a total reaction volume of 10μL. All reactions were run in triplicate. Cycling conditions for all SYBR® Green-based reactions included initial denaturation at 95°C for 5 min, followed by 50 amplification cycles of denaturation at 94°C for 15 sec, annealing at 60°C for 30 sec and elongation at 82°C for 15 sec. The final extension period was performed at 72°C for 10 min. For those oligonucleotide primers being used for the first time, qPCR products were subjected to electrophoresis on a 2.5% (w/v) agarose gel as previously described to confirm the presence of a single transcript.

As for PCR, for each gene of interest, a positive and negative control was used. Calibration was used across plates as required. Transcript quantities were calculated using the Roche LightCycler Analysis Software and were normalized to *HPRT* and/or *Actin* housekeeper values.

2.14. Protein preparation + techniques

2.14.1. Whole cell lysate generation

Whole cell lysates were generated from total / sorted bone marrow cells or from cell lines as required. Bone marrow cells were harvested or collected into PBS with 2% FCS. Cell lines were harvested by protease treatment as necessary. Having been quantified, samples were pelleted by centrifugation (5min at 300g). and then washed twice with cold PBS and resuspended in an appropriate volume

of lysis buffer (5 x SLAB made up with dH_2O). Generally, 100µL of buffer was used for every 5 x 10^5 cells. Following resuspension, samples were heated to 95-100°C for 5-10 min to ensure adequate lysis was achieved. Protein was then stored at -70°C until required.

2.14.2. SDS-Polyacrylamide gel formation

To generate an in-house polyacrylamide gel– a separating and stacking gel were initially prepared as per the 'Molecular solutions' section above. The separating gel was usually made up at 10%, although this was varied depending on the size of the protein being analyzed for. After setting up the gel formation apparatus, the separating gel was poured (with isopropanol on top) and incubated for at least 20 min to allow it to solidify adequately. Once this had been achieved, the isopropanol was poured off and washed with dH_2O (x 3). A piece of Whatmann's paper was then used to blot away any remaining water from the top of the gel. The stacking gel was then poured (with a comb in place). After allowing this to set, the comb was removed and the sample slots were washed with running buffer. Samples were then loaded as per the details below.

2.14.3. Western Blotting

Detailed Western Blot conditions are provided in ***Table 2.9***

Prior to loading, samples were boiled to 100°C for 5 min and then placed on ice. For equal loading, the same number of cells was loaded for each sample. For small volume lysates, these were diluted further with 1 x SLAB buffer to ensure equivalent volume loading. An in-house or commercially acquired Tris-Glycine polyacrylamide gel of the appropriate percentage (Invitrogen) was placed into a BioRad Mini Protean II electrophoresis chamber (Hercules, USA) and was subsequently filled with 1 x Western Blot running buffer. A pre-stained ladder was used and the gel was allowed to run for 15 min at 85V at RT, then 120-140V until the blue dye began to run out of the gel.

Prior to the end of electrophoresis, a piece of Hybond-P PVDF nitrocellulose membrane (Amersham) and two pieces of Whatman filter paper were cut to size

(~ 7.5cm x 10.5cm). The PVDF was soaked in 100% MeOH for 10 sec for activation and then washed in dH_2O for a few minutes before being left in Western Blot transfer buffer to equilibrate. Whatman paper was similarly equilibrated in Western Blot transfer buffer.

After electrophoresis was complete, the polyacrylamide gel was removed from the apparatus, trimmed and then soaked in 1 x Western Blot transfer buffer. A Western Blot transfer 'sandwich' was then assembled using a BioRad Mini Trans-Blot Cell cassette (Hercules, USA). This was equilibrated with the 1 x Western Blot transfer buffer and layered with the following in order from the black side: sponge, Whatman filter paper, polyacrylamide gel, membrane, second piece of Whatman filter paper and another sponge. The 'sandwich' continued to be soaked in Western Blot transfer buffer during assembly and a pipette was rolled over to ensure no air was trapped between the layers. Once assembled, the cassette was placed into a BioRad Mini Trans-Blot Cell and filled with 1 x Western Blot transfer buffer. This was left to run at 100V for 2 hrs at 4°C with stirring or 20V overnight at 4°C. An ice-block was added to the Blot Cell to prevent overheating during the transfer process.

Following transfer, the membrane was briefly stained with Ponceau S to ensure adequate protein transfer. The membrane was then rinsed with dH_2O and blocked using the appropriate blocking buffer for 1 hr at RT to prevent non-specific binding. After blocking, the membrane was rinsed with wash buffer and then incubated with the primary antibody at its appropriate dilution in 5% BSA in TBST at 4°C overnight.

The following day, the membrane was rinsed three times with wash buffer (TBST – 15 min per wash) and then incubated with the appropriate HRP-linked secondary antibody for 1hr at RT at a dilution of 1:5000. A further three washes were undertaken after incubation. For detection of protein levels, the ECL chemi-luminescence kit (Amersham) was used.

In the event that a different antibody needed to be tested on the same membrane, the membrane was stripped using an antibody stripping solution (Re-blot Plus, Millipore). After making up the stripping solution as per manufacturer's guidelines, the membrane was incubated with gentle mixing for 15 min at room temperature. The membrane was subsequently re-blocked two times for 5 min intervals and then re-probed with the next antibody of interest.

Table 2.9. ***Western Blot conditions***

Western blots were performed using an in-house or commercially-acquired tris-glycine polyacrylamide gel. Membranes were blocked for 1hr at RT using 5% skim milk / TBST, incubated with primary antibodies overnight at 4°C and then incubated in secondary antibodies for 1hr at RT on the following day. Details of buffer recipes are provided in Section 2.2 above. All washes involved 3 x 15min in TBST – unless otherwise specified.

Antibody (size)	**Primary**		**Secondary**	
	Antibody	**Conditions**	**Antibody**	**Conditions**
Total p53 (53kDa)	P53 (1C12) – Cell Signaling	1/1000 dilution in 5% skim milk / TBST; overnight incubation at 4°C	Anti-Mouse IgG, HRP-linked antibody	1/5000 dilution in 5% skim milk / TBST; 1hr at room temperature
Phospho-p53 (Ser 15) (53kDa)	Phospho-p53 (Ser 15) - #9284 – Cell Signaling	1/1000 dilution in 5% BSA / TBST; overnight incubation at 4°C	Anti-Rabbit IgG, HRP-linked antibody	1/5000 dilution in 5% skim milk / TBST; 1hr at room temperature
Caspase 8 (45kDa)	Caspase 8 - #4927 – Cell Signaling	1/1000 dilution in 5% skim milk / TBST; overnight incubation at 4°C	Anti-Rabbit IgG, HRP-linked antibody	1/5000 dilution in 5% skim milk / TBST; 1hr at room temperature
Actin (45kDa)	β-actin HRP (13E5) – #5125 - Cell Signaling	1/1000 dilution in 5% BSA / TBST; overnight incubation at 4°C	N/A	N/A
GAPDH (37kDa)	GAPDH HRP (14C10) - #3683 – Cell Signaling	1/1000 dilution in 5% skim milk / TBST; overnight incubation at 4°C	N/A	N/A

Cell preparations + techniques

2.15 Cell suspensions

2.15.1. Tissue culture cells

Cells were harvested using tryptase treatment as required. Resultant suspensions were pelleted by centrifugation (5 min at 300g at 4°C) and resuspended as appropriate.

2.15.2. Bone marrow

Bone marrow was harvested routinely from a femur and tibia (i.e one leg) or both legs depending on the required use. Marrow was flushed with 2-3mL of PBS / 2% FCS using 3mL syringes fitted with 23 gauge needles. Cells were then routinely enumerated prior to further use.

2.15.3. Whole blood analysis (blood counts and films)

Peripheral blood was harvested by cardiac puncture or submandibular bleed depending on the fate of the mouse at the time into buffered saline glucose citrate (BSGC)-lined syringes. Blood was subsequently expunged into EDTA tubes (Sarstedt) and kept at 4°C until time of analysis. Sample analysis was undertaken on the Hemavet Multispecies Hematology Analyzer (Drew Scientific). For cell counts, a minimum volume of 10μL was collected for the purpose of the analysis.

For the analysis of blood cell morphology, blood films were prepared on glass microscope slides (Superfrost) using 5-10μL of freshly obtained peripheral blood. After air-drying, films were stained by the Alfred Hospital Haematology Department using a May-Grunwald-Giemsa (MGG) stain. Slides were then covered with DePeX mounting medium (Merck/BDH) and cover-slipped before being examined using a Nikon light microscope.

2.15.4. Whole organ analysis (liver / spleen / thymus)

2.15.4.1 Whole organ homogenization

Whole organs were harvested from mice in 2-3mL of PBS/2% FCS. Organs were subsequently homogenized using 3mL syringe plungers and then flushed through a 40µm cell strainer. The homogenized suspension was then enumerated.

2.15.4.2 Whole organ histology

Histological sections were acquired from bones, spleen, liver and thymi. After collection, whole organs were fixed in 10% formaldehyde solution for at least one day and were then sent to Monash Histology (Monash University) for decalcification (if required), sectioning and staining. Sections were stained with a haematoxylin and eosin stain and examined by light microscopy (Nikon).

2.16 Cell cryopreservation and thawing

For long-term liquid nitrogen storage, 1 x 10^6 - 1 x 10^7 cells were pelleted and resuspended in freezing medium typically consisting of FCS solution with 10% (v/v) of the cryoprotectant dimethyl sulphoxide (DMSO). Samples were usually aliquoted into cryotubes (Nunc) and placed into an isopropanol bath. Samples were kept in the bath at -80°C overnight to allow for slow freezing and were then transferred to liquid nitrogen tanks.

For thawing, cryopreserved cells were removed from liquid nitrogen and allowed to rapidly thaw in a 37°C water bath. The cells were then mixed in with the appropriate culture medium in a drop-wise fashion to make up a final sample volume of 25mL in order to wash away the DMSO. Cells were subsequently centrifugated (300g, 5 min at 4°C) and the supernatant was aspirated. Cells were gently resuspended in the appropriate complete growth medium.

2.17 Cell counting

For evaluating cell counts (per mL) and viability, cells were enumerated using a haemocytometer chamber (Neubauer) or the Muse Cell Analyzer (Merck Millipore) using a dye exclusion method. Depending on sample cellularity,

variable dilutions were made and diluted with 0.4% trypan blue solution (Sigma-Aldrich) for enumeration using the haemocytometer or with Muse® Count and Viability Reagent for enumeration using the Muse machine. For the haemocytometer, a minimum of 50 cells was counted per sample to ensure accuracy of the overall cell count. Dilutions on the Muse Cell Analyzer were adjusted to ensure the machine did not deem the sample as 'too dilute' or 'too concentrated' (generally 1/100 or 1/200).

2.18 Flow cytometric analysis

Flow cytometric analysis was used extensively throughout this study. Immunostaining with fluorochrome-labelled antibodies against surface markers was usually undertaken first (except when caspase staining was used). Staining was performed in a 96 V-well plate. Plates were centrifuged at 300g for 5 min at 4°C throughout and samples were washed with PBS/2%FCS unless otherwise specified. After the cells of interest were harvested and counted, aliquots of 2 x 10^6 cells were pipetted into each well for single colour controls and actual samples. In cases where rarer haematopoietic stem cell populations were analysed or where a significant number of events needed to be recorded, 3 x 10^6 cells were used instead. Antibody concentrations were adjusted accordingly. After centrifugation, 10µL of 1:20 (v/v) IgG from rat serum (Sgma) was added to each sample and incubated on ice for at least 5 min to prevent any non-specific antibody binding. Primary antibody was made up as a master-mix in PBS/2% FCS and 30µL of this mix was added to each well. Total volume per well was calculated as 10µL for cell pellet, 10µL of block and 30µL of antibody master-mix = 50µL per well. Concentration of antibodies used has been summarized in ***Table 2.10.*** After primary antibody was added, samples were incubated for 20 min on ice in the dark. If a secondary antibody was required, samples were washed with PBS/2%FCS and centrifuged and resuspended in 30µL of the secondary antibody master-mix for 15 min on ice. Prior to analysis, samples were again washed, centrifuged and resuspended in 150µL of PBS/2% FCS. Analysis was undertaken on the BD FACSCanto II or the BD LSR II cell analyser (depending on the stains) using the BD FACS Diva software. Cell populations were analysed on the basis of their forward and side scatter properties. Control

tubes were used to set the appropriate voltage for each fluorochrome channel and for compensation purposes. FlowJo™ analysis software was used for post-acquisition analysis of samples. For samples that could not be analysed immediately, 100µL of FACS fixative was used to enable later analysis.

2.18.1. Caspase staining

Caspase 3/7 staining was undertaken using the Vybrant FAM Caspase-3/7 Assay Kit (Life Technologies) as per the manufacturer's guidelines. This technology uses fluorescent inhibitor of caspases (FLICA™) methodology that is cell-permeant and non-cytotoxic. Using a fluorescein reporter group (detected in the FITC channel), the reagent interacts with activated caspase by recognizing a specific aspartic acid-glutamic acid-valine-aspartic acid (DEVD) sequence. In this manner, the FLICA inhibitor directly measures the amount of active caspase present at the time the caspase is added. To prepare the 150x FLICA reagent stock solution, 50µL of DMSO was added to the lyophilized reagent. The vial was mixed thoroughly to ensure adequate dissolving of the reagent. At time of use, the 150x FLICA stock solution was diluted a further 1 in 5 by adding 1 part FLICA reagent to 4 parts PBS to prepare a 30x FLICA reagent working solution. For each sample, 8µL of stock solution was added to 240µL of PBS/2% FCS. Unused 30x FLICA reagent was discarded at the end of the day. 150x FLICA reagent stock solution was stored at -30°C protected from light. It was thawed a further two times after which it was discarded. Staining was undertaken for 1 hr at 37°C and cells were agitated every 20 min. Cells were washed in PBS/2% FCS twice prior to additional surface staining.

2.18.2. Annexin-V / 7AAD staining

Annexin-V and 7-aminoactinomycin D (7-AAD) staining were undertaken after surface staining was complete and immediately before analysis on the flow cytometer. Annexin-V acts by binding to exposed phosphatidylserine residues on the surface of a cell undergoing apoptosis. 7-AAD is a nucleic acid stain and can be used as a viability exclusion stain. For annexin-V staining, a 1/20 dilution of antibody was used (i.e 5µL in a total volume of 100µL). For 7AAD, 7.5µL of antibody was used per 100µL. Annexin buffer was used prior, during and after

staining. Samples were incubated for 15min at RT in the dark and were then analysed without spinning.

2.18.3. Cell fixation and permeabilization

After initial surface staining and prior to intracellular staining, cells were usually fixed and permeabilized. Depending on the population of interest, two different techniques were used (Cytofix/Cytoperm vs 4% PFA). Following centrifugation, cells resuspended in 100µL of the Cytofix/Cytoperm solution (BD Biosciences) were incubated for 20 min at 4°C before washing twice with Perm/Wash™ buffer. If 4% PFA was used to fix cells (10 min at 4°C), cells were subsequently permeabilized using 100µL of the Perm/Wash™ buffer (30 min at 4°C). This was followed by an additional wash step with the buffer prior to the addition of intracellular stains.

2.18.4. Intracellular stains (Ki67 and γH2AX)

Intracellular staining with Ki67 and γH2AX was used to analyse cell cycle and DNA damage respectively. Ki67 antibody was resuspended in PBS/FCS 2% at a 1/10 dilution (i.e 5µL / sample) and samples were stained overnight. On the following day, samples were washed as previous before proceeding to DAPI staining. For γH2AX staining, a 1/25 dilution of antibody (i.e 2µL/sample) was made up with the Perm/Wash buffer. Cells were incubated for two hours at room temperature. After washing, cells were resuspended in PBS for analysis the following day.

2.18.5. DAPI staining

DAPI staining was typically undertaken just before analysis on the flow cytometer machines. The DAPI stain was made up from a 500µM (500x) stock solution. 80µL of the 500x solution was diluted in 10mL of PBS to make a 4µM (4x) solution. The DAPI was then diluted a further 1:4 with PBS (35µL DAPI + 135µL PBS) before being added to samples (final concentration = 1µM). Cells were stained for 15 min at 4°C in the dark and were subsequently analysed without additional washing.

2.18.6. Chimerism analysis on peripheral blood

Peripheral blood was used for chimerism analysis (Ly5.1 vs Ly5.2) to determine the percentage of donor-derived blood cells after chimeric transplantation. Mice were typically bled on a four-weekly basis using submandibular bleeds. For accurate analysis with minimal background interference, red cells were lysed using red cell lysis buffer. Cells were incubated for 5-10 min at room temperature until the red cell solution became clear and then centrifuged following which the supernatant was discarded. Surface staining was undertaken as previously described. After washing, cells were then analysed on the BD FACSCanto II.

2.19 Lineage depletion and cell sorting

To isolate pure haematopoietic stem cell populations for the purpose of qPCR / RNAseq analysis or for chimeric transplantation, cell sorting was undertaken. If cells were to be used for subsequent transplantation purposes, the procedure was undertaken in a tissue culture laminar flow hood to maintain sterility as much as possible. Bone marrow was first harvested by flushing femora and tibiae of the appropriate mice and enumerated as previously described. Samples were pooled as required. Cells were then stained with Biotinylated Mouse Lineage Panel antibodies (BD Biosciences) using 1µL / per 2 $x10^6$ cells and incubated for 30 min on ice. After incubation and centrifugation, cells were resuspended in Qiagen Biomag Goat Anti-Rat IgG bead suspension (Qiagen) and incubated for 45 min at 4°C on a rotating wheel in the dark. Using a magnetic separation system, samples were subsequently mounted and lineage-positive cells bound to biotinylated antibodies were permitted to attach to the magnet. The bead-free fraction comprised of the lineage-negative population was collected, enumerated and re-stained with surface lineage markers (Lin PE, Sca-1 PE-Cy7 and Kit APC). Cells were then washed and resuspended at the appropriate concentration for the purpose of sorting. Prior to sorting, 1 µL of PI (at 1µg/mL) was added as applicable, to enable exclusion of dead cells. Cell sorting was undertaken on the BD FACS Aria II using BD FACS Diva software and cells were usually collected into 100% FCS to ensure their integrity. Once again, control tubes were used to enable accurate voltage setting and compensation.

After sorting, cells were pelleted by centrifugation and resuspended in TRIzol for RNA extraction or prepared for subsequent transplantation into donor mice by resuspending at the appropriate concentration.

Table 2.10. *Antibody cocktails used for flow cytometric analysis*

Concentrations are based on a final volume of 50µL in the 96-V-well plates; PB = peripheral blood.

* Protocols for flow-cytometric analysis of immature myeloerythroid precursors have been derived from work by Pronk et al. (Pronk and Bryder 2011).

Organ	Purpose of stain	Antibody cocktails	Cell marker profile	Antibody concentrations
Bone marrow	HSC staining (LK/LSK)	Lin-Bio (or Lin PE for sorting) SA-BV605; Kit-APC; Sca-1 PE-Cy7	Mature lineage markers: Gr-1, Mac-1, Ter119, B220, CD3 LK: Lin^-,Kit^+,$Sca\text{-}1^-$ LSK: Lin^-,Kit^+,$Sca\text{-}1^+$	Gr-1: 1/1000 Rest of lineage antibodies: 1/500 Kit: 1/100; Sca-1: 1/100 SA-BV605:1/500
Bone marrow	SLAM markers (LT-HSC/ ST-HSC/ MPP)	LSK as above CD150 PE; CD48 APC-Cy7	Gated on LSK LT-HSC: $CD150^+$,$CD48^-$ ST-HSC: $CD150^-$,$CD48^-$ MPP: $CD150^-$,$CD48^+$	CD150: 1/100; CD48: 1/100
Bone marrow	Progenitor subsets (BFU-E / CFU-E / GMP / Meg-E)	LK as above, Sca-1 Bio, CD41 Bio CD16/32 PCP; CD150 PE; CD105 PB	Gated on LK, $Sca\text{-}1^-$, $CD41^-$ BFU-E: $CD16/32^{lo}$,$CD150^+$, $CD105^+$ CFU-E: $CD16/32^{lo}$,$CD150^-$, $CD105^+$ GMP: $CD16/32^{hi}$ Meg-E: $CD16/32^{lo}$,$CD150^+$, $CD105^-$	CD16/32:1/100; CD105: 1/100

Organ	Purpose of stain	Antibody cocktails	Cell marker profile	Antibody concentrations
Bone marrow	Cell cycle	Surface stains as above DAPI, Ki67-FITC	G0: $Ki67^{lo}$, DAPI G0 peak G1: $Ki67^{hi}$, DAPI G0 peak G2SM: $Ki67^{hi}$, DAPI G2SM phase	Ki67: 1/10 DAPI: 1μM final concentration
Bone marrow	DNA damage	Surface stains as above γH2AX APC		γH2AX: 1/25
Bone marrow	Apoptosis	Surface stains as above Caspase-FITC OR Annexin-V PE/FITC and 7-AAD		Caspase: 1/30 dilution (8μL in 240μL) 7AAD: 5μL
Bone marrow, liver, spleen, thymus	Leukaemic profile (Lineage markers)	CD3 PE, B220 PE-Cy5, CD19 APC-Cy7, Ter119 FITC, Gr-1 PE-Cy7, Mac-1 APC	T-cells: CD3; B-cells: CD19 and B220; Erythroid: Ter119; Granulocytes, macrophages and monocytes: Gr-1 and Mac-1	CD3: 1/500; CD19: 1/500; B220: 1/500; Ter119: 1/500; Gr-1: 1/500; Mac-1: 1/250
Bone marrow, liver, spleen, thymus	Leukaemic profile (T-cell markers including DN1-4)	CD4 APC; CD8 PB; Thy1.2 FITC; TCRβ PE; CD44 APC-Cy7; CD25 PE-Cy7	SP T-cells: $CD4^+$ or $CD8^+$ DN T-cell populations: $CD4^-CD8^-$ DN1: $CD44^+CD25^-$ DN2: $CD44^+CD25^+$ DN3: $CD44^-CD25^+$ DN4: $CD44^-CD25^-$	CD4: 1/500; CD8: 1/500; Thy1.2: 1/500: TCR-β: 1/500; CD44: 1/1000; CD25: 1/400
PB	Chimerism analysis	Ly5.1 PE Ly5.2 FITC	CD45.1: Ly5.1 CD45.2: Ly5.2	Ly5.1 and Ly5.2 – 0.4μL/sample

2.20 Haematopoietic progenitor assays

Progenitor assays were used as a functional means of assessing the ability of haematopoietic cells to generate both myeloid and erythroid progenitors. Assays involved the use of semi-solid agar or methylcellulose for the analysis of colony-forming units granulocyte-myeloid (CFU-GM) or burst-forming units / colony-forming units erythroid respectively (BFU-E/CFU-E). This is based on previously described methods (Metcalf 1984).

2.20.1. Reagent preparation

2.20.1.1. 0.6% agar

0.6g of BactoAgar was dissolved per 100mL of MQH_2O by heating in a microwave until boiling. The solution was regularly swirled to allow the agar to dissolve in an even manner and was subsequently maintained at 42°C until time of use.

2.20.1.2. Methylcellulose

The methylcellulose used for colony assays was either made in-house using Methylcellulose (MeC) Powder (Fluka Biochemika) or commercially acquired MethoCult™ (Stem Cell Technologies). For the powder formulation, 30g of MeC powder was added to a 2L flask followed by 500mL of boiling dH_2O. The solution was permitted to reboil for a few minutes whilst being stirred using a magnetic stirrer. After allowing the MeC to cool to about 45°C, IMDM x 2 was added. The flask was subsequently placed at 4°C, covered in foil and allowed to stir overnight. The following morning the MeC was poured into 50mL tubes and frozen at -20°C. Tubes were subsequently thawed as required. For commercially acquired MethoCult™, additional components (IMDM + FCS) were added as per the manufacturer's guidelines. The methylcellulose solution was then aliquoted and stored at -20°C until use.

2.20.1.3. Cytokine cocktail for agar plates

Cytokines were added to agar plates prior to the addition of other components. To each plate, 20µL of 50 x mIL-3, 20µL of 50 x mIL-6 and 20µL of 50 x rSCF was added. Final concentrations of each cytokine were 5ng/mL mIL-3, 1ng/mL mIL-6 and 50ng/mL rSCF.

2.20.1.4. Cytokine cocktail for methylcellulose plates

Cytokines were added to methylcellulose plates prior to the addition of other components. To each plate, 20µL of 50 x mIL-3, 10µL of 100 x EPO and 20µL of 50 x rSCF was added. Final concentrations of each cytokine were 5ng/mL mIL-3, 8U/mL EPO and 50ng/mL rSCF.

2.20.1.5. Progenitor assay generation

All agar and methylcellulose cultures were performed in triplicate. For the agars – 0.6% agar was used to make up a media mix with the following ratios: 5 parts 0.6% Agar: 3 parts 2 x DMEM : 2 parts FCS giving a final agar medium of 0.3% agar in DMEM with 20% FCS. For methylcellulose assays, a media mix was made up with the following ratios: 8 parts methylcellulose, 3 parts (2 x IMDM), 3 parts dH_2O and 5 parts FCS. Cell suspensions were prepared and enumerated as previously described. Bone marrow harvest in these cases was undertaken under sterile conditions to minimize contamination. Bone marrow cells were then combined with 3mL of the appropriate media mix at a concentration of 5 x 10^4 cells / mL for agar cultures and 1 x 10^5 cells / mL for methylcellulose cultures. The 3mL cell and media mix was subsequently divided between three 35mm petri dishes (Sarstedt) to which the appropriate cytokines had been added. Dishes were swirled briefly to enable adequate mixture of the various components and were then left to air dry for at least 10 min at RT before being incubated at 37°C in a humidified incubator with 10% CO_2 for a period of seven days.

2.20.1.6. Staining of methylcellulose progenitor assays

To allow for more accurate differentiation between erythroid and myeloid progenitor colonies, methylcellulose colony assays were stained with 3,3'-di-amino-benzidine (DAB). One DAB tablet was dissolved in 10mL of PBS after which 10µL of hydrogen peroxide (30% w/w) was added. 500mcL of the staining mixture was added to each plate and incubated for at least 5 min prior to counting.

Animal experimentation

2.21 Animal ethics approval

Animal experiments performed in this study were approved by the Melbourne Health Research Directorate and University of Melbourne Animal Ethics Committee or the Alfred Medical Research and Education Precinct (AMREP) Animal Ethics Committee – depending on the site at which the experiments were undertaken. All experimental procedures were conducted in accordance with the Australian Code of Practice for the Care and Use of Animals for Scientific Purposes (2004).

2.22 Animal Husbandry

Mice used in this study were bred and maintained in either the BIO21 Institute animal facility under the supervision of the Facility Manager, Mr Max Walker and Animal Technologists, Ms Lan Ta and Ms Samantha Zahra; the University of Melbourne (Medicine) animal facility under the supervision of Facility Manager, Ms Jenny David and Animal Technologists, Ms Rebecca Bowyer and Ms Lara Mizhiritsky; Monash University Animal Research Laboratories (ARL) under the supervision of Facility Managers, Ms Emma Morgan and Ms Liliana Jackanic and Animal Technologists, Ms Naomi Borg and Ms Elyse Eble or the Alfred Medical Research and Education Precinct under the supervision of Facility Manager, Mr Steven Comber and Animal Technologist, Ms Kylie Spark. Mice were housed under standard conditions in a 12-hour dark/light cycle and were fed irradiated chow pellets and acidified water (tap water) as required. When euthanized, mice were sacrificed by CO_2 asphyxiation.

2.23 Animal procedures

2.23.1. Tail sampling for genotyping

Tail samples were acquired for the purpose of genotyping at the time of weaning. DNA was extracted as previously described in ***Section 2.11.1***. In older mice, where a repeat sample was required for analysis, ear notches were used.

2.23.2. Whole blood analysis

For peripheral blood analysis, submandibular bleeds were used as a simple and easy method for blood sampling from mice that were to be kept alive. This was used for haematological analyses (eg full blood examination or blood smears) or for chimerism studies. After immobilizing the mouse, an 18-20G needle was used to make a puncture towards the posterior portion of the cheek pouch. Up to 100µL of blood (2 drops) was collected into ethylene-diamine-tetra-acetic acid-(EDTA, Sarstedt) coated tubes. Pressure was subsequently applied to the puncture site using a clean gauze pad or cotton bud to stop blood flow. The mouse was observed for a further 15 min to ensure there were no complicating sequelae.

In cases where the mouse was to be sacrificed, CO_2 asphyxiation was undertaken and blood was collected immediately after death by cardiac puncture into BSGC-lined syringes and injected into EDTA Sarstedt tubes.

2.23.3. Irradiation + tail vein injections (for competitive transplants)

Competitive transplants were performed to study the repopulating potential of various stem and progenitor cell populations. Briefly, 6-week old WT and *NHD13* mice were used as donors. Ly5.1 mice were used as recipients and as the source of competitor cells. Mice were lethally irradiated with 2 doses of 550 rad (5.5Gy) of γ-irradiation, administered at least 3 hours apart using a Rad Source γ-irradiator. After resting the mice for 2-3 hours, tail vein injection was used for transplantation. To maximise the success of injection, mice were heated under a heat lamp for a minimum of 15 min to dilate the tail vein. Mice were transplanted with a sterile inoculum of donor Ly5.2 cells resuspended in a total volume of 200µL of PBS/2% FCS. Cells were admixed with 5 $x10^5$ competitor splenic Ly5.1 cells. For each cell population transplanted, four recipient mice were inoculated. After transplantation, mice were monitored daily for four weeks and were given antibiotic water to reduce the risk of bacterial infection.

Statistical analysis

Throughout this study, unless stated otherwise, all experiments were performed with a minimum of n = 3 for each genotype. Each experiment was performed at least two separate times. Where analyses have been combined, results have often been normalized. Results of experiments have generally been expressed as mean +/- standard error of the mean (SEM). For statistical significance testing, data was analyzed using the appropriate test and the associated p-value has been denoted using asterix symbols as defined in the figure legends. Kaplan-Meier curves have been used for analysis of survival data.

CHAPTER THREE

The Role of p53 in the Apoptosis of NHD13 MDS progenitors

Abstract

The role of p53 in the pathogenesis of malignancy has been studied for over 30 years. In this time, p53's importance in apoptosis, cell cycle arrest, DNA damage repair, autophagy, metabolism and senescence has been progressively deduced. Mutations of this gene have been described in MDS since the 1990s and portend a poor prognosis in various subcategories - contributing to ~ 10-15% of overall cases. In a subgroup of MDS cases (such as the 5q- syndrome), activation of p53 has been postulated as a mechanism of erythroid apoptosis implicating the intrinsic pathway. In this context, targeting p53 has been associated with an amelioration of this phenotype. In this Chapter, we show evidence of activation of the intrinsic pathway in our model and hypothesize this to be the key process underlying the apoptosis of *NHD13* HSCs. By generating *NHD13* mice deficient for p53, we demonstrate that the apoptosis of *NHD13* HSCs is p53-dependent and that erythroid survival in particular is more highly dependent on p53. Although the abrogation of apoptosis and rescue of cell numbers by targeting p53 presents a somewhat attractive possibility of improving the cytopenias associated with MDS, we show evidence of an expected detrimental effect through loss of p53. These findings provide initial clarification for the mechanism of apoptosis upstream of BCL-2 and form the basis of investigating downstream mediators within the intrinsic pathway in subsequent Chapters.

Background

3.1. P53

The tumour suppressor gene '*p53*' located on chromosome 17p has been considered one of the most highly mutated genes in human malignancy over the last three decades (Vogelstein 1990; Hollstein et al. 1991). Belonging to a small family of related proteins which includes p63 and p73, p53 was first isolated as a cellular partner of Simian Virus 40 (SV40)-derived tumour antigens in 1979 - although its exact role and significance at the time was not clear (Lane and Crawford 1979; Linzer and Levine 1979). The gene encodes a 53-kD nuclear phosphoprotein. Initial work in the 1980s seemed to suggest it was primarily an oncogene capable of transforming cells independently or co-operating with other oncogenes (Eliyahu et al. 1984; Jenkins et al. 1984; Parada et al. 1984; Eliyahu et al. 1985). However, approximately one decade later, p53's role as a tumour suppressor gene begun to emerge (Baker et al. 1989; Donehower et al. 1992).

In its wild-type form, P53 acts to prevent malignant transformation either by inducing cell cycle arrest (through induction of cyclin-dependent kinase 1a (*Cdkn1a* aka *p21*) and allowing for DNA damage repair; or driving cells towards apoptosis and/or senescence particularly when DNA damage is too great to repair. This multi-faceted role of p53 and the ultimate outcome (i.e repair vs senescence vs apoptosis) not only depends on the source and degree of DNA damage, but also on how dispensible the affected cell population is to the organism. In keeping with this, distinct differences in response to DNA damage are noted in haematopoietic stem cells (HSCs) in contrast to progenitor populations (HPCs) (Insinga et al. 2013; Insinga et al. 2014).

p53 also appears to have distinct functions under conditions of cellular homeostasis vs cellular 'stress.' During normal cellular homeostasis, p53 levels are held in check by the action of MDM2 (and similar E3 ubiquitin ligases) through post-translational mechanisms (Kubbutat et al. 1997). Although *Mdm2* is a transcriptional target of p53 (Barak et al. 1993), its associated protein MDM2 *(Hdm2* in humans), functions in a negative feedback loop targeting p53 for

proteasomal degradation through ubiquitylation (Haupt et al. 1997; Fuchs et al. 1998). MDM2 also acts to inhibit p53's transcriptional activity by binding to its N-terminal transactivation domain. As such, p53's half-life during cellular homeostasis is generally very short and its function is tightly regulated.

In contrast, p53 levels rise in the setting of various cellular stressors and through the activity of different signalling molecules. Genotoxic stressors include but are not limited to ionizing radiation (Lowe et al. 1993; de Vries et al. 2002), hypoxia, oncogenic stress and DNA damage (Halazonetis et al. 2008), ribosomal dysfunction (Dai et al. 2004; Panić et al. 2006) and oxidative stress. Often signalling thru downstream kinases such as ATM and ATR, cellular stress generally stabilizes p53 through post-translational modifications at various sites; the most common being N- and C- terminal phosphorylation, C-terminal acetylation, methylation, ubiquitylation and sumoylation (Appella and Anderson 2001). As an additional layer of complexity, different residues are modified in response to different 'stressors'. Ultimately, these modifications serve to disrupt the interaction between p53 and its main negative regulator, MDM2 (Jabbour et al. 2010).

The effects of p53 induced by these two opposing scenarios (cellular homeostasis / low stress vs high / acute stress) are strikingly different. Under conditions of low stress, an organism will often attempt to prevent damage to cells or repair those cells that have been damaged. This is in contrast to high-stress scenarios where the damaged cells are often eliminated. These seemingly opposite functions of p53 have been reviewed extensively by Vousden and Lane (Vousden and Lane 2007).

Once stabilized, p53 generally functions most efficiently as a tetramer, although functional dimeric forms do exist (Warnock et al. 2008). P53's main mechanism of action is that of a transcription factor in which it proceeds to activate or repress various target genes by binding to p53-binding sites within regulatory regions. Such effects are far-reaching and influence a number of cellular functions including apoptosis (Clarke et al. 1993; Schuler et al. 2003; Villunger et

al. 2003), G1/S cell-cycle arrest (el-Deiry et al. 1993), quiescence (Liu et al. 2009), co-ordination of DNA damage repair (Canman et al. 1995), autophagy and metabolism. Transcription-independent mechanisms of action have also been described. These may potentiate the apoptotic response in particular and are discussed below. A summary of a number of p53's downstream targets is provided in ***Figure 3.1***

3.1.1. P53 and haematopoietic stem cells

p53's role in regulating quiescence and as a negative regulator of HSC self-renewal (TeKippe et al. 2003; Akala et al. 2008; Chen et al. 2008; Liu et al. 2009) has long been recognised. These functions play an important role in ensuring the survival, longevity and integrity of this vital HSC population. In this context, p53 is most highly expressed in LSK cells and in particular, LT-HSCs.

Under stressful conditions, haematopoietic stem cells are permitted to cycle and divide in a symmetric fashion allowing expansion of the progenitor 'pool' (Passegué et al. 2005). Additionally, cell division allows repair of any acquired double-stranded breaks via homologous recombination – a process that requires cells to be actively cycling.

3.1.2. P53 and apoptosis

Within the apoptotic pathway, p53 is recognised for its important role in the regulation of a number of key target genes and proteins. As a transcription factor, it serves as a key activator of genes involved in the intrinsic apoptotic pathway such as *Bax* (Miyashita and Reed 1995), *Puma* (Nakano and Vousden 2001; Yu et al. 2001; Han et al. 2001; Jeffers et al. 2003)*, Bid* and *Noxa* (Oda et al. 2000; Shibue et al. 2003; Villunger et al. 2003). However, the role of p53 is not limited to the intrinsic pathway alone. Some evidence indicates it may contribute, albeit to a lesser extent, to the activation of the extrinsic pathway by engaging particular death-associated proteins (eg Fas and KILLER/DR5) at the cell surface (Owen-Schaub et al. 1995). P53 may also drive apoptosis independent of its transcriptional function by localizing to the mitochondria and regulating mitochondrial permeability directly. Studies indicate that in some

cases, it may behave in a similar fashion to the 'BH3-only proteins' and directly displace anti-apoptotic Bcl-2 like proteins (such as BCL-2 or BCL-xL) activating pro-apoptotic BAX or BAK signalling (Erster et al. 2004).

3.1.3. P53, cell cycle regulation and DNA damage

P53's role in cell cycle regulation is primarily mediated through its transcriptional activation of *Cdkn1a* (or *p21*) (el-Deiry et al. 1993). As the name suggests, p21 acts as a cyclin-dependent kinase inhibitor inducing reversible cell cycle arrest and allowing DNA repair to occur as required. In this context, one of p53's target genes involved in the DNA damage response and examined in this Chapter is *GADD45* (growth arrest and DNA damage) (Hollander et al. 1993).

3.1.4. P53 and tumour suppression

Loss of tumour suppression may occur in a number of ways and is not limited to loss of the p53 allele alone. In some cases, the mutated p53 protein may exhibit a dominant-negative effect acting to silence wild-type p53 function without loss of this allele (Vogelstein 1990; de Vries et al. 2002). Additionally, gain of function mutations within p53 may drive the development of a more aggressive tumour phenotype and broader tumour spectrum. In other cases however, mechanisms upstream of p53 may act to hinder its usual activation (eg mutations of ARF or CHK2 may allow MDM2 – its negative inhibitor - to function independently). Alternatively, downstream mediators of p53 function may be mutated.

Mutations are generally considered to fall into two main groups – those that alter the structure of the p53 protein itself and those that alter amino acids crucial for DNA binding. These two categories are not mutually exclusive in all situations.

The mechanism of p53's tumour suppressive role is one that has attracted much attention over the years. Apoptosis, cell cycle arrest and senescence in particular have been flagged as being pivotal for p53's function as a tumour suppressor gene. However, recent mouse models have raised some suspicions that this might not actually be the case (Dudgeon et al. 2006).

In the case of apoptosis, it is notable that mice deficient in PUMA, the key protein responsible for mediating the apoptotic response following p53 activation (Yu and Zhang 2008), do not exhibit increased spontaneous tumour formation (Shibue et al. 2003). However, loss of PUMA in the setting of an oncogene such as *Myc* can promote tumorigenesis (Michalak et al. 2009). These findings suggest that in the absence of potent apoptosis, p53 can still function as a tumour suppressor in certain cases. More recently, by generating mice deficient for *p21, Puma* and *Noxa,* Valente et al have been able to more definitively demonstrate that apoptosis and cell-cycle arrest are not key to p53's tumour suppressive role (Valente et al. 2013). As senescence was not completely abrogated, the authors were unable to definitively exclude this as a means of tumour suppression. Ultimately, it may be that p53 is capable of suppressing tumour formation using different mechanisms – and dependant on the source of cellular damage, the degree of damage and the cell-type affected. Findings in this area are eagerly awaited in years to come.

3.2. P53 mutations + MDS

As in lymphoid disease, p53 mutations are also associated with an unfavourable prognosis in myeloid disease (Wattel et al. 1994; Misawa et al. 1997). Point mutations in p53 were first described in MDS as early as 1994 (Adamson et al. 1995; Mori et al. 1995) and generally occur within the central DNA-binding domain. P53 itself is mutated in approximately 8-14% of MDS cases and is more often associated with high-risk and therapy-related MDS where it typically occurs in conjunction with complex karyotypes (i.e $\geq$ 3 cytogenetic abnormalities) (Haase et al. 2007). Invariably, it portends a fairly dismal prognosis in these cases, is associated with disease progression and poor response to therapy (Bejar et al. 2011b).

P53 mutations also occur in the low-risk, del(5q) subgroup of MDS patients at a frequency of approximately 15%. Although patients with del(5q) usually respond well to lenalidomide (List et al. 2006), the presence of a p53 mutation negates this favourable prognosis and is associated with an increased risk of leukaemic progression, shorter time to progression and failure to achieve a

complete cytogenetic response (Jädersten et al. 2011; Sebaa et al. 2012). Although many studies suggest that a p53 mutation is a later event in the progression of MDS to AML, Jadersten et al. suggest that the mutation may actually occur at an early stage and that clone size increases with disease progression and selection pressures.

3.3. P53 + Ribosomopathies

Not to be confused with p53 "mutations" in MDS, defective ribosomal biosynthesis has in recent years been associated with "activation" of p53; thus implicating the intrinsic pathway as a significant driver of apoptosis in MDS. Disorders that fall into this category have been coined as 'ribosomopathies' (Narla and Ebert 2010). The most well described example is the haploinsufficiency of RPS14 which is associated with the '5q- syndrome' (Ebert et al. 2008). RPS14 encodes for the 40S ribosomal subunit and is required for processing of 18S pre-rRNA. In this context, ribosomal proteins are thought to accumulate in the cell due to defective assembly, ultimately binding and sequestering MDM2. By inducing 'ribosomal stress' and through MDM2's inhibition, p53 is stabilised and activated, inducing cell cycle arrest and apoptosis. This process is believed to preferentially target erythroid cells - inducing their apoptosis and driving the anaemia that is characteristic of this disease (Dutt et al. 2011).

In vitro, this process has been replicated in SKM-1 cell lines (an MDS line). Lentiviral suppression of RPS14 reduced proliferation rates, activating p53 and inducing apoptosis (Wang et al. 2014b)

An in vivo mouse model by Barlow et al reveals similar results. Loss of a section of chromosome 18 (syntenic to the 5q region and containing the RPS14 gene) generates an 'MDS mouse model' with evidence of a dysplastic macrocytic anaemia, high levels of p53 and increased apoptosis (Barlow et al. 2010). Of significance, when these mice are crossed with mice deficient in p53, the MDS phenotype is rescued with disappearance of dysplasia and rescue of progenitor and stem cell populations (including CMPs, MEPs, GMPs + HSCs). These findings

highlight the role and contribution of p53 in the apoptosis of MDS progenitors and importantly, implicate the intrinsic pathway.

3.4. P53 deficient mice

P53-deficient mice have been quite well characterized since they were first described in 1992 (Donehower et al. 1992). Although normal at birth, there is evidence that some p53-deficient mice exhibit developmental abnormalities due to failure of neural tissue to undergo apoptosis. These findings appear to be strain dependent. Haematopoiesis generally appears to proceed normally with these mice exhibiting normal peripheral blood counts and bone marrow cellularity (TeKippe et al. 2003). However, given the role p53 plays as a negative regulator of HSC self-renewal, it is not surprising that these mice exhibit an increase in stem cells numbers (both LSK and LT-HSC) (Chen et al. 2008). This is most likely the result of enhanced self-renewal and not the prevention of apoptosis (Liu et al. 2009). Functional assays corroborate an associated gain of function and these stem cells show evidence of an engraftment advantage during competitive bone marrow transplant assays, when transplanted as a subset of whole bone marrow cells (Chen et al. 2008).

Although these findings have provided a rationale for targeting p53 as a means of expanding the stem cell 'pool', the unregulated proliferation associated with p53-deficiency, exposes HSCs to a higher risk of accumulating mutations and DNA damage. In keeping with this, mice deficient for p53 typically develop thymic lymphoma or sarcoma with an invariably fatal outcome from about 6-7 months of age onwards (Jacks et al. 1994). An increased incidence in tumour formation is also noted in p53 heterozygous mice (+/-) and in secondary bone marrow transplant recipients when whole bone marrow is used as the source of stem cells (TeKippe et al. 2003). These findings suggest an inherent issue within the bone marrow cells themselves and are relevant to findings in this Chapter.

3.5. *NHD13* mice and p53

The Nimer group have previously published some work in which p53 was increased in immature LSK cells and $CD71^{+}Ter119^{-}$ erythroid cells using flow

cytometric analysis. In this context, the use of a p53 inhibitor was shown to have some partial benefit on myeloid abnormalities, but the effect and actual relationship to apoptosis was never examined. Of significance, p53 inhibition through the use of pfithrin did not rescue the associated anaemia or result in improved overall survival. Additionally, no change in LSK or SLAM population numbers was reported in this context. Generation of *NHD13*.p53 deficient mice showed similar results – with no rescue of the associated anaemia. In contrast, loss of both p53 alleles resulted in a rescue of LT- and ST-HSC numbers, LSK cells, GMPs and MEPs. The mechanism for this was not clearly examined (Xu et al. 2012b).

Results

3.6. Characterizing *NHD13* stem cell and progenitor subpopulations

3.6.1. *NHD13* LK and LSK progenitors are reduced in number

Throughout this study, we have used the *NUP98-HOXD13* transgenic mouse model as it recapitulates some of the key features of human myelodysplastic syndrome (MDS). Peripheral blood cytopenias typically develop from approximately 3 months of age onwards and are usually represented by a macrocytic anaemia and associated thrombocytopenia. The cytopenias occur in spite of a normo- or hypercellular bone marrow (Lin et al. 2005) giving rise to the phenomenon referred to as 'ineffective haematopoiesis'.

To further understand the basis of this discrepancy, we begun by enumerating the numbers and percentages of well-defined haematopoietic stem cell and progenitor cell populations using flow cytometry. Within the lineage-negative population, bone marrow progenitors can be divided into an immature $lineage^{neg}$, KIT^{+}, $SCA\text{-}1^{+}$ (LSK) population and a more mature $lineage^{neg}$, KIT^{+}, $SCA\text{-}1^{-}$ (LK) population. Analysis of *NHD13* mice revealed relative proportions of LK and LSK cells are reduced 4-fold and 6-fold respectively in keeping with previous reports (Chung et al. 2008; Xu et al. 2012b). Absolute cell numbers mirrored these findings ***(Figure 3.2).***

3.6.2. *NHD13* results in significant loss of stem cell subsets – particularly LT and ST-HSCs

Within the LSK population, we analyzed more refined stem cell subsets as defined by the Signaling Lymphocyte Activation Molecules (SLAM) surface markers, CD48 and CD150. These include long term (LT)-HSCs ($CD150^{+}CD48^{-}$), short term (ST)-HSCs ($CD150^{-}CD48^{-}$) and multi-potent progenitors (MPPs) ($CD150^{-}CD48^{+}$) (Chen et al. 2008). We noted a significant reduction in all three cell populations which was more marked for LT- and ST-HSC (> 10-fold reduction). Absolute cell numbers of these populations again mirrored these findings ***(Figure 3.3)***

In contrast to the LSK population, the LK population is comprised of more mature and terminally differentiated progenitors – including burst-forming units erythroid (BFU-E), colony-forming units erythroid (CFU-E), granulocyte-macrophage progenitors (GMP) and megakaryocyte erythroid (Meg-E) progenitors. Within this population, we found an approximate two-fold reduction in GMP and BFU-E cell numbers. The reduction in Meg-E was less striking ***(Figure 3.4)***. Thus, we see a widespread reduction in stem-cell and progenitor cell numbers with the greatest effect seen in the LT- and ST-HSC sub-populations.

3.6.3. *NHD13* LT-HSC exhibit reduced engraftment capacity from a functional perspective

Although reduced in numbers, flow cytometric results do not provide insight into the function of various progenitor subsets. Previous studies have confirmed the presence of self-renewing cells capable of generating MDS within the lineage negative population of cells (Chung et al. 2008). However, a more detailed phenotype has not been defined to date.

To evaluate stem cell repopulating potential and define which cell might be most relevant in leukaemic transformation, we set up a number of chimeric transplants. Briefly, WT and *NHD13* LK cells or LT-HSC or MPPs were transplanted into lethally irradiated recipient Ly5.1 mice – with additional engraftment support provided by splenic cells ***(Figure 3.5A).*** Mice were bled on a monthly basis and peripheral blood chimerism was analyzed based on Ly5.1 vs Ly5.2 expression. WT and *NHD13* LK cells did not show any repopulating potential – with peripheral blood wholly comprised of recipient Ly5.1 cells over the first two months ***(Figure 3.5B).*** In contrast, WT LT-HSC cells showed increasing repopulating potential over time as expected. Somewhat differently, *NHD13* LT-HSC showed impaired repopulating potential and comprised only a very small percentage of haematopoietic cells (< 1%) over the 4-month course of observation. Both WT and *NHD13* MPP cells showed somewhat better reconstitution than the *NHD13* LT-HSC. This diminished with time but did not all together disappear at 4 months post-transplant. From these results, we infer that

the phenotype of the predominant long-term repopulating cell in mice expressing the *NHD13* transgene most closely resembles that of the MPP cell, although the period of observation does not entirely exclude the *NHD13* LT-HSC population.

3.6.4. Apoptosis characterization in *NHD13* stem cell and progenitor subsets

Within the various subsets described, we sought to determine if increased apoptosis might be responsible for the reduced cell numbers seen. Using caspase-3/7 staining, which we found to be fairly sensitive for detecting apoptosis, we were able to demonstrate that apoptosis is increased in the more immature LSK population and MPP subset by about 2-fold in each case ***(Figure 3.6)***. However, due to significantly reduced numbers of LT- and ST-HSCs in *NHD13* mice, we were unable to accurately quantify apoptosis in these subpopulations. In the more mature progenitor subsets (BFU-E, CFU-E and GMP) – apoptosis was significantly reduced ***(Figure 3.7)***.

Thus, in keeping with human MDS, we note that apoptosis in the *NHD13* mouse is increased in the more immature stem-cell subpopulation. This most likely accounts for reduced HSC numbers and is the likely cause of reduced numbers of more differentiated cells downstream (BFU-E, CFU-E and GMP).

3.6.5. Apoptosis of *NHD13* HSCs is not mediated by the extrinsic pathway

As BCL-2 overexpression has previously been shown to rescue the apoptosis of *NHD13* HSCs (Slape et al. 2012), these findings implicate the intrinsic pathway as the predominant driver of apoptosis in this model. However, other groups have attributed the excessive apoptosis of early-stage human MDS to activation of the death receptor pathway (Gersuk et al. 1998; Claessens et al. 2002; Sawanobori et al. 2003). Therefore, we sought to determine the specific mechanism of increased apoptosis in *NHD13* LSK cells. Increased apoptosis as measured by caspase-3/7 or annexin may be secondary to cell extrinsic factors (such as TNF-α or Fas ligand) or cell intrinsic factors.

To address this question, we generated *NHD13* mice deficient in TNF-α or Fas ligand and noted no reduction in apoptosis as measured by flow cytometric analysis ***(Figure 3.8A)*** and no rescue of progenitor numbers using agar and methylcellulose progenitor assays ***(Figure 3.8B)***. Analysis for cleaved caspase 8, as a marker of activation of the extrinsic pathway was also negative for *NHD13* HSCs ***(Figure 3.9)***. Thus we conclude that the extrinsic pathway of apoptosis does not contribute significantly to the apoptosis of *NHD13* HSCs.

3.6.6. Apoptosis of NHD13 HSCs is predominantly mediated by the intrinsic pathway

Although the truncated BH3-only protein (t-Bid) allows for communication between the intrinsic and extrinsic pathways of apoptosis (Wei et al. 2000), this tends to be specific for certain cell types alone such as hepatocytes (Yin et al. 1999). Having excluded the extrinsic pathway as a significant contributor in the apoptosis of *NHD13* progenitors, we sought to corroborate our findings with BCL-2 overexpression which implicate a cell-intrinsic mechanism.

In this context, P53 is a well-described activator of the intrinsic pathway – through its transcriptional regulation of BH3-only genes, *Puma* (Nakano and Vousden 2001; Jeffers et al. 2003), *Noxa* (Oda et al. 2000; Shibue et al. 2003; Villunger et al. 2003; Michalak et al. 2008) and *Bax* (Miyashita and Reed 1995; Thornborrow et al. 2002; Chipuk et al. 2004). Western blot analysis of whole bone marrow for total p53 and phospho-p53 Serine 18 (a marker of response to DNA damage and the equivalent of Serine 15 in the human p53 protein) (Warnock et al. 2008) did not show a significant difference between WT and *NHD13* (not shown). Flow cytometric analysis allowed us to examine rarer populations and in this setting, LT-HSCs and MPPs were shown to have increased levels of total p53 and phospho-p53 Serine 18 ***(Figure 3.10)***. From this, we surmise there is some evidence that in the *NHD13* model, p53 may drive the apoptosis of immature haematopoietic stem cells.

To further validate our findings, we analysed the expression of an assortment of p53 transcriptional target genes in a sorted LSK population of cells. Genes

analysed included the pro-apoptotic BH3-only genes, *Puma* and *Noxa,* the cyclin-dependent kinase inhibitor, *CDKN1a* (aka *p21*) and the DNA damage response gene, *GADD45*. Of the four genes, we found *Noxa* to be the only gene significantly upregulated ***(Figure 3.11)*** with no significant change in *Puma* or *GADD45.* For p21, we noted reduced expression levels in NHD13 LSK cells – an observation that likely explains the increased cell cycling seen in this stem cell population. We reviewed these same genes using RNA-seq analysis data and found this accurately aligned with our qPCR findings (Not shown)

From this, we conclude that *NHD13* HSCs show modest evidence of p53 activation – through increased total and activated p53 levels and increased expression of p53's transcriptional target, *Noxa.*

3.7. Deducing the role of p53 in the apoptosis of *NHD13* HSCs

3.7.1. Loss of p53 rescues LSK and MPP cell numbers

To further investigate a cell-intrinsic mechanism for the increased apoptosis of NHD13 progenitors, we devised a breeding strategy to generate *NHD13.p53* heterozygote and *NHD13.p53* homozygote knockout mice. Breeding was limited somewhat by the increased tumour susceptibility of p53 deficient mice as has previously been described by Donehower et al (Donehower et al. 1992). We proceeded to quantify cell populations following loss of p53.

In the setting of the *NHD13* transgene, both LK and LSK populations revealed a rescue of cell numbers upon removal of p53 ***(Figure 3.12A)*** in keeping with p53's role in maintaining stem cell quiescence (Liu et al. 2009). We proceeded to analyse further subpopulations of the LSK and LK populations. Within the LSK population, the marked reduction in LT-HSC and ST-HSC numbers was surprisingly not rescued following loss of p53. This was in contrast to the MPP population, which demonstrated a rescue of both absolute and relative numbers not too dissimilar from wild-type levels ***(Figure 3.12A & B).*** As the MPP subset comprises the majority of LSK cells (in NHD13 mice), we surmised that the rescue of LSK cell numbers was predominantly a reflection of MPP cell number rescue. Further analysis of the LK population and its subsets will be discussed

later in this chapter. Thus, we note that loss of p53 is associated with a rescue of LSK and MPP cell numbers but not LT- or ST-HSCs.

3.7.2. P53 drives the apoptosis of NHD13 LSK and MPP cells

Flow cytometric analysis for activated caspase 3/7 was used to determine if rescue of LSK and MPP cell numbers in *NHD13*.p53 deficient mice was explained by reduced apoptosis. We found that the removal of p53 prevented the apoptosis of LSK cells which is predominantly comprised of MPP cells in the NHD13 mouse ***(Figure 3.13).*** Due to significantly reduced cell numbers, we were unable to measure apoptosis in the more primitive LT-HSC and ST-HSC populations.

Thus we conclude that the increased apoptosis of NHD13 LSK (and MPP cells) occurs by way of a cell-intrinsic mechanism that is p53-dependent. Targeting p53 is additionally associated with rescue of these populations.

3.7.3. P53's differential role in the apoptosis of mature erythroid vs myeloid progenitors

P53 activation in the context of ribosomal dysfunction in MDS has been well documented by a number of groups (Barlow et al. 2010; Dutt et al. 2011) and has been linked to a phenotype of 'anaemia'. This is particularly evident in association with the '5q- syndrome' (Ebert et al. 2008) – a subtype of MDS with a relatively good prognosis. Despite the somewhat limited evidence for p53 activation in our model, we sought to determine if there might be a lineage-specific effect in association with p53-deficiency. To determine the role of p53 in the more mature progenitor populations of *NHD13* mice, we used agar and methylcellulose colony assays.

Surprisingly, colony assays revealed a significant differential effect. NHD13 mice lacking p53 exhibited a potent rescue of erythroid (BFU-E) but not myeloid (CFU-GM) progenitors ***(Figure 3.14)***. We proceeded to examine similar LK subpopulations using flow cytometry and corroborated our colony assay results – loss of p53 rescued erythroid progenitor subsets. In the case of GMP, these were reduced in $p53^{-/-}$ mice alone making interpretation somewhat difficult

(Figure 3.15A & B). Further examination of total p53 protein expression levels using flow cytometry revealed higher expression in erythroid subpopulations compared to myeloid subpopulations suggesting a greater contribution and thus dependence on p53 in erythroid but not myeloid apoptosis ***(Figure 3.16)***. Thus, these findings suggest a differential role of p53 in programmed cell death of erythroid progenitors compared to myeloid progenitors.

As ribosomal dysfunction correlates with anaemia in human MDS, we examined ribosomal gene expression in *NHD13* mice based on RNA-seq analysis. We found that of 108 ribosomal proteins, only the expression of ribosomal protein S4-like (*RPS4l*) was significantly reduced ***(Figure 3.17A)***. Additionally, genes usually increased by loss of RPS14 (Ebert et al. 2008) were reduced in NHD13 LK cells based on gene set enrichment analysis (GSEA) ***(Figure 3.17B).*** These results favour a non-ribosomal mechanism for activation of p53 in this model.

3.7.4. Loss of p53 is associated with significantly shortened survival in *NHD13* mice

To examine the long-term effects that loss of p53 might have on the MDS phenotype, we aged the *NHD13.p53*$^{+/-}$ (heterozygous) and *NHD13.p53*$^{-/-}$ (homozygous) mice. Not surprisingly, loss of p53 was associated with a significant reduction in the time to tumour development in both *NHD13.p53*$^{+/-}$ and *NHD13.p53*$^{-/-}$ mice. The median survival of *NHD13.p53*$^{-/-}$ mice was 95 days compared with 126 days for p53-deficient mice alone ($p < 0.01$) and 353 days for NHD13 mice alone ($p < 0.0001$). *NHD13. p53*$^{+/-}$ also had a shortened median survival of 250 days compared with p53 heterozygous mice alone ***(Figure 3.18)***. Although, p53 deficient mice typically develop thymomas or soft tissue sarcomas by an age of 6 months (Donehower et al. 1992), examination of the tumour spectrum in our mice revealed a mixture of acute myeloid and acute T-cell lymphoblastic leukaemia ***(Figure 3.19)***. Therefore, in keeping with p53's tumour suppressive role, loss of p53 in the presence of the *NHD13* oncogene contributed to increased leukaemic transformation with a shorter time to disease development.

Figures

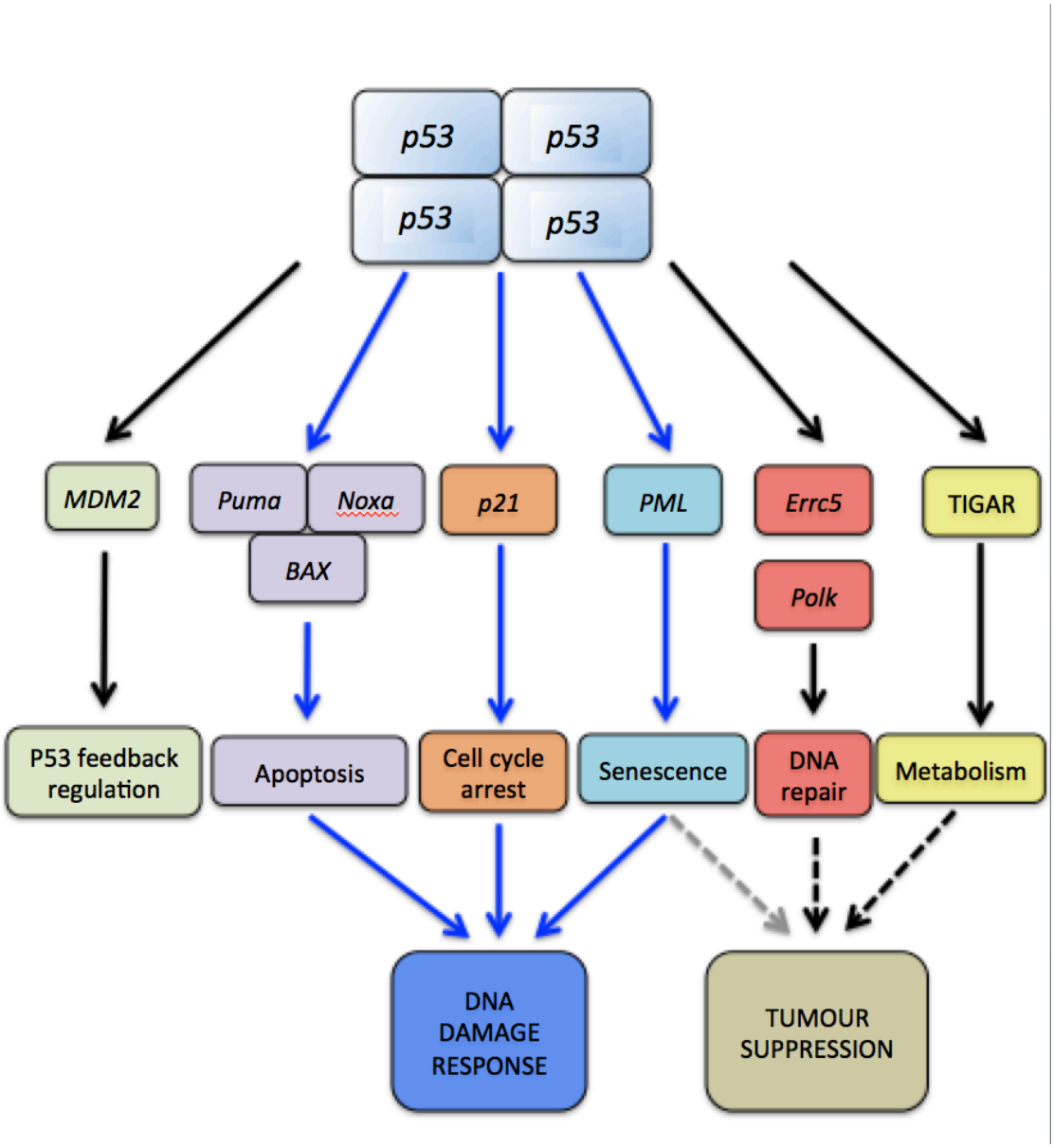

Figure 3.1. ***Downstream targets of p53 and their associated cellular processes***

Schematic of a limited repertoire of p53 target genes and the cellular processes they control. In its activated form, p53 exists as a tetramer. Current schematic is based on recent work by Valente et al (Valente et al. 2013).

Figure 3.2. ***Quantification of NHD13 HSC and progenitor populations***

(A) Relative quantification of the more mature lineage^{neg}, KIT^{+}, SCA-1^{-} (LK) cell population and the immature lineage^{neg}, KIT^{+} SCA^{+} (LSK) cell populations. Flow plots are initially gated on lineage negative cells. Numbers shown represent percentages of total nucleated cells. Results are representative of multiple replicates with three mice used per genotype per experiment (> 3); (B) Absolute number of cells per mouse leg (tibia + femur). Numbers represent the aggregate of > 5 experiments; ** = $p < 0.01$.

A

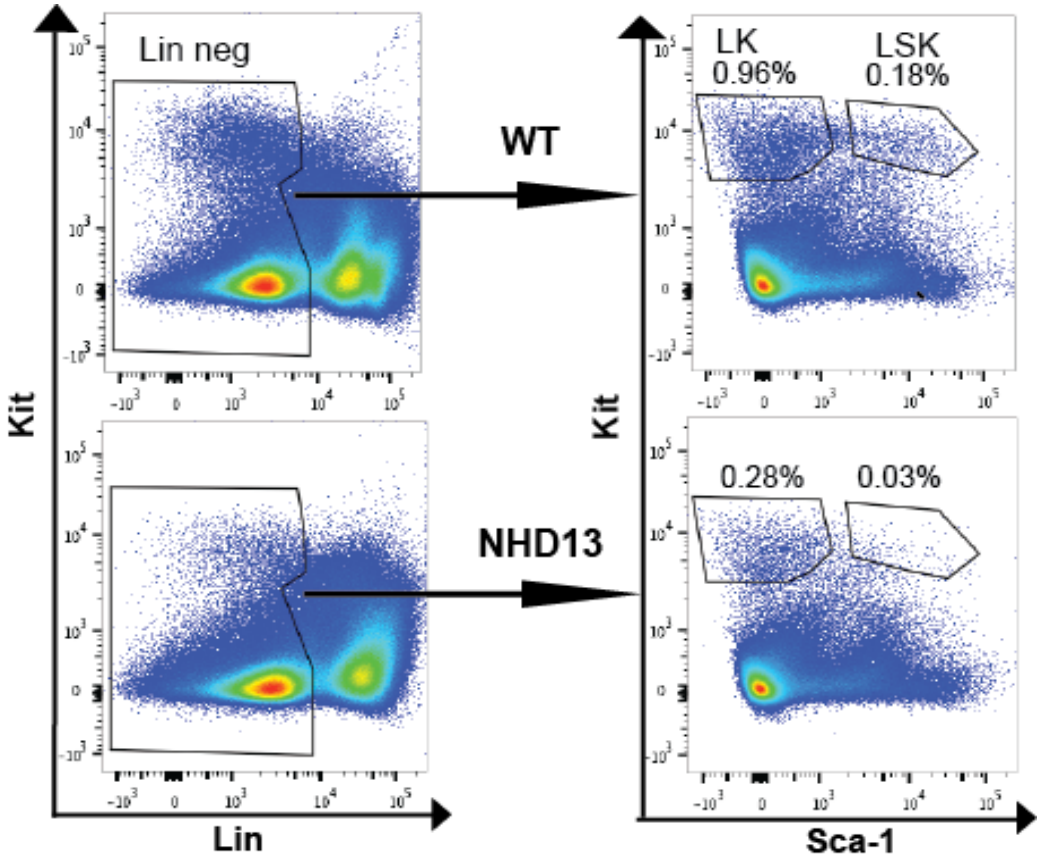
Lin neg
WT
NHD13
LK
0.96%
LSK
0.18%
0.28%
0.03%
Kit
Lin
Sca-1

B

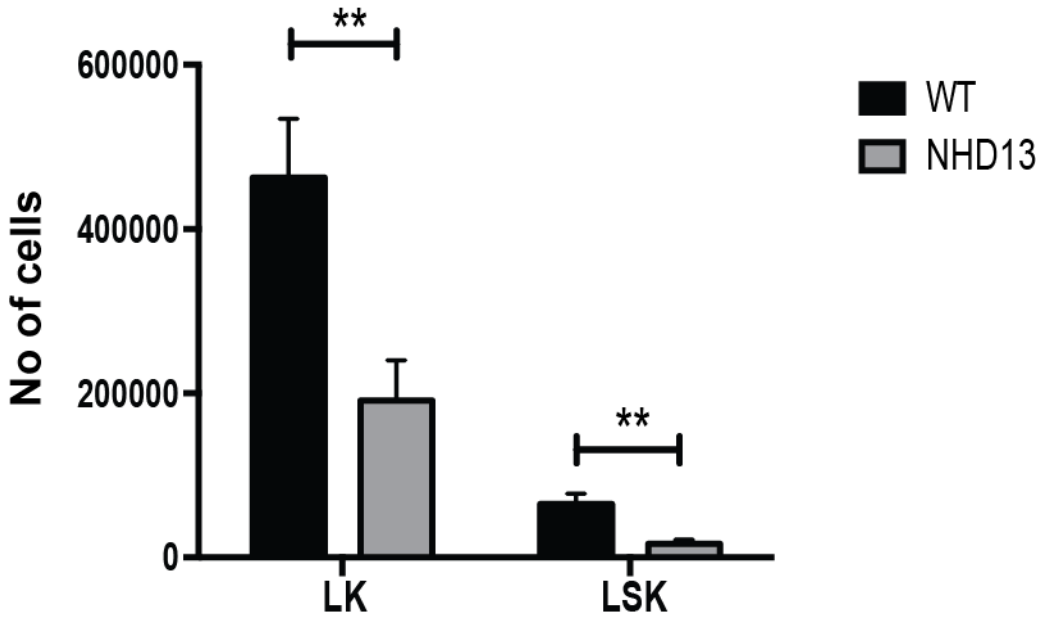
**
**
600000
400000
200000
0
No of cells
LK
LSK
WT
NHD13

<u>Figure 3.3.</u> ***Quantification of NHD13 HSC sub-populations***

(A) Relative quantification of HSC subpopulations. Numbers shown represent percentages of total nucleated cells. Flow cytometry plots are initially gated on LSK cells. HSC populations shown include LT-HSCs ($CD150^{+}CD48^{-}$), ST-HSCs ($CD150^{-}CD48^{-}$) and MPPs ($CD150^{-}CD48^{+}$); (B) Absolute number of cells per mouse leg (tibia + femur). Numbers represent the aggregate of > 5 experiments; ** = $p < 0.01$; *** = $p < 0.001$; **** = $p < 0.0001$

A

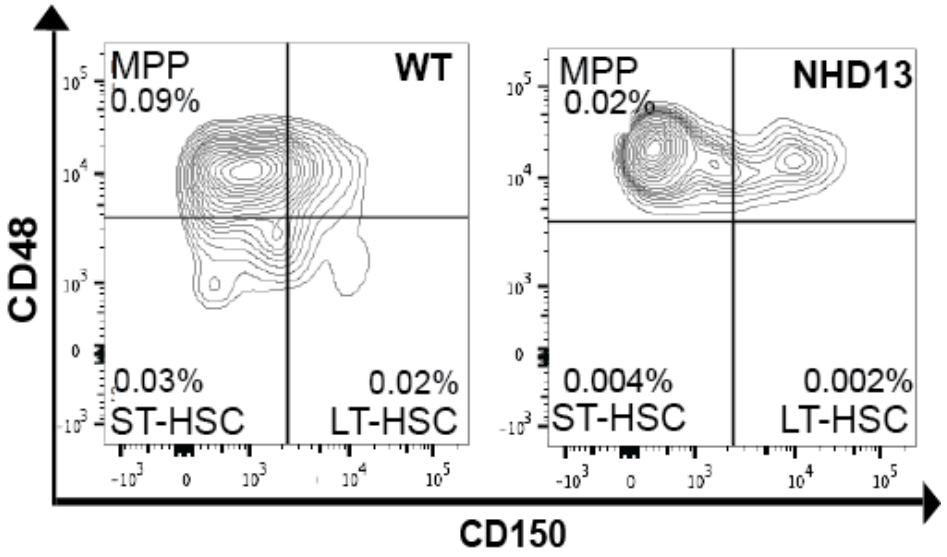
MPP
0.09%
WT
0.03%
ST-HSC
0.02%
LT-HSC
MPP
0.02%
NHD13
0.004%
ST-HSC
0.002%
LT-HSC
CD48
CD150

B

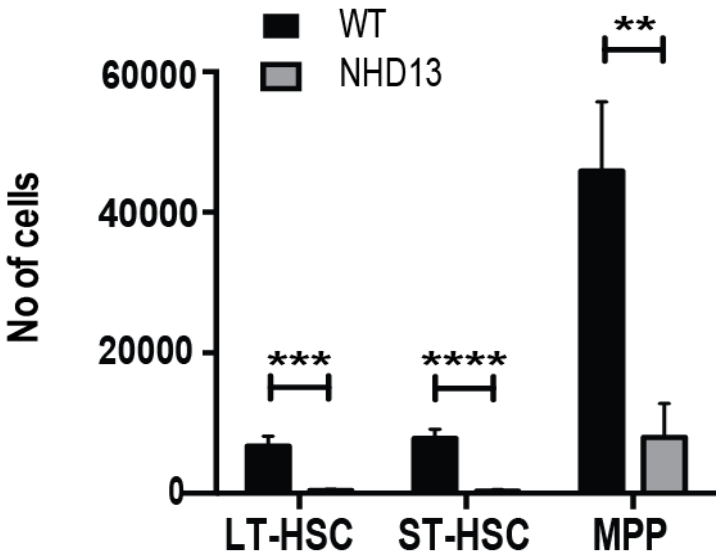
WT
NHD13
No of cells
60000
40000
20000
0
***
****
**
LT-HSC
ST-HSC
MPP

.

Figure 3.4. ***Quantification of mature progenitor subsets***

(A) Relative quantification of more mature progenitor subsets using flow cytometric analysis. Numbers shown represent percentages of total nucleated cells. Flow cytometry plots are initially gated on LK.Sca-CD41- cells. Populations shown include GMPs (LK.Sca-CD41-CD16/32+), BFU-E (LK.Sca-CD41-CD16/32loCD150+CD105+), CFU-E (LK.Sca-CD41-CD16/32loCD150-CD105+) and Meg-E (LK.Sca-CD41-CD16/32loCD150+ CD105-); (B) Absolute number of cells per mouse leg (tibia + femur). Numbers represent results extracted from three experimental replicates.

A

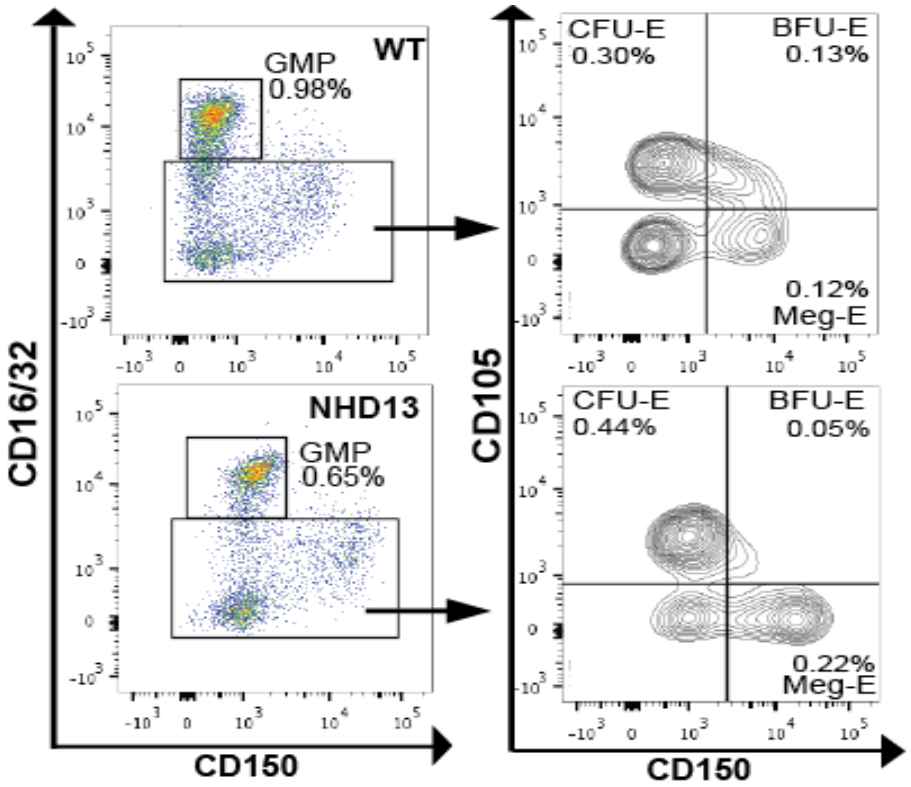
WT
GMP
0.98%
NHD13
GMP
0.65%
CD16/32
CD150
CFU-E
0.30%
BFU-E
0.13%
0.12%
Meg-E
CFU-E
0.44%
BFU-E
0.05%
0.22%
Meg-E
CD105
CD150

B

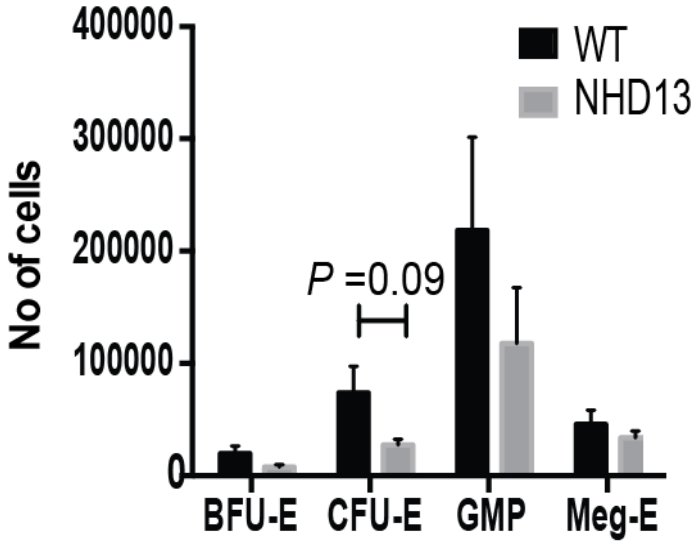
400000
300000
200000
100000
0
No of cells
WT
NHD13
P =0.09
BFU-E
CFU-E
GMP
Meg-E

Figure 3.5. ***Characterizing repopulating potential of specific haematopoietic stem cell subtypes in WT and NHD13 mice***

(A) Schematic for chimeric transplants: FACS sorted LK, LT-HSC and MPP cells from WT and NHD13 (Ly5.2) donor mice were transplanted into 6-week old lethally irradiated recipient Ly5.1 mice. Each sorted population was transplanted into 4 recipient mice. 2 x 10^5 splenic cells were transplanted concurrently to aid with engraftment. Mice were monitored frequently and bled four weekly for a total of 16 weeks and analysed for Ly5.2:Ly5.1 chimerism; (B) Percentage of donor Ly5.2 cells over time based on peripheral blood chimerism analysis. WT LK, NHD13 LK and NHD13 LT-HSC all share the first two data points sitting on the x-axis (at 4 and 8 weeks).

A

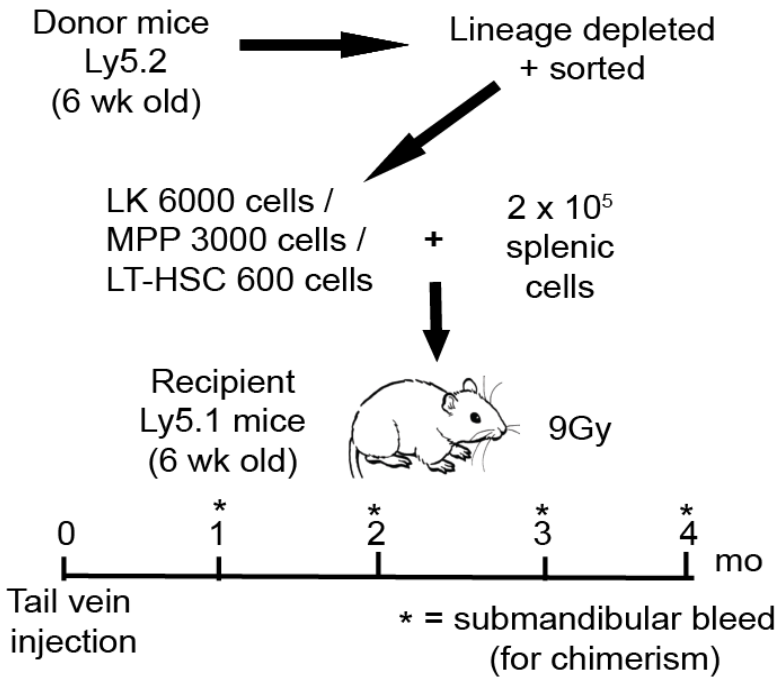
Donor mice
Ly5.2
(6 wk old)
Lineage depleted
+ sorted
LK 6000 cells /
MPP 3000 cells /
LT-HSC 600 cells
+
2 x 10^5
splenic
cells
Recipient
Ly5.1 mice
(6 wk old)
9Gy
0
1
2
3
4
mo
Tail vein
injection
* = submandibular bleed
(for chimerism)

B

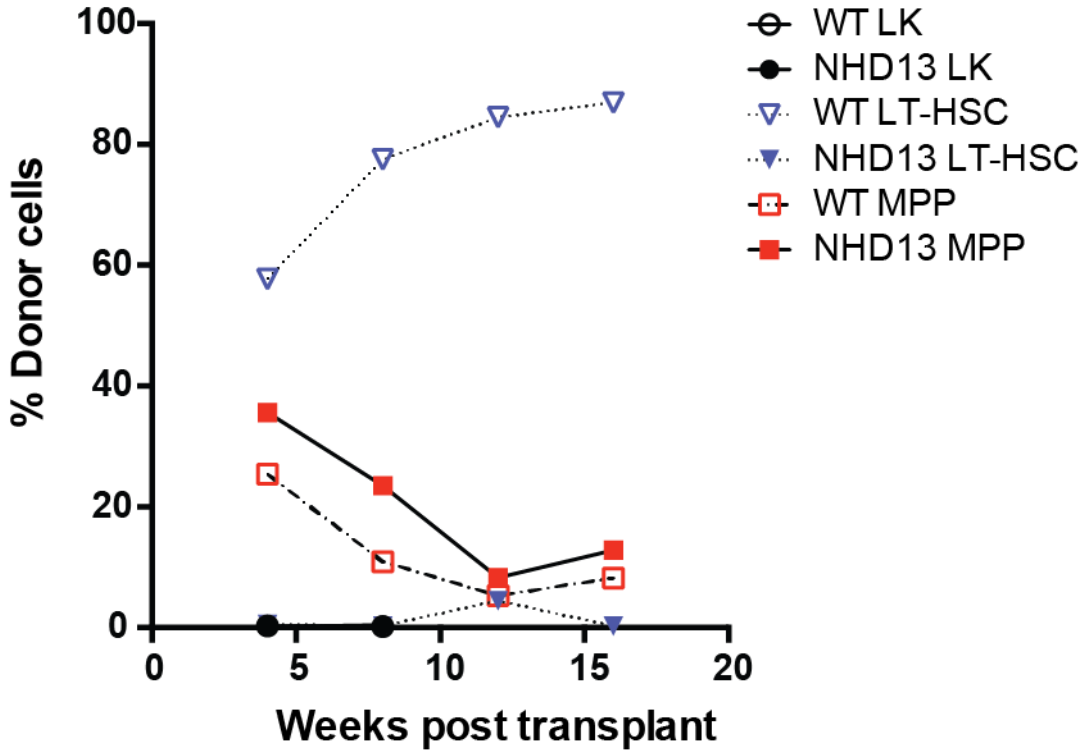
% Donor cells
100
80
60
40
20
0
0
5
10
15
20
Weeks post transplant
WT LK
NHD13 LK
WT LT-HSC
NHD13 LT-HSC
WT MPP
NHD13 MPP

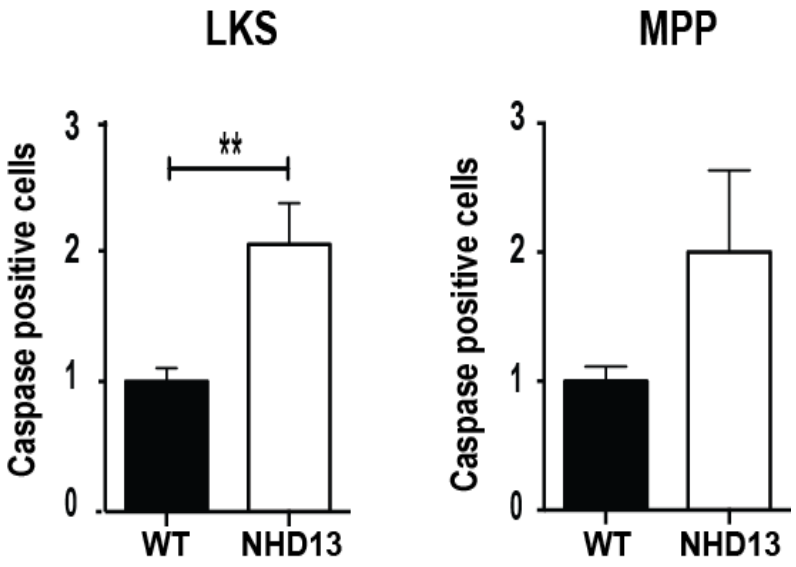

Figure 3.6. ***Normalized caspase-3/7 measurements for LSK and MPP cells***

Apoptosis as measured by caspase-3/7 staining using flow cytometric analysis. Results are shown for LSK and MPP cells. To account for multiple analyses, results have been normalized to wild-type caspase levels. For LSK and MPP analyses, n = 14 and 8 respectively; ** = $p < 0.01$.

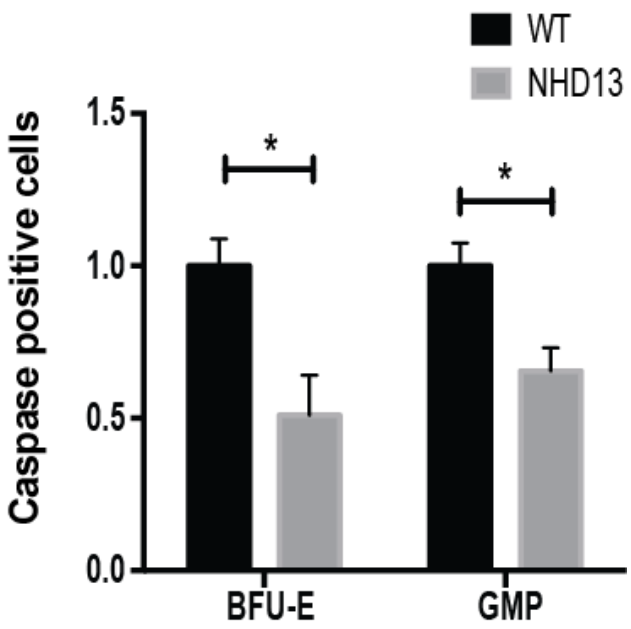

Figure 3.7. ***Normalized caspase-3/7 measurements for BFU-E and GMP progenitors***

Apoptosis of more mature myeloid and erythroid progenitors as measured by caspase-3/7 staining using flow cytometric analysis. Results are shown for BFU-E and GMP progenitors cells. To account for multiple analyses, results have been normalized to wild-type caspase. For BFU-E and GMP analyses, n = 6; * = $p < 0.05$.

A.

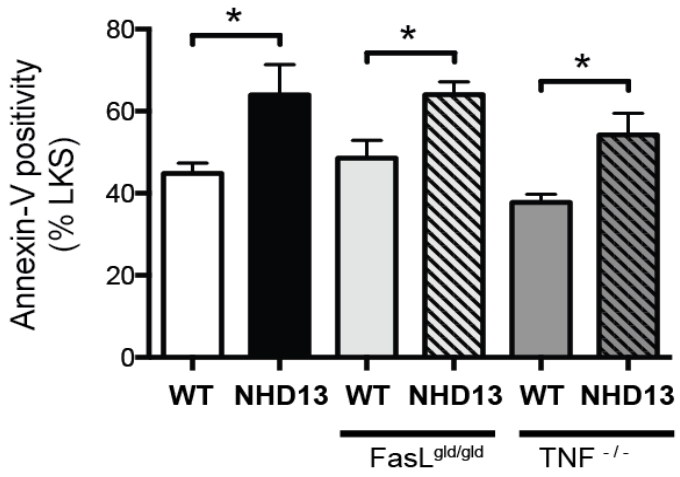

B.

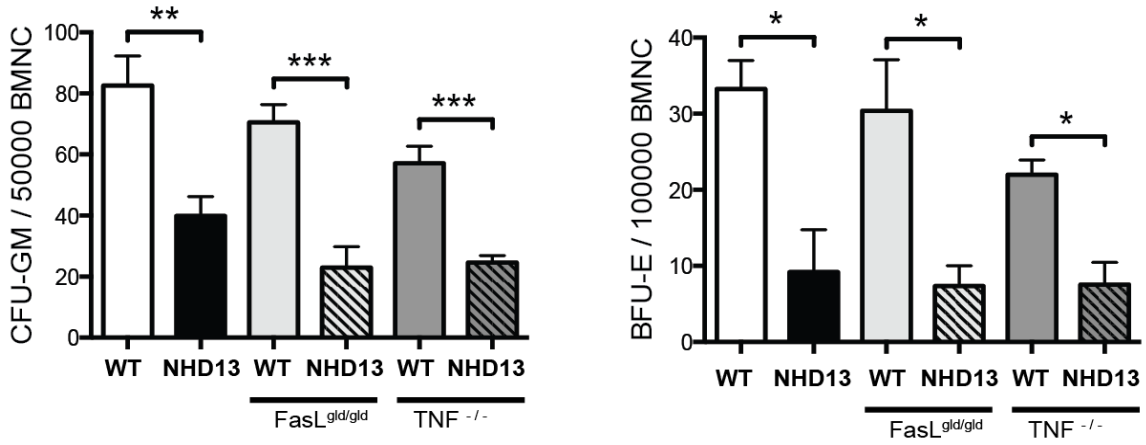

Figure 3.8. ***The death receptor pathway does not mediate apoptosis of NHD13 progenitors***

(A) Measurement of apoptosis in LSK HSCs as measured by Annexin-V using flow cytometric analysis. Comparison is made between WT or NHD13 mice in which the extrinsic pathway is functional and mice in whom the Fas ligand is mutated (gld mutation) or TNF-α is absent ($TNF^{-/-}$). Results are expressed as percentage of LSK cells; (B) Analysis of progenitor colony numbers as measured by agar and methylcellulose assays. Numbers are expressed per number of BM nucleated cells (BMNC) plated; * = $p < 0.05$; ** = $p < 0.01$; *** = $p < 0.001$.

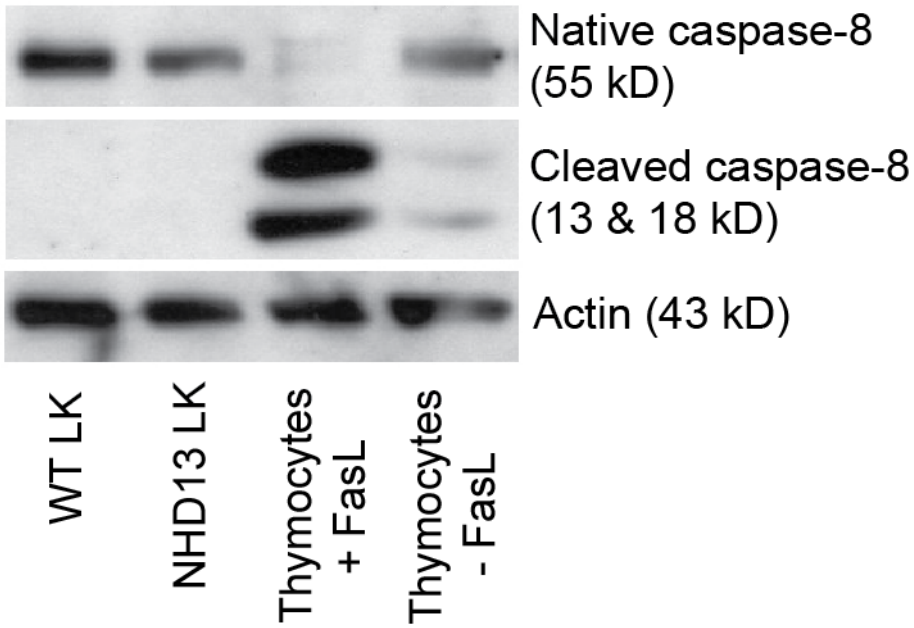

Figure 3.9. ***Caspase 8 – a marker of the extrinsic pathway – is not activated in NHD13 progenitors***

Western blot analysis for activated or cleaved caspase-8 (denoted by 13 and 18kD fragments) in comparison with native (uncleaved) caspase-8 (55kD). WT LK cells are compared with NHD13 LK cells and depict no activation of caspase-8. Thymocytes treated with or without Fas-L have been used as a positive and negative control respectively. Actin has been used as a loading control in this case.

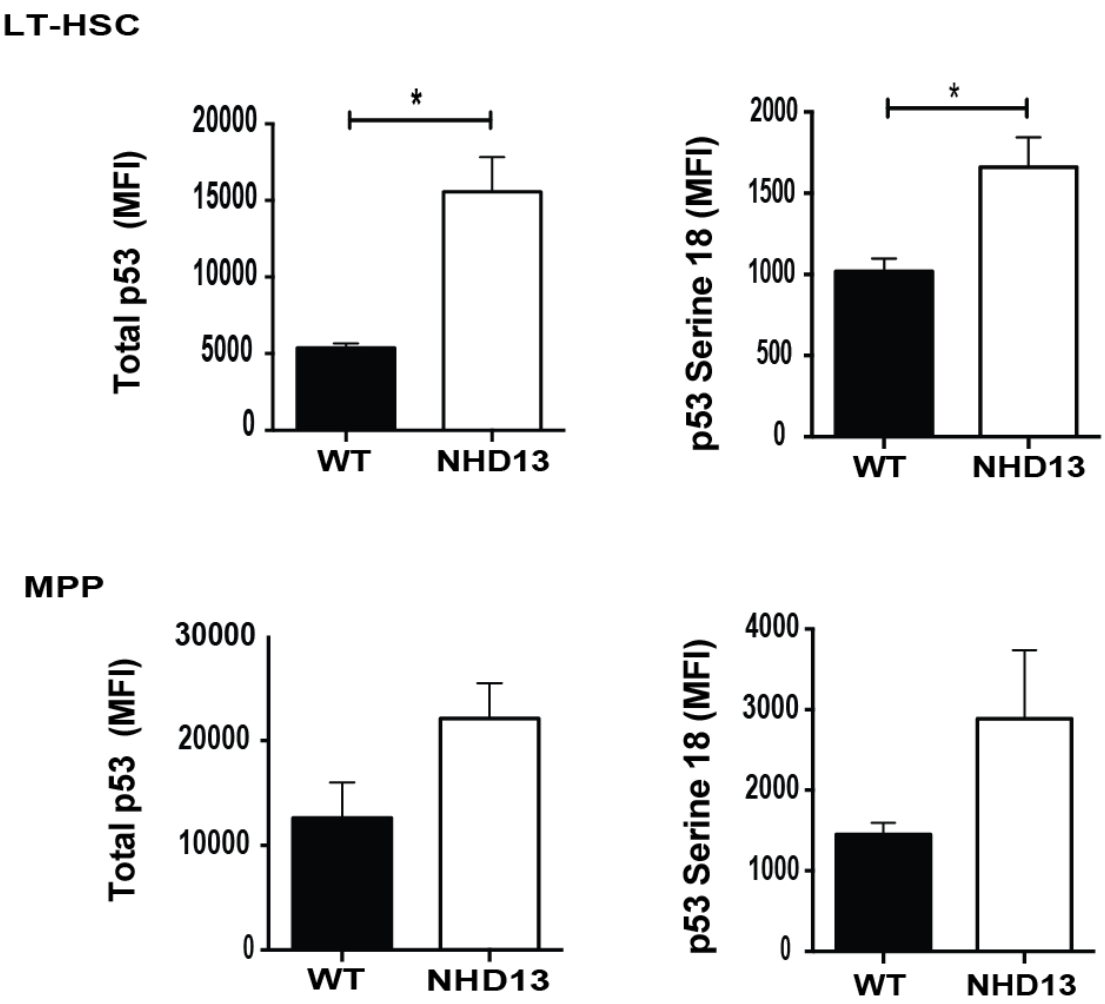

Figure 3.10. ***P53 protein expression levels in LT-HSC and MPP populations***

Expression of total p53 protein and phospho-p53 Serine 18 as measured by flow cytometric analysis and expressed as mean fluorescence intensity (MFI). Results are shown for LT-HSC and MPP populations (n = 3 for each genotype); * = $p < 0.05$.

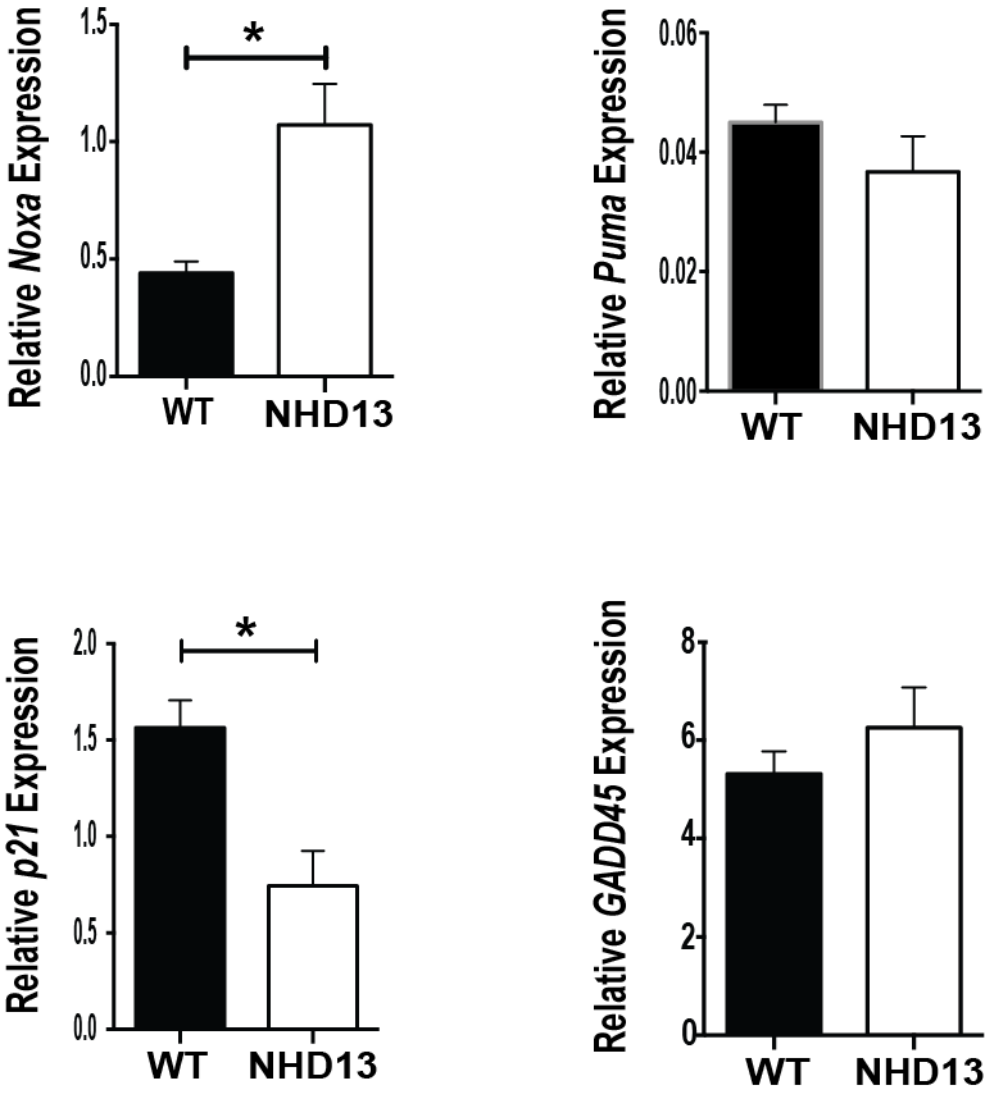

Figure 3.11. ***P53's transcriptional target Noxa is significantly increased in LSK progenitor cells***

qPCR analysis on sorted LSK populations for a selection of p53 target genes – *Noxa, Puma, p21 (*aka *Cdkn1a)* and *GADD45*. Results are expressed relative to *Actin* and *HPRT* expression; * = $p < 0.05$.

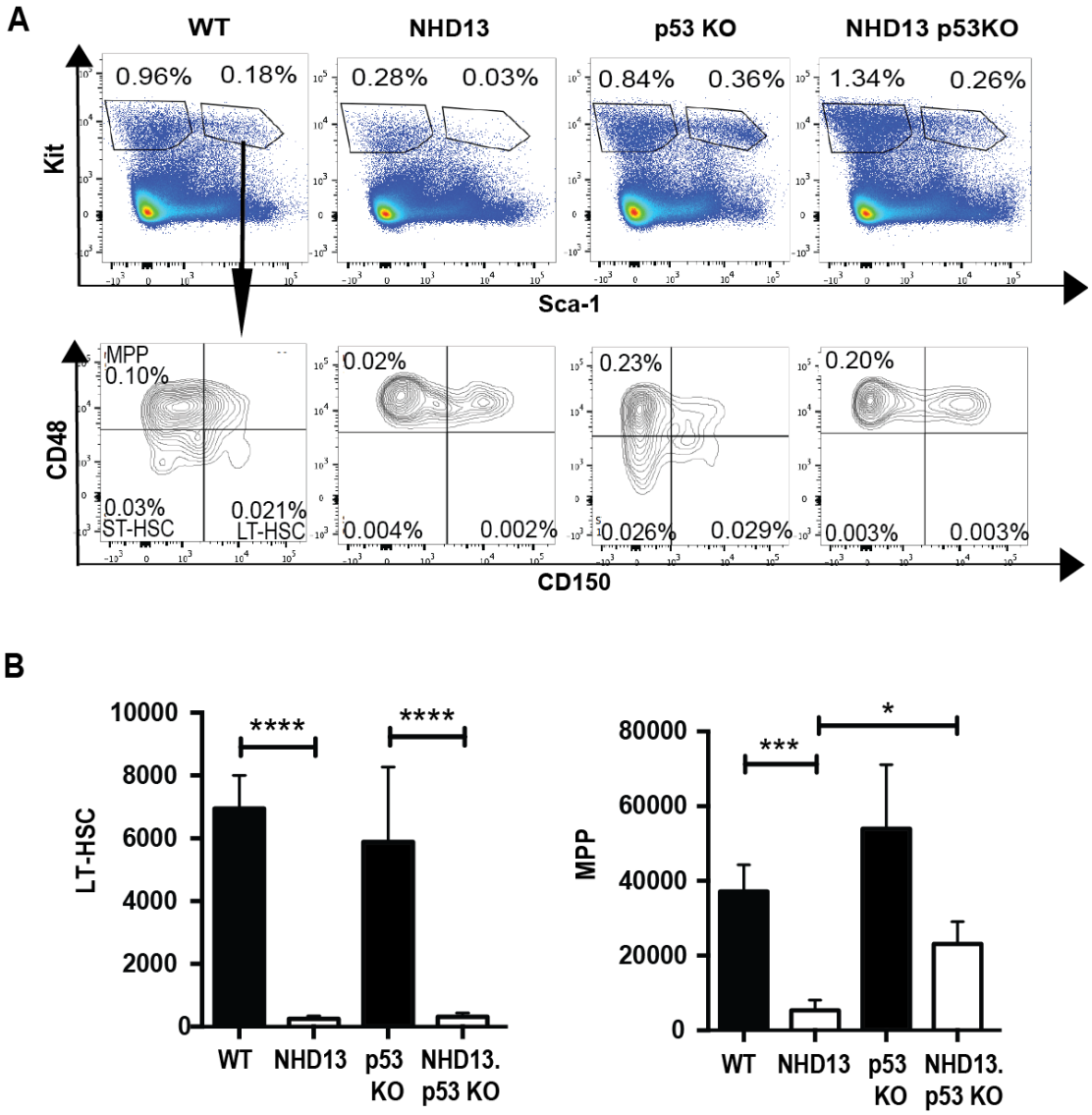

Figure 3.12. ***Removal of p53 results in a rescue of LSK and MPP cell numbers but no rescue of LT-HSC or ST-HSCs***

(A) Flow cytometric analysis of LK and LSK cell populations gated on lineage negative cells with subsequent analysis of SLAM markers for WT, *NHD13*, p53 knockout (KO) and *NHD13*;p53 knockout mice. Results are representative of one of four replicates for this experiment and numbers represent percentages of total nucleated cells; (B) Absolute quantification of LT-HSC and MPP cell populations. Number of cells calculated using flow cytometric analysis represents the number of cells per mouse leg (tibia + femur). These results represent the aggregation of all four experiments; * = $p < 0.05$; *** = $p < 0.001$; **** = $p < 0.0001$.

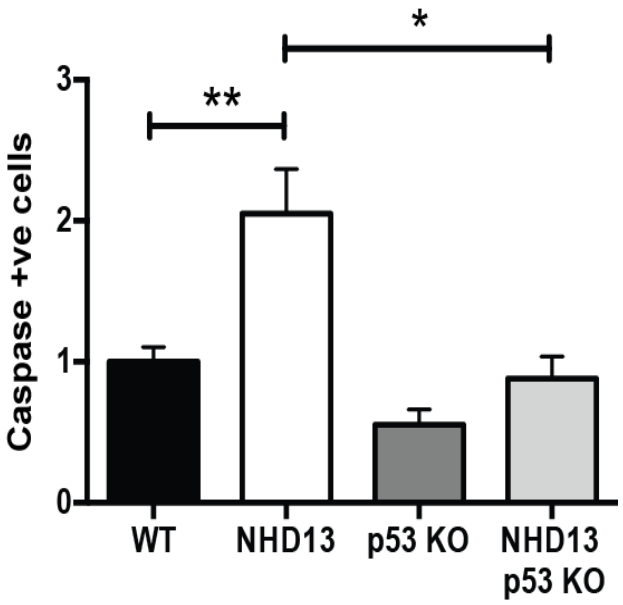

Figure 3.13. ***Measurement of LSK apoptosis***

Flow cytometric analysis of apoptosis as measured by caspase 3/7 staining for LSK cells of *NHD13* mice deficient for *p53.* Results have been normalized to WT LSK cells and represent the aggregation of three separate experiments; * = $p < 0.05$; ** = $p < 0.01$. As shown in Figure 3.12, *NHD13* and *NHD13*.p53$^{-/-}$ LSK cells are predominantly composed of MPP subpopulations.

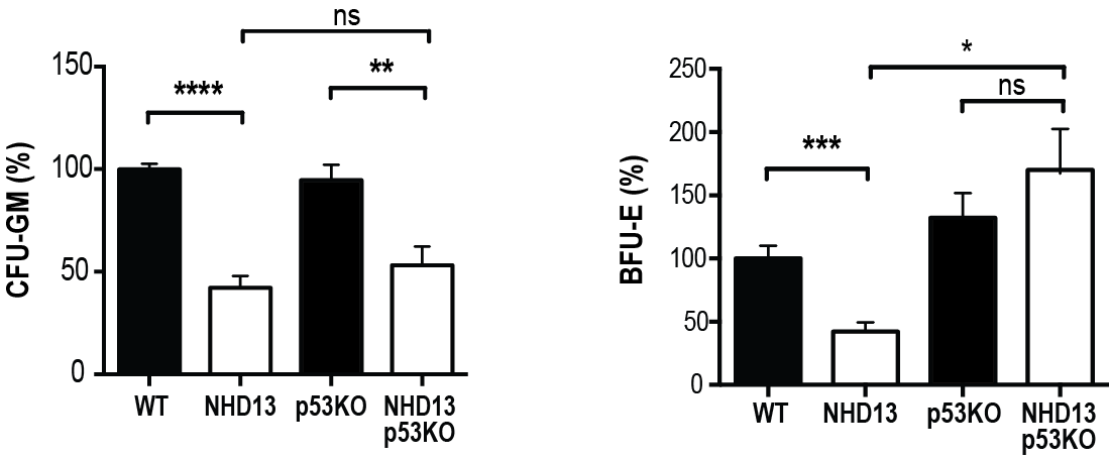

Figure 3.14. ***Haematopoietic progenitor assays for NHD13 mice deficient for p53***

Methylcellulose and agar haematopoietic progenitor assays were performed for the measurement of colony-forming units granulocyte-macrophage (CFU-GM) and burst-forming units erythroid (BFU-E) respectively. Assays were performed in triplicate and 1 x 10^5 and 5 x 10^4 whole bone marrow cells were plated respectively with the appropriate semi-solid culture medium and cytokines. Colony numbers were enumerated after one week incubation at 37°C in 10% CO_2. Results represent the aggregation of four individual experiments (n = 3 per genotype) and have been normalized to wild-type levels (100%); * = $p < 0.05$; ** = $p < 0.01$; *** = $p < 0.001$; **** = $p < 0.0001$; ns = not significant.

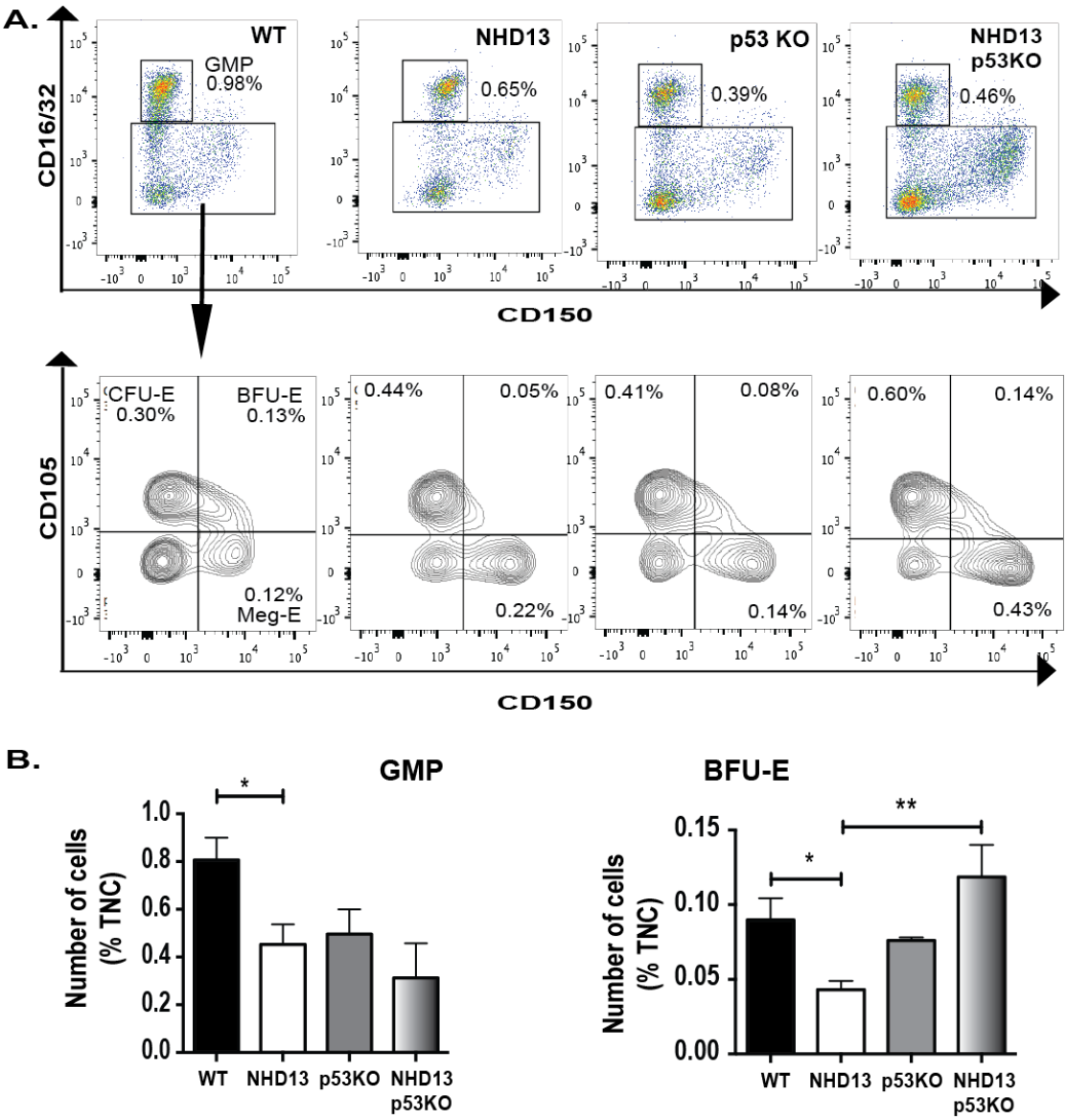

Figure 3.15. ***Quantification of progenitor subsets using flow cytometric analysis***

(A) Flow cytometric analysis of myeloid and erythroid progenitor subsets including GMP, BFU-E, CFU-E, MegE. Numbers represent percentages of total nucleated cells (TNC) and plots are a single representation of two individual experiments. Cells are initially gated on $Lin^{-}Sca\text{-}1^{-}CD41^{-}$ cells; (B) Column graph representation of myeloid (GMP) and erythroid (BFU-E) subset proportions. Numbers represent the combined results of two individual experiments; * = $p < 0.05$; ** = $p < 0.01$.

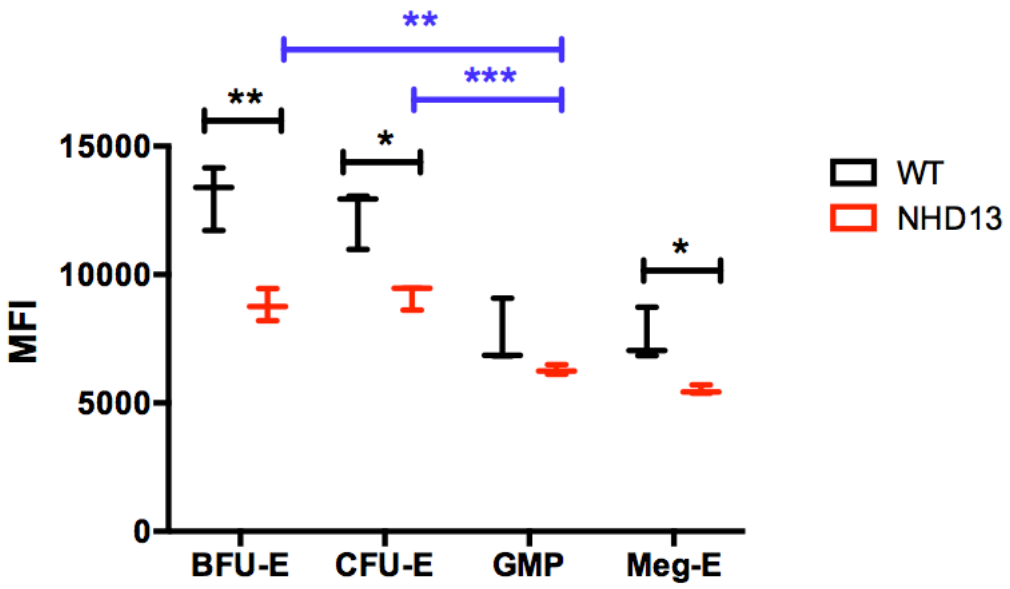

Figure 3.16. ***Total p53 expression levels of mature erythroid and myeloid progenitor subsets quantified using flow cytometric analysis***

Flow cytometric analysis of total p53 expression levels within erythroid and myeloid progenitor subsets comparing WT to NHD13 mice. Results are expressed as mean fluorescence intensity. n = 3 for each genotype. In general p53 levels appear to be higher in wild-type mice compared to NHD13 mice across all subgroups. Within the NHD13 subgroup, p53 levels are significantly increased in erythroid subsets (BFU-E and CFU-E) compared to the GMP myeloid subset; * = $p < 0.05$; ** = $p < 0.01$; *** = $p < 0.001$.

A

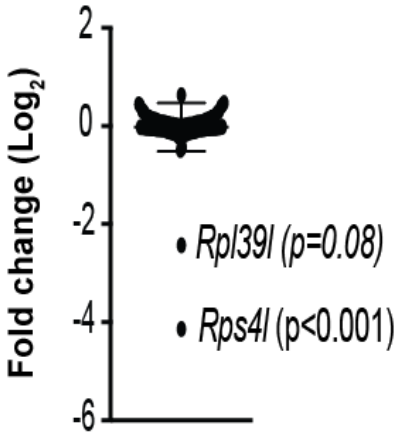

B

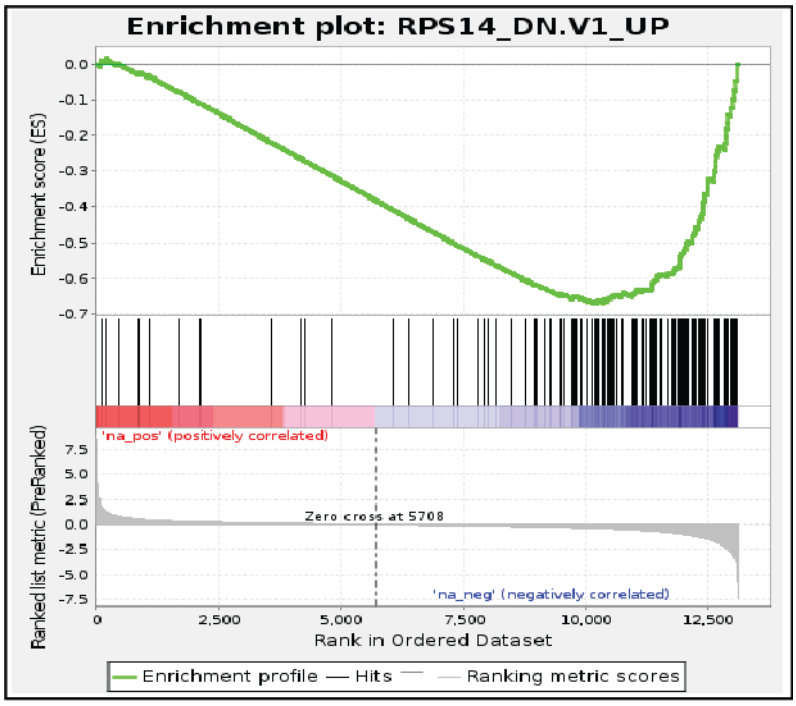

Figure 3.17. ***Ribosomal gene expression levels and GSEA analysis***

(A) Gene expression levels of ribosomal genes extracted from RNA-seq analysis and expressed as log2 fold-change comparing WT to *NHD13*; (B) GSEA enrichment plot of gene dataset typically up-regulated in response to *RPS14* knockdown. Results show that there is a negative correlation in this case - implying the lack of a 'ribosomal dysfunction' gene signature in *NHD13* HSCs.

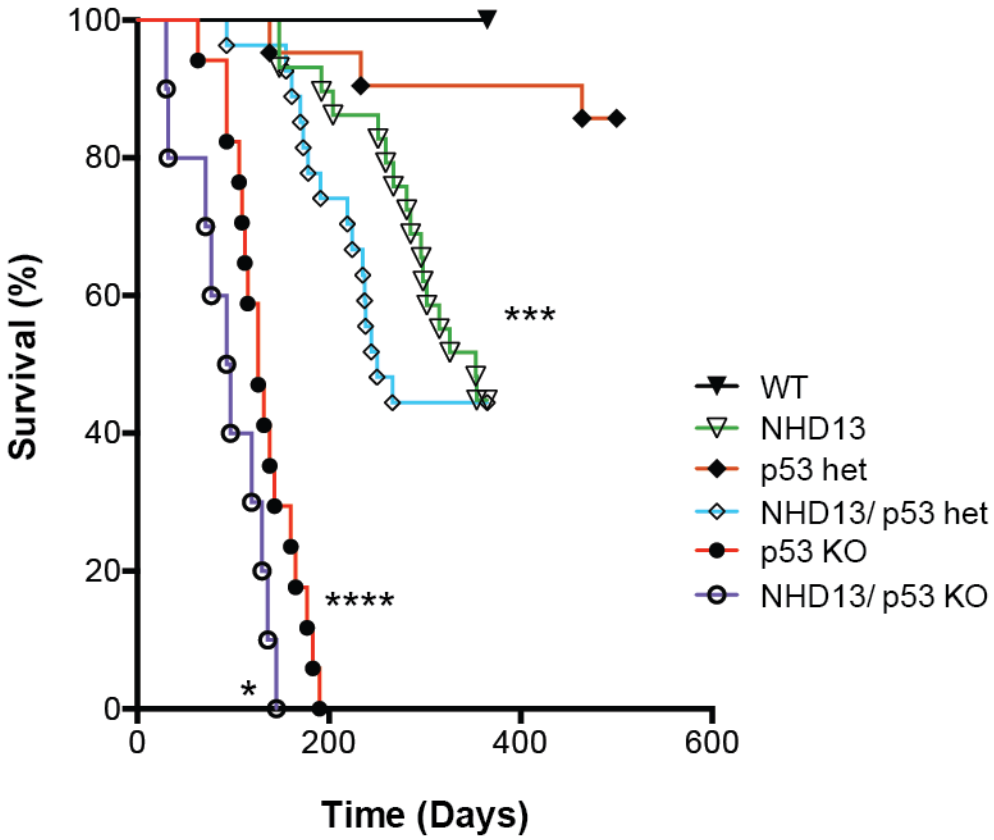

Figure 3.18. ***Kaplan-Meier survival curves for NHD13;p53$^{+/-}$ and NHD13;p53$^{-/-}$***

Kaplan-Meier survival curves comparing overall survival of *NHD13 mice* with those deficient for one allele of p53 *(NHD13;p53$^{+/-}$)* or both alleles of p53 *(NHD13;p53$^{-/-}$);* * = $p < 0.05$; *** = $p < 0.001$; **** = $p < 0.0001$.

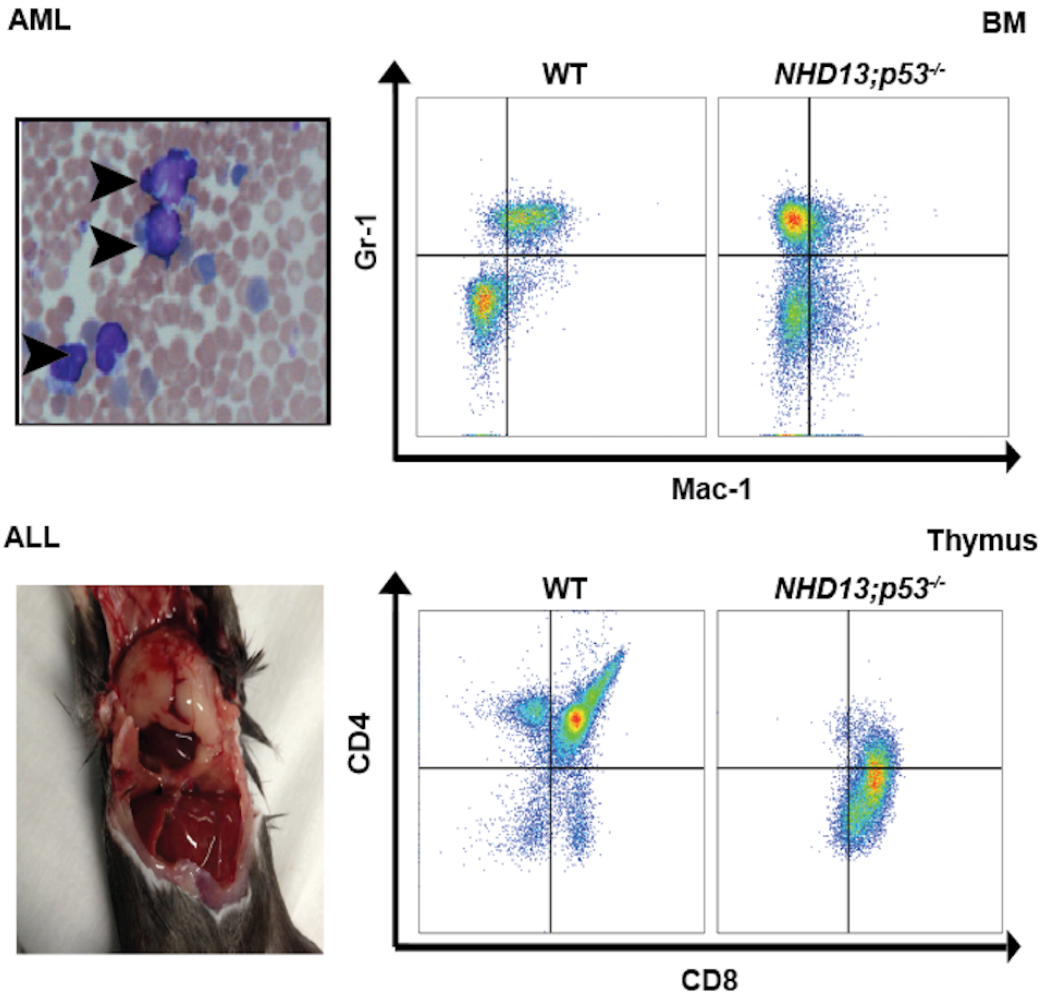

Figure 3.19. ***Leukaemic profiles of NHD13;p53$^{-/-}$ mice***

Illustrative examples of leukaemic progression as seen in *NHD13;p53$^{-/-}$* mice; (Top) Peripheral blood smear showing evidence of immature leukaemic blasts (arrowheads) with open immature chromatin and high nuclear:cytoplasmic ratio. Flow cytometric analysis shows normal Mac-1 vs Gr-1 gating on the bone marrow of a wild-type mouse and similar gating on the *NHD13;p53$^{-/-}$* mouse showing evidence of an abnormal Gr-1^{+} population; (Bottom) Macroscopic dissection showing thymic lymphoma in keeping with T-ALL. Flow cytometric analysis on the thymus reveals an abnormal single positive CD8 T-cell population.

Discussion

P53 mutations in MDS occur in ~ 15% of cases and generally portend a poor prognosis even in the favourable '5q-' category (Jädersten et al. 2011; Kulasekararaj et al. 2013). A distinction however must be drawn between 'p53 mutations' that likely provide a survival advantage for clonal haematopoietic cells and 'p53 activation', a phenomenon that has been described in association with ribosomal dysfunction and that has been linked to the 'anaemia' of related disorders.

In this Chapter, we confirm that the reduction in *NHD13* haematopoietic stem cells is likely the result of p53-mediated apoptosis implicating the intrinsic pathway as a key player within this model and confirming our previous results with BCL-2 overexpression. We demonstrate persistence of increased apoptosis after excluding key drivers of the extrinsic pathway ***(Figure 3.8)*** and show that p53's transcriptional target *Noxa* (a pro-apoptotic BH3-only member), but not *Puma* is significantly increased in *NHD13* LSK HSCs ***(Figure 3.11)***. By targeting p53, we are able to confirm apoptosis is p53-dependent ***(Figure 3.13)***. We also show evidence of a differential effect on the apoptosis of erythroid vs myeloid precursors ***(Figure 3.14 & 3.15)***. Finally, we confirm that not surprisingly, targeting p53 results in accelerated leukaemogenesis - highlighting its role as a potent tumour suppressor gene in both myeloid and lymphoid disease ***(Figure 3.18)***.

Although the loss of p53 within this model has previously been shown to portend a poor prognosis with increased leukaemic transformation (Xu et al. 2012b), p53's pivotal role in oncogene-induced apoptosis in this context has not been studied before. Importantly, we demonstrate a rescue of MPP cells (which make up a significant proportion of LSK cells in *NHD13* mice), but not LT- or ST-HSCs. Using a chimeric transplantation model, we refine the definition of the MDS-repopulating cell adding to the previous body of work by Chung et al

(Chung et al. 2008) and demonstrate that this cell most likely has an MPP phenotype.

Although the evidence for increased p53 activity is limited, this might be explained for a number of reasons. Firstly, the half-life of p53 is extremely short under normal homeostatic conditions – a result of the efficient inhibitory activity of MDM2. Secondly, unlike the acute effects of chemotherapy and ionizing radiation on p53 expression which have been well studied, protracted exposure to an oncogene (in this case, *NHD13*) may yield a more subtle effect on p53 activation. In spite of this, we show modest evidence for the activation of p53 and demonstrate an unquestionable increase in the expression of its transcriptional target, *Noxa,* but not *Puma.* We additionally show that targeting important ligands that mediate apoptosis via the extrinsic pathway (i.e TNF-α and FasL) does not abrogate the increase in apoptosis seen in *NHD13* progenitors. In constellation, these results suggest that apoptosis is predominantly driven by the intrinsic pathway and that the likely mediator of this is NOXA.

Given these findings, we proceeded to generate *NHD13*-mice deficient in *p53.* The rescue of *NHD13* LSK HSC apoptosis confirms that programmed cell death in this population is indeed mediated by p53 ***(Figure 3.13)***. This rescue correlates with increased numbers of LSK cells and their predominant MPP HSC subpopulation. Apoptosis within LT- and ST-HSCs could not be examined in these cases, as these populations exist in very low numbers in NHD13 mice.

Within more mature progenitor subsets, we note a differential effect on erythroid progenitors compared to myeloid cells. This is supported by haematopoietic agar and methylcellulose progenitor assays and corroborated by flow cytometric analysis confirming a prominent role for p53 in erythroid apoptosis of MDS as demonstrated by other groups (Barlow et al. 2010; Dutt et al. 2011) ***(Figure 3.14 & 3.15)***. Of significance, we were unable to demonstrate a 'ribosomal dysfunction' signature using RNA-seq expression data and GSEA analysis in these mice ***(Figure 3.17)***. This suggests that p53 activation in MDS

may not be limited to cases of 'ribosomal dysfunction' alone and that other means of activation may indeed exist (eg increased reactive oxygen species). Although not extensively examined, the mode of p53 activation certainly warrants further investigation. For instance, case reports that have shown iron chelation therapy in human MDS may be of potential therapeutic benefit, support a possible role for targeting the production of reactive oxygen species as a means of preventing programmed cell death.

Our work supports that of Xu et al and confirms that loss of p53 accelerates leukaemic progression – in this case to both acute myeloid and acute lymphoblastic leukaemia ***(Figure 3.18)***. The main possibilities in this case are two-fold: prevention of apoptosis may permit the expansion of the pool of self-renewing MDS-repopulating cells allowing for the acquisition of additional genetic mutations and ultimately driving leukaemic progression. These findings are in line with the cancer pathogenesis paradigm in which resistance to apoptosis is generally associated with disease progression (Hanahan and Weinberg 2000; Hanahan and Weinberg 2011). Alternatively, p53's tumour suppressor role in myeloid disease is independent of its pro-apoptotic function - as *NHD13* mice deficient for p53 still develop leukaemia in spite of a demonstrable rescue in apoptosis. These findings are in keeping with those recently shown by Valente et al (Valente et al. 2013).

From a clinical perspective, although we could extrapolate and anticipate an improvement in peripheral blood cell parameters secondary to the rescue in apoptosis; we are unable to demonstrate these findings due to the significantly shortened lifespan of the *NHD13*;p53-deficient mice. However, the results to date, do suggest that if apoptosis alone could be targeted, this may improve the associated cytopenias. The effect on disease progression remains largely unanswered (particularly for myeloid disease) and will be explored in subsequent Chapters.

In conclusion, we demonstrate that apoptosis of *NHD13* HSCs is p53-dependent. Although targeting p53 may have some merit in improving cytopenias and rendering patients transfusion-independent, this work highlights p53's importance in tumour suppression and suggests that this likely extends beyond its pro-apoptotic function alone. In keeping with p53 mutations in human MDS, the heterozygous or homozygous loss of p53 in the *NHD13* model portends a significantly poor prognosis.

Subsequent Chapters will explore the role of apoptotic proteins downstream of p53 and upstream of BCL-2 to further dissect and clarify the role of apoptosis in the myelodysplastic phenotype and in myeloid disease progression.

CHAPTER FOUR

The Contribution of BH3-only Proteins to the Apoptosis of *NHD13* Stem Cells

Abstract

After initial DNA-damage inducing events, the BH3-only class of proteins function to initiate mitochondrial-dependent apoptosis within a cell. These proteins are regulated by various transcriptional and post-translational mechanisms and act to bind downstream BCL-2-related proteins and BAK/BAX. In the setting of DNA damage induced by ionizing radiation or through cytokine withdrawal, both *Puma* and *Noxa* have been described as direct transcriptional targets of p53. PUMA (and NOXA to a lesser degree) have also been implicated as tumour suppressors in the presence of an oncogene - particularly for lymphoid malignancies. In Chapter 3, we show evidence for activation and induction of the intrinsic pathway of apoptosis via a p53-dependent mechanism. In this Chapter, we look downstream of p53 to determine which proteins within the BH3-only family drive apoptosis and the effects seen when this is abrogated. We demonstrate that apoptosis of MDS HSCs is primarily mediated by PUMA. As seen when apoptosis is prevented by BCL-2 overexpression, long-term survival analysis unexpectedly reveals that *NHD13* mice deficient for PUMA do not develop myeloid leukaemia – further supporting a role for apoptosis in myeloid disease progression. The contrasting effect with loss of p53 is examined in greater detail. In correlative work with human MDS, we show evidence for increased *Puma* expression in MDS samples and discuss a possible therapeutic avenue in this regard. To our knowledge, this is the first body of work examining the specific roles of NOXA, PUMA and (to a lesser extent) BIM in MDS.

Introduction

4.1. BH3-only proteins

The BH3-only proteins are notable for two common features. Firstly, as suggested by their name, they all share homology for the "BH3-domain" alone. Secondly, they are all pro-apoptotic in nature. These two features are in fact interdependent; the pro-apoptotic function of these proteins is mediated by the α-helical BH3-domain – enabling them to bind to a groove formed by BH1 and BH2 domains of multi-domain BCL-2 family members (Letai et al. 2002).

A number of differences between these proteins however, warrants discussion; including the manner by which individual members are regulated at a transcriptional and post-translational level and additionally their specificity for downstream proteins. For instance, p53's transcriptional regulation of *Noxa* (Oda et al. 2000; Shibue et al. 2003) and *Puma* has been well documented (Nakano and Vousden 2001; Jabbour et al. 2010). Other proteins such as BID may be cleaved (as previously discussed) and BAD, BIM and BMF may be phosphorylated or sequestered providing additional post-translational levels of regulation (Puthalakath et al. 1999; Puthalakath and Strasser 2002). A variety of inducers are known to activate these proteins by p53–dependent and independent pathways. These include but are not limited to: physiological stimuli (such as cytokine deprivation), DNA damage, chemotherapeutic drugs, oncogenic stress and γ-irradiation. The various manners of induction and regulation have been extensively reviewed by Willis et al (Willis and Adams 2005).

Downstream, the BH3-only proteins exhibit differential binding to their respective pro-survival partners. BIM and PUMA engage all pro-survival proteins; BAD binds BCL-2, BCL-xL and BCL-w, whilst NOXA binds MCL-1 and A1 (Chen et al. 2005). A summary of these binding specificities is provided in ***Figure 4.1***. These interactions provide an insight into the complementary function induced by certain BH3-only protein combinations. Of note, those proteins with restricted targets are typically less potent killers – a reflection of their inability

to neutralize all pro-survival molecules. Of further significance is the dependence of different cell types on different BH3-only proteins to execute apoptosis. As an example, BIM plays a particular role in the apoptosis of self-reactive lymphocytes and thymocytes (Bouillet et al. 1999; Bouillet et al. 2000); BID is specific for the apoptosis of hepatocytes (Yin et al. 1999) and A1 is suggested to play a role in neutrophil apoptosis.

Further downstream, some BH3-only proteins such as BID and BIM may act directly to oligomerize BAK and BAX (Letai et al. 2002; Cartron et al. 2004). These have been termed 'activators'. Other proteins such as BAD and NOXA are known as 'sensitizers' as they 'sensitize' BAX/BAK to direct binding by the 'activator' BH3-only proteins by displacing their attachment to anti-apoptotic BCL-2 related proteins.

As the BH3-only proteins, NOXA, PUMA and BIM have been extensively studied in this work, these proteins will be discussed in more detail in subsequent sections. A more succinct summary will be given for some of the other well-characterized BH3-only proteins here. As HRK, BMF and BIK lie beyond the scope of this current study, they have been purposefully excluded from the current discussion.

BID:

This BH3-only protein is reported to be important in the apoptosis of hepatocytes and fibroblasts as mice lacking BID have reduced sensitivity to Fas-induced hepatocyte destruction (Yin et al. 1999). Of all BH3-only proteins, BID is the main protein that allows for communication between the extrinsic and intrinsic pathways of apoptosis. After initial activation of caspase-8 by Fas or TNFR ligation, BID is cleaved to its truncated form (tBID). Downstream, tBID's apoptotic function appears to be mediated through BAK inducing the release of cytochrome c (Wei et al. 2000).

BAD:

Unlike BIM and PUMA which can neutralize all BCL-2 like proteins, BAD exhibits limited activity against BCL-2, BCL-xL and BCL-w alone (Chen et al. 2005). Typically localized in the cytoplasm under physiological conditions, there is some evidence that similar to *Noxa* and *Puma, Bad* may also act as a transcriptional target of p53 (Jiang et al. 2006).

4.1.1. PUMA

The pro-apoptotic BH3-only gene *Puma (**p**53 **u**pregulated **m**odulator of **a**poptosis)* is one of the main transcriptional targets of p53 within the apoptotic pathway (Nakano and Vousden 2001; Yu et al. 2001; Han et al. 2001) and its most potent killer. In similar fashion to other members of its family, PUMA relies upon its BH3-domain for interactions with downstream BCL-2-related proteins such as BCL-2 and BCL-xL.

A mouse model of PUMA deficiency has revealed its pivotal role in haematopoietic cell apoptosis triggered by γ-ionizing radiation (IR), oncogenic stress (through deregulated Myc-expression) and cytokine withdrawal (Jeffers et al. 2003). During steady-state homeostasis, PUMA appears to have a minimal role in HSC apoptosis with no difference seen in HSC and HPC population numbers in comparison to PUMA wild-type mice (Shao et al. 2010). However, under conditions of cellular 'stress' such as IR, loss of PUMA was able to afford a protective effect (Yu et al. 2010) – particularly for LT-HSCs and ST-HSCs, improving overall survival (Shao et al. 2010). This was also apparent for apoptosis-dependent thymic lymphoma development following IR (Michalak et al. 2010). As loss of PUMA appears to ablate tumour development in these cases, this suggests that loss of PUMA (and prevention of IR-induced apoptosis) may act to limit DNA damage by maintaining cells in a state of quiescence allowing more efficient DNA repair to occur. In keeping with this, PUMA-deficient mice do not exhibit evidence of increased tumour susceptibility even after exposure to multiple courses of IR (Yu et al. 2010).

Within the realm of myeloid cells, resistance to apoptosis is seen in PUMA deficient myeloid progenitors exposed to γ-IR. Factor-dependent myeloid cells are also dependent on PUMA for apoptosis provoked by cytokine deprivation and mediated by p53 (Jabbour et al. 2010).

Although its predominant means of activation is through transcriptional activity of p53, *Puma* can also be induced by means of transcription independent of p53 (Han et al. 2001). Although not exhaustive, some examples include induction by glucocorticoids, the forkhead box O3 protein (FoxO3a) under growth factor deprivation conditions (You et al. 2006) and the p53 homologue p73. Conversely, negative regulation of *Puma* transcription may occur through repressors such as the Snail family member, *Slug* in response to DNA damage (Wu et al. 2005). Unlike BIM, PUMA is not exposed to significant post-translational modification.

In contrast to the weakly pro-apoptotic BH3-only proteins BAD and NOXA, which inhibit a limited repertoire of pro-apoptotic BCL-2 related proteins; PUMA is considered one of the most potent killers – and is capable of inducing apoptosis indirectly by inhibiting ALL pro-apoptotic BCL-2 related proteins (Chen et al. 2005). Reports indicates that PUMA is also capable of directly activating BAX (Cartron et al. 2004; Gallenne et al. 2009), even in the absence of other known direct activators (such as BIM and t-BID) (Garrison et al. 2012).

As a tumour suppressor, PUMA appears to have a minimal role in tumour suppression during normal haematopoiesis. In keeping with this, PUMA-deficient mice are not abnormally susceptible to tumours (Yu et al. 2010). However, PUMA's tumour suppressive role becomes more apparent in the presence of an oncogene particularly in the setting of lymphoid malignancies. In contrast to the protective effect induced by loss of PUMA in γ-irradiated mice; in the setting of Myc overexpression, loss of PUMA results in a more aggressive lymphoma phenotype with higher leukocyte and B-lymphoid cell counts (Michalak et al. 2009).

These findings suggest that the effect of preventing apoptosis is very much 'context' dependent and may vary based on the tissue involved and the mode of 'stressful' injury.

4.1.2. NOXA

Deriving its name from the Latin word for 'damage', *Noxa* (aka PMA-induced protein 1 or PMAIP) is the second pro-apoptotic 'BH-3 only' gene that is a direct target of p53 (Oda et al. 2000). In similar fashion to other BH3-only proteins, the BH3 domain within NOXA has been shown to be crucial for its pro-apoptotic activity. However, unlike PUMA, it is only weakly pro-apoptotic – a reflection of its ability to bind the anti-apoptotic BCL-2-related proteins MCL-1 and A1 alone. As such, its activity must be complemented by that of BH3-only proteins such as BAD, which can neutralize all remaining BCL-2-related proteins (Chen et al. 2005). Unlike some of the other BH3-only proteins which are capable of binding BAX / BAK directly (Donehower et al. 1992), NOXA can only act as a 'sensitizer', indirectly activating BAX/BAK through its inhibition of MCL1 and A1.

Although it is mainly induced in a p53-dependent manner in response to DNA damage, NOXA can also be induced by the activity of Hif1α in response to hypoxia and by Protein Kinase C (PKC) family members, cytokine signalling such as IL7 and IL15 and by the polycomb repressive complex member, Bmi1.

In a similar manner to PUMA-deficient mice, NOXA deficient mice do not exhibit an overt phenotype with no spontaneous tumour development (Shibue et al. 2003).

4.1.3. BIM

As with other BH3-only proteins, BCL-2 Interacting Mediator of cell death or BIM shares the common 'BH3 domain' comprised of 9-16 amino acids. First isolated in 1998, it is known to have three different but functional isoforms – the result of alternative splicing. These are denoted as Bim_S, Bim_{EL} and Bim_L (O'Connor et al. 1998). In its inactive state, the Bim_L and Bim_{EL} isoforms are typically bound to LC8 (the cytoplasmic dynein light chain) and sequestered to the microtubule-

associated dynein motor complex (Puthalakath et al. 1999; STRASSER et al. 2000). This interaction harnesses the pro-apoptotic activity of this BH3-only protein. Upon activation, the interaction is disrupted and freed BIM bound to LC8 is then capable of translocating and interacting with a number of anti-apoptotic BCL-2- related proteins.

Unlike NOXA which targets a limited number of anti-apoptotic BCL-2 related proteins (namely Mcl-1 and A1); in similar fashion to PUMA, BIM is capable of binding all five BCL-2-like proteins (Chen et al. 2005). 'Direct' and 'indirect' activation models have been described with the latter likely playing a greater role in inducing apoptosis. Direct interaction occurs when BIM binds to BAX 'directly' either through the typical hydrophobic groove:BH3 interaction or another independent mechanism. Indirect activation involves the binding of the BCL-2 related proteins releasing their inhibition of BAX and BAK.

As is the case for individual BH3-only proteins, BIM's importance is also cell-specific. Expressed in many haematopoietic cell types, BIM is specifically essential for eliminating autoreactive lymphocytes / thymocytes (van Delft and Huang 2006). When absent, mice develop a leucocytosis involving a spectrum of white blood cells including B and T lymphocytes, granulocytes and monocytes (Bouillet et al. 1999). More recent work has shown that the leucocytosis associated with these mouse is related to a specific effect of BIM on the haematopoietic system itself (Herold et al. 2014). Although megakaryocytic numbers are normal, platelet counts are often reduced and this is thought to relate to BIM's role in platelet shedding. In addition to the leucocytosis and thrombocytopenia, BIM-deficient mice develop a progressive lymphadenopathy with age together with features in keeping with a systemic autoimmune disorder with splenic enlargement (akin somewhat to systemic lupus erythematosus). A significant proportion of mice develop a fatal form of glumerulonephritis to which they ultimately succumb (Bouillet et al. 1999). Given its significant role in lymphocyte development and homeostasis, it is not surprising that BIM functions as a tumour suppressor and may be lost in cases of lymphoma development.

From a developmental perspective, BIM knockout foetuses may often die before E10; however, the penetrance of this phenotype is largely dependent on the genetic background of these mice (Bouillet et al. 1999).

4.2. BH3-only proteins and myelodysplastic syndrome

There is no literature to date that discusses the role of PUMA, NOXA or BIM in association with the myelodysplastic syndrome.

Results

4.3. Determining the mediator of apoptosis within *NHD13* HSCs downstream of p53

4.3.1. NOXA does not mediate apoptosis of *NHD13* progenitor cells

Although the apoptosis of *NHD13* HSCs can be abrogated through loss of p53, this approach from a therapeutic view is not without its perils as demonstrated by the increase in leukaemic transformation seen in *NHD13* mice deficient for p53 ***(Figure 3.18)***. As discussed, these results suggest that p53's tumour suppressive function most likely occurs independent of its apoptotic function - in keeping with more recent reports (Dudgeon et al. 2006; Valente et al. 2013).

Downstream, p53's role as a transcription factor of *Noxa* (Oda et al. 2000) and *Puma* (Nakano and Vousden 2001; Shao et al. 2010) has been well-defined. We have shown that of p53's main transcriptional pro-apoptotic targets, *Noxa* (but not *Puma*) demonstrates significantly increased expression in LSK cells ***(Figure 3.11)***. This is supported by RNA-seq data. We therefore attempted to define which of p53's downstream apoptosis-inducing targets might be responsible for the increase in apoptosis seen in *NHD13* HSCs. Based on our findings to date, it seems reasonable to assume that NOXA is responsible for mediating the apoptosis of *NHD13* LSK cells.

To examine this further, we bred NOXA-deficient mice with *NHD13* transgenic mice to generate *NHD13;Noxa* heterozygous *($Noxa^{+/-}$)* mice and subsequently used these mice to generate *NHD13.Noxa* homozygous knockout *($Noxa^{-/-}$)* mice. *NHD13;$Noxa^{-/-}$* were subsequently analysed at 3 months of age for apoptosis as measured by annexin-V staining using flow cytometry. NOXA-deficiency in the setting of the *NHD13* transgene did not rescue the apoptosis of progenitor populations ***(Figure 4.2A)***. Additionally, examination of progenitor colony assays did not reveal any rescue of erythroid or myeloid colony numbers on methylcellulose or agar plates respectively ***(Figure 4.2B)***.

These results suggest that although the apoptosis of *NHD13* LKS cells is mediated by p53, this appears to occur independent of NOXA. As NOXA did not appear to play a significant role in the apoptosis of *NHD13* LKS progenitors, we did not age these mice further and did not examine for leukaemic progression.

4.3.2. The apoptosis of *NHD13* progenitor cells is dependent on PUMA

Of p53's transcriptional targets within the apoptotic pathway, *Puma* appears to be the most important. In part, this is likely explained by its more widespread inhibitory activity against all the anti-apoptotic Bcl-2 related proteins. In view of this and although mRNA levels did not reveal an increase in *Puma* expression, we proceeded to generate *NHD13* mice deficient in PUMA (*NHD13;Puma*$^{-/-}$) using a similar breeding strategy to that used for the NOXA-deficient mice.

Of note, analysis of human microarray data as provided by Pellagatti et al reveals that *Puma* expression is significantly increased in MDS CD34+ cells compared to wild-type samples across all subtypes of MDS. This is in contrast to *Noxa* expression which was not altered between wild-type and MDS samples ***(Figure 4.3)***.

4.3.2.1. PUMA prevents apoptosis of *NHD13* haematopoietic stem cells and rescues the number of MPP cells

In stark contrast to the *NHD13* NOXA-deficient mice, loss of PUMA was associated with a rescue of apoptosis within the LSK population of *NHD13* mice ***(Figure 4.4A)***. Although a similar pattern was seen in the LK population, the results did not achieve statistical significance.

To determine the functional significance of preventing apoptosis within the LSK cell population, we proceeded to enumerate more defined subpopulations. Similar to loss of p53, the absence of PUMA rescued relative and absolute LSK cell numbers and the MPP subpopulation, but not LT- or ST-HSCs ***(Figure 4.5)***. Apoptosis within the MPP subpopulation closely correlated with results seen for the LSK cell population ***(Figure 4.4B)***. Once again we were unable to measure

apoptosis in either LT- or ST-HSC subsets due to significantly reduced cell numbers. Thus in similar fashion to p53 deficiency, loss of PUMA from *NHD13* HSCs prevents apoptosis and rescues the LSK cell population and its MPP subset.

We proceeded to perform haematopoietic progenitor assays as a functional measure of haematopoietic stem cell function. In contrast to p53's differential effect on erythroid vs myeloid progenitors (as determined using agar and methylcellulose colony assays), PUMA deficiency in the setting of *NHD13* bone marrow stem cells restored both erythroid and myeloid colony numbers to wild-type levels ***(Figure 4.6)***

Thus, we demonstrate that the apoptosis of *NHD13* progenitors is dependent predominantly on the activity of p53's transcriptional target, *Puma* and that PUMA-deficiency rescues *NHD13* haematopoietic stem cell numbers (namely the MPP subpopulation). To our knowledge, this is the first time that PUMA has been implicated in the excessive apoptosis associated with MDS.

4.3.2.2. PUMA deficiency results in rescue of the macrocytic anaemia associated with *NHD13* mice

Having demonstrated the dependence of *NHD13* HSCs on PUMA for apoptosis, we proceeded to examine the implications of preventing apoptosis on the MDS phenotype. *NHD13;Puma*$^{-/-}$ mice were aged and submandibular bleeds were undertaken at 8 months of age. Analysis of haematological parameters revealed a rescue of the macrocytic anaemia ordinarily seen in *NHD13* mice at this age; but no rescue of the associated thrombocytopenia ***(Figure 4.7)***

We therefore demonstrate the importance of apoptosis in the cytopenias of MDS. The absence of PUMA rescues *NHD13* LSK cells from undergoing apoptosis and in doing so rectifies the anaemia (but not the thrombocytopenia) associated with their development.

4.3.2.3. PUMA deficiency prevents myeloid disease progression in *NHD13* deficient mice

In the context of an oncogene, PUMA's role as a tumour suppressor protein has been highlighted particularly for lymphoid disease as reported by Michalak et al (Michalak et al. 2009). However, the role of PUMA in myeloid disease progression has not been clearly defined.

Therefore, to examine PUMA's role in disease progression in the *NHD13* mice, we generated a survival cohort. Mice were observed until they became unwell and were subsequently euthanized. Bone marrow, spleens and thymi were harvested after macroscopic examination and were analyzed using flow cytometry for lineage and T-cell markers. Peripheral blood haematological analysis was also undertaken. Of the *NHD13;Puma*$^{-/-}$ mice analyzed, somewhat unexpectedly, all of them developed T-cell acute lymphoblastic leukaemia alone (based on macroscopic and/or flow cytometric analysis) with no evidence of acute myeloid leukaemia ***(Table 4.1)***. Median survival of *NHD13* mice with or without PUMA was comparable (301 days vs 327 days respectively; p = 0.15) excluding the possibility that these mice simply developed ALL at an earlier time point ***(Figure 4.8)***.

These results suggest that PUMA may have dual function in preventing or permitting tumour progression and that this likely depends on the tumour type and source of oncogenic stress.

4.3.2.4. Loss of a single *Puma* allele affords a degree of restoration of peripheral blood anaemia and also prevents AML transformation

In examining long-term survival of *NHD13;Puma*$^{-/-}$ mice, we aged a number of *NHD13; Puma heterozygous (Puma*$^{+/-}$*)* littermates. Loss of a single *Puma* allele resulted in an intermediate rescue of the anaemia and the macrocytosis at a level between *NHD13* and *NHD13;Puma*$^{-/-}$ mice, although these results did not achieve statistical significance ***(Figure 4.7)***.

Of those mice aged, five were available for macroscopic dissection and flow cytometric analysis. Of these, four died from ALL/thymic lymphoma and one was deemed to have died from cytopenic complications of MDS alone. Of importance, we did not observe any transformation to acute myeloid leukaemia once again ***(Table 4.2)***.

4.4. Disease progression in *NHD13* mice and the disparate effects of PUMA vs p53

The generation of *NHD13* mice deficient in PUMA or p53 has one significant similarity and yet quite strikingly different outcomes. Loss of p53 or PUMA in *NHD13* mice rescues the apoptosis of HSCs in both cases; however p53-deficient mice exhibit a more aggressive phenotype of disease progression to both AML and thymic lymphoma / ALL as would be expected; whilst PUMA-deficient mice surprisingly do not develop AML at all.

As we have demonstrated in Chapter 3 and as others have shown, p53's tumour suppressive role is likely mediated independent of its apoptotic function (Valente et al. 2013). To explain the discrepancy with respect to disease progression, we compared cell cycle characteristics and DNA damage of LSK cells in *NHD13* mice deficient in PUMA or p53.

Cell cycle analysis, as performed using flow cytometric analysis, was undertaken using the nucleic acid stain DAPI and the proliferation marker, Ki67. *NHD13* LSK cells were demonstrated to have reduced quiescence compared to wild-type mice (i.e reduced G0) – a finding that may be in keeping with reduced *Cdkn1a* (p21) expression ***(Figure 3.11)***. In the absence of PUMA or p53 however, we did not see any difference in cell cycle analysis ***(Figure 4.9)***. This suggests the difference in survival and disease progression between *NHD13*;*Puma*$^{-/-}$ and *NHD13;p53*$^{-/-}$ mice is not the result of an altered impact on cell cycle progression.

We proceeded to quantify DNA damage in LSK cells by analyzing phospho-γ-H2AX levels using flow cytometry. *NHD13* LSK cells in this case, exhibit a 4-fold increase in γ-H2AX staining indicative of increased DNA damage. This increase

was abrogated by the loss of PUMA. However, in contrast, absence of p53 had no effect on the proportion of γ-H2AX positive LSK cells with a level maintained at 4-fold above baseline ***(Figure 4.10)***.

Therefore, we report opposing effects for disease progression in *NHD13* mice deficient in PUMA or p53 and demonstrate that this is most likely the result of alterations in DNA damage responses, but not due to apoptosis or cell cycling. Although, a number of DNA damage response genes affecting homologous recombination (HR) and non-homologous end joining (NHEJ) were analyzed using qPCR analysis, no significant differences were found (data not shown).

4.5. In addition to PUMA, BIM mediates apoptosis of *NHD13* HSCs

Although not a direct transcriptional target of p53, BIM, like PUMA is capable of inhibiting all five anti-apoptotic BCL-2 related proteins (Chen et al. 2005). In particular scenarios, BIM has also been shown to co-operate with PUMA to activate effector proteins, BAX/BAK.

In view of this, we sought to determine if BIM could also rescue the apoptosis of *NHD13* HSCs and its effect on individual HSC subsets. In similar fashion to PUMA, deficiency of BIM in *NHD13* HSCs rescued the apoptosis of the immature LSK cell population alone ***(Figure 4.11)***. Unlike PUMA however, we only saw a partial rescue of LSK and MPP numbers with no rescue whatsoever of LT- or ST-HSCs ***(Figure 4.12)***.

In combination therefore, the apoptosis of *NHD13* stem cells (MPP cells in particular) appears to be primarily mediated by PUMA, with a possible contribution (albeit significantly smaller) by BIM. As we saw no complete rescue of MPP or LSK cell numbers – mice were not aged for longer-term analysis.

Tables

Table 4.1. ***Phenotype of NHD13 mice completely deficient for Puma***

Table outlining the phenotypic features of *NHD13* mice completely deficient for PUMA. The table outlines the age of mice when they were culled and their appearance; together with peripheral blood parameters, macroscopic appearance of organs and diagnosis based on these features and flow cytometric analysis (as required); Hb = haemoglobin, MCV = mean corpuscular volume, neut = neutrophils; lymph = lymphocytes; DP = double positive; SP = single positive; Pl = platelets.

Age (days)	**Appearance**	**Peripheral blood parameters**	**Macroscopic features**	**Flow cytometry findings**	**Diagnosis**
326	Pale feet, reduced mobility	Hb 36 / MCV 64 / WCC 44.6 (Neut 8.16, Lympho 26.2) / Pl 115	Normal thymus, large spleen, abnormal mottling of liver	Abnormal DP population	DP-ALL
173	Hunched and skinny		Massive thymoma		ALL
187		Hb 133 / MCV 58 / WCC 22.9 (Lymph. 17.31) / Pl 296	Small thymoma, pale bone marrow, enlarged spleen	Abnormal SP8 population	SP8 ALL
327	Shallow breathing, reduced mobility	Hb 49 / WCC 130 (Neut high, Lymph high) / Pl 487	Massive thymoma, enlarged spleen,		ALL
321	Reduced mobility, weight loss	Hb 111 / MCV 63.4 / WCC high (Neut high, Lymph high) / Pl 730	Medium-size thymoma, massive splenomegaly	Abnormal SP8 profile	SP8 ALL

<u>Table 4.2.</u> ***Phenotype of NHD13 mice that are heterozygous deficient for Puma***

Table outlining the phenotypic features of *NHD13* mice deficient for a single allele of *Puma*. The table outlines the age of mice when they were culled and their appearance; together with peripheral blood parameters, macroscopic appearance of organs and diagnosis based on these features and flow cytometric analysis (as required)

Age (days)	**Appearance**	**Peripheral blood parameters**	**Macroscopic features**	**Flow cytometry findings**	**Diagnosis**
257	Lethargic, reduced mobility	Hb 63 (MCV 59) / WCC 49 (Neut 16 / Lymph 25) / Pl 93	Mild splenomegaly	Normal myeloid profile, small T-cell population	MDS-related death
248	Hunched, increased breathing	Hb 148 (MCV 49) / WCC 2.74 / Pl 317	Huge thymoma, normal sized spleen, pale liver	Not done	T-ALL
215	Unwell, hunched	Hb 111 (MCV 53) / WCC 14.9 (Lymph. 11.61) / Pl 252	Large thymus	Normal myeloid maturation, abnormal DP population	DP T-ALL
231	Reduced mobility	Hb 148 (MCV 50) / WCC 60 (Neut 12.16 / Lymph. 40.9) / Pl 663	Enlarged thymus, enlarged spleen	Normal myeloid maturation, abnormal DP population	DP T-ALL
297	Unwell, reduced mobility, unkempt	Hb 74 (MCV 63) / WCC 147 (Neut. 146 / Mono. 34)	Large thymus, massive spleen	Normal myeloid maturation, expanded B220 population	ISP8 ALL

Figures

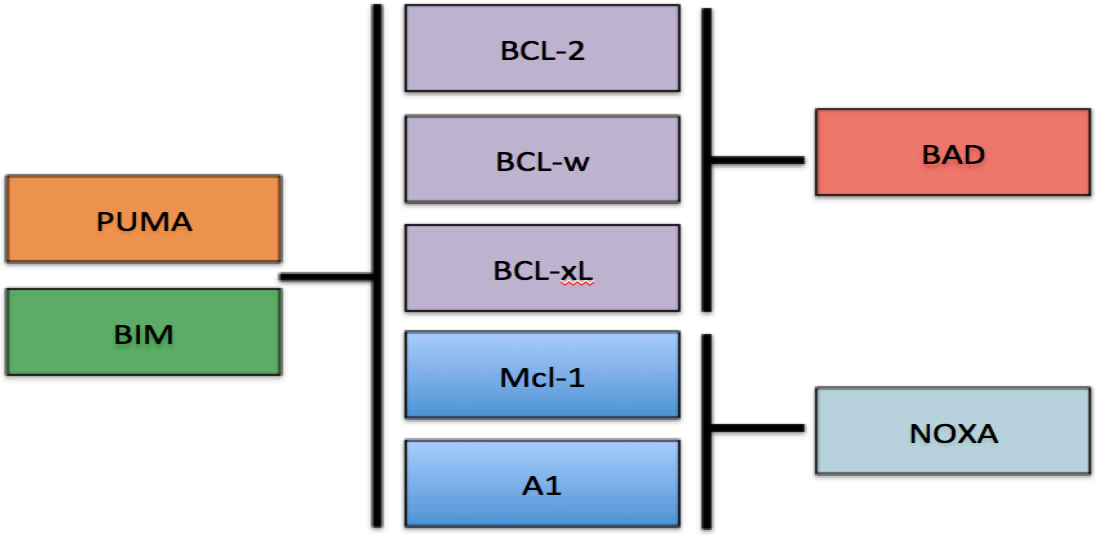

Figure 4.1. ***Specificity of various BH3-only proteins***

This schema indicates the relative specificity of some of the major pro-apoptotic BH3-only proteins against the class of anti-apoptotic BCL-2-related proteins (BCL-2, BCL-w, BCL-xL, Mcl-1 and A1). The proteins PUMA and BIM are the most potent inhibitors of this class of proteins - capable of inhibiting all five well-described members. This is in contrast to BAD and NOXA, which both have a limited repertoire of targets and are thus not as potent, but nonetheless appear to be complementary in combination.

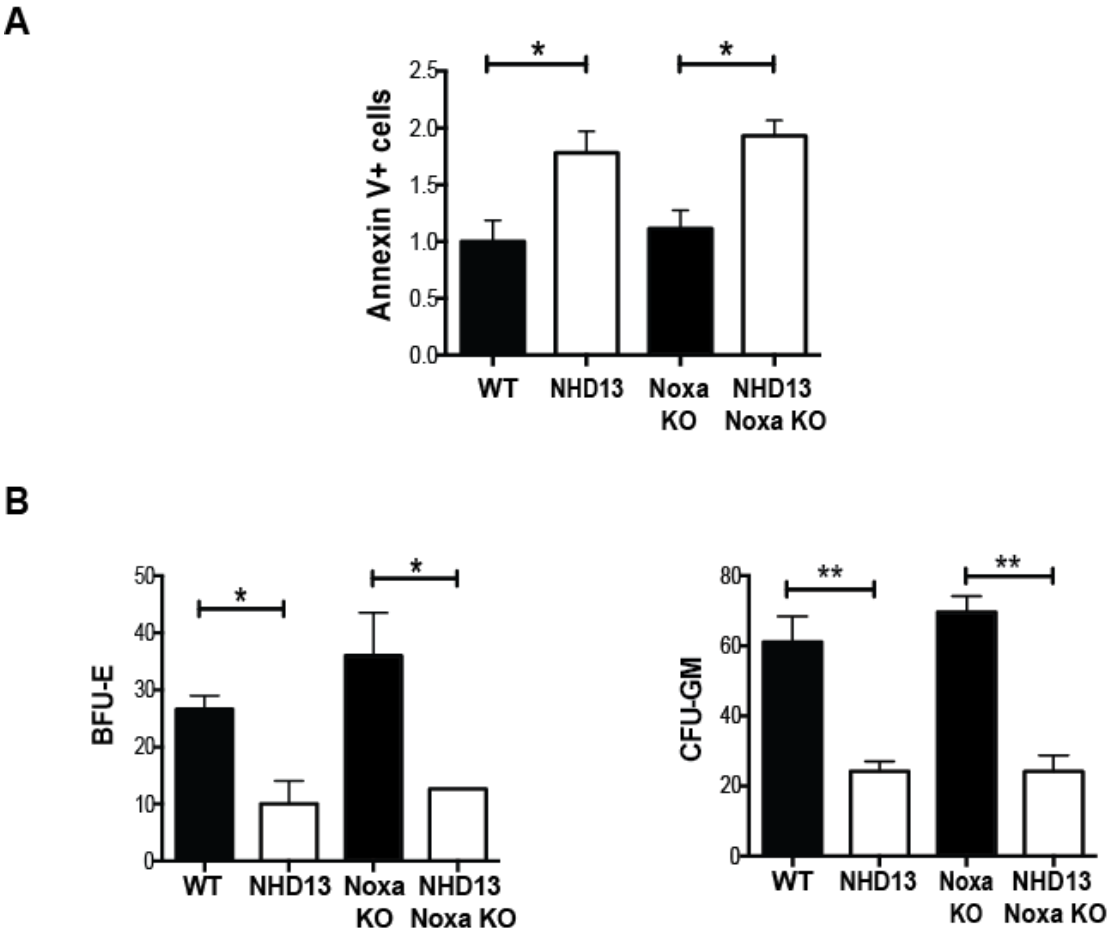

Figure 4.2. ***The effect of NOXA-deficiency on apoptosis and haematopoietic progenitor assays***

NHD13 mice were generated deficient for *Noxa;* (A) Apoptosis as measured by annexin-V using flow cytometry. Results have been normalized to wild-type levels; n = 3 for each genotype; (B) Haematopoietic progenitor assays (methylcellulose and agars) were performed to quantify BFU-E and CFU-GM respectively. Results are expressed as number of colonies per 100,000 cells for BFU-E and per 50,000 cells for CFU-GM; * = $p < 0.05$; ** = $p < 0.01$.

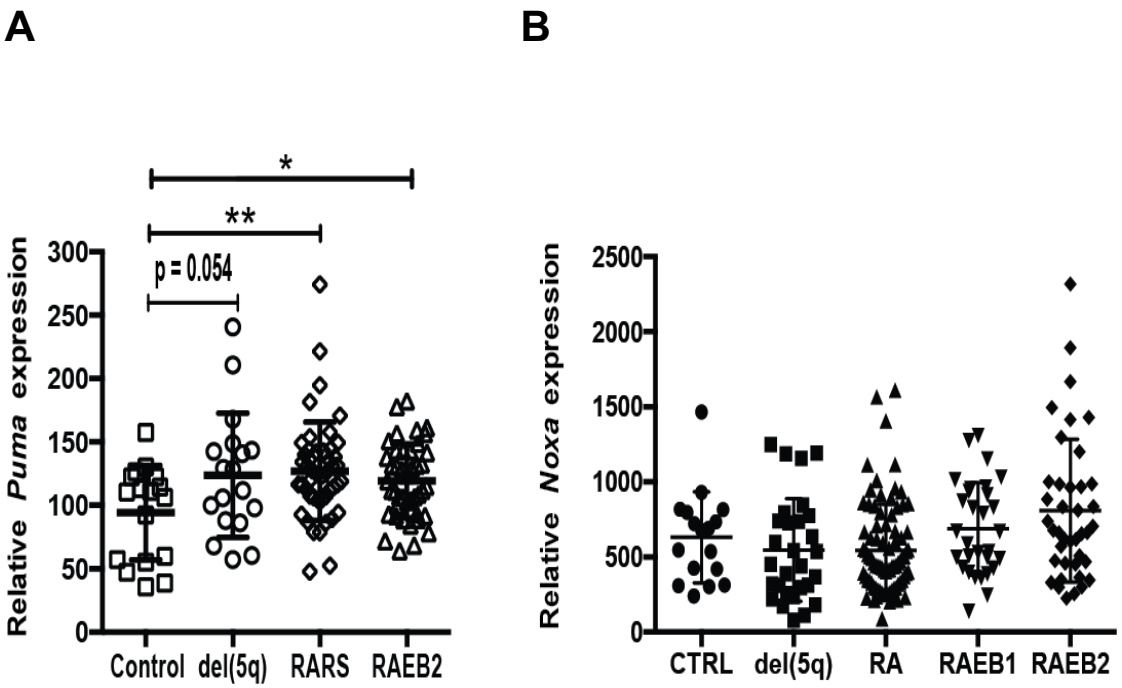

Figure 4.3. ***Microarray data of Puma and Noxa expression in human MDS***

Data as derived and extracted from Pellagatti et al (Pellagatti et al. 2010) . Plots show mRNA expression levels of (A) *Puma* and (B) *Noxa* for control samples and various subtypes of human MDS. Each point represents a single sample. Relative expression levels are plotted on the y-axis; * = $p < 0.05$; ** = $p < 0.01$

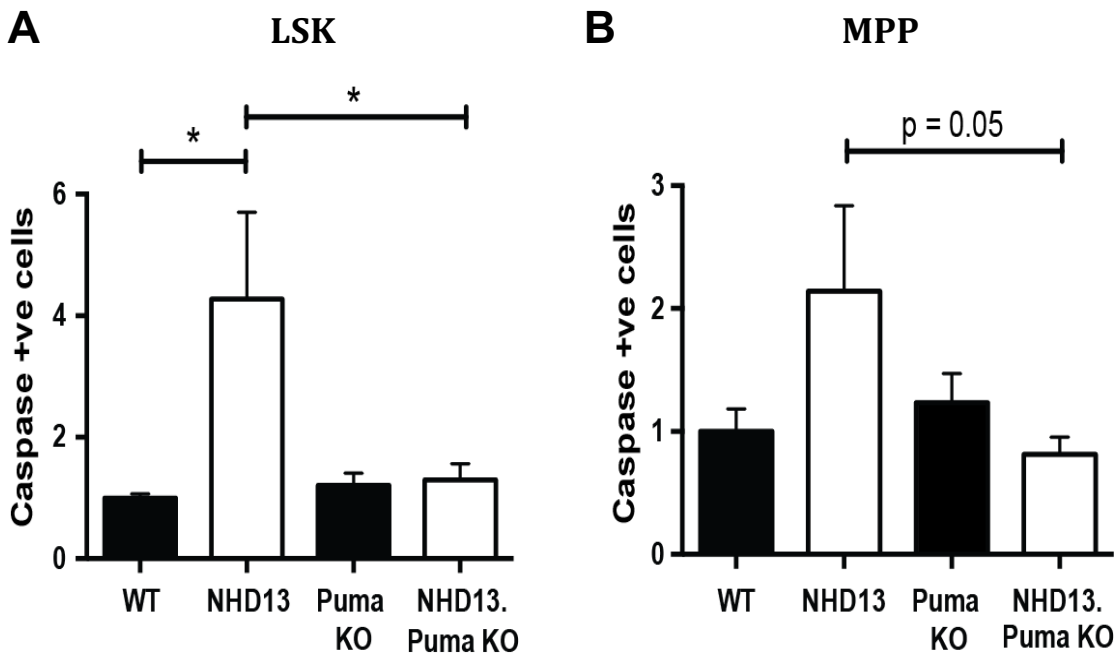

Figure 4.4. ***Effect of PUMA-deficiency on apoptosis of NHD13 HSCs***

NHD13 mice were generated deficient for *Puma;* (A) Apoptosis of LSK cells as measured by caspase-3/7 using flow cytometry. Results have been normalized to wild-type levels; n = 9 mice in total for each genotype (3 individual experiments); (B) Apoptosis of MPP progenitors (a subset of LSK cells) as measured by caspase-3/7 using flow cytometry. Results have again been normalized to wild-type levels; n = 5 for each genotype; * = $p < 0.05$.

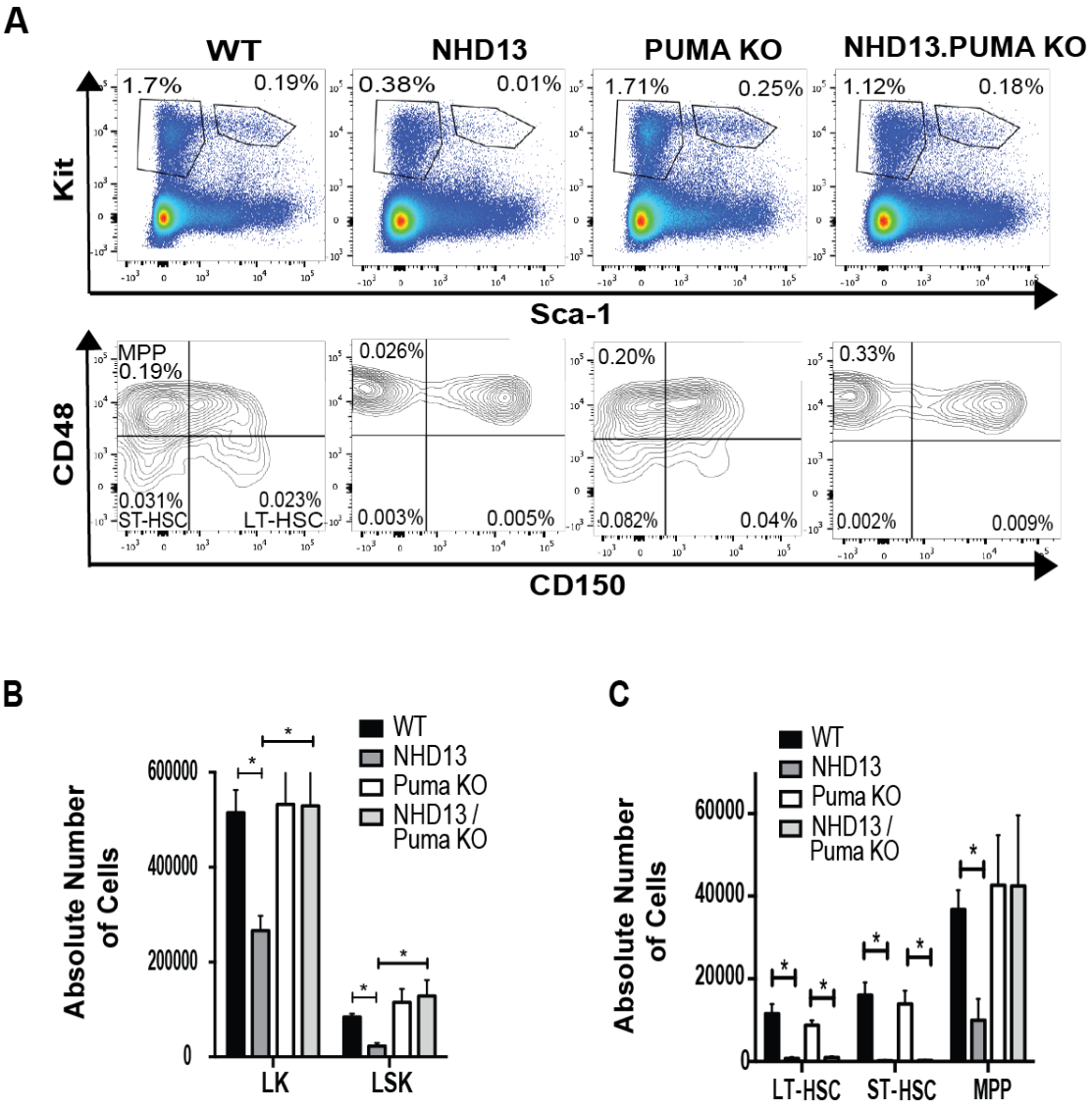

Figure 4.5. ***PUMA deficiency rescues relative and absolute numbers of LSK (and MPP) NHD13 HSCs***

(A) Flow cytometric analysis of relative proportions of LSK cells and associated SLAM subsets. Numbers represent percentages of total nucleated cells. Cells have initially been gated on lineage negative subsets. Results shown are representative of at least three individual experimental replicates; (B) Absolute quantification of LK and LSK cells (per mouse leg) using flow cytometric analysis. Numbers represent the aggregation of three individual experiments (i.e n = 9 / genotype); (C) Absolute quantification of SLAM subsets – as for (B); * = $p < 0.05$.

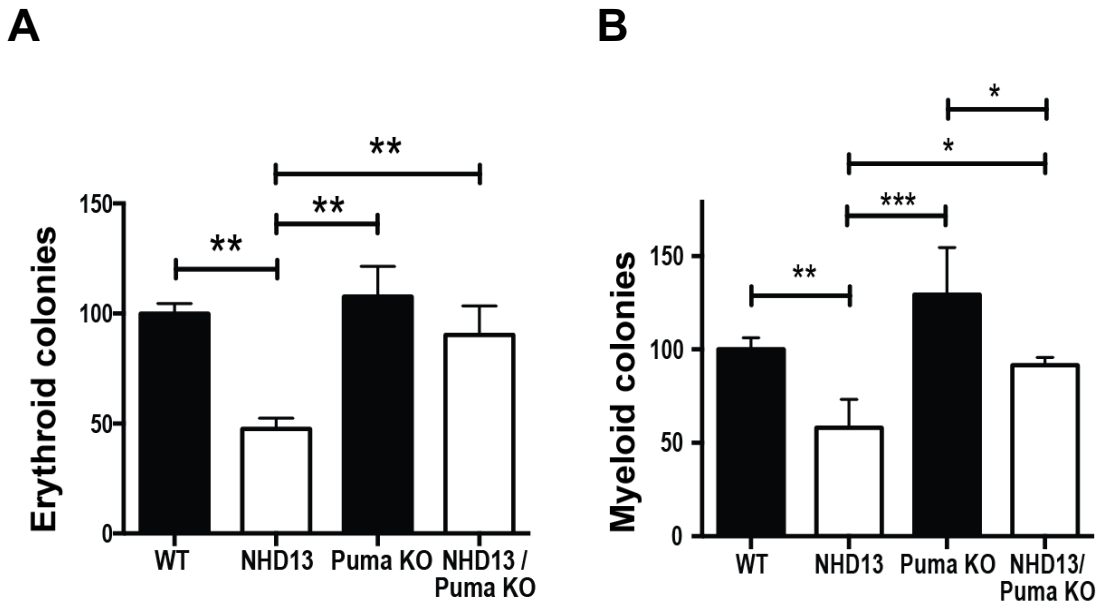

Figure 4.6. ***PUMA deficiency restores erythroid and myeloid colony numbers as determined by haematopoietic progenitor assays***

(A) Analysis of erythroid progenitors as determined by methylcellulose colony assays for *NHD13* mice deficient for PUMA. Results shown represent normalized values of two individual experiments with n = 3 per genotype per experiment. Assays were performed in triplicate for individual mice; (B) Myeloid progenitor analysis as determined by agar progenitor assays. As for methylcellulose assays, results have been normalized and performed in triplicate for each sample; n = 3 per genotype per experiment; * = $p < 0.05$, ** = $p < 0.01$, *** = $p < 0.001$.

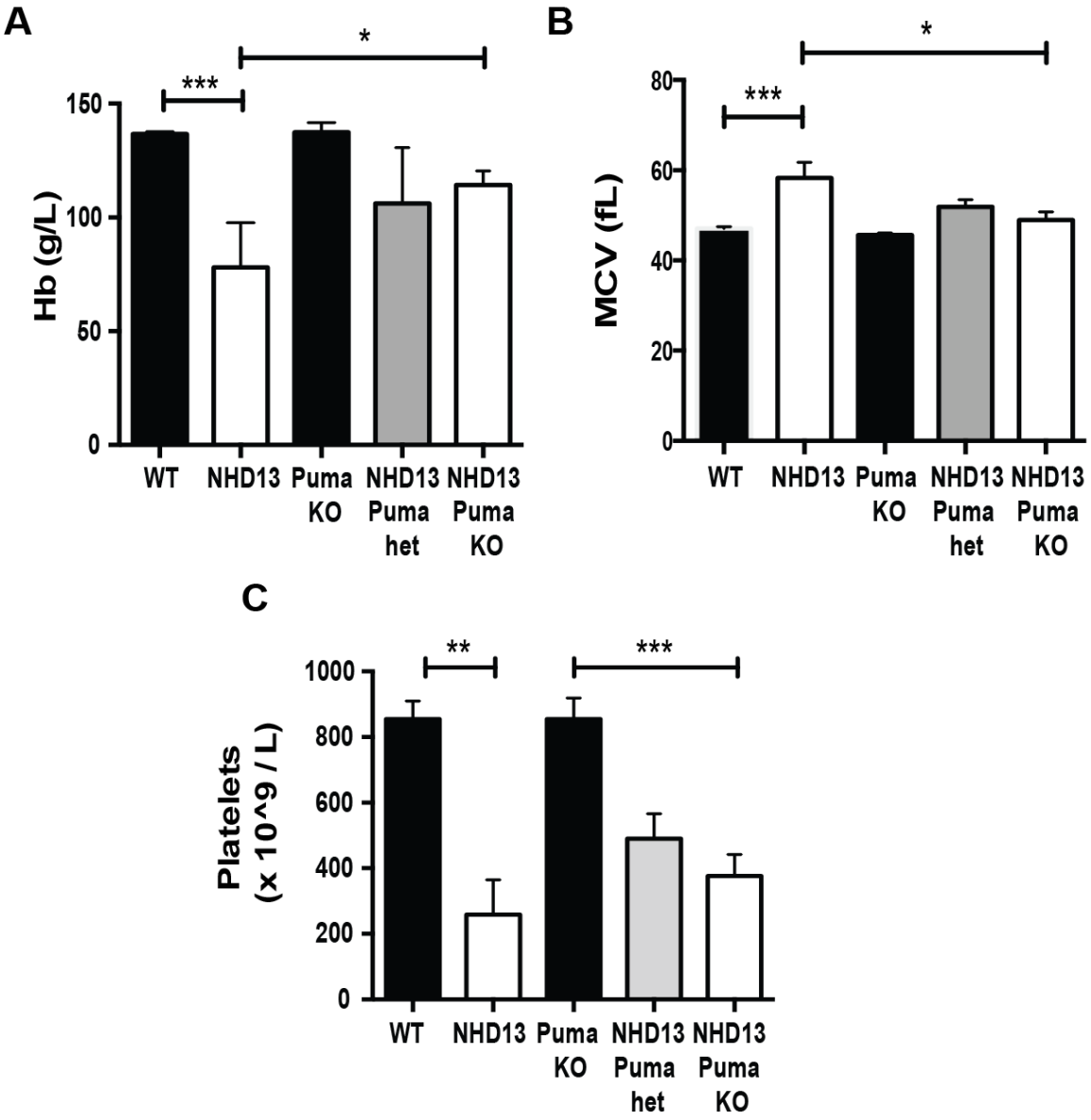

Figure 4.7. ***PUMA deficiency rescues the macrocytic anaemia of NHD13 mice but not the associated thrombocytopenia***

Peripheral blood parameters of *NHD13* mice deficient for one or both allele(s) of *Puma.* Mice are all 8 months old; n = > 6. Parameters shown include (A) haemoglobin in g/L; (B) mean corpuscular volume (MCV) in fL and (C) platelet count; * = $p < 0.05$; ** = $p < 0.01$; *** = $p < 0.001$.

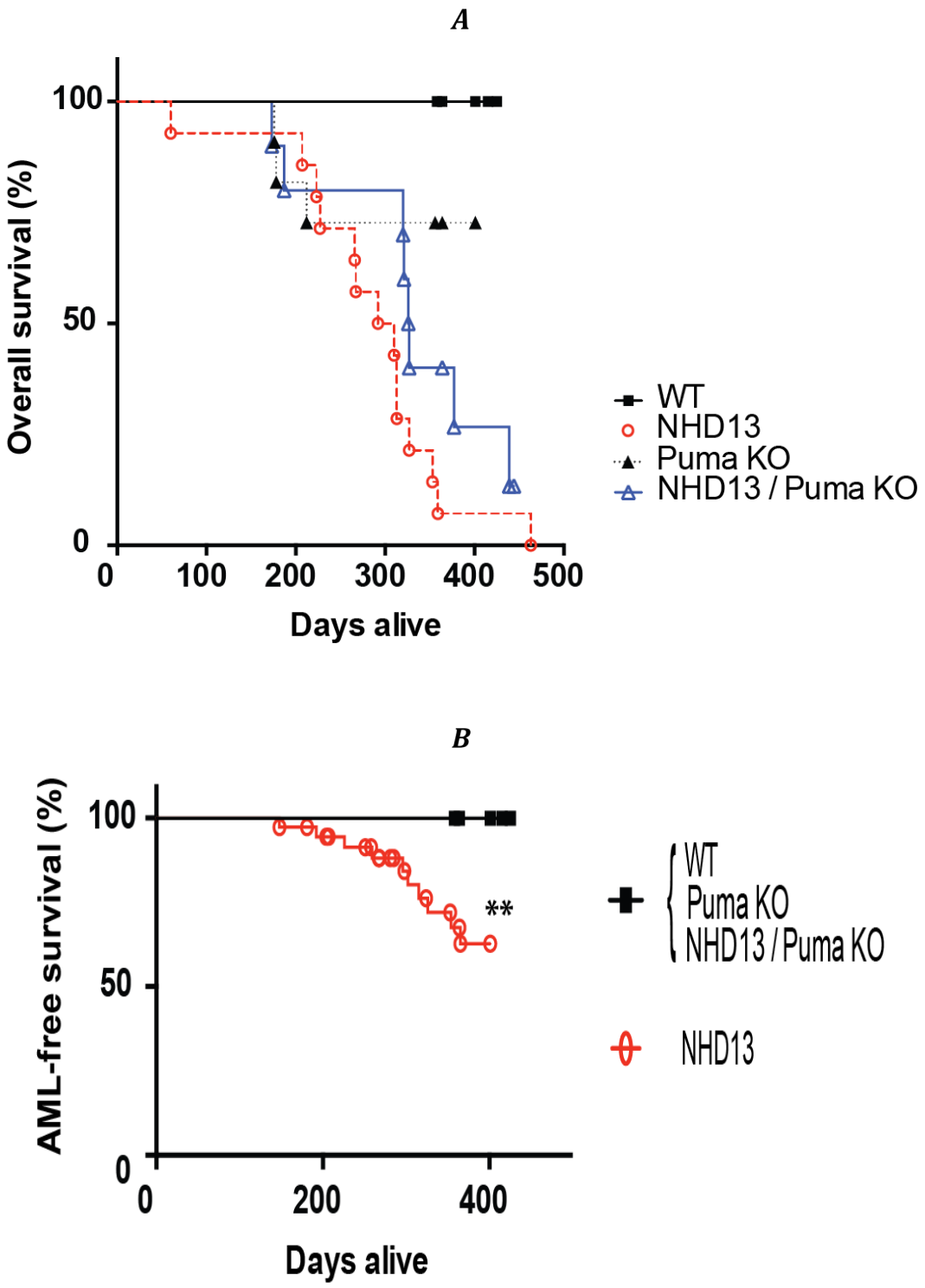

Figure 4.8. ***Survival curves for NHD13 mice deficient for PUMA***

Kaplan-Meier curve analysis of (A) overall survival and (B) AML-free survival for *NHD13* mice and those deficient for PUMA; ** = $p < 0.01$.

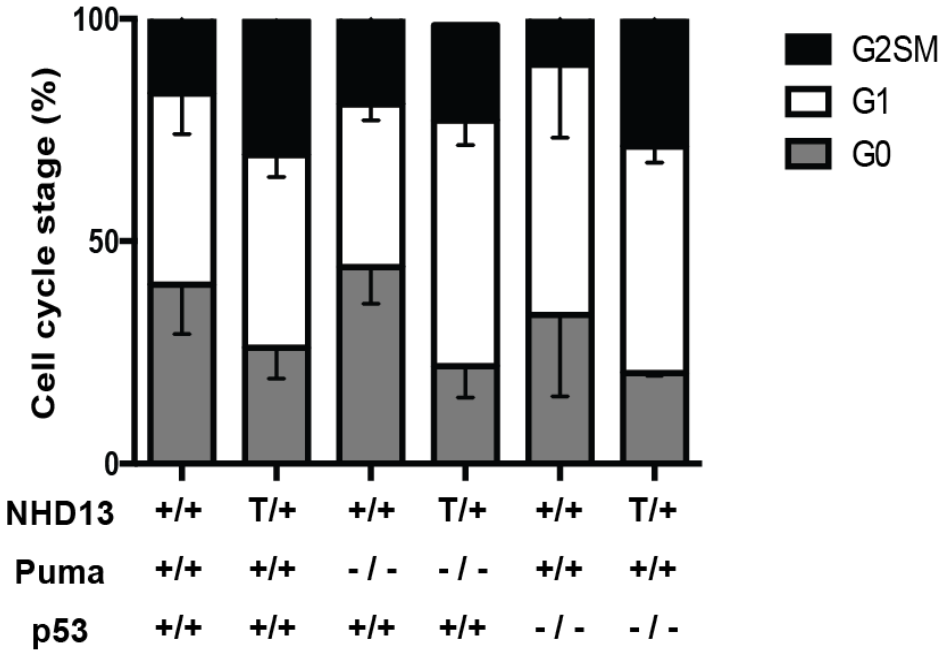

<u>Figure 4.9.</u> ***Cell cycle analysis of NHD13 mice deficient for PUMA or p53***

Cell cycle analysis of LSK cells as determined by flow cytometry. Results are based on gating of DAPI vs Ki67 (proliferation marker). Gating includes G0 (non-cycling) cells: $Ki67^{lo}$, DAPI peak; G1 cells: $Ki67^{hi}$, DAPI peak; G2SM (cycling cells): $Ki67^{hi}$, DAPI tail. Results shown are the aggregation of three individual experiments for PUMA deficient mice (n = 3 per genotype) and p53 deficient mice (n = 3 per genotype) and have been normalized to wild-type G0. Results show no significant effect on cell cycle through loss of PUMA or loss of p53 on the *NHD13* phenotype.

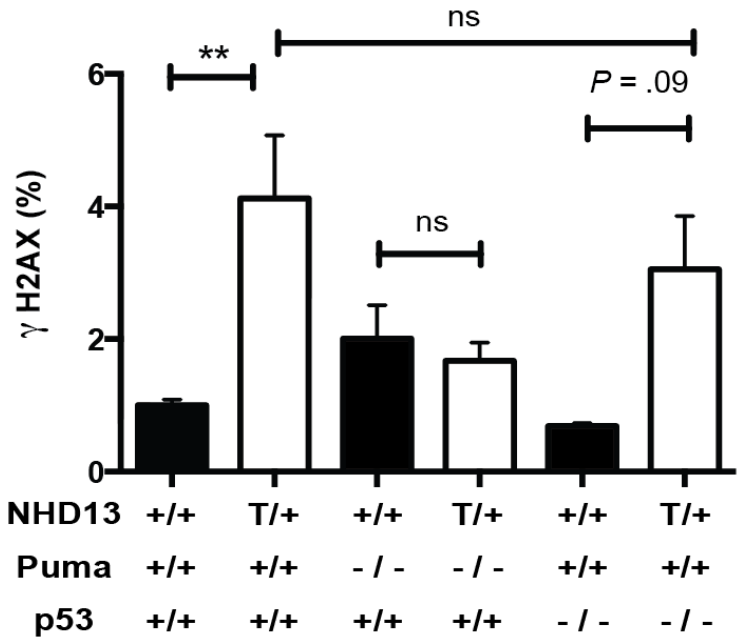

Figure 4.10. ***DNA damage analysis (γH2AX) as determined for NHD13 mice and those deficient in PUMA or p53***

DNA damage (γH2AX) as determined using flow cytometric analysis. Results are expressed as percentage of G0 (i.e non-cycling) cells that are positive for γH2AX. n = > 5 for each genotype. Once again, results represent the aggregate of multiple experiments and have been normalized to wild-type γH2AX levels; ** = $p < 0.01$.

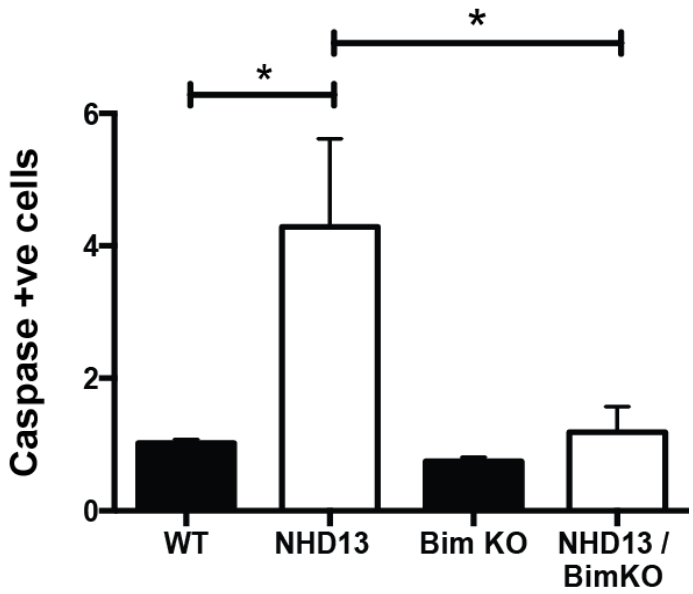

Figure 4.11. ***The effect of BIM deficiency on apoptosis of NHD13 HSCs***

Flow cytometric analysis of apoptosis as measured by caspase staining for *NHD13* LSK progenitor cells deficient for BIM. As for PUMA, loss of BIM appears to protect LSK cells from undergoing apoptosis. Results shown have been normalized to WT caspase and represent 2 separate experiments (n = 10 for WT and *NHD13*; n = 6 for *Bim* KO and *NHD13*;*Bim KO*); * = $p < 0.05$.

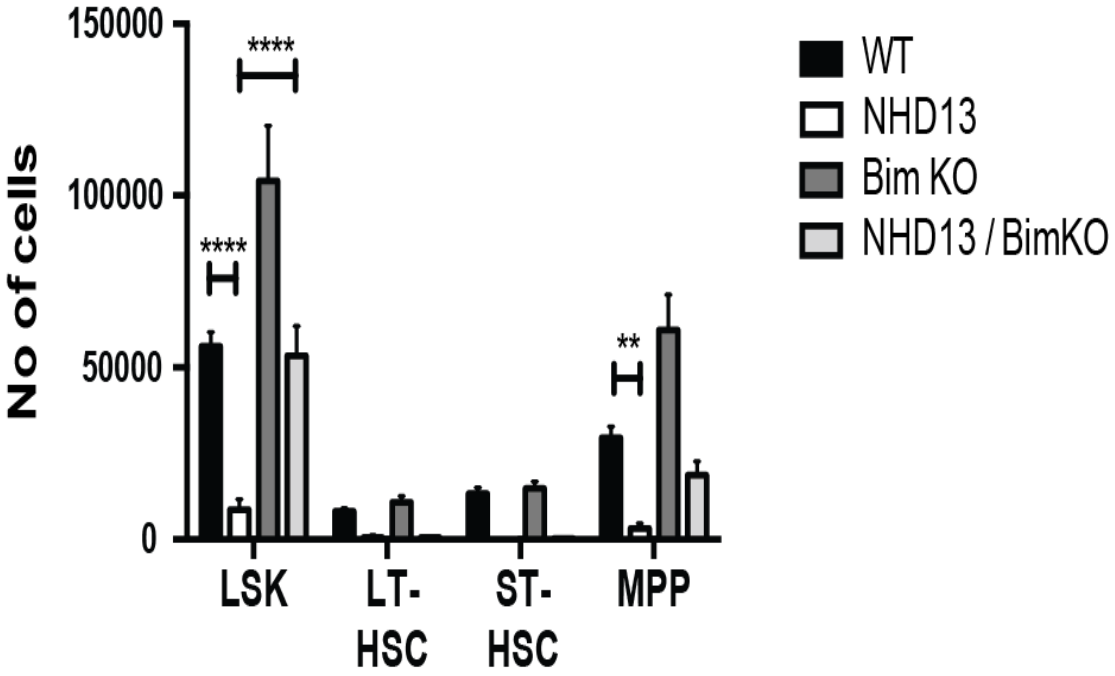

Figure 4.12. ***Loss of BIM partially rescues LSK and MPP cell numbers***

Absolute enumeration of LSK cells and SLAM subsets reveals partial rescue of LSK and MPP subsets. Absolute numbers are expressed per mouse leg (tibia + fibula); n = 6 per genotype; ** = $p < 0.01$; **** = $p < 0.0001$.

Discussion

Although multiple groups have demonstrated that apoptosis is increased particularly in early-stage myelodysplastic syndrome (Raza et al. 1995; Parker and Mufti 2000), much of this data remains observational with few attempts having been made to decipher which particular proteins drive this phenotype and what the effect might be if apoptosis were modulated.

Having excluded a significant role for the extrinsic pathway in this model, in this Chapter we focus on intrinsic pathway pro-apoptotic proteins, PUMA, NOXA and BIM – all of which sit upstream of BCL-2 and downstream of p53. We demonstrate that although *Noxa* is increased at the mRNA level, the principle driver of apoptosis of MDS progenitors is PUMA. Our work shows that removal of PUMA not only normalizes apoptosis to wild-type levels ***(Figure 4.4)***, but also rescues the haematopoietic stem cell populations (LSK and MPP cells) ***(Figure 4.5)***. This is associated with a rescue of the macrocytic anaemia typically seen in these mice ***(Figure 4.7)***. In contrast to removal of p53, which also rescues the apoptosis of *NHD13* haematopoietic stem cells, but accelerates leukaemic progression, removal of PUMA surprisingly prevents progression of disease to acute myeloid leukaemia ***(Figure 4.8)***. These findings highlight a potential role for apoptosis in myeloid disease progression. Furthermore, to our knowledge, this is the first body of work demonstrating a role for PUMA in the phenotype of MDS.

Having demonstrated that apoptosis in this model is p53-mediated and that *Noxa's* expression is increased at the mRNA level, we begin this Chapter by first examining the role of NOXA in the apoptosis of MDS progenitors. Together with *Puma, Noxa* is also a downstream transcriptional target of p53 and the production of both proteins is predominantly regulated at the transcriptional level (Oda et al. 2000; Nakano and Vousden 2001; Shibue et al. 2003). However, despite its increased expression, we are unable to demonstrate any rescue of apoptosis or of progenitor colony numbers when *Noxa* is removed from *NHD13* stem cells, suggesting that apoptosis of these cells occurs independent of *Noxa.*

We subsequently focused our attention on PUMA. At a transcriptional level, we were unable to demonstrate any significant increase in *Puma* expression. However, it is worthy of mention, that in human MDS samples, based on analysis of microarray data from Pellagatti et al (Pellagatti et al. 2010), *Puma* is significantly increased in all subtypes of MDS compared with control samples, whilst *Noxa* is not ***(Figure 4.3)***. Unlike NOXA, removal of PUMA was associated with a significant amelioration of apoptosis to wild-type levels and rescue of LSK (+ MPP) cell numbers ***(Figure 4.4 & 4.5)***. In contrast to the differential rescue of erythroid vs myeloid progenitors and numbers seen with removal of p53; removal of PUMA restored both myeloid and erythroid colony numbers ***(Figure 4.6)***. From a functional and clinically significant perspective, rescue of apoptosis translated into a rescue of the macrocytic anaemia associated with the *NHD13* phenotype. However, as for BCL-2 overexpression the thrombocytopenia was not rescued - suggesting this occurs in an apoptosis-independent manner or that the apoptosis is driven by an alternate mechanism that is not dependent on PUMA ***(Figure 4.7)***.

Although once again counterintuitive, but similar to BCL-2 overexpression, is the effect loss of PUMA has on disease progression. Of note, *NHD13* mice deficient for PUMA, do not develop AML – suggesting a significant role for apoptosis in myeloid disease progression. Importantly, loss of PUMA is still associated with lymphoid disease progression as has been shown in the setting of other oncogenes such as c-Myc - highlighting its tumour suppressive role in this context (Michalak et al. 2009). Importantly, our survival data does not indicate that *NHD13* mice deficient for PUMA develop ALL at an earlier timepoint masking the development of AML. In fact, survival of *NHD13* mice alone and *NHD13; Puma*$^{-/-}$ mice was comparable ***(Figure 4.8)***.

These findings generate a number of important questions:

a) Why does removal of PUMA but not NOXA rescue apoptosis? And why are *Puma* levels not elevated?

b) Are these findings significant from a clinical perspective for patients with human MDS? and;
c) Why does loss of p53, which also rescues the apoptosis of *NHD13* HSCs accelerate leukaemic progression in stark contrast to loss of PUMA?

Although at a transcriptional level *Puma* is not increased, that apoptosis of *NHD13* HSCs is PUMA-dependent is not entirely unexpected. Of the two BH3-only proteins, PUMA is known to be the more potent activator of apoptosis due to its ability to inhibit all BCL-2 related proteins, unlike NOXA which only binds MCL-1 and A1 (Chen et al. 2005). One of the difficulties studying apoptosis particularly in MDS, is the inherent nature of the population being studied to undergo cell death. We postulate that *Puma* levels may actually be increased at a transcriptional level; however as cells overexpressing PUMA undergo increased apoptosis, it may be that these cells are actually not available for interrogation when samples are analyzed. Although not shown, unpublished data in which BCL-2 is overexpressed (thus preventing apoptosis) in the presence of the *NHD13* transgene shows elevated levels of *Puma* at levels higher than those seen in *NHD13* samples alone.

That *Puma* levels are increased in human MDS samples compared with controls and that *Puma* heterozygosity in *NHD13* HSCs results in an intermediate rescue of the peripheral blood anaemia and reduced AML progression is of great significance. These findings suggest that therapeutically targeting PUMA may potentially be beneficial in ameliorating the cytopenias of MDS. Additionally, the PUMA heterozygosity data indicates that PUMA may not have to be completely inhibited to achieve some of these benefits. This certainly warrants further investigation particularly given that small-molecule PUMA inhibitors have recently been described (Mustata et al. 2011).

Although the Hanahan and Weinberg model (Hanahan and Weinberg 2000; Hanahan and Weinberg 2011) suggests that overcoming apoptosis is typically associated with disease progression, our findings in this Chapter challenge this paradigm and align with our previously published work regarding BCL-2

overexpression. By preventing cells from undergoing apoptosis, we surprisingly found no progression to acute myeloid leukaemia. To some degree, this may seem counterintuitive. However, it is possible that apoptosis in this disorder drives a 'proliferative' phenotype which is subsequently associated with the acquisition of additional genetic mutations. This has certainly been demonstrated in lymphoid disease (Michalak et al. 2010). What remains unclear however, is at what point does preventing apoptosis become detrimental in this context, accelerating leukaemic progression. This remains an ongoing area of interest in our laboratory at present. Additionally, these findings challenge the paradigm that 'chemotherapy' is always the answer for malignancies. It may be that chemotherapy, through its induction of apoptosis actually drives more rapid leukaemic progression. This suggests that newer therapies may need to target alternative pathways.

One striking difference between the removal of PUMA vs p53 is the effect on longer-term survival and disease progression. Whilst loss of either gene prevented apoptosis in *NHD13* HSCs, loss of p53 accelerated leukaemic progression whilst loss of PUMA abrogated the development of myeloid leukaemia. To address this dichotomy, we proceeded to examine the effect on cell cycle using Ki67 and DAPI staining and DNA damage as measured using γH2AX measurement. Whilst we saw no difference in the cycling of *NHD13* cells that are deficient in PUMA or p53 – i.e there is reduced quiescence regardless; we did see a significant different in DNA damage. *NHD13* progenitors have repeatedly been shown to harbour more DNA damage cf their wild-type counterparts (Slape et al. 2012). Of note, loss of PUMA appears to prevent DNA damage somewhat in contrast to loss of p53, where DNA damage remains abundant. These findings highlight p53's promiscuous roles ranging from apoptosis to cell cycle control and DNA damage responses. It is likely therefore that loss of p53 not only prevents apoptosis, but also results in significant impairment of other tumour-suppressive functions, that are independent of apoptosis alone. This has been demonstrated in other models (Valente et al. 2013) and suggests that targeting p53 would be exceptionally deleterious.

In concluding remarks, although we show some evidence that BIM may also play a role in the apoptosis of MDS HSCs, its loss only provides a partial rescue of HSC numbers. These findings suggest that PUMA remains the primary BH3-only protein responsible for the apoptosis of MDS HSCs in the *NHD13* model.

CHAPTER FIVE

Apoptosis and myeloid leukaemic transformation: the tale of BCL-2

Abstract

BCL-2 and its related proteins comprise the anti-apoptotic machinery of the intrinsic pathway and lie downstream of the BH3-only proteins. Although these proteins have a postulated role in inducing cell cycle arrest, their primary function is to bind and inhibit pro-apoptotic function of BH3-only proteins. Previous gene expression analysis of NHD13 MDS progenitors reveals that of all the BCL-2 related proteins, BCL-2 itself is most significantly reduced - suggesting that this may prime MDS progenitors to undergo apoptosis. In this Chapter, we confirm that BCL-2 overexpression prevents the apoptosis of NHD13 LSK cells. In an attempt to mechanistically understand how preventing apoptosis might prevent leukaemic disease progression, we present the findings of RNA-seq and Ingenuity Pathway analyses specifically examining the effect BCL-2 overexpression has on the NHD13 transgene. We show evidence that prevention of apoptosis through the overexpression of BCL-2 is associated with a dampened 'inflammatory' signature when compared with gene expression associated with the NHD13 transgene alone. These findings suggest that inflammation associated with apoptosis of MDS progenitors may play a pivotal role not only in the cytopenias of this disease, but also in disease progression. Recent 'anti-inflammatory' based therapies are discussed in light of these results.

Background

5.1. BCL-2

The anti-apoptotic protein BCL-2 belongs to the family of BCL-2-related proteins including BCL-xL, BCL-w, MCL-1 and A1. These proteins all share homology for the BH1-4 domains. The basis of BCL-2 as an oncogene was first suggested when it was identified from the breakpoint region of the recurrent chromosomal translocation t(14;18) associated with human follicular lymphoma (Finger 1984). In this context, BCL-2 overexpressing mice have an increased incidence of lymphoma. Furthermore, BCL-2 may co-operate with oncogenes such as c-Myc, immortalizing pre-B cells, promoting proliferation and ultimately driving more rapid malignant progression (Vaux et al. 1988; Strasser et al. 1990).

As discussed in Chapter 1, overexpression of the anti-apoptotic protein BCL-2 has generally been associated with more advanced disease in MDS. Higher levels of expression portend a worse overall prognosis with increased risk of leukaemic progression and shorter overall survival (Rajapaksa et al. 1996; Kurotaki et al. 2000; Parker et al. 2000; Boudard et al. 2002).

5.2. Apoptosis + inflammation

Although apoptosis has been classically considered 'anergic' in comparison to necrosis (Scaffidi et al. 2002), the apoptotic corpse may at times promote pro-inflammatory factors. Under ordinary circumstances, anti-inflammatory cytokines such as TGF-β and IL-10 are often released by macrophages and act to suppress the inflammation seen during apoptotic corpse clearance (Savill and Fadok 2000). However, defective clearance can occur in diseases processes, particularly if this mechanism is overwhelmed (Velegraki et al. 2013). In this context, a pro-inflammatory milieu may be associated with apoptosis.

The association of inflammation with various disease entities such as atherosclerosis and cancer has drawn significant interest over recent years having been proposed by Virchow more than 140 yrs ago. In this context, the role of various tumour macrophages as a source of pro- and anti-inflammatory

cytokines (eg IL-1β, IL-18, IL-6, IL-12 vs IL-10, IL-4, IL-13 respectively) is noted. Although beyond the scope of this current study, the function of myeloid derived suppressor cells induced by inflammation and facilitating tumour growth has been previously reviewed (Biswas et al. 2008; Ostrand-Rosenberg and Sinha 2009).

In solid tumours, the link between inflammation and malignancy has certainly been well described. A number of examples highlight this and include:

- patients with ulcerative colitis or Crohn's disease (inflammatory bowel disorders) generally exhibit an increased propensity for development of colorectal cancer (Nieminen and Färkkilä 2015);
- chronic pancreatitis may be associated with pancreatic cancer and often portends a worse prognosis (Dzeletovic et al. 2014);
- gastric cancer with H. pylori infection (Graham 2015);
- nasopharyngeal cancer in the context of EBV infection (Busson et al. 2004) and
- hepatocellular tumours in the setting of hepatitis.

Inflammation in these contexts likely causes significant DNA and tissue damage predisposing cells towards malignant transformation. Of recent interest, the use of aspirin as an anti-inflammatory agent has been shown to reduce the likelihood of developing colorectal cancer and other gastrointestinal malignancies possibly supporting this hypothesis (Cuzick et al. 2014). Although beyond the scope of this current work, a number of reviews have been published regarding inflammation and its role in the development and progression of malignancies in general (Grivennikov et al. 2010; Diakos et al. 2014).

In MDS, an immune or inflammatory milieu may contribute to the pathogenesis as has previously been discussed in Chapter 1. Inflammation in MDS is supported by studies which show an increase in immunomodulatory cytokines such as TNF-α (Sawanobori et al. 2003; Stifter et al. 2005) or IFN-γ in various haematopoietic cells. In some cases, TNF-α levels have been correlated with increased caspase-3 levels supporting a potential causal link between

inflammation and apoptosis (Mundle et al. 1999a; Mundle et al. 1999b). Mundle et al also report higher IL-1β levels in MDS patients and a reduction in apoptosis when IL-1β converting enzyme (aka ICE = Caspase 1), an important component of the inflammasome is inhibited (Mundle et al. 1996). What remains somewhat unclear in these cases is whether inflammation drives apoptosis or whether it might represent a by-product of the process as previously discussed.

An immune-mediated basis is also described in "hypoplastic" MDS, a subtype that makes up 10% of cases and shares common features with aplastic anaemia. Autoreactive and oligoclonal T-cell clones have been characterized in these disorders and correlated with higher rates of apoptosis (Pülhorn et al. 2012) and inhibition of normal haematopoiesis. In this context, the use of immunosuppressive therapies has exhibited some efficacy in the treatment of MDS - particularly in those expressing the HLA-DR15 antigen which often associates with this subtype (Molldrem et al. 1998; Sauntharajah et al. 2002; Dobbelstein and Ganser 2012).

In striking contrast to these cases, other studies have suggested that inhibition of an immune response may actually be permissive for leukaemic progression of MDS. Kondo et al report the expression of B7-H1 (CD274), a T-cell immunoinhibitory molecule, on MDS blasts in response to IFN-γ and TNF-α through the activation of NF-κB. Of note, blasts expressing B7-H1 demonstrated greater proliferative capacity and suppressed T-cell proliferation and were generally associated with higher risk disease (Kondo et al. 2010).

The numerous reports of MDS associated with other immune-mediated disorders such as vasculitis, polychondritis and sarcoidosis also warrants mention in this context and suggests underlying immune dysfunction as a possible common aetiology (Berthelot et al. 1997; Airaghi et al. 2000; Banerjee et al. 2001; Amberger et al. 2004).

Results

5.3. Exploring the effects of BCL-2 overexpression in *NHD13* stem cells

We have thus far demonstrated that abrogation of apoptosis alone (without influencing cell cycle) by targeting *Puma* is sufficient to prevent transformation to acute myeloid leukaemia. Although BCL-2 overexpression restored cellular quiescence in *NHD13* HSCs (Slape et al. 2012), the results with PUMA deficiency suggest that BCL-2 overexpression prevents leukaemic progression predominantly through its effects on apoptosis, but not on cell cycle. In contrast, P53's roles in cellular processes other than apoptosis alone (eg cell cycle arrest, DNA damage response, senescence, metabolism) may go towards explaining the opposing effect seen on long-term survival as has been discussed at the end of Chapter 4.

In analysing stem cell subsets, BCL-2 overexpression associates with a rescue of LSK cell numbers. Within this stem cell population, MPP cell numbers are rescued, but not LT- or ST-HSCs ***(Figure 5.1)***. These findings are similar to those seen in association with knockdown of p53 or PUMA as has previously been discussed.

5.4. Deciphering how preventing apoptosis prevents leukaemic progression

Our findings to date indicate that inhibition of apoptosis can prevent or at least delay transformation to AML. To investigate a possible underlying mechanism for this, we performed RNA-seq analysis of WT, *NHD13* transgenic, *BCL-2* transgenic and *NHD13-BCL-2* transgenic mice to determine the effect of BCL-2 overexpression on the genetic signature of *NHD13* mice.

Briefly, ~ 3 mice were pooled per sample to allow a sufficient amount of RNA to be extracted. Three samples were then generated for each genotype (4 genotypes x 3 samples x 3 mice = 36 mice). After performing RNA-seq, results were analyzed using Ingenuity Pathway Analysis.

As shown in ***Figure 5.2***, the top five canonical pathways that appear to be downregulated when BCL-2 is overexpressed in *NHD13* mice are:

a) the production of nitric oxide and ROS in macrophages,
b) leukocyte extravasation signalling,
c) triacyglycerol biosynthesis,
d) IL-8 signaling and
e) granulocyte adhesion and diapedesis

Analysis of specific regulators revealed significant inhibition of lipopolysaccharide, TNF, tretinoin and TGFβ1 – many of which are mediators of inflammation. Detailed pathway analysis of leukocyte extravasation and of ROS production by macrophages is also shown ***(Figure 5.3 and 5.4)***. Highlighted genes are those that have been downregulated. In combination, these findings suggest that BCL2 overexpression prevents apoptosis and reduces inflammation.

Figures

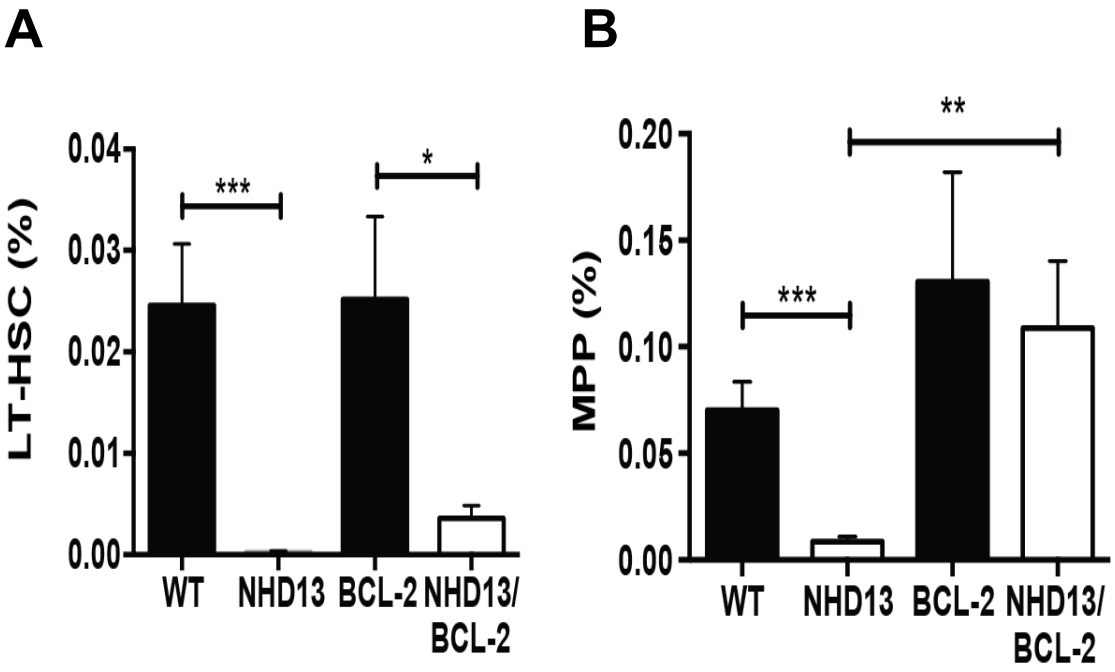

Figure 5.1. ***Overexpression of BCL-2 prevents apoptosis of LSK cells and specifically rescues MPP cell numbers***

Flow cytometric relative quantification of (A) LT-HSC and (B) MPP examining the effect of BCL-2 overexpression. Results reflect percentages of total nucleated cells; (n = 5 per genotype); * = $p < 0.05$; ** = $p < 0.01$; *** = $p < 0.001$..

Top Canonical Pathways

Name	p-value	Ratio
Production of Nitric Oxide and Reactive Oxygen Species in Macrophages	6.36E-09	16/180 (0.089)
Leukocyte Extravasation Signaling	9.58E-07	14/198 (0.071)
Triacylglycerol Biosynthesis	8.88E-06	6/35 (0.171)
IL-8 Signaling	1.24E-05	12/183 (0.066)
Granulocyte Adhesion and Diapedesis	4.69E-05	11/177 (0.062)

Top Upstream Regulators

Upstream Regulator	p-value of overlap	Predicted Activation State
lipopolysaccharide	2.46E-20	Inhibited
TNF	1.44E-19	Inhibited
tretinoin	6.29E-17	Inhibited
TGFB1	2.11E-13	Inhibited

Figure 5.2. ***Ingenuity Pathway Analysis comparing NHD13 transgenic mice to NHD13;BCL-2 double transgenic mice***

(Top panel) Ingenuity Pathway Analysis (IPA) results showing the top five canonical pathways that are significantly downregulated when BCL-2 is overexpressed in NHD13 transgenic mice. All of these results are highly significant; (Lower panel): IPA results of the four most significantly downregulated upstream regulators again showing the effects of BCL-2 overexpression on the NHD13 phenotype at the gene expression level.

Figure 5.3. ***Detailed IPA pathway mapping of macrophage production of ROS and nitric oxide***

IPA pathway map detailing ROS and nitric oxide production by macrophages – the most significantly down-regulated pathway in NHD13;BCL-2 double transgenic mice (compared with NHD13 mice alone). Highlighted genes are those that exhibit significantly reduced expression levels. Specific note is made of reduced expression of TNF-α and of components of the membrane-associated enzyme NADPH-oxidase complex including the 'phox' genes.

Production of Nitric Oxide and Reactive Oxygen Species in Macrophages

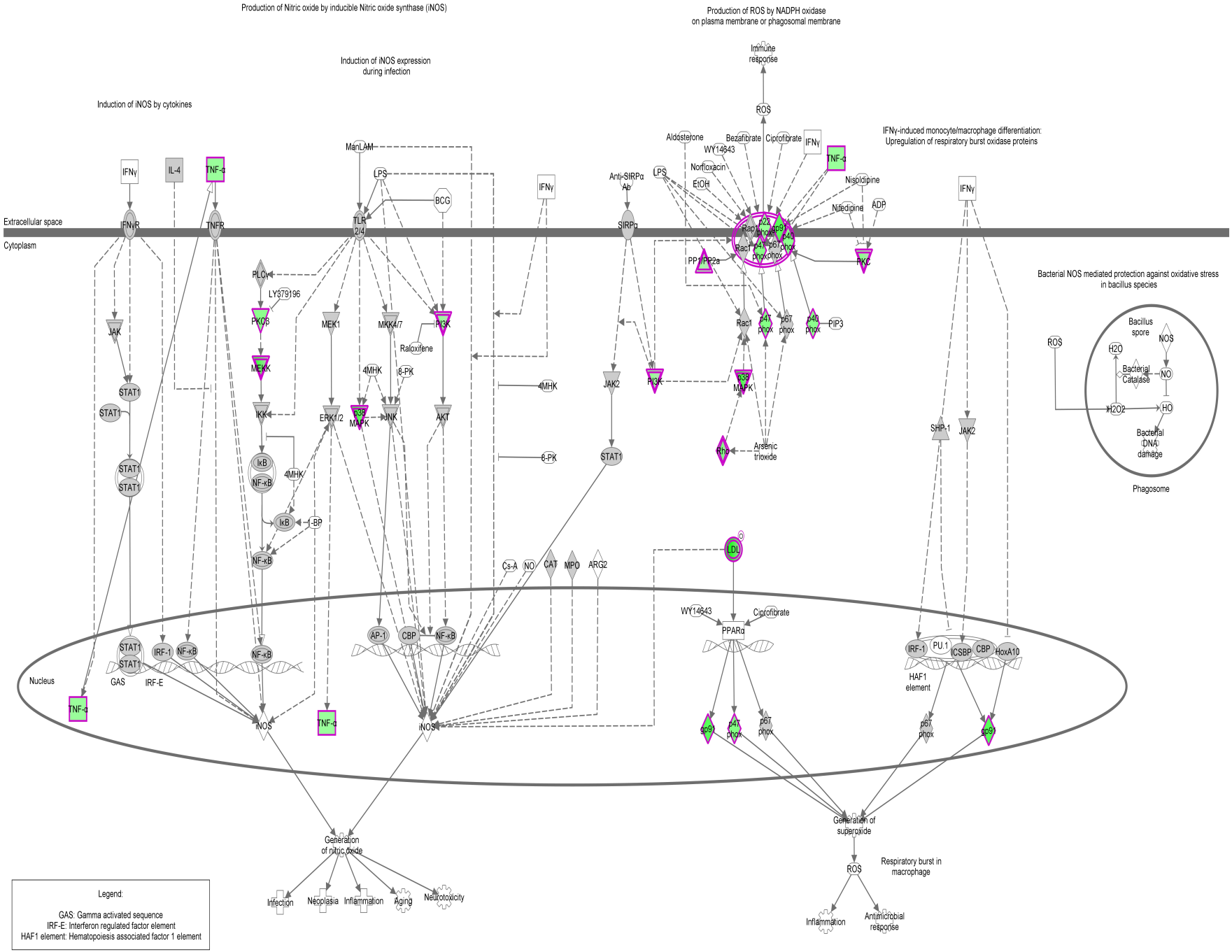

<u>Figure 5.4.</u> ***Detailed IPA pathway mapping of leukocyte extravasation signalling***

IPA pathway map of the leukocyte extravasation signalling pathway – the second most highly downregulated pathway in NHD13;BCL-2 double transgenic mice (when compared with NHD13 mice alone). Highlighted genes are those within this pathway that exhibit significantly reduced expression levels. Note is made of specific involvement of the integrins involved in leukocyte adhesion and rolling. Components of the NADPH oxidase complex are also significantly downregulated including neutrophil cytosolic factor (NCF), cytochrome b-245 alpha polypeptide (CYBA) and NADPH oxidase genes (NOX). Note is also made of downregulation of p38MAPK.

Leukocyte Extravasation Signaling

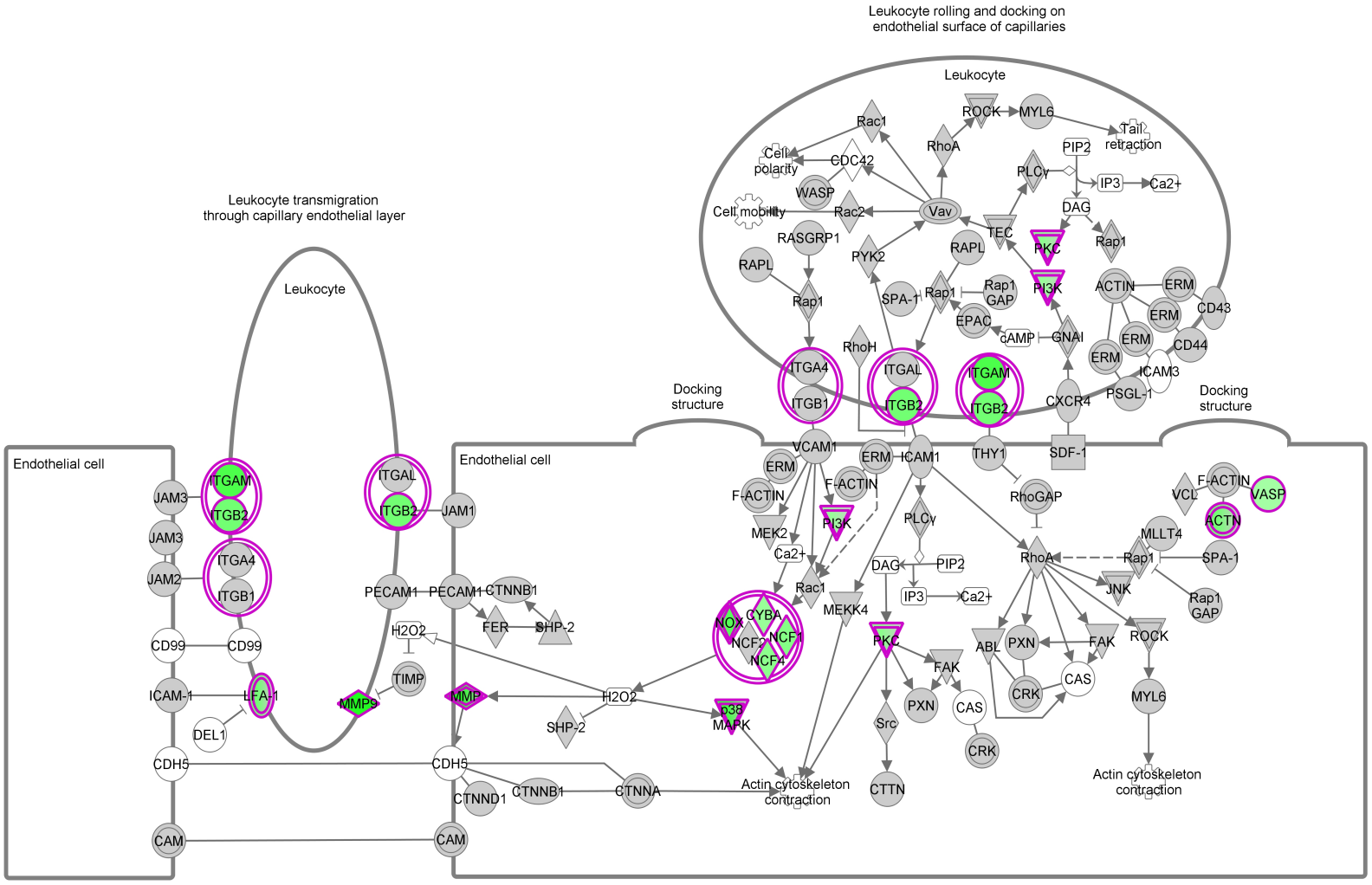

Discussion

Using RNA-seq analysis, we sought to understand at a molecular level, how preventing apoptosis through BCL-2 overexpression (or PUMA deficiency) acts to ameliorate the cytopenias of MDS and more importantly, prevent progression of MDS to more aggressive myeloid leukaemia.

We note in gene expression analysis, that of all the anti-apoptotic genes, BCL-2 is the most significantly reduced at an mRNA and protein level (Slape et al. 2012). These findings suggest that reduced BCL-2 may sensitize MDS progenitor cells, lowering the 'threshold' required to induce apoptosis of this population. It also explains how BCL-2 overexpression acts to block apoptosis of *NHD13* HSCs and rescue the associated cytopenias.

Although, other studies have demonstrated that BCL-2 overexpression in the context of an oncogene (for example, c-Myc) is associated with more aggressive disease progression (Vaux et al. 1988; Strasser et al. 1990); these studies have focused on the effects in lymphoid disease. Our previous work with BCL-2 (Slape et al. 2012) and current work with PUMA, suggest that the opposite may be true for myeloid disease progression.

Whilst BCL-2 overexpression restores quiescence, the fact that loss of PUMA within *NHD13* HSCs does not ***(Figure 4.8)***; and yet both scenarios reduce myeloid leukaemia progression - suggests that cell cycle is not the crucial factor in disease transformation. Importantly, both BCL-2 overexpression and PUMA deficiency restore DNA damage. This is in significant contrast to p53 deficiency ***(Figure 4.9).*** In constellation, our findings suggest that the anti-apoptotic function of BCL2 rather than its effect on cell cycle is responsible for delaying leukaemic transformation. One possible explanation is that the cells undergo oncogene-induced senescence as a means of protecting against DNA damage, thus halting any further disease progression. Direct assays for senescence would help to clarify this possibility.

To obtain a more in-depth understanding into why prevention of apoptosis might reduce myeloid leukaemic transformation, we undertook RNA-seq analysis comparing wild-type mice with *NHD13* transgenic, *BCL-2* transgenic and *NHD13-BCL-2* double transgenic mice. Results were further assessed using Ingenuity Pathway Analysis specifically trying to address the means by which BCL-2 overexpression might function to prevent leukaemic progression. Our results identify a number of 'inflammation-associated pathways' that are significantly down-regulated when BCL-2 is overexpressed. Pathways involving the production of nitric oxide or leukocyte adhesion and extravasation are markedly suppressed, suggesting that inhibition of apoptosis through BCL-2 overexpression may act to dampen down an inflammatory response. Metabolic pathways involving lipid biosynthesis are also affected and these may also associate with inflammation. Reduction of IL-8 signalling which functions as a neutrophil chemotactic factor may also contribute to the dampened response.

In combination, these findings suggest that inflammation, as a by-product of apoptosis, may play a significant role in myeloid disease progression. Although apoptosis is considered a highly regulated process and apoptotic cells do not usually trigger inflammation under ordinary physiological conditions (Scaffidi et al. 2002), there is evidence to suggest that mechanisms by which apoptotic bodies are usually cleared, might actually be overwhelmed in MDS (Velegraki et al. 2013). In their study, Velegraki et al show evidence for the production of soluble factors from monocytes of MDS patients – including IL-1β, IL-6 and TNF-α. Downstream, impaired apoptotic cell clearance by bone marrow macrophages leads to a release of high mobility group box-1 protein (HMGB-1) – the levels of which correlate with the apoptotic load. Through ligation of TLR4 and activation of the NFκB and JNK/p38 pathways, further inflammation may be incited.

At a molecular level, the most significantly downregulated signalling molecules in our IPA analysis include lipopolysaccharide, TNF, tretinoin and TGFβ1 (transforming growth factor) – a number of which are also involved in inflammation.

Our findings therefore suggest that targeting these signalling pathways or molecules (or the classes they belong to), may present a means of ameliorating the MDS phenotype. One recent study using the Activin receptor fusion protein (ACE-536), which acts as a ligand trap for TGF-β family members has shown some promising results in normal mice as well as the *NHD13* model with evidence of significant improvements in haematological parameters (Suragani et al. 2014). Of note, mice treated with this agent showed slower progression of anaemia and a possible reduction in leukaemic transformation with no significant increase in blast numbers. In contrast, TNF inhibitors in the treatment of MDS have only been met with limited success as discussed in Chapter 1 (Deeg et al. 2002; Maciejewski et al. 2002; Scott et al. 2010). One phase 2, randomized, double-blinded multicentre study comparing an IL-6 inhibitor with placebo did not show any benefit in MDS patients and was terminated prematurely (Garcia-Manero et al. 2014). These findings suggest that not all 'anti-inflammatory' therapies exhibit equivalent efficacy. However, the positive data to date does appear promising. A discussion of signal transduction inhibition in this context has been presented by Bachegowda et al and certainly warrants further consideration (Bachegowda et al. 2013).

FINAL DISCUSSION

The myelodysplastic syndromes are comprised of a heterogeneous group of disorders whose pathological basis has only recently begun to be deciphered (Bejar and Ebert 2010; Bejar et al. 2011b; Haferlach et al. 2014). In keeping with this, much is yet to be understood regarding the specific basis of their clinical variability. Work in this field has been further impaired by the lack of appropriate cell lines and animal models that phenotypically replicate features of this disorder in an accurate manner (Thanopoulou et al. 2004; Kerbauy et al. 2004; Drexler et al. 2009). Our limited armamentarium of therapeutics in this arena is therefore a reflection of our limited pathophysiological knowledge. Despite their efficacy, the exact mechanism of action of agents such as azacitidine and lenalidomide has not been fully elucidated and we are still a way off 'individualising' therapy and predicting response.

Although mainly observational, there is general consensus that apoptosis is usually increased in early-stage MDS. The mechanism by which this occurs is debated and both the extrinsic (Mundle et al. 1999b; Campioni et al. 2005) and intrinsic pathways (Parker et al. 2000; Gyan et al. 2008) have been implicated. In spite of this, there are only a limited number of studies that have sought to examine the effects of modulating apoptosis on the associated phenotype (Bouscary et al. 2000; Deeg et al. 2002; Scott et al. 2010). These have been met with variable success.

Our current study has sought to understand which specific proteins mediate apoptosis in the *NHD13* murine model of MDS and the effect modulating apoptosis has on the MDS phenotype and ultimately on disease progression. This tool has been chosen to study MDS as it accurately recapitulates features of the disease and appears more reliable than the use of cell lines or xenograft models.

Our work implicates the intrinsic pathway as the predominant mediator of apoptosis in *NHD13* HSCs and reveals the apoptosis to be both p53 and PUMA-

dependent. In removing PUMA (as shown for BCL-2 overexpression), not only do we see a rescue of the associated macrocytic anaemia, but somewhat counter-intuitively reduced progression to acute myeloid leukaemia is noted – challenging the paradigm that resistance to apoptosis generally associates with more aggressive disease progression. As expected, although removal of p53 also prevents apoptosis, these mice exhibit a more aggressive phenotype highlighting p53's tumour suppressive role, which occurs independent of its apoptotic function (Valente et al. 2013). To our knowledge, this is the first study examining a specific role for PUMA, NOXA and BIM in MDS.

This work challenges the current treatment paradigm that supports the use of therapies, which induce apoptosis – such as chemotherapy. Our results suggest that although counterintuitive, under particular circumstances, preventing apoptosis may be of benefit in ameliorating the cytopenias associated with human MDS without necessarily driving increased leukaemic transformation.

A caveat of this work however, is that the overexpression of BCL-2 or the deletion of PUMA is constitutive – i.e it occurs at such an early time point prior to disease development. As such, these models do not fully capture the chain of events seen with human disease. It is worthwhile therefore to consider what the consequences of preventing apoptosis at later time points might be on disease progression - a form of modelling that would be particularly relevant to the chronology seen with human disease. This work would further clarify which subset of patients might benefit from this approach and in which cases it might actually be detrimental to prevent apoptosis.

Of interest, the RNA-seq data from Chapter 5 suggests that the 'inflammatory' milieu, which is potentially induced by apoptosis that overwhelms the usual protective response, might also present itself as a valuable therapeutic target. Commonly used chemotherapeutic agents may also induce inflammation by stimulating IL-1β production – permitting tumour growth as has been shown by some (Bruchard et al. 2012). Our results suggest that targeting this milieu may be of benefit and some preliminary work has shown promising results in this

regard. Additionally, this approach might bypass the need to target apoptosis directly, which might be a cause for concern by many people. Previous trials and the modest results obtained with the TNF-α inhibitor, etanercept, suggest that the 'inflammatory' target needs to be carefully chosen. Whether this target might be different in different patients depending on the underlying pathophysiology is yet to be determined.

In summary, the work presented here further investigates the mechanism of apoptosis associated with MDS examines the effect modulating this has on the MDS phenotype. Our work to date suggests that apoptosis plays an important role in myeloid disease progression and generates a number of potential therapeutic targets which warrant further examination. We show evidence that apoptosis may indeed be a double-edged sword and that inducing cell death might not always be associated with a favourable outcome.

REFERENCES

Abdel-Wahab O, Gao J, Adli M, et al (2013) Deletion of Asxl1 results in myelodysplasia and severe developmental defects in vivo. J Exp Med 210:2641–2659. doi: 10.1084/jem.20131141

Acehan D, Jiang X, Morgan DG, et al (2002) Three-dimensional structure of the apoptosome: implications for assembly, procaspase-9 binding, and activation. Mol Cell 9:423–432.

Adams JM, Cory S (2007) The Bcl-2 apoptotic switch in cancer development and therapy. Oncogene 26:1324–1337. doi: 10.1038/sj.onc.1210220

Adamson DJ, Dawson AA, Bennett B, et al (1995) p53 mutation in the myelodysplastic syndromes. 89:61–66. doi: 10.1111/j.1365-2141.1995.tb08910.x/pdf

Adolfsson J, Borge OJ, Bryder D, et al (2001) Upregulation of Flt3 expression within the bone marrow Lin(-)Sca1(+)c-kit(+) stem cell compartment is accompanied by loss of self-renewal capacity. Immunity 15:659–669.

AIHW (2012) Cancer in Australia: an overview 2012 (full report, 29 November 2012 edition) (AIHW). 1–215.

Airaghi L, Montori D, Zorzi F, et al (2000) Sarcoidosis in a patient with 5q- myelodysplasia. A possible pathogenetic link between the two diseases. Monaldi Arch Chest Dis 55:378–380.

Akala OO, Park I-K, Qian D, et al (2008) Long-term haematopoietic reconstitution by Trp53-/-p16Ink4a-/-p19Arf-/- multipotent progenitors. Nature 453:228–232. doi: 10.1038/nature06869

Albain KS, Le Beau MM, Vardiman JW, et al (1983) Development of dysmyelopoietic syndrome in a hairy cell leukemia patient treated with chlorambucil: cytogenetic and morphologic evaluation. Cancer Genet Cytogenet 8:107–115.

Albitar M, Manshouri T, Shen Y, et al (2002) Myelodysplastic syndrome is not merely "preleukemia". Blood 100:791–798.

Ali A, Mundle SD, Ragasa D, et al (1999) Sequential activation of caspase-1 and caspase-3-like proteases during apoptosis in myelodysplastic syndromes. J Hematother Stem Cell Res 8:343–356.

Amberger C, Denzlinger C, Janzen J, et al (2004) Takayasu's arteritis secondary to myelodysplasia as a predictor of poor outcome: two case reports. Clin Exp Rheumatol 22:346–348.

Amin HM, Jilani I, Estey EH, et al (2003) Increased apoptosis in bone marrow B lymphocytes but not T lymphocytes in myelodysplastic syndrome. 102:1866–1868. doi: 10.1182/blood-2003-01-0221

Appella E, Anderson CW (2001) Post-translational modifications and activation of p53 by genotoxic stresses. Eur J Biochem 268:2764–2772.

Armand P, Kim HT, Cutler CS, et al (2007) Prognostic impact of elevated pretransplantation serum ferritin in patients undergoing myeloablative stem cell transplantation. Blood 109:4586–4588. doi: 10.1182/blood-2006-10-054924

Bachegowda L, Gligich O, Mantzaris I, et al (2013) Signal transduction inhibitors in treatment of myelodysplastic syndromes. J Hematol Oncol 6:50. doi:

10.1186/1756-8722-6-50
Baker SJ, Fearon ER, Nigro JM, et al (1989) Chromosome 17 deletions and p53 gene mutations in colorectal carcinomas. Science 244:217–221.
Banerjee SS, Morris DP, Rothera MP, Routledge RC (2001) Relapsing polychondritis associated with monoclonal gammopathy in a patient with myelodysplastic syndrome. J Laryngol Otol 115:482–484.
Barak Y, Juven T, Haffner R, Oren M (1993) mdm2 expression is induced by wild type p53 activity. EMBO J 12:461–468.
Barlow JL, Drynan LF, Hewett DR, et al (2010) A p53-dependent mechanism underlies macrocytic anemia in a mouse model of human 5q- syndrome. Nature Medicine 16:59–66. doi: 10.1038/nm.2063
Basañez G, Soane L, Hardwick JM (2012) A new view of the lethal apoptotic pore. PLoS Biol 10:e1001399. doi: 10.1371/journal.pbio.1001399
Beachy SH, Aplan PD (2010) Mouse models of myelodysplastic syndromes. Hematol Oncol Clin North Am 24:361–375. doi: 10.1016/j.hoc.2010.02.002
Bejar R, Ebert BL (2010) The genetic basis of myelodysplastic syndromes. Hematol Oncol Clin North Am 24:295–315. doi: 10.1016/j.hoc.2010.02.001
Bejar R, Levine R, Ebert BL (2011a) Unraveling the molecular pathophysiology of myelodysplastic syndromes. J Clin Oncol 29:504–515. doi: 10.1200/JCO.2010.31.1175
Bejar R, Lord A, Stevenson K, et al (2014) TET2 mutations predict response to hypomethylating agents in myelodysplastic syndrome patients. 124:2705–2712. doi: 10.1182/blood-2014-06-582809
Bejar R, Stevenson K, Abdel-Wahab O, et al (2011b) Clinical effect of point mutations in myelodysplastic syndromes. N Engl J Med 364:2496–2506. doi: 10.1056/NEJMoa1013343
Bejar R, Stevenson KE, Caughey BA, et al (2012) Validation of a prognostic model and the impact of mutations in patients with lower-risk myelodysplastic syndromes. J Clin Oncol 30:3376–3382. doi: 10.1200/JCO.2011.40.7379
Benito AI, Bryant E, Loken MR, et al (2003) NOD/SCID mice transplanted with marrow from patients with myelodysplastic syndrome (MDS) show long-term propagation of normal but not clonal human precursors. Leuk Res 27:425–436.
Bennett JM, Catovsky D, Daniel MT, et al (1982) Proposals for the classification of the myelodysplastic syndromes. 51:189–199. doi: 10.1111/j.1365-2141.1982.tb02771.x/pdf
Berthelot JM, Hamidou M, Dauty M, et al (1997) Joint manifestations in myelodysplastic syndromes. A report of three cases presenting as polymyalgia rheumatica. Rev Rhum Engl Ed 64:95–100.
Bhatia M, Wang JC, Kapp U, et al (1997) Purification of primitive human hematopoietic cells capable of repopulating immune-deficient mice. Proc Natl Acad Sci USA 94:5320–5325.
Biswas SK, Sica A, Lewis CE (2008) Plasticity of macrophage function during tumor progression: regulation by distinct molecular mechanisms. The Journal of Immunology 180:2011–2017.
Blair TR, Bayrd ED, Pease GI (1966) Atypical leukemia. JAMA 198:139–142.
Bogdanović AD, Janković GM, Colović MD, et al (1996) Apoptosis in bone marrow of myelodysplastic syndrome patients. 87:3064.
Boudard D, Vasselon C, Berthéas M-F, et al (2002) Expression and prognostic

significance of Bcl-2 family proteins in myelodysplastic syndromes. Am J Hematol 70:115–125. doi: 10.1002/ajh.10108
Bouillet P, Huang DC, O'Reilly LA, et al (2000) The role of the pro-apoptotic Bcl-2 family member bim in physiological cell death. Ann N Y Acad Sci 926:83–89.
Bouillet P, Metcalf D, Huang DC, et al (1999) Proapoptotic Bcl-2 relative Bim required for certain apoptotic responses, leukocyte homeostasis, and to preclude autoimmunity. Science 286:1735–1738.
Boultwood J, Perry J, Pellagatti A, et al (2010) Frequent mutation of the polycomb-associated gene ASXL1 in the myelodysplastic syndromes and in acute myeloid leukemia. Leukemia 24:1062–1065. doi: 10.1038/leu.2010.20
Bouscary D, Chen YL, Guesnu M, et al (2000) Activity of the caspase-3/CPP32 enzyme is increased in "early stage" myelodysplastic syndromes with excessive apoptosis, but caspase inhibition does not enhance colony formation in vitro. Exp Hematol 28:784–791.
Bouscary D, De Vos J, Guesnu M, et al (1997) Fas/Apo-1 (CD95) expression and apoptosis in patients with myelodysplastic syndromes. Leukemia 11:839–845.
Bruchard MEL, Mignot GEG, re VDE, et al (2012) Chemotherapy-triggered cathepsin B release in myeloid-derived suppressor cells activates the Nlrp3 inflammasome and promotes tumor growth. Nature Medicine 19:57–64. doi: 10.1038/nm.2999
Buonamici S, Li D, Chi Y, et al (2004) EVI1 induces myelodysplastic syndrome in mice. J Clin Invest 114:713–719. doi: 10.1172/JCI21716
Busson P, Keryer C, Ooka T, Corbex M (2004) EBV-associated nasopharyngeal carcinomas: from epidemiology to virus-targeting strategies. Trends Microbiol 12:356–360. doi: 10.1016/j.tim.2004.06.005
Campioni D, Secchiero P, Corallini F, et al (2005) Evidence for a role of TNF-related apoptosis-inducing ligand (TRAIL) in the anemia of myelodysplastic syndromes. Am J Pathol 166:557–563. doi: 10.1016/S0002-9440(10)62277-8
Canman CE, Gilmer TM, Coutts SB, Kastan MB (1995) Growth factor modulation of p53-mediated growth arrest versus apoptosis. Genes Dev 9:600–611.
Cartron P-F, Gallenne T, Bougras G, et al (2004) The first alpha helix of Bax plays a necessary role in its ligand-induced activation by the BH3-only proteins Bid and PUMA. Mol Cell 16:807–818. doi: 10.1016/j.molcel.2004.10.028
Chen J, Ellison FM, Keyvanfar K, et al (2008) Enrichment of hematopoietic stem cells with SLAM and LSK markers for the detection of hematopoietic stem cell function in normal and Trp53 null mice. Exp Hematol 36:1236–1243. doi: 10.1016/j.exphem.2008.04.012
Chen L, Willis SN, Wei A, et al (2005) Differential targeting of prosurvival Bcl-2 proteins by their BH3-only ligands allows complementary apoptotic function. Mol Cell 17:393–403. doi: 10.1016/j.molcel.2004.12.030
Chen ML, Logan TD, Hochberg ML, et al (2009) Erythroid dysplasia, megaloblastic anemia, and impaired lymphopoiesis arising from mitochondrial dysfunction. Blood 114:4045–4053. doi: 10.1182/blood-2008-08-169474
Chipuk JE, Kuwana T, Bouchier-Hayes L, et al (2004) Direct activation of Bax by p53 mediates mitochondrial membrane permeabilization and apoptosis. Science 303:1010–1014. doi: 10.1126/science.1092734

Chomczynski P, Sacchi N (1987) Single-step method of RNA isolation by acid guanidinium thiocyanate-phenol-chloroform extraction. Anal Biochem 162:156–159. doi: 10.1006/abio.1987.9999

Christensen JL, Weissman IL (2001) Flk-2 is a marker in hematopoietic stem cell differentiation: a simple method to isolate long-term stem cells. Proc Natl Acad Sci USA 98:14541–14546. doi: 10.1073/pnas.261562798

Chung YJ, Choi CW, Slape C, et al (2008) Transplantation of a myelodysplastic syndrome by a long-term repopulating hematopoietic cell. Proc Natl Acad Sci USA 105:14088–14093. doi: 10.1073/pnas.0804507105

Chung YJ, Robert C, Gough SM, et al (2014) Oxidative stress leads to increased mutation frequency in a murine model of myelodysplastic syndrome. Leuk Res 38:95–102. doi: 10.1016/j.leukres.2013.07.008

Claessens Y-E, Bouscary D, Dupont J-M, et al (2002) In vitro proliferation and differentiation of erythroid progenitors from patients with myelodysplastic syndromes: evidence for Fas-dependent apoptosis. 99:1594–1601.

Claessens Y-E, Park S, Dubart-Kupperschmitt A, et al (2005) Rescue of early-stage myelodysplastic syndrome-deriving erythroid precursors by the ectopic expression of a dominant-negative form of FADD. 105:4035–4042. doi: 10.1182/blood-2004-08-3166

Clarke AR, Purdie CA, Harrison DJ, et al (1993) Thymocyte apoptosis induced by p53-dependent and independent pathways. Nature 362:849–852. doi: 10.1038/362849a0

Coiffier B, Adeleine P, Viala JJ, et al (1983) Dysmyelopoietic syndromes. A search for prognostic factors in 193 patients. Cancer 52:83–90.

Cortelezzi A, Cattaneo C, Cristiani S, et al (2000) Non-transferrin-bound iron in myelodysplastic syndromes: a marker of ineffective erythropoiesis? Hematol J 1:153–158. doi: 10.1038/sj/thj/6200028

Cuzick J, Thorat MA, Bosetti C, et al (2014) Estimates of benefits and harms of prophylactic use of aspirin in the general population. Ann Oncol 26:47–57. doi: 10.1093/annonc/mdu225

Dai M-S, Zeng SX, Jin Y, et al (2004) Ribosomal protein L23 activates p53 by inhibiting MDM2 function in response to ribosomal perturbation but not to translation inhibition. Mol Cell Biol 24:7654–7668. doi: 10.1128/MCB.24.17.7654-7668.2004

Danial NN, Korsmeyer SJ (2004) Cell death: critical control points. Cell 116:205–219.

de Vries A, Flores ER, Miranda B, et al (2002) Targeted point mutations of p53 lead to dominant-negative inhibition of wild-type p53 function. Proc Natl Acad Sci USA 99:2948–2953. doi: 10.1073/pnas.052713099

Deeg HJ, Gotlib J, Beckham C, et al (2002) Soluble TNF receptor fusion protein (etanercept) for the treatment of myelodysplastic syndrome: a pilot study. Leukemia 16:162–164. doi: 10.1038/sj.leu.2402356

del Rey M, O'Hagan K, Dellett M, et al (2013) Genome-wide profiling of methylation identifies novel targets with aberrant hypermethylation and reduced expression in low-risk myelodysplastic syndromes. Leukemia 27:610–618. doi: 10.1038/leu.2012.253

Deng X, Gao F, May WS (2003) Bcl2 retards G1/S cell cycle transition by regulating intracellular ROS. 102:3179–3185. doi: 10.1182/blood-2003-04-1027

Denisov AY, Chen G, Sprules T, et al (2006) Structural model of the BCL-w-BID peptide complex and its interactions with phospholipid micelles. Biochemistry 45:2250–2256. doi: 10.1021/bi052332s
Diakos CI, Charles KA, McMillan DC, Clarke SJ (2014) Cancer-related inflammation and treatment effectiveness. Lancet Oncol 15:e493–503. doi: 10.1016/S1470-2045(14)70263-3
Dobbelstein C, Ganser A (2012) Immunosuppressive Therapy for Myelodysplastic Syndromes. CPD 18:3184–3189. doi: 10.2174/1381612811209023184
Donehower LA, Harvey M, Slagle BL, et al (1992) Mice deficient for p53 are developmentally normal but susceptible to spontaneous tumours. Nature 356:215–221. doi: 10.1038/356215a0
Drexler HG, Dirks WG, MacLeod RAF (2009) Many are called MDS cell lines: one is chosen. Leuk Res 33:1011–1016. doi: 10.1016/j.leukres.2009.03.005
Dudgeon C, Kek C, Demidov ON, et al (2006) Tumor susceptibility and apoptosis defect in a mouse strain expressing a human p53 transgene. Cancer Res 66:2928–2936. doi: 10.1158/0008-5472.CAN-05-2063
Dutt S, Narla A, Lin K, et al (2011) Haploinsufficiency for ribosomal protein genes causes selective activation of p53 in human erythroid progenitor cells. 117:2567–2576. doi: 10.1182/blood-2010-07-295238
Dzeletovic I, Harrison ME, Crowell MD, et al (2014) Pancreatitis before pancreatic cancer: clinical features and influence on outcome. J Clin Gastroenterol 48:801–805. doi: 10.1097/MCG.0b013e3182a9f879
Ebert BL, Pretz J, Bosco J, et al (2008) Identification of RPS14 as a 5q- syndrome gene by RNA interference screen. Nature 451:335–339. doi: 10.1038/nature06494
el-Deiry WS, Tokino T, Velculescu VE, et al (1993) WAF1, a potential mediator of p53 tumor suppression. Cell 75:817–825.
Eliyahu D, Michalovitz D, Oren M (1985) Overproduction of p53 antigen makes established cells highly tumorigenic. Nature 316:158–160.
Eliyahu D, Raz A, Gruss P, et al (1984) Participation of p53 cellular tumour antigen in transformation of normal embryonic cells. Nature 312:646–649.
Erster S, Mihara M, Kim RH, et al (2004) In vivo mitochondrial p53 translocation triggers a rapid first wave of cell death in response to DNA damage that can precede p53 target gene activation. Mol Cell Biol 24:6728–6741. doi: 10.1128/MCB.24.15.6728-6741.2004
Fenaux P, Mufti GJ, Hellstrom-Lindberg E, et al (2009) Efficacy of azacitidine compared with that of conventional care regimens in the treatment of higher-risk myelodysplastic syndromes: a randomised, open-label, phase III study. Lancet Oncol 10:223–232. doi: 10.1016/S1470-2045(09)70003-8
Finger LR (1984) Cloning of the chromosome breakpoint of neoplastic B cells with the t(14;18) chromosome translocation. Science 226:1097–1099.
Flores-Figueroa E, Gutiérrez-Espíndola G, Montesinos JJ, et al (2002) In vitro characterization of hematopoietic microenvironment cells from patients with myelodysplastic syndrome. Leuk Res 26:677–686.
Font P, Loscertales J, Benavente C, et al (2013) Inter-observer variance with the diagnosis of myelodysplastic syndromes (MDS) following the 2008 WHO classification. Ann Hematol 92:19–24. doi: 10.1007/s00277-012-1565-4
Frytak JR, Henk HJ, De Castro CM, et al (2009) Estimation of economic costs

associated with transfusion dependence in adults with MDS. Curr Med Res Opin 25:1941–1951. doi: 10.1185/03007990903076699
Fuchs SY, Adler V, Buschmann T, et al (1998) Mdm2 association with p53 targets its ubiquitination. Oncogene 17:2543–2547. doi: 10.1038/sj.onc.1202200
Fütterer A, Campanero MR, Leonardo E, et al (2005) Dido gene expression alterations are implicated in the induction of hematological myeloid neoplasms. J Clin Invest 115:2351–2362. doi: 10.1172/JCI24177
Gallenne T, Gautier F, Oliver L, et al (2009) Bax activation by the BH3-only protein Puma promotes cell dependence on antiapoptotic Bcl-2 family members. J Cell Biol 185:279–290. doi: 10.1083/jcb.200809153
Garcia-Manero G (2014) Myelodysplastic syndromes: 2014 update on diagnosis, risk-stratification, and management. Am J Hematol 89:97–108. doi: 10.1002/ajh.23642
Garcia-Manero G, Gartenberg G, Steensma DP, et al (2014) A phase 2, randomized, double-blind, multicenter study comparing siltuximab plus best supportive care (BSC) with placebo plus BSC in anemic patients with International Prognostic Scoring System low- or intermediate-1-risk myelodysplastic syndrome. Am J Hematol 89:E156–62. doi: 10.1002/ajh.23780
Garrison SP, Phillips DC, Jeffers JR, et al (2012) Genetically defining the mechanism of Puma- and Bim-induced apoptosis. Cell Death Differ 19:642–649. doi: 10.1038/cdd.2011.136
Gavathiotis E, Suzuki M, Davis ML, et al (2008) BAX activation is initiated at a novel interaction site. Nature 455:1076–1081. doi: 10.1038/nature07396
Gersuk GM, Beckham C, Loken MR, et al (1998) A role for tumour necrosis factor-alpha, Fas and Fas-Ligand in marrow failure associated with myelodysplastic syndrome. 103:176–188.
Gersuk GM, Lee JW, Beckham CA, et al (1996) Fas (CD95) receptor and Fas-ligand expression in bone marrow cells from patients with myelodysplastic syndrome. 88:1122–1123.
Geyh S, Oz S, Cadeddu R-P, et al (2013) Insufficient stromal support in MDS results from molecular and functional deficits of mesenchymal stromal cells. Leukemia 27:1841–1851. doi: 10.1038/leu.2013.193
Gondek LP, Haddad AS, O'Keefe CL, et al (2007a) Detection of cryptic chromosomal lesions including acquired segmental uniparental disomy in advanced and low-risk myelodysplastic syndromes. Exp Hematol 35:1728–1738. doi: 10.1016/j.exphem.2007.08.009
Gondek LP, Tiu R, Haddad AS, et al (2007b) Single nucleotide polymorphism arrays complement metaphase cytogenetics in detection of new chromosomal lesions in MDS. Leukemia 21:2058–2061. doi: 10.1038/sj.leu.2404745
Gonzalez MF, Freeman JK (2012) Myelofibrosis associated with romiplostim treatment in a patient with immune thrombocytopenia. Case Rep Hematol 2012:318597–4. doi: 10.1155/2012/318597
Graham DY (2015) Helicobacter pylori update: gastric cancer, reliable therapy, and possible benefits. Gastroenterology 148:719–31.e3. doi: 10.1053/j.gastro.2015.01.040
Graubert TA, Shen D, Ding L, et al (2012) Recurrent mutations in the U2AF1 splicing factor in myelodysplastic syndromes. Nat Genet 44:53–57. doi:

10.1038/ng.1031
Greenberg P, Cox C, LeBeau MM, et al (1997) International scoring system for evaluating prognosis in myelodysplastic syndromes. 89:2079–2088.
Greenberg PL, Tuechler H, Schanz J, et al (2012) Revised international prognostic scoring system for myelodysplastic syndromes. 120:2454–2465. doi: 10.1182/blood-2012-03-420489
Grisendi S, Bernardi R, Rossi M, et al (2005) Role of nucleophosmin in embryonic development and tumorigenesis. Nature 437:147–153. doi: 10.1038/nature03915
Grivennikov SI, Greten FR, Karin M (2010) Immunity, inflammation, and cancer. Cell 140:883–899. doi: 10.1016/j.cell.2010.01.025
Gu S, Zhao Y, Guo J, et al (2014) High expression of APAF-1 elevates erythroid apoptosis in iron overload myelodysplastic syndrome. Tumour Biol 35:2211–2218. doi: 10.1007/s13277-013-1294-x
Guralnik JM, Eisenstaedt RS, Ferrucci L, et al (2004) Prevalence of anemia in persons 65 years and older in the United States: evidence for a high rate of unexplained anemia. 104:2263–2268. doi: 10.1182/blood-2004-05-1812
Gyan E, Frisan E, Beyne-Rauzy O, et al (2008) Spontaneous and Fas-induced apoptosis of low-grade MDS erythroid precursors involves the endoplasmic reticulum. Leukemia 22:1864–1873. doi: 10.1038/leu.2008.172
Haase D, Germing U, Schanz J, et al (2007) New insights into the prognostic impact of the karyotype in MDS and correlation with subtypes: evidence from a core dataset of 2124 patients. 110:4385–4395. doi: 10.1182/blood-2007-03-082404
Haferlach T, Nagata Y, Grossmann V, et al (2014) Landscape of genetic lesions in 944 patients with myelodysplastic syndromes. Leukemia 28:241–247. doi: 10.1038/leu.2013.336
Halazonetis TD, Gorgoulis VG, Bartek J (2008) An oncogene-induced DNA damage model for cancer development. Science 319:1352–1355. doi: 10.1126/science.1140735
Han J, Flemington C, Houghton AB, et al (2001) Expression of bbc3, a pro-apoptotic BH3-only gene, is regulated by diverse cell death and survival signals. Proc Natl Acad Sci USA 98:11318–11323. doi: 10.1073/pnas.201208798
Hanahan D, Weinberg RA (2000) The hallmarks of cancer. Cell 100:57–70.
Hanahan D, Weinberg RA (2011) Hallmarks of cancer: the next generation. Cell 144:646–674. doi: 10.1016/j.cell.2011.02.013
Harada H, Harada Y, Niimi H, et al (2004) High incidence of somatic mutations in the AML1/RUNX1 gene in myelodysplastic syndrome and low blast percentage myeloid leukemia with myelodysplasia. 103:2316–2324. doi: 10.1182/blood-2003-09-3074
Haupt Y, Maya R, Kazaz A, Oren M (1997) Mdm2 promotes the rapid degradation of p53. Nature 387:296–299. doi: 10.1038/387296a0
Hengartner MO, Horvitz HR (1994) C. elegans cell survival gene ced-9 encodes a functional homolog of the mammalian proto-oncogene bcl-2. Cell 76:665–676.
Herold MJ, Stuchbery R, Mérino D, et al (2014) Impact of conditional deletion of the pro-apoptotic BCL-2 family member BIM in mice. Cell Death Dis 5:e1446. doi: 10.1038/cddis.2014.409

Hikita H, Kodama T, Shimizu S, et al (2012) Bak deficiency inhibits liver carcinogenesis: A causal link between apoptosis and carcinogenesis. Journal of Hepatology 57:92–100. doi: 10.1016/j.jhep.2012.01.027
Hollander MC, Alamo I, Jackman J, et al (1993) Analysis of the mammalian gadd45 gene and its response to DNA damage. J Biol Chem 268:24385–24393.
Hollstein M, Sidransky D, Vogelstein B, Harris CC (1991) p53 mutations in human cancers. Science 253:49–53.
Insinga A, Cicalese A, Faretta M, et al (2013) DNA damage in stem cells activates p21, inhibits p53, and induces symmetric self-renewing divisions. Proc Natl Acad Sci USA 110:3931–3936. doi: 10.1073/pnas.1213394110
Insinga A, Cicalese A, Pelicci PG (2014) DNA damage response in adult stem cells. Blood Cells Mol Dis. doi: 10.1016/j.bcmd.2013.12.005
Ishibashi M, Tamura H, Ogata K (2011) Disease progression mechanism in myelodysplastic syndromes: insight into the role of the microenvironment. Leuk Res 35:1449–1452. doi: 10.1016/j.leukres.2011.06.022
Jabbour AM, Daunt CP, Green BD, et al (2010) Myeloid progenitor cells lacking p53 exhibit delayed up-regulation of Puma and prolonged survival after cytokine deprivation. 115:344–352. doi: 10.1182/blood-2009-07-230730
Jacks T, Remington L, Williams BO, et al (1994) Tumor spectrum analysis in p53-mutant mice. Curr Biol 4:1–7.
Jädersten M, Saft L, Smith A, et al (2011) TP53 Mutations in Low-Risk Myelodysplastic Syndromes With del(5q) Predict Disease Progression. J Clin Oncol 29:1971–1979. doi: 10.1200/JCO.2010.31.8576
Jeffers JR, Parganas E, Lee Y, et al (2003) Puma is an essential mediator of p53-dependent and -independent apoptotic pathways. Cancer Cell 4:321–328.
Jenkins JR, Rudge K, Currie GA (1984) Cellular immortalization by a cDNA clone encoding the transformation-associated phosphoprotein p53. Nature 312:651–654.
Jiang P, Du W, Heese K, Wu M (2006) The Bad guy cooperates with good cop p53: Bad is transcriptionally up-regulated by p53 and forms a Bad/p53 complex at the mitochondria to induce apoptosis. Mol Cell Biol 26:9071–9082. doi: 10.1128/MCB.01025-06
Kaferle J, Strzoda CE (2009) Evaluation of macrocytosis. Am Fam Physician 79:203–208.
Kantarjian H, O'Brien S, Ravandi F, et al (2008) Proposal for a new risk model in myelodysplastic syndrome that accounts for events not considered in the original International Prognostic Scoring System. Cancer 113:1351–1361. doi: 10.1002/cncr.23697
Kantarjian HM, O'Brien S, Huang X, et al (2007) Survival advantage with decitabine versus intensive chemotherapy in patients with higher risk myelodysplastic syndrome: comparison with historical experience. Cancer 109:1133–1137. doi: 10.1002/cncr.22508
Kerbauy DMB, Lesnikov V, Torok-Storb B, et al (2004) Engraftment of distinct clonal MDS-derived hematopoietic precursors in NOD/SCID-beta2-microglobulin-deficient mice after intramedullary transplantation of hematopoietic and stromal cells. 104:2202–2203. doi: 10.1182/blood-2004-04-1518
Kerr JF, Wyllie AH, Currie AR (1972) Apoptosis: a basic biological phenomenon

with wide-ranging implications in tissue kinetics. Br J Cancer 26:239–257.
Kiel MJ, Yilmaz OH, Iwashita T, et al (2005) SLAM family receptors distinguish hematopoietic stem and progenitor cells and reveal endothelial niches for stem cells. Cell 121:1109–1121. doi: 10.1016/j.cell.2005.05.026
Kirito K, Komatsu N (2013) [Progression of bone marrow fibrosis with reticulin and collagen hyperplasia during treatment with the thrombopoietin receptor agonist romiplostim in a patient with immune thrombocytopenia]. Rinsho Ketsueki 54:295–299.
Knudson CM, Tung KS, Tourtellotte WG, et al (1995) Bax-deficient mice with lymphoid hyperplasia and male germ cell death. Science 270:96–99.
Kondo A, Yamashita T, Tamura H, et al (2010) Interferon-γ and tumor necrosis factor-α induce an immunoinhibitory molecule, B7-H1, via nuclear factor-κB activation in blasts in myelodysplastic syndromes. 116:1124–1131. doi: 10.1182/blood-2009-12-255125
Körner H, Riminton DS, Strickland DH, et al (1997) Critical points of tumor necrosis factor action in central nervous system autoimmune inflammation defined by gene targeting. J Exp Med 186:1585–1590.
Kubbutat MH, Jones SN, Vousden KH (1997) Regulation of p53 stability by Mdm2. Nature 387:299–303. doi: 10.1038/387299a0
Kulasekararaj AG, Smith AE, Mian SA, et al (2013) TP53 mutations in myelodysplastic syndrome are strongly correlated with aberrations of chromosome 5, and correlate with adverse prognosis. 160:660–672. doi: 10.1111/bjh.12203
Kurotaki H, Tsushima Y, Nagai K, Yagihashi S (2000) Apoptosis, bcl-2 expression and p53 accumulation in myelodysplastic syndrome, myelodysplastic-syndrome-derived acute myelogenous leukemia and de novo acute myelogenous leukemia. Acta Haematol 102:115–123.
Kushnareva Y, Andreyev AY, Kuwana T, Newmeyer DD (2012) Bax activation initiates the assembly of a multimeric catalyst that facilitates Bax pore formation in mitochondrial outer membranes. PLoS Biol 10:e1001394. doi: 10.1371/journal.pbio.1001394
Kutler DI, Singh B, Satagopan J, et al (2003) A 20-year perspective on the International Fanconi Anemia Registry (IFAR). 101:1249–1256. doi: 10.1182/blood-2002-07-2170
Labi V, Erlacher M, Krumschnabel G, et al (2010) Apoptosis of leukocytes triggered by acute DNA damage promotes lymphoma formation. Genes Dev 24:1602–1607. doi: 10.1101/gad.1940210
Lane DP, Crawford LV (1979) T antigen is bound to a host protein in SV40-transformed cells. Nature 278:261–263.
Langmead B, Salzberg SL (2012) Fast gapped-read alignment with Bowtie 2. Nat Methods 9:357–359. doi: 10.1038/nmeth.1923
Laster SM, Wood JG, Gooding LR (1988) Tumor necrosis factor can induce both apoptic and necrotic forms of cell lysis. The Journal of Immunology 141:2629–2634.
Law CW, Chen Y, Shi W, Smyth GK (2014) voom: Precision weights unlock linear model analysis tools for RNA-seq read counts. Genome Biol 15:R29. doi: 10.1186/gb-2014-15-2-r29
Letai A, Bassik MC, Walensky LD, et al (2002) Distinct BH3 domains either sensitize or activate mitochondrial apoptosis, serving as prototype cancer

therapeutics. Cancer Cell 2:183–192.
Li X, Bryant CE, Deeg HJ (2004) Simultaneous demonstration of clonal chromosome abnormalities and apoptosis in individual marrow cells in myelodysplastic syndrome. Int J Hematol 80:140–145.
Lin YW, Slape C, Zhang Z, Aplan PD (2005) NUP98-HOXD13 transgenic mice develop a highly penetrant, severe myelodysplastic syndrome that progresses to acute leukemia. 106:287–295. doi: 10.1182/blood-2004-12-4794
Lindsten T, Ross AJ, King A, et al (2000) The combined functions of proapoptotic Bcl-2 family members bak and bax are essential for normal development of multiple tissues. Mol Cell 6:1389–1399.
Linette GP, Li Y, Roth K, Korsmeyer SJ (1996) Cross talk between cell death and cell cycle progression: BCL-2 regulates NFAT-mediated activation. Proc Natl Acad Sci USA 93:9545–9552.
Linzer DI, Levine AJ (1979) Characterization of a 54K dalton cellular SV40 tumor antigen present in SV40-transformed cells and uninfected embryonal carcinoma cells. Cell 17:43–52.
List A, Dewald G, Bennett J, et al (2006) Lenalidomide in the myelodysplastic syndrome with chromosome 5q deletion. N Engl J Med 355:1456–1465. doi: 10.1056/NEJMoa061292
List A, Kurtin S, Roe DJ, et al (2005) Efficacy of lenalidomide in myelodysplastic syndromes. N Engl J Med 352:549–557. doi: 10.1056/NEJMoa041668
Liu X, Dai S, Zhu Y, et al (2003) The structure of a Bcl-xL/Bim fragment complex: implications for Bim function. Immunity 19:341–352.
Liu Y, Elf SE, Miyata Y, et al (2009) p53 regulates hematopoietic stem cell quiescence. Cell Stem Cell 4:37–48. doi: 10.1016/j.stem.2008.11.006
Louz D, van den Broek M, Verbakel S, et al (2000) Erythroid defects and increased retrovirally-induced tumor formation in Evi1 transgenic mice. Leukemia 14:1876–1884.
Lowe SW, Schmitt EM, Smith SW, et al (1993) p53 is required for radiation-induced apoptosis in mouse thymocytes. Nature 362:847–849. doi: 10.1038/362847a0
Lübbert M, Suciu S, Baila L, et al (2011) Low-dose decitabine versus best supportive care in elderly patients with intermediate- or high-risk myelodysplastic syndrome (MDS) ineligible for intensive chemotherapy: final results of the randomized phase III study of the European Organisation for Research and Treatment of Cancer Leukemia Group and the German MDS Study Group. J Clin Oncol 29:1987–1996. doi: 10.1200/JCO.2010.30.9245
Ma X (2012) Epidemiology of myelodysplastic syndromes. Am J Med 125:S2–5. doi: 10.1016/j.amjmed.2012.04.014
Ma Y, Cui W, Yang J, et al (2006) SALL4, a novel oncogene, is constitutively expressed in human acute myeloid leukemia (AML) and induces AML in transgenic mice. Blood 108:2726–2735. doi: 10.1182/blood-2006-02-001594
Maciejewski JP, Risitano AM, Sloand EM, et al (2002) A pilot study of the recombinant soluble human tumour necrosis factor receptor (p75)-Fc fusion protein in patients with myelodysplastic syndrome. Br J Haematol 117:119–126. doi: 10.1046/j.1365-2141.2002.03381.x/epdf
Malcovati L (2007) Impact of transfusion dependency and secondary iron

overload on the survival of patients with myelodysplastic syndromes. Leuk Res 31 Suppl 3:S2–6. doi: 10.1016/S0145-2126(07)70459-9
Malcovati L, Germing U, Kuendgen A, et al (2007) Time-dependent prognostic scoring system for predicting survival and leukemic evolution in myelodysplastic syndromes. J Clin Oncol 25:3503–3510. doi: 10.1200/JCO.2006.08.5696
Malcovati L, Porta Della MG, Strupp C, et al (2011) Impact of the degree of anemia on the outcome of patients with myelodysplastic syndrome and its integration into the WHO classification-based Prognostic Scoring System (WPSS). Haematologica haematol.2011.044602v1. doi: 10.3324/haematol.2011.044602
McQuilten ZK, Polizzotto MN, Wood EM, Sundararajan V (2013) Myelodysplastic syndrome incidence, transfusion dependence, health care use, and complications: an Australian population-based study 1998 to 2008. Transfusion 53:1714–1721. doi: 10.1111/trf.12054
McQuilten ZK, Wood EM, Polizzotto MN, et al (2014) Underestimation of myelodysplastic syndrome incidence by cancer registries: Results from a population-based data linkage study. Cancer 120:1686–1694. doi: 10.1002/cncr.28641
Messa E, Cilloni D, Messa F, et al (2008) Deferasirox treatment improved the hemoglobin level and decreased transfusion requirements in four patients with the myelodysplastic syndrome and primary myelofibrosis. Acta Haematol 120:70–74. doi: 10.1159/000158631
Metcalf D (1984) Clonal culture of hemopoietic cells. Elsevier Publishing Company
Michalak EM, Jansen ES, Happo L, et al (2009) Puma and to a lesser extent Noxa are suppressors of Myc-induced lymphomagenesis. Cell Death Differ 16:684–696. doi: 10.1038/cdd.2008.195
Michalak EM, Vandenberg CJ, Delbridge ARD, et al (2010) Apoptosis-promoted tumorigenesis: gamma-irradiation-induced thymic lymphomagenesis requires Puma-driven leukocyte death. Genes Dev 24:1608–1613. doi: 10.1101/gad.1940110
Michalak EM, Villunger A, Adams JM, Strasser A (2008) In several cell types tumour suppressor p53 induces apoptosis largely via Puma but Noxa can contribute. Cell Death Differ 15:1019–1029. doi: 10.1038/cdd.2008.16
Misawa S, Horiike S, Kaneko H, Kashima K (1997) Genetic aberrations in the development and subsequent progression of myelodysplastic syndrome. Leukemia 11 Suppl 3:533–535.
Miyashita T, Reed JC (1995) Tumor suppressor p53 is a direct transcriptional activator of the human bax gene. Cell 80:293–299.
Mohamedali A, Gäken J, Twine NA, et al (2007) Prevalence and prognostic significance of allelic imbalance by single-nucleotide polymorphism analysis in low-risk myelodysplastic syndromes. Blood 110:3365–3373. doi: 10.1182/blood-2007-03-079673
Moldoveanu T, Liu Q, Tocilj A, et al (2006) The X-ray structure of a BAK homodimer reveals an inhibitory zinc binding site. Mol Cell 24:677–688. doi: 10.1016/j.molcel.2006.10.014
Molldrem JJ, Jiang YZ, Stetler-Stevenson M, et al (1998) Haematological response of patients with myelodysplastic syndrome to antithymocyte globulin is

associated with a loss of lymphocyte-mediated inhibition of CFU-GM and alterations in T-cell receptor Vbeta profiles. 102:1314–1322.
Moody JL, Xu L, Helgason CD, Jirik FR (2004) Anemia, thrombocytopenia, leukocytosis, extramedullary hematopoiesis, and impaired progenitor function in Pten+/-SHIP-/- mice: a novel model of myelodysplasia. Blood 103:4503–4510. doi: 10.1182/blood-2003-09-3262
Mori N, Hidai H, Yokota J, et al (1995) Mutations of the p53 gene in myelodysplastic syndrome and overt leukemia. Leuk Res 19:869–875.
Morrison VA, Rai KR, Peterson BL, et al (2002) Therapy-related myeloid leukemias are observed in patients with chronic lymphocytic leukemia after treatment with fludarabine and chlorambucil: results of an intergroup study, cancer and leukemia group B 9011. J Clin Oncol 20:3878–3884.
Mundle SD, Ali A, Cartlidge JD, et al (1999a) Evidence for involvement of tumor necrosis factor-alpha in apoptotic death of bone marrow cells in myelodysplastic syndromes. Am J Hematol 60:36–47.
Mundle SD, Reza S, Ali A, et al (1999b) Correlation of tumor necrosis factor alpha (TNF alpha) with high Caspase 3-like activity in myelodysplastic syndromes. Cancer Lett 140:201–207.
Mundle SD, Shetty VT, Raza A (2000) Caspases and apoptosis in myelodysplastic syndromes. Exp Hematol 28:1310–1312.
Mundle SD, Venugopal P, Cartlidge JD, et al (1996) Indication of an involvement of interleukin-1 beta converting enzyme-like protease in intramedullary apoptotic cell death in the bone marrow of patients with myelodysplastic syndromes. 88:2640–2647.
Mustata G, Li M, Zevola N, et al (2011) Development of small-molecule PUMA inhibitors for mitigating radiation-induced cell death. Curr Top Med Chem 11:281–290.
Nakano K, Vousden KH (2001) PUMA, a novel proapoptotic gene, is induced by p53. Mol Cell 7:683–694.
Naqvi K, Garcia-Manero G, Sardesai S, et al (2011a) Association of comorbidities with overall survival in myelodysplastic syndrome: development of a prognostic model. J Clin Oncol 29:2240–2246. doi: 10.1200/JCO.2010.31.3353
Naqvi K, Jabbour E, Bueso-Ramos C, et al (2011b) Implications of discrepancy in morphologic diagnosis of myelodysplastic syndrome between referral and tertiary care centers. 118:4690–4693. doi: 10.1182/blood-2011-03-342642
Narla A, Ebert BL (2010) Ribosomopathies: human disorders of ribosome dysfunction. 115:3196–3205. doi: 10.1182/blood-2009-10-178129
Neukirchen J, Fox F, Kündgen A, et al (2012) Improved survival in MDS patients receiving iron chelation therapy - a matched pair analysis of 188 patients from the Düsseldorf MDS registry. Leuk Res 36:1067–1070. doi: 10.1016/j.leukres.2012.04.006
Ng AK, Travis LB (2008) Subsequent malignant neoplasms in cancer survivors. Cancer J 14:429–434. doi: 10.1097/PPO.0b013e31818d8779
Nieminen U, Färkkilä M (2015) Malignancies in inflammatory bowel disease. Scand J Gastroenterol 50:81–89. doi: 10.3109/00365521.2014.992041
Nilsson L, Astrand-Grundström I, Anderson K, et al (2002) Involvement and functional impairment of the CD34(+)CD38(-)Thy-1(+) hematopoietic stem cell pool in myelodysplastic syndromes with trisomy 8. 100:259–267. doi:

10.1182/blood-2001-12-0188
Nilsson L, Astrand-Grundström I, Arvidsson I, et al (2000) Isolation and characterization of hematopoietic progenitor/stem cells in 5q-deleted myelodysplastic syndromes: evidence for involvement at the hematopoietic stem cell level. Blood 96:2012–2021.
Nimer SD (2008) Myelodysplastic syndromes. 111:4841–4851. doi: 10.1182/blood-2007-08-078139
Nisse C, Haguenoer JM, Grandbastien B, et al (2001) Occupational and environmental risk factors of the myelodysplastic syndromes in the North of France. 112:927–935.
O'Connor L, Strasser A, O'Reilly LA, et al (1998) Bim: a novel member of the Bcl-2 family that promotes apoptosis. EMBO J 17:384–395. doi: 10.1093/emboj/17.2.384
Oda E, Ohki R, Murasawa H, et al (2000) Noxa, a BH3-only member of the Bcl-2 family and candidate mediator of p53-induced apoptosis. Science 288:1053–1058.
Okada S, Nakauchi H, Nagayoshi K, et al (1991) Enrichment and characterization of murine hematopoietic stem cells that express c-kit molecule. 78:1706–1712.
Okada S, Nakauchi H, Nagayoshi K, et al (1992) In vivo and in vitro stem cell function of c-kit- and Sca-1-positive murine hematopoietic cells. 80:3044–3050.
Omidvar N, Kogan S, Beurlet S, et al (2007) BCL-2 and mutant NRAS interact physically and functionally in a mouse model of progressive myelodysplasia. Cancer Res 67:11657–11667. doi: 10.1158/0008-5472.CAN-07-0196
Orkin SH, Zon LI (2008) Hematopoiesis: an evolving paradigm for stem cell biology. Cell 132:631–644. doi: 10.1016/j.cell.2008.01.025
Osawa M, Hanada K, Hamada H, Nakauchi H (1996) Long-term lymphohematopoietic reconstitution by a single CD34-low/negative hematopoietic stem cell. Science 273:242–245.
Ostrand-Rosenberg S, Sinha P (2009) Myeloid-derived suppressor cells: linking inflammation and cancer. J Immunol 182:4499–4506. doi: 10.4049/jimmunol.0802740
Owen-Schaub LB, Zhang W, Cusack JC, et al (1995) Wild-type human p53 and a temperature-sensitive mutant induce Fas/APO-1 expression. Mol Cell Biol 15:3032–3040.
Pang WW, Pluvinage JV, Price EA, et al (2013) Hematopoietic stem cell and progenitor cell mechanisms in myelodysplastic syndromes. Proc Natl Acad Sci USA 110:3011–3016. doi: 10.1073/pnas.1222861110
Panić L, Tamarut S, Sticker-Jantscheff M, et al (2006) Ribosomal protein S6 gene haploinsufficiency is associated with activation of a p53-dependent checkpoint during gastrulation. Mol Cell Biol 26:8880–8891. doi: 10.1128/MCB.00751-06
Papaemmanuil E, Cazzola M, Boultwood J, et al (2011) Somatic SF3B1 mutation in myelodysplasia with ring sideroblasts. N Engl J Med 365:1384–1395. doi: 10.1056/NEJMoa1103283
Papaemmanuil E, Gerstung M, Malcovati L, et al (2013) Clinical and biological implications of driver mutations in myelodysplastic syndromes. Blood 122:3616–27– quiz 3699. doi: 10.1182/blood-2013-08-518886

Parada LF, Land H, Weinberg RA, et al (1984) Cooperation between gene encoding p53 tumour antigen and ras in cellular transformation. Nature 312:649–651.
Parker JE, Fishlock KL, Mijovic A, et al (1998) "Low-risk" myelodysplastic syndrome is associated with excessive apoptosis and an increased ratio of pro- versus anti-apoptotic bcl-2-related proteins. 103:1075–1082.
Parker JE, Mufti GJ (2000) Excessive apoptosis in low risk myelodysplastic syndromes (MDS). Leuk Lymphoma 40:1–24. doi: 10.3109/10428190009054877
Parker JE, Mufti GJ, Rasool F, et al (2000) The role of apoptosis, proliferation, and the Bcl-2-related proteins in the myelodysplastic syndromes and acute myeloid leukemia secondary to MDS. 96:3932–3938.
Passegué E, Wagers AJ, Giuriato S, et al (2005) Global analysis of proliferation and cell cycle gene expression in the regulation of hematopoietic stem and progenitor cell fates. J Exp Med 202:1599–1611. doi: 10.1084/jem.20050967
Pelengaris S, Khan M, Evan GI (2002) Suppression of Myc-induced apoptosis in beta cells exposes multiple oncogenic properties of Myc and triggers carcinogenic progression. Cell 109:321–334.
Pellagatti A, Cazzola M, Giagounidis A, et al (2010) Deregulated gene expression pathways in myelodysplastic syndrome hematopoietic stem cells. Leukemia 24:756–764. doi: 10.1038/leu.2010.31
Porwit A, van de Loosdrecht AA, Bettelheim P, et al (2014) Revisiting guidelines for integration of flow cytometry results in the WHO classification of myelodysplastic syndromes-proposal from the International/European LeukemiaNet Working Group for Flow Cytometry in MDS. Leukemia 28:1793–1798. doi: 10.1038/leu.2014.191
Pronk CJ, Attema J, Rossi DJ, et al (2008) Deciphering developmental stages of adult myelopoiesis. Cell Cycle 7:706–713. doi: 10.4161/cc.7.6.5565
Pronk CJH, Bryder D (2011) Flow cytometry-based identification of immature myeloerythroid development. Methods Mol Biol 699:275–293. doi: 10.1007/978-1-61737-950-5_13
Pronk CJH, Rossi DJ, Månsson R, et al (2007) Elucidation of the phenotypic, functional, and molecular topography of a myeloerythroid progenitor cell hierarchy. Cell Stem Cell 1:428–442. doi: 10.1016/j.stem.2007.07.005
Puthalakath H, Huang DC, O'Reilly LA, et al (1999) The proapoptotic activity of the Bcl-2 family member Bim is regulated by interaction with the dynein motor complex. Mol Cell 3:287–296.
Puthalakath H, Strasser A (2002) Keeping killers on a tight leash: transcriptional and post-translational control of the pro-apoptotic activity of BH3-only proteins. Cell Death Differ 9:505–512. doi: 10.1038/sj/cdd/4400998
Pülhorn H, Herrmann M, Harms H, et al (2012) Apoptotic cells and clonally expanded cytotoxic T cells in bone marrow trephines of patients with myelodysplastic syndrome. Histopathology 61:200–211. doi: 10.1111/j.1365-2559.2012.04209.x
Raaijmakers MHGP, Mukherjee S, Guo S, et al (2010) Bone progenitor dysfunction induces myelodysplasia and secondary leukaemia. Nature 464:852–857. doi: 10.1038/nature08851
Radu A, Moore MS, Blobel G (1995) The peptide repeat domain of nucleoporin Nup98 functions as a docking site in transport across the nuclear pore

complex. Cell 81:215–222.
Rajapaksa R, Ginzton N, Rott LS, Greenberg PL (1996) Altered oncoprotein expression and apoptosis in myelodysplastic syndrome marrow cells. 88:4275–4287.
Ramos F, Fuertes-Núñez M, Suárez-Vilela D, Fernández-López A (2002) What does apoptosis have to do with clinical features in myelodysplastic syndrome? Haematologica 87:381–391.
Rassool FV, Gaymes TJ, Omidvar N, et al (2007) Reactive oxygen species, DNA damage, and error-prone repair: a model for genomic instability with progression in myeloid leukemia? Cancer Res 67:8762–8771. doi: 10.1158/0008-5472.CAN-06-4807
Raza A, Alvi S, Borok RZ, et al (1997) Excessive proliferation matched by excessive apoptosis in myelodysplastic syndromes: the cause-effect relationship. Leuk Lymphoma 27:111–118. doi: 10.3109/10428199709068277
Raza A, Galili N (2012) The genetic basis of phenotypic heterogeneity in myelodysplastic syndromes. Nat Rev Cancer 12:849–859. doi: 10.1038/nrc3321
Raza A, Gezer S, Mundle S, et al (1995) Apoptosis in bone marrow biopsy samples involving stromal and hematopoietic cells in 50 patients with myelodysplastic syndromes. 86:268–276.
Raza A, Mundle S, Shetty V, et al (1996) Novel insights into the biology of myelodysplastic syndromes: excessive apoptosis and the role of cytokines. Int J Hematol 63:265–278.
Raza A, Reeves JA, Feldman EJ, et al (2008) Phase 2 study of lenalidomide in transfusion-dependent, low-risk, and intermediate-1 risk myelodysplastic syndromes with karyotypes other than deletion 5q. 111:86–93. doi: 10.1182/blood-2007-01-068833
Raza-Egilmez SZ, Jani-Sait SN, Grossi M, et al (1998) NUP98-HOXD13 gene fusion in therapy-related acute myelogenous leukemia. Cancer Res 58:4269–4273.
Reindl C, Quentmeier H, Petropoulos K, et al (2009) CBL exon 8/9 mutants activate the FLT3 pathway and cluster in core binding factor/11q deletion acute myeloid leukemia/myelodysplastic syndrome subtypes. Clin Cancer Res 15:2238–2247. doi: 10.1158/1078-0432.CCR-08-1325
Rigolin GM, Cuneo A, Roberti MG, et al (1998) Exposure to myelotoxic agents and myelodysplasia: case-control study and correlation with clinicobiological findings. 103:189–197.
Rose C, Brechignac S, Vassilief D, et al (2010) Does iron chelation therapy improve survival in regularly transfused lower risk MDS patients? A multicenter study by the GFM (Groupe Francophone des Myélodysplasies). Leuk Res 34:864–870. doi: 10.1016/j.leukres.2009.12.004
Roths JB, Murphy ED, Eicher EM (1984) A new mutation, gld, that produces lymphoproliferation and autoimmunity in C3H/HeJ mice. J Exp Med 159:1–20.
Sanford D, Hsai CC (2015) A case of transfusion independence in a patient with myelodysplastic syndrome using deferasirox, sustained for two years after stopping therapy. Curr Oncol 22:128–5. doi: 10.3747/co.22.2100
Sattler M, Liang H, Nettesheim D, et al (1997) Structure of Bcl-xL-Bak peptide complex: recognition between regulators of apoptosis. Science 275:983–986.

Saunthararajah Y, Nakamura R, Nam J-M, et al (2002) HLA-DR15 (DR2) is overrepresented in myelodysplastic syndrome and aplastic anemia and predicts a response to immunosuppression in myelodysplastic syndrome. 100:1570–1574.
Savill J, Fadok V (2000) Corpse clearance defines the meaning of cell death. Nature 407:784–788. doi: 10.1038/35037722
Sawanobori M, Yamaguchi S, Hasegawa M, et al (2003) Expression of TNF receptors and related signaling molecules in the bone marrow from patients with myelodysplastic syndromes. Leuk Res 27:583–591.
Scaffidi P, Misteli T, Bianchi ME (2002) Release of chromatin protein HMGB1 by necrotic cells triggers inflammation. Nature 418:191–195. doi: 10.1038/nature00858
Schanz J, Tüchler H, Solé F, et al (2012) New comprehensive cytogenetic scoring system for primary myelodysplastic syndromes (MDS) and oligoblastic acute myeloid leukemia after MDS derived from an international database merge. J Clin Oncol 30:820–829. doi: 10.1200/JCO.2011.35.6394
Schuler M, Maurer U, Goldstein JC, et al (2003) p53 triggers apoptosis in oncogene-expressing fibroblasts by the induction of Noxa and mitochondrial Bax translocation. Cell Death Differ 10:451–460. doi: 10.1038/sj.cdd.4401180
Scott BL, Ramakrishnan A, Fosdal M, et al (2010) Anti-thymocyte globulin plus etanercept as therapy for myelodysplastic syndromes (MDS): a phase II study. 149:706–710. doi: 10.1111/j.1365-2141.2010.08145.x
Scott FL, Stec B, Pop C, et al (2009) The Fas-FADD death domain complex structure unravels signalling by receptor clustering. Nature 457:1019–1022. doi: 10.1038/nature07606
Sebaa A, Ades L, Baran Marzack F, et al (2012) Incidence of 17p deletions and TP53 mutation in myelodysplastic syndrome and acute myeloid leukemia with 5q deletion. Genes Chromosomes Cancer 51:1086–1092. doi: 10.1002/gcc.21993
Seymour JF, Fenaux P, Silverman LR, et al (2010) Effects of azacitidine compared with conventional care regimens in elderly (≥ 75 years) patients with higher-risk myelodysplastic syndromes. Crit Rev Oncol Hematol 76:218–227. doi: 10.1016/j.critrevonc.2010.04.005
Shah DR, Daver N, Borthakur G, et al (2014) Pernicious Anemia With Spuriously Normal Vitamin B12 Level Might Be Misdiagnosed As Myelodysplastic Syndrome. Clinical Lymphoma Myeloma and Leukemia 14:e141–e143. doi: 10.1016/j.clml.2014.02.002
Shao L, Sun Y, Zhang Z, et al (2010) Deletion of proapoptotic Puma selectively protects hematopoietic stem and progenitor cells against high-dose radiation. 115:4707–4714. doi: 10.1182/blood-2009-10-248872
Shetty V, Mundle S, Alvi S, et al (1996) Measurement of apoptosis, proliferation and three cytokines in 46 patients with myelodysplastic syndromes. Leuk Res 20:891–900.
Shi Y (2002) Mechanisms of caspase activation and inhibition during apoptosis. Mol Cell 9:459–470.
Shibue T, Takeda K, Oda E, et al (2003) Integral role of Noxa in p53-mediated apoptotic response. Genes Dev 17:2233–2238. doi: 10.1101/gad.1103603
Silverman LR, Demakos EP, Peterson BL, et al (2002) Randomized controlled

trial of azacitidine in patients with the myelodysplastic syndrome: a study of the cancer and leukemia group B. J Clin Oncol 20:2429–2440.
Silverman LR, Greenberg P, Raza A, et al (2014) Clinical activity and safety of the dual pathway inhibitor rigosertib for higher risk myelodysplastic syndromes following DNA methyltransferase inhibitor therapy. Hematol Oncol n/a–n/a. doi: 10.1002/hon.2137
Slape C, Aplan PD (2004) The role of NUP98 gene fusions in hematologic malignancy. Leuk Lymphoma 45:1341–1350.
Slape C, Lin YW, Hartung H, et al (2008a) NUP98-HOX translocations lead to myelodysplastic syndrome in mice and men. J Natl Cancer Inst Monographs 64–68. doi: 10.1093/jncimonographs/lgn014
Slape C, Liu LY, Beachy S, Aplan PD (2008b) Leukemic transformation in mice expressing a NUP98-HOXD13 transgene is accompanied by spontaneous mutations in Nras, Kras, and Cbl. 112:2017–2019. doi: 10.1182/blood-2008-01-135186
Slape CI, Saw J, Jowett JBM, et al (2012) Inhibition of apoptosis by BCL2 prevents leukemic transformation of a murine myelodysplastic syndrome. 120:2475–2483. doi: 10.1182/blood-2012-05-430736
Smolewski P, Grabarek J, Halicka HD, Darzynkiewicz Z (2002) Assay of caspase activation in situ combined with probing plasma membrane integrity to detect three distinct stages of apoptosis. J Immunol Methods 265:111–121.
Sportoletti P, Grisendi S, Majid SM, et al (2008) Npm1 is a haploinsufficient suppressor of myeloid and lymphoid malignancies in the mouse. Blood 111:3859–3862. doi: 10.1182/blood-2007-06-098251
Starczynowski DT, Kuchenbauer F, Argiropoulos B, et al (2010) Identification of miR-145 and miR-146a as mediators of the 5q- syndrome phenotype. Nature Medicine 16:49–58. doi: 10.1038/nm.2054
Steensma DP (2012) Dysplasia Has A Differential Diagnosis: Distinguishing Genuine Myelodysplastic Syndromes (MDS) From Mimics, Imitators, Copycats and Impostors. Curr Hematol Malig Rep 7:310–320. doi: 10.1007/s11899-012-0140-3
Stifter G, Heiss S, Gastl G, et al (2005) Over-expression of tumor necrosis factor-alpha in bone marrow biopsies from patients with myelodysplastic syndromes: relationship to anemia and prognosis. Eur J Haematol 75:485–491. doi: 10.1111/j.1600-0609.2005.00551.x
Strasser A, Cory S, Adams JM (2011) Deciphering the rules of programmed cell death to improve therapy of cancer and other diseases. EMBO J 30:3667–3683. doi: 10.1038/emboj.2011.307
Strasser A, Harris AW, Bath ML, Cory S (1990) Novel primitive lymphoid tumours induced in transgenic mice by cooperation between myc and bcl-2. Nature 348:331–333. doi: 10.1038/348331a0
STRASSER A, PUTHALAKATH H, BOUILLET P, et al (2000) The Role of Bim, a Proapoptotic BH3-Only Member of the Bcl-2 Family, in Cell-Death Control. Ann N Y Acad Sci 917:541–548. doi: 10.1111/j.1749-6632.2000.tb05419.x
Streuli RA, Testa JR, Vardiman JW, et al (1980) Dysmyelopoietic syndrome: sequential clinical and cytogenetic studies. Blood 55:636–644.
Subramanian A, Tamayo P, Mootha VK, et al (2005) Gene set enrichment analysis: a knowledge-based approach for interpreting genome-wide expression profiles. Proc Natl Acad Sci USA 102:15545–15550. doi:

10.1073/pnas.0506580102
Suda T, Takahashi T, Golstein P, Nagata S (1993) Molecular cloning and expression of the Fas ligand, a novel member of the tumor necrosis factor family. Cell 75:1169–1178.
Suragani RNVS, Cadena SM, Cawley SM, et al (2014) Transforming growth factor-β superfamily ligand trap ACE-536 corrects anemia by promoting late-stage erythropoiesis. Nature Medicine 20:408–414. doi: 10.1038/nm.3512
Suzuki M, Youle RJ, Tjandra N (2000) Structure of Bax: coregulation of dimer formation and intracellular localization. Cell 103:645–654.
Takahashi T, Tanaka M, Brannan CI, et al (1994) Generalized lymphoproliferative disease in mice, caused by a point mutation in the Fas ligand. Cell 76:969–976.
Talwalkar SS, Yin CC, Naeem RC, et al (2010) Myelodysplastic syndromes arising in patients with germline TP53 mutation and Li-Fraumeni syndrome. Arch Pathol Lab Med 134:1010–1015. doi: 10.1043/2009-0015-OA.1
Tehranchi R, Fadeel B, Forsblom A-M, et al (2003) Granulocyte colony-stimulating factor inhibits spontaneous cytochrome c release and mitochondria-dependent apoptosis of myelodysplastic syndrome hematopoietic progenitors. 101:1080–1086. doi: 10.1182/blood-2002-06-1774
Tehranchi R, Fadeel B, Schmidt-Mende J, et al (2005) Antiapoptotic role of growth factors in the myelodysplastic syndromes: concordance between in vitro and in vivo observations. Clin Cancer Res 11:6291–6299. doi: 10.1158/1078-0432.CCR-04-1850
TeKippe M, Harrison DE, Chen J (2003) Expansion of hematopoietic stem cell phenotype and activity in Trp53-null mice. Exp Hematol 31:521–527.
Thanopoulou E, Cashman J, Kakagianne T, et al (2004) Engraftment of NOD/SCID-beta2 microglobulin null mice with multilineage neoplastic cells from patients with myelodysplastic syndrome. 103:4285–4293. doi: 10.1182/blood-2003-09-3192
Thornberry NA, Lazebnik Y (1998) Caspases: enemies within. Science 281:1312–1316.
Thornborrow EC, Patel S, Mastropietro AE, et al (2002) A conserved intronic response element mediates direct p53-dependent transcriptional activation of both the human and murine bax genes. Oncogene 21:990–999. doi: 10.1038/sj.onc.1205069
Thota S, Viny AD, Makishima H, et al (2014) Genetic alterations of the cohesin complex genes in myeloid malignancies. Blood 124:1790–1798. doi: 10.1182/blood-2014-04-567057
Tsoplou P, Kouraklis-Symeonidis A, Thanopoulou E, et al (1999) Apoptosis in patients with myelodysplastic syndromes: differential involvement of marrow cells in 'good' versus “poor” prognosis patients and correlation with apoptosis-related genes. Leukemia 13:1554–1563.
Valente LJ, Gray DHD, Michalak EM, et al (2013) p53 efficiently suppresses tumor development in the complete absence of its cell-cycle inhibitory and proapoptotic effectors p21, Puma, and Noxa. Cell Rep 3:1339–1345. doi: 10.1016/j.celrep.2013.04.012
van de Loosdrecht AA, Alhan C, Béné MC, et al (2009) Standardization of flow cytometry in myelodysplastic syndromes: report from the first European

LeukemiaNet working conference on flow cytometry in myelodysplastic syndromes. In: Haematologica. pp 1124–1134
van de Loosdrecht AA, Westers TM (2011) Flow cytometry in myelodysplastic syndromes: Ready for translation into clinical practice. Leuk Res 35:850–852. doi: 10.1016/j.leukres.2011.03.030
van Delft MF, Huang DCS (2006) How the Bcl-2 family of proteins interact to regulate apoptosis. Cell Res 16:203–213. doi: 10.1038/sj.cr.7310028
Vaux DL, Cory S, Adams JM (1988) Bcl-2 gene promotes haemopoietic cell survival and cooperates with c-myc to immortalize pre-B cells. Nature 335:440–442. doi: 10.1038/335440a0
Veda P (2013) Evaluation of macrocytosis in routine hemograms. Indian J Hematol Blood Transfus 29:26–30. doi: 10.1007/s12288-011-0142-7
Velegraki M, Papakonstanti E, Mavroudi I, et al (2013) Impaired clearance of apoptotic cells leads to HMGB1 release in the bone marrow of patients with myelodysplastic syndromes and induces TLR4-mediated cytokine production. Haematologica 98:1206–1215. doi: 10.3324/haematol.2012.064642
Vermes I, Haanen C, Steffens-Nakken H, Reutelingsperger C (1995) A novel assay for apoptosis. Flow cytometric detection of phosphatidylserine expression on early apoptotic cells using fluorescein labelled Annexin V. J Immunol Methods 184:39–51.
Villunger A, Michalak EM, Coultas L, et al (2003) p53- and drug-induced apoptotic responses mediated by BH3-only proteins puma and noxa. Science 302:1036–1038. doi: 10.1126/science.1090072
Vogelstein B (1990) Cancer. A deadly inheritance. Nature 348:681–682. doi: 10.1038/348681a0
Voukelatou G, Thanopoulou E, Dallas K, et al (2009) P060 CD34+ marrow cells from MDS patients are characterized by higher levels of intracellular reactive oxygen species and inadequate antioxidant defences. Leuk Res 33:S93–S94. doi: 10.1016/S0145-2126(09)70140-7
Vousden KH, Lane DP (2007) p53 in health and disease. Nat Rev Mol Cell Biol 8:275–283. doi: 10.1038/nrm2147
Walensky LD, Pitter K, Morash J, et al (2006) A stapled BID BH3 helix directly binds and activates BAX. Mol Cell 24:199–210. doi: 10.1016/j.molcel.2006.08.020
Walter MJ, Shen D, Ding L, et al (2012) Clonal Architecture of Secondary Acute Myeloid Leukemia. N Engl J Med 366:1090–1098. doi: 10.1056/NEJMoa1106968
Walter MJ, Shen D, Shao J, et al (2013) Clonal diversity of recurrently mutated genes in myelodysplastic syndromes. Leukemia 27:1275–1282. doi: 10.1038/leu.2013.58
Wang J, Li Z, He Y, et al (2014a) Loss of Asxl1 leads to myelodysplastic syndrome–like disease in mice. 123:541–553. doi: 10.1182/blood-2013-05-500272
Wang L, Luo J, Nian Q, et al (2014b) Ribosomal protein S14 silencing inhibits growth of acute myeloid leukemia transformed from myelodysplastic syndromes via activating p53. Hematology 19:225–231. doi: 10.1179/1607845413Y.0000000127
Warnock LJ, Knox A, Mee TR, et al (2008) Influence of tetramerisation on site-

specific post-translational modifications of p53: comparison of human and murine p53 tumor suppressor protein. cbt 7:1481–1489.
Watanabe-Okochi N, Kitaura J, Ono R, et al (2008) AML1 mutations induced MDS and MDS/AML in a mouse BMT model. Blood 111:4297–4308. doi: 10.1182/blood-2007-01-068346
Wattel E, Preudhomme C, Hecquet B, et al (1994) p53 mutations are associated with resistance to chemotherapy and short survival in hematologic malignancies. Blood 84:3148–3157.
Wei MC, Lindsten T, Mootha VK, et al (2000) tBID, a membrane-targeted death ligand, oligomerizes BAK to release cytochrome c. Genes Dev 14:2060–2071.
Wen X-M, Hu J-B, Yang J, et al (2015) CEBPA methylation and mutation in myelodysplastic syndrome. Med Oncol 32:605. doi: 10.1007/s12032-015-0605-z
Wijsman JH, Jonker RR, Keijzer R, et al (1993) A new method to detect apoptosis in paraffin sections: in situ end-labeling of fragmented DNA. J Histochem Cytochem 41:7–12.
Wiley SR, Schooley K, Smolak PJ, et al (1995) Identification and characterization of a new member of the TNF family that induces apoptosis. Immunity 3:673–682.
Willis SN, Adams JM (2005) Life in the balance: how BH3-only proteins induce apoptosis. Curr Opin Cell Biol 17:617–625. doi: 10.1016/j.ceb.2005.10.001
Willis SN, Chen L, Dewson G, et al (2005) Proapoptotic Bak is sequestered by Mcl-1 and Bcl-xL, but not Bcl-2, until displaced by BH3-only proteins. Genes Dev 19:1294–1305. doi: 10.1101/gad.1304105
Willis SN, Fletcher JI, Kaufmann T, et al (2007) Apoptosis initiated when BH3 ligands engage multiple Bcl-2 homologs, not Bax or Bak. Science 315:856–859. doi: 10.1126/science.1133289
Wlodkowic D, Skommer J, Darzynkiewicz Z (2009) Flow Cytometry-Based Apoptosis Detection. In: Flow cytometry-based apoptosis detection. Humana Press, Totowa, NJ, pp 19–32
Woll PS, Kjällquist U, Chowdhury O, et al (2014) Myelodysplastic Syndromes Are Propagated by Rare and Distinct Human Cancer Stem Cells In Vivo. Cancer Cell. doi: 10.1016/j.ccr.2014.03.036
Wolter KG, Hsu YT, Smith CL, et al (1997) Movement of Bax from the cytosol to mitochondria during apoptosis. J Cell Biol 139:1281–1292.
Wu L, Li X, Xu F, et al (2012) Over-expression of RPL23 in myelodysplastic syndromes is associated with apoptosis resistance of CD34+ cells and predicts poor prognosis and distinct response to CHG chemotherapy or decitabine. Ann Hematol 91:1547–1554. doi: 10.1007/s00277-012-1486-2
Wu M-Y, Eldin KW, Beaudet AL (2008) Identification of chromatin remodeling genes Arid4a and Arid4b as leukemia suppressor genes. J Natl Cancer Inst 100:1247–1259. doi: 10.1093/jnci/djn253
Wu W-S, Heinrichs S, Xu D, et al (2005) Slug antagonizes p53-mediated apoptosis of hematopoietic progenitors by repressing puma. Cell 123:641–653. doi: 10.1016/j.cell.2005.09.029
Xu F, Yang R, Wu L, et al (2012a) Overexpression of BMI1 confers clonal cells resistance to apoptosis and contributes to adverse prognosis in myelodysplastic syndrome. Cancer Lett 317:33–40. doi: 10.1016/j.canlet.2011.11.012

Xu H, Menendez S, Schlegelberger B, et al (2012b) Loss of p53 accelerates the complications of myelodysplastic syndrome in a NUP98-HOXD13-driven mouse model. 120:3089–3097. doi: 10.1182/blood-2012-01-405332

Yin XM, Wang K, Gross A, et al (1999) Bid-deficient mice are resistant to Fas-induced hepatocellular apoptosis. Nature 400:886–891. doi: 10.1038/23730

Yoshida K, Sanada M, Shiraishi Y, et al (2011) Frequent pathway mutations of splicing machinery in myelodysplasia. Nature 478:64–69. doi: 10.1038/nature10496

You H, Pellegrini M, Tsuchihara K, et al (2006) FOXO3a-dependent regulation of Puma in response to cytokine/growth factor withdrawal. J Exp Med 203:1657–1663. doi: 10.1084/jem.20060353

Yu H, Shen H, Yuan Y, et al (2010) Deletion of Puma protects hematopoietic stem cells and confers long-term survival in response to high-dose gamma-irradiation. 115:3472–3480. doi: 10.1182/blood-2009-10-248278

Yu J, Zhang L (2008) PUMA, a potent killer with or without p53. Oncogene 27 Suppl 1:S71–83. doi: 10.1038/onc.2009.45

Yu J, Zhang L, Hwang PM, et al (2001) PUMA induces the rapid apoptosis of colorectal cancer cells. Mol Cell 7:673–682.

Zamai L, Secchiero P, Pierpaoli S, et al (2000) TNF-related apoptosis-inducing ligand (TRAIL) as a negative regulator of normal human erythropoiesis. 95:3716–3724.

Zhou T, Hasty P, Walter CA, et al (2013) Myelodysplastic syndrome: an inability to appropriately respond to damaged DNA? Exp Hematol 41:665–674. doi: 10.1016/j.exphem.2013.04.008

(2008) WHO Classification of Tumours of Haematopoietic and Lymphoid Tissue, Fourth Edition. World Health Organization

(2014) Abstracts of the HAA 2014 Annual Scientific Meeting. 1–492.